AN INVESTIGATION INTO THE ROLE OF GLUCURONIDATION ON THE DISPOSITION AND TOXICITY OF MYCOPHENOLIC ACID USING TARGETED QUANTITATIVE PROTEOMICS

David Edward Harbourt

A dissertation submitted to the faculty of the University of North Carolina at Chapel Hill in partial fulfillment of the requirements for the degree of Doctor of Philosophy in the Curriculum of Toxicology.

Chapel Hill
2009

Approved by:
Advisor and Committee Chair: Philip C. Smith, Ph.D.
Reader: Michael J. DeVito, Ph.D.
Reader: Gary L. Glish, Ph.D.
Reader: Mary F. Paine, Ph.D.
Reader: Joseph K. Ritter, Ph.D.

ABSTRACT

DAVID HARBOURT: "An Investigation into the Role of Glucuronidation on the Disposition and Toxicity of Mycophenolic Acid using Targeted Quantitative Proteomics"
(Under the direction of Dr. Philip C. Smith)

The prodrug mycophenolate mofetil (MMF) is used clinically for prophylaxis of organ rejection in transplant patients. MMF is metabolized to the active metabolite mycophenolic acid (MPA). While proven useful in this setting, a significant fraction of patients receiving MMF chronically experience delayed-onset diarrhea, which limits the long term effectiveness of their treatment. MPA is eliminated primarily through glucuronidation by the action of UDP-glucuronosyltransferase (UGT) 1A enzymes within the liver and intestine. Glucuronides in the liver are excreted into the bile by the canalicular transporter multidrug resistance-associated protein 2 (MRP2) where they are subject to enterohepatic cycling and excretion through the urine as glucuronides. Glucuronidation results in the formation of the inactive phenolic glucuronide (MPAG) and the labile acyl glucuronide (acMPAG). While the formation of MPAG is the primary method of detoxification of MPA *in vivo,* studies have attempted to link formation of acyl glucuronides with adverse drug reactions (ADRs). While evidence has been inconclusive in directly linking acyl glucuronides with toxicity, some drugs forming acyl glucuronides have been removed from the marketplace due to ADRs. The overall hypothesis of this

dissertation project is that variable glucuronidation formation and efflux within the liver and gastrointestinal tract results in differential MPAG formation rates and thus modulates MPA toxicity.

The study of the relationships between metabolism and transport was aided by quantitative measurement of relevant enzymes in humans and animals. This methodology was used to establish assays to quantify precise differences in UGT1A enzymes between the tissues in rats and humans to understand the differences in metabolism and toxicity of MPA between species. This dissertation research examined the disposition of acMPAG and MPAG in relation to expression levels of Ugt1a enzymes and efflux transporters using targeted quantitative proteomics. By correlating glucuronide catalysis and efflux with absolute quantification of Ugts and transporters, we increased our understanding of relationships between glucuronide formation and disposition and UGT enzymes. This research helps explain some differences in metabolism and elimination observed between rats and humans administered MPA and these relationships may be applied to other xenobiotics with Phase II substrates.

ACKNOWLEDGEMENTS

I am forever indebted to my committee chair and advisor, Dr. Philip Smith for his guidance and mentorship over the course of my graduate work. His advice and thoughtful comments during my numerous inquiries throughout my experiments have taught me how to think critically during problem solving. My graduate work in Dr. Smith's lab has shaped me into the scientist I am today and it is my hope that he can be proud of the work presented as it is a testament to his guidance and thoughtfulness as my mentor.

I also have the deepest gratitude for my committee members, Drs. Mike DeVito, Gary Glish, Mary Paine and Joe Ritter for their thoughtful comments and advice over the course of my project. I would especially like to thank the members of the Glish and Ritter labs along with Dr. Peter Bullock and Saber Malecki of Panacos Pharmaceuticals for their assistance and camaraderie as this work would not have been possible without their help.

I would like to thank my parents, Cyrus and Bonnie, and my sister Diana for providing me with a solid foundation and for always believing in me. The many lessons they have taught me beginning in my early childhood help shape the kind of person I hope to be through the duration of my adult life.

I would also like to thank the members of the Cho lab as my daily interactions with them helped me through all of the ups and downs of graduate school.

I would like to thank all of my friends and members of my extended family for their support during the course of my graduate education. My friends have always been supportive of me during the course of my studies and have helped me in many ways that are too numerous to list. I will always be grateful for all of my interactions with them because they formed many of my fondest memories from graduate school.

Finally, I would like to express my sincerest gratitude to my wonderful girlfriend Kelly Ennis. The past two years that we have spent together have been the happiest of my life as she has always given me someone to talk to and has been the person that I can always lean on during difficult times. I will always cherish her love and company and meeting her during the course of my graduate studies has been one of the best things that has ever happened to me.

Table of Contents

List of Tables

List of Figures

List of Abbreviations

ABC= Adenosine Triphosphate Binding Cassette

ACN= Acetonitrile

AcMPAG= Mycophenolic Acid Acyl Glucuronide

ADRs= Adverse Drug Reactions

AhR= Aryl Hydrocarbon Receptor

BCA = Bicinchoninic Acid

BD= Bile duct

BEH= Bridged ethylene hybrid

BSA= Bovine Serum Albumin

CAR= Constitutive Androstane Receptor

Cdx2= Caudal Homeodomain Protein 2

CHAPS = 3-((3-cholamidopropyl)dimethylammonio)-1-propanesulfonic acid

CID= Collision induced dissociation

CRP= C-Reactive Protein

% C.V. = Percentage coefficient of variation

DIGE= Differential Gel Electrophoresis

DPP-IV= Dipeptidyl Peptidase IV

DS-L= D-Sacchric Acid 1, 4 Lactone

ELISA= Enzyme Linked ImmunoSorbant Assay

ESI= Electrospray Ionization

FA= Formic Acid

GI= Gastronintestinal

HOAc= Acetic Acid

HSA= Human Serum Albumin

HIM = Human intestinal microsomes

HLM = Human liver microsomes

HNF1-α= Human Nuclear Factor 1-Alpha

ICAT= Isotope Coded Affinity Tag

IMPDH= Ionosine Monophosphate Dehydrogenase

IV= Intravenous

iTRAQ= Isobaric Tagging for Relative and Absolute Quantification

LC = Liquid Chromatography

LC-MS = Liquid Chromatography - Mass Spectrometry

LC-MS/MS = Liquid Chromatography – Tandem Mass Spectrometry

LIT-TOF= Linear Ion Trap-Time of Flight

$MgCl_2$= Magnesium Chloride

MMF= Mycophenolate Mofetil

MPA = Mycophenolic Acid

MPAG= Mycophenolic Acid Glucuronide

MPA Na^+= Mycophenolic Acid Sodium Salt

MRM= Multiple Reaction Monitoring

Mrp2= Rat Mutidrug Resistance-Associated Protein 2

Mrp3= Rat Mutidrug Resistance-Associated Protein 3

Nano-UPLC= Nano-Ultra Performance Liquid Chromatography

NCBI Blast = National Center for Biotechnology Information Basic Local Alignment Search tool

NSAIDs= Non-Steroidal Anti-Inflammatory Drugs

PAR = Peak Area Ratio

PMSF= Phenylmethylsulfonyl Fluoride

PSA= Prostate Specific Antigen

PO= Oral Dosing

PXR= Pregnane X Receptor

QconCAT/QCAT= Quantitative Concatomer

Q-TOF= Quadrupole-Time of Flight

RLM = Rat liver microsomes

RT-PCR= Real Time Polymerase Chain Reaction

SDS-PAGE = Sodium dodecyl sulfate polyacrylamide gel electrophoresis

SILAC = Stable isotope labeling with amino acids in cell culture

SNP = Single nucleotide polymorphism

SPE = Solid Phase Extraction

TFE = 2,2,2-Trifluoroethanol

TPCK = L-1-tosylamido-2-phenylethyl chloromethyl ketone

$T_{1/2}$= Half-Life

UGT = Uridine-Diphosphate Glucuronosyl Transferase

VPA= Valproic Acid

CHAPTER 1

INTRODUCTION

A. INTRODUCTION

Drug metabolizing enzymes affect the disposition and toxicity of many endogenous and exogenous chemicals. These enzymes can alter compounds in a number of ways, either through the addition or subtraction of functional groups or by the alteration of oxidation state or arrangement of the molecule (Bock and Lilienblum, 1994; Ionescu C and Caira MR, 2005). Through the actions of drug metabolizing enzymes, the body is able to eliminate many potential harmful compounds, primarily as inactive biproducts, by the usual methods of excretion and elimination.

While the impact of drug metabolizing enzymes on the disposition and elimination of xenobiotics is well known, additional factors include protein binding, metabolite disposition and toxicity, and transporters (Bock and Lilienblum, 1994; Coleman M, 2005; Ionescu C and Caira MR, 2005). A single compound may be metabolized by different enzymes, resulting in many different metabolites, and are subsequently excreted into either the blood or bile by separate transporters, further complicating absorption, disposition, metabolism and excretion (ADME) studies necessary for pharmaceutical compounds.

The rapid development of new methods and instruments designed for quantitative proteomics has the potential to advance our understanding of relationships between drug metabolizing enzymes and transporters when conducting ADME studies of particular compounds of interest. The example of linking the expression of particular enzymes and transporters of interest with the metabolism and disposition of a compound can be highlighted with the

immunosuppressive agent mycophenolic acid (MPA; 1,3-dihydro-4-hydroxy-6-methoxy-7-methyl-3-oxo-5-isobenzylfuranyl-4-methyl-4-hexenoate, Figure 1.1). MPA is a substrate for uridine diphosphate glucuronosyltransferase (UGT) enzymes in the liver, kidney and intestinal tract. Following UGT conjugation, MPA is excreted first into either the bile or blood by canalicular or basolateral transporters located in hepatocytes. Subsequent metabolism following efflux into the bile or blood, hydrolysis by β-glucuronidase enzymes found in the gut flora of the intestinal lumen by enterocytes of the intestine, or the tubules of the kidney leads to elimination of glucuronide conjugates in the urine or feces (Bullingham et al., 1996; Bullingham et al., 1998). While MPA is generally well tolerated, a large fraction of patients experience delayed-onset diarrhea, impacting lifestyle and potentially resulting in allograft rejection and life threatening complications (Davies et al., 2007). It is possible that variability in UGT enzymes and transporters within the gastrointestinal tract affect MPA exposure levels, leading to gastrointestinal toxicity (Stern et al., 2007; Tallman et al., 2007; Tukey and Strassburg, 2000).

The structure and function of UGT enzymes within the body, along with differences between metabolism and expression levels between rats and humans are examined. Furthermore, a background on the clinical uses of MPA is given, along with its fate within the body following administration. The potential impact of labile acyl glucuronides are examined along with a short background on the recent developments within the field of quantitative proteomics. This introduction should provide the reader with an understanding of the benefits that

quantitative proteomics can provide biological scientists, illustrated by the effect of altered UGT enzyme and transporter levels have on MPA disposition and toxicity.

B. UDP-Glucuronosyltransferases

B.1. Background and Function

UDP-glucuronosyltransferases (UGTs) are a family of phase II metabolism enzymes that primarily convert lipophilic exogenous and endogenous compounds to conjugated products through the nucleophilic addition of glucuronic acid onto the compound. The glucuronic acid side chain addition is accomplished through a nucleophilic attack onto the C1 pryanose acid side chain in a S_N2 reaction mediated by the cofactor UDPGA and UGT enzymes (Clarke and Burchell, 1994; Ionescu C and Caira MR, 2005). The UGT family of enzymes consists of four gene families, UGT1, UGT2, UGT3 and UGT8, with 52 UGT enzymes described between vertebrate and invertebrate species (Tukey and Strassburg, 2000; Tukey and Strassburg, 2001). In humans, 19 UGT enzymes have been described and separated into two gene families, UGT1 and UGT2, with two subfamilies each. The UGT1A locus is found within chromosome 2q37 encoding nine separate functional isoforms and the inactive pseudogenes UGT1A2, UGT1A11, UGT1A12 and UGT1A13 (Tukey and Strassburg, 2001). The UGT locus consists of a 528-534 amino acid sequence divided between a conserved domain toward the carboxyl tail, spanning 250

amino acids and a divergent domain unique to each isoform spanning approximately 280 amino acids starting at the amino terminus.

The primary function of UGT enzymes within the body is the detoxification of endogenous and exogenous lipophilic compounds. Conjugation results in the formation of a product that is more hydrophilic and excreted into the blood or into the bile after a change in charge state and molecular weight addition. In addition, conjugation results in the loss of pharmacological activity, with the some exceptions including morphine 6-glucuronide (Bailey and Dickinson, 2003; Ritter 2000; Ionescu C and Caira MR, 2005). Compounds that undergo conjugation are also less likely to form electrophilic adducts with proteins or other macromolecules including DNA (Bock and Lilienbaum, 1994). A source of bioactivation involves the formation of electrophilic N-O-glucuronides of hydroxamic acids potentially resulting in hypersensitivity or chemical carcinogenesis (Ritter, 2000). While electrophilic adducts of DNA have been linked to carcinogenesis, there is inconsistent evidence linking drug protein adduct formation via acyl glucuronides with toxicological outcomes (Bailey and Dickinson, 2003).

Following conjugation within the liver, it is common for glucuronide conjugates to be excreted into the biliary tract by the ATP-binding cassette (ABC) family of canalicular membrane transporters, including the multidrug resistance-associated protein 2 (MRP2) (ABCC2/Abcc2) and the breast cancer resistance protein (BCRP) (ABCG2/Abcg2). Conjugated metabolites may be cleaved back to the parent aglycone molecule by β-glucuronidase enzymes within the gut flora

of the intestinal lumen. The parent aglycone that is liberated within the intestinal lumen may then be taken back up into the liver through the portal vein in a process known as enterohepatic cycling (EHC). Generally, glucuronides are not passively absorbed due to their polarity and charge. EHC can be manifested in plasma concentration versus time curves as secondary peaks after initial dose administration. EHC values vary between compounds but may be responsible for as much as 60% of MPA systemic exposure in humans and can serve to both increase efficacy of the parent compound along with potential side effects (Bullingham et al., 1998; Naderer et al., 2005).

B.2. Human UGTs

UGTs are expressed widely in humans and have been found in some capacity in virtually every major organ within the body. In humans, genes are expressed within two separate families and four subfamilies. Nomenclature for the UGT gene family is denoted with an Arabic numeral, the gene subfamily with a letter and specific gene with an Arabic numeral (Mackenzie et al., 1997). In humans, UGT genes are transcribed from chromosomes 2q37 (1A) and 4q2 (2B). The UGT1A enzymes are transcribed from 12 unique promoter sequences with the four common 3' exons and one unique 5' exon to form nine functional enzymes and four pseudogenes (Ritter et al., 1992; Owens and Ritter, 1995; Tukey and Strassburg, 2000; Tukey and Strassburg, 2001; <http://som.flinders.edu.au/FUSA/ClinPharm/UGT/>).

UGT1A1 is the most widely expressed of the human UGT enzymes (hUGTs) and is known to conjugate numerous endogenous steroid and thyroid hormones, in addition to many exogenous compounds, but is best known for bilirubin detoxification (Ritter et al., 1991; Tukey and Strassburg, 2000). Its role in bilirubin conjugation is responsible for this being the most intensly studied UGT isoform. Expression of UGT1A1 has been detected primarily in the liver and throughout the gastrointestinal tract. Unlike other drug metabolizing enzymes, UGTs undergo oligermerization, either within or between isoforms, drastically impacting activity levels (Bock and Kohle, 2009; Meech and Mackenzie, 1997; Levesque et al., 2007). UGT1A6 has a similar distribution of tissue expression compared to 1A1 but has been found to catalyze and detoxify primarily exogenous compounds. The advent of RT-PCR technology allowed for tissue expression studies of individual UGT isoforms but quantification has still proven difficult. Because human UGT1A3, UGT1A4, UGT1A5 and UGT1A7, UGT1A8, UGT1A9 and UGT1A10 display up to 93% sequence homology, antibody generation for Western blotting has proven to be an arduous task and perhaps unresolvable. Of the 17 active human UGT isoforms identified, only UGT1A1, UGT1A6 and UGT2B7 display proper structural diversity to allow for specific or selective antibody generation (Tukey and Strassburg, 2001). A fourth antibody for quantification of UGT1A9 has been generated from the laboratory of J. Ritter at Virginia Commenwealth University (VCU), but cross-reactivity with UGT1A7-10 due to structural homology has hindered reliability of quantification. A similar attempt has been made with UGT1A4 and UGT1A8, but again, cross-reactivity

with analogous isoforms has deterred development. Because of their high genome sequence homology, coupled with extensive tissue expression and diverse substrate conjugation, a need exists for an accurate, reproducible method for UGT quantification.

B.3. Rat Ugts

In rats, the UGT gene family is separated between two families and four subfamilies but displays a different set of conjugating isoforms. Unlike humans, rat Ugt1a enzymes are encoded from the gene locus of chromosome 9q35, with the gene subfamilies denoted with lower case letters (Nagai et al., 1995). Within the rat Ugt1a locus, Ugt1a1 is seen as a functional homolog to the human counterpart, but the additional Ugt1a isoforms diverge from their human counterparts with respect to location, sequence and substrate specificity. In conjunction with the active isoforms within the rat UGT1A locus, two pseudogenes encoding Ugt1a4 and Ugt1a9 have been discovered within the genome (Shelby et al., 2003). Despite these differences, rat models have long since been used for glucuronidation studies due to comparable metabolite generation capabilities compared to humans and the ability to perform cannulation studies for pharmacokinetic analyses. Furthermore, the rat also serves as a powerful tool for mimicking the human hyperbilirubinemic disease state through the Gunn rat model. The Gunn rat is devoid of functional Ugt1a enzymes due to a frameshift mutation on exon 2 and subsequently develops hyperbilirubinemia in addition to an increased sensitivity to xenobiotics

undergoing detoxification through glucuronidation (Chowdury et al., 1993). Unlike humans with Criglar-Najjar Syndrome, however, the rat has some bilirubin conjugation ability, making the Gunn rat mutation nonlethal. Recent work involving Gunn rats revolves around adenovirus mediated gene therapy to restore expression of UGT1A isoforms within the liver and gastrointestinal tract. Specifically, adenovirus gene therapy Gunn rat models have been more sensitive to gastrointestinal toxicity of irinotecan and mycophenolic acid due to increased biliary efflux and subsequent hydrolysis of glucuronide conjugates resulting in elevated exposure of of the GI tract to toxic aglycones (Miles et al., 2006; Tallman et al., 2007).

B.4. Detoxification and Toxicity associated with glucuronidation

Despite the role of UGTs in the detoxification and excretion of numerous endogenous and exogenous compounds, there has been evidence indicating glucuronide conjugates have toxicological implications. The link between UGTs and cancer has not yet been directly made, but mutations in UGT genomes have been observed in colorectal carcinoma (Guillemette, 2003; Tukey and Strassburg, 2000; Tukey and Strassburg, 2001). In addition, UGT activity has been shown to be highly polymorphic within the gastrointestinal tract, yet interindividual differences are small within the liver (Strassburg et al., 1999). One of the most prominent detoxification mechanisms prevalent in the UGT genome is the formation of bilirubin diacylglucuronide through UGT1A1 catalysis. In Gunn rats and humans stricken with Crigler-Najjar or Gilbert's Syndrome,

hyperbilirubinemia results from the buildup of lipophilic bilirubin that then can penetrate the blood brain barrier to result in encephalopathy, neural necrosis and death if untreated (Tukey and Strassburg, 2000). Though a vast majority glucuronide conjugates are pharmacologically inactive, certain compounds such as morphine-6-glucuronide display increased pharmacological activity (Bailey and Dickinson, 2003; Ritter, 2000). In addition to active glucuronides, an area of active research and continued debate revolves around acyl glucuronide catalysis and toxicity (Shipkova et al., 2003). Acyl glucuronide conjugates occur through conjugation of carboxylic acid moiety within the affected compound, resulting in a product whose link to adverse drug reactions and adduct formation has been implicated but yet to be established (Bailey and Dickinson, 2003; Faed, 1984; Shipkova et al., 2003).

C. Acyl Glucuronides

C.1. Background

Acyl glucuronides are controversial in drug toxicology due to their ability to form protein adducts with liver and plasma proteins and may have a role in adverse drug reactions (ADRs) (Bailey and Dickinson, 2003). After arising from a carboxylate moiety within a substrate, acyl glucuronides have a series of potential fates within the body that may either predispose the affected organism to toxicity or result in harmless excretion outside the body. One of these fates includes the acyl glucuronide being produced through a UGT catalyzed reaction followed by excretion from the liver into the bloodstream or via biliary tract into the intestine. Acyl glucuronides make excellent substrates for transporters within

the hepatocyte, with the most active transporters in acyl glucuronide excretion including the basolateral organic anion transporters (OAT) transporters or the canalicular MRP2 transporter (Bailey and Dickinson, 2003).

Besides excretion, acyl glucuronides can be subject to hydrolysis through the actions of esterases within the liver, blood or gastrointestinal tract. This aspect is unique to acyl glucuronides compared other glucuronide conjugates because of the carboxylate moiety binding to the glucuronide conjugate resulting in ester linkage (Faed, 1984). Unlike other glucuronides which are resistant to hydrolysis by esterase enzymes, acyl glucuronides may be cleaved back to the parent compound through the actions of esterases which are found throughout the body. The cleavage of acyl glucuronides can increase a patient's exposure to the parent drug, and subsequently its efficacy, through enterohepatic cycling or even engage the compound in systemic "futile cycling" through continuous cleavage and conjugation within the body (Bailey and Dickinson, 2003). This is important for toxicological consequences if glucuronidation of a carboxylate moiety is the primary means of elimination and detoxification for a compound. The parent compound may exhibit cellular toxicity due to increased exposure throughout the body because of esterase cleavage of the acyl glucuronide.

C.2. Acyl Migration of Ester Glucuronides

Another possible fate of acyl glucuronide metabolites *in vivo* concerns acyl migration. Acyl migration of glucuronide conjugates involves the initial conversion of O-β-1 acyl glucuronide into either an O-β-2 or an O-α-2 isomeric conjugate via intramolecular trans-esterification (Faed, 1984). This reaction is

the result of a nucleophilic attack on an adjacent carbon by the hydroxyl group of the glucuronide conjugate. Additional isomeric conjugates O-β-3, O-β-4, O-α-3, O-α-4 can be created during this process and each reaction beyond the initial O-β-1 conjugate is reversible (Bailey and Dickinson, 2003; Faed, 1984). Some studies have shown that back conversion into the initial biologically synthesized β-1 acyl glucuronide metabolite is possible at low levels within *in vitro* systems but this reaction is rare and not significant in *in vivo* biological systems (Bailey and Dickinson, 2003). While the isomeric conjugates are similar to the O-β-1 acyl glucuronide, they are unique because biological systems are unable to create them as primary products and they are resistant to β-glucuronidase enzymes present within the gastrointestinal tract and liver. Even though many isomeric conjugates exhibit no apparent biological consequences, the ability of these isomers to form covalent bonds with cellular proteins and macromolecules may have toxicological implications resulting in ADRs seen in some compounds containing carboxylate moeities.

C.3. Potential Toxicity

Once the parent acyl glucuronide conjugate or any of its isomeric conjugates form protein adducts *in vivo,* a number of consequences are possible. One of the most contentious debates is the fate of the acyl glucuronide-protein adducts within the biological system (Bailey and Dickinson, 2003; Shipkova et al., 2003). Protein adducts have been demonstrated frequently with albumin, plasma and liver *in vitro* systems, yet within each system, few direct links to toxicity have been made (Bailey and Dickinson, 2003; Shipkova et al., 2003). Many

compounds including NSAIDS rapidly form acyl glucuronides and subsequent protein adducts with plasma proteins and albumin, yet these drugs are generally regarded as safe and some such as ibuprofen are available without a prescription (Bailey and Dickinson, 2003).

Drug-protein adducts formed from acyl glucuronides have been shown to affect cellular function of certain proteins within rats, including disruption of tubulin and dipeptidyl-peptidase IV function by diclofenac and zomepirac acyl glucuronides (Bailey et al., 1998; Bailey and Dickinson, 2003). In addition to drug-protein adducts, acyl glucuronides have also been implicated in hypersensitivity and idiosyncratic adverse drug reactions with mixed results (Shipkova et al., 2003). Numerous acyl glucuronide forming compounds including suprofen, zomepirac and ibufenac have been withdrawn from the market because of hepatoxicity, yet compared to the large number of patients administered these compounds, the number of adverse reactions remains small and unpredictable. Moreover, no direct link between toxicity and acyl glucuronide exposure has been reported in animals and humans (Bailey and Dickinson, 2003).

Mycophenolic acid is an immunosuppressant for prophylaxis in organ and solid graft transplant patients that forms both a phenolic and acyl glucuronide in humans (Young and Sollinger, 1994). While the phenolic glucuronide is inactive, *in vitro* testing of the acyl glucuronide conjugate exhibited a greater efficacy for inhibition of leukocyte proliferation than the unconjugated parent drug (Shipkova et al., 2001). Along with this evidence, cellular protein adducts have been found

to form as a result of the acyl glucuronide, which has led some scientists to believe that this metabolite is the source of delayed-onset diarrhea observed within patients on extended therapy along with additional side effects including leucopenia (Shipkova et al., 2004). However, the evidence basing MPA toxicity on acyl glucuronide formation (acMPAG) remains inconsistent, not only due to the lack of conclusive data from *in vitro* testing, but also due to the fact that negative clinical outcomes of MPA have not been directly linked to exposure of acMPAG (Kypers et al., 2003).

D. Quantitative Proteomics

D.1. Background

While traditional methods of quantitative proteomics involved 2D-gel electrophoresis or immunoassays for relative quantification, the field began to take off with the advent of refined electrospray ionization (ESI) and tandem mass spectrometry (MS/MS) techniques in the late 1980s (Whitehouse et al., 1985; Cañas et al., 2006). Even though immunoassays including ELISA and Western Blots have been used for clinical biomarker detection for years, they have a number of shortcomings. Many antibody-based assays can vary significantly between laboratories and are subject to cross-reactivity along with the hook effect (antibody saturation resulting in declining signal) that compromises the linear range of the assays (Hoofnagle and Wener, 2009). The refinements in both ionization and mass spectrometry have enabled the development of methods involving isotope dilution mass spectrometry applied for the quantification of intact proteins and peptides. Coupled with the newer stable isotope internal

standards available today with an increasing assortment of mass spectrometer platforms and LC configurations, the field of quantitative proteomics through tandem mass spectrometry continues its evolvement as a primary research initiative for investigators interested in biomarker discovery, enzyme quantification, cancer research and global proteomics (Gstaiger and Aebersold, 2009).

While numerous methods of stable isotope labeling are offered today, one of the more reliable and cost effective methods involves N^{15} and C^{13} isotopes of peptide side chains such as the AQUA™ method (Gerber et al., 2003). In addition to the AQUA™ method, other methods that have been developed within this decade include stable isotope labeling with amino acids in cell culture (SILAC), isotope coated affinity tags (ICAT), isobaric tagging for relative and absolute quantification (iTRAQ) reagents. The most recent development by SJ Gaskell's lab involves stable isotopes expressed and grown in *E. Coli* cell culture to form quality concatamer internal standards (QConCAT) (Beynon et al., 2005). As opposed to the SILAC and QConCAT methodology involving stable isotopes grown in cell culture, the ICAT and iTRAQ methods involve targeting the entire protein through either cysteine labeling (ICAT) or N-terminal labeling (iTRAQ) (Cañas B 2006). One problem with the ICAT and SILAC strategy is that each of these methods are not suitable for wide-scale quantification due to the limited number of peptides containing cysteine residues and the difficulty in purifying proteins of interest from SILAC cultures, respectively. While iTRAQ and QConCAT have been applied in absolute quantification, iTRAQ peptides have

been beset by problems due to lack of specificity compared to true MS/MS and QConCAT peptides are no longer commercially produced for proteomic applications (Wu et al., 2006).

D.2. Biological Applications

Recently, a number of new methodologies have been used for quantifying biological enzymes in complex matrices. Biological enzymes such as the cytochrome P450 family (CYP450s), hUGTs, cancer biomarkers and membrane transporters have been quantified across a number of different matrices (Barnidge et al., 2004; Jenkins et al., 2006; Kamiie et al., 2008; Li et al., 2008; Wang et al., 2008). The AQUA™ method was selected for this research project because the synthetic peptides are readily available for purchase through numerous vendors and their accuracy in quantification of specific enzymes and proteins has been demonstrated through previous experiments (Fallon et al, 2008; Gerber et al., 2003). Two AQUA™ peptides are usually selected per protein through a specific series of selection criteria, including the elimination of cysteine, methionine and tryptophan due to ionization difficulties, size limited to 8-15 residues and no aspartic acid/glycine N-terminus to prevent cyclization. These selection rules, coupled with the understanding that each peptide must be unique to the targeted protein, two AQUA™ peptides are chosen for quantification of both human and rat UGT enzymes, whereas three peptides are used for each rat membrane transporter.

E. Mycophenolic Acid

E.1. Clinical Uses

Mycophenolic acid (MPA) is an immunosuppressant designed for prophylaxis in renal and hepatic transplant patients or as treatment for autoimmune disorders such as systemic lupus erythmatosus (Bullingham et al., 1996; Young and Sollinger, 1994; Stern et al., 2007). Currently MPA is available in either the prodrug form mycophenolate mofetil (CellCept©, Novartis) or as an enteric coated sodium salt (Myfortic©, Roche). The immunosuppressive action of MPA is obtained through the inhibition of the ionsine monophosphate dehydrogenase type II (IMPDH) enzyme which converts xanthine monophosphate (XMP) into guanine monophosphate (GMP) in the *de novo* purine biosynthesis pathway (Young and Sollinger, 1994). This particular pathway is important for lymphocyte proliferation because lymphocytes are unable to undergo the secondary salvage pathway for purine biosynthesis and IMPDH type II is unique to both B and T lymphocytes (Carr et al., 1993; Young and Sollinger, 1994). MPA is coadministered as part of immunosuppressive therapy for transplant patients with cyclosporin A, tacrolimus or sirolimus combined with corticosteroids for maximum efficacy. MPA is extensively protein bound (97%) and metabolized almost exclusively by UGTs into either MPA-7-O-glucuronide (MPAG) or MPA-acyl-glucuronide (acMPAG) and eliminated through biliary or urinary excretion (Table 1.2, Bullinghman et al., 1996; Bullingham et al., 1998; Hofmann La Roche; Parker et al., 1996). While it is generally regarded as a safe drug and is well tolerated by patients, side effects of MPA include

leucopenia and an elevated infection rate. The most severe effect exhibited in patients is delayed-onset diarrhea seen in 20-30% of patients (Davies et al., 2007; Hebert et al., 1999; McDiarmid, 1996; Wang et al., 2004).

E.2. Toxicity

In humans, the toxicological source of MPA is a conflicted argument revolving around the fate of the acyl glucuronide within the bloodstream and intestinal tract. MPA metabolized to its phenolic glucuronide by UGT1A1, UGT1A8 and UGT1A9 within the liver followed by excretion into the bloodstream or into the biliary tract by MRP2 and BCRP (Mackenzie, 2000; Miura et al., 2008). Peak plasma concentrations of MPA, MPAG and acMPAG are observed within forty five to ninety minutes of oral dosing of MMF (Bullingham et al., 1996; Bullingham et al., 1998; Hofmann La Roche). While UGT1A1, UGT1A8, UGT1A9 and UGT1A10 are the source of the phenolic glucuronide in humans, acyl glucuronidation of MPA exclusively involves UGT2B7 (Mackenzie, 2000; Saitoh et al., 2006). After excretion into the biliary tract or bloodstream, acMPAG has the ability to form covalent bonds with plasma proteins and cellular macromolecules, creating protein adducts (Shipkova et al., 2003). More troubling is that *in vitro* cell systems have shown that acMPAG incubation results in significantly elevated cytokine levels, possibly resulting in immunogenic reactions (Wieland et al., 2000). However, this evidence has yet to be shown in *in vivo* experiments which may indicate that acMPAG is excreted out of the system before cytokine elevation occurs.

A further complication of MPA metabolism and excretion involves polymorphisms in UGT enzymes, MRP2 and BCRP transcripts that result in decreased MPA clearance that is possibly be associated with intestinal toxicity in transplant patients (Djedi et al., 2007; Miura et al., 2008; Shipkova et al., 2005). Unlike its glucuronide metabolites, MPA has also shown the ability to penetrate the enterocyte membranes within the intestinal tract and be a source of direct cellular toxicity (Shipkova et al., 2005). While attempts have been made to link acMPAG exposure levels with toxicity, recent studies have not been able to correlate elevated acMPAG exposure with GI toxicity (Kuypers et al., 2003; Shaw et al., 1996; Staatz et al., 2007). This indicates that within humans, glucuronidation serves as a protective mechanism although the potential immunogenic properties of acMPAG should be monitored.

E.3. Rat and Human MPA Metabolism

The fate of MPA is similar between rats and humans despite the different UGT isoforms involved between the two species. In rats, MPA is glucuronidated at the phenol ring by Ugt1a1, Ugt1a6 and Ugt1a7 and at the carboxylate functional group by rUgt2b7 to form acMPAG followed by excretion into the biliary tract by Mrp2 (Koboyashi et al., 2004; Miles et al., 2006; Takekuma et al., 2007). Compared to humans, a significantly elevated amount or fraction of the dose of MPAG is excreted into the biliary tract as opposed to the bloodstream (Takekuma et al., 2007). Thus, the ratio between MPAG and MPA exposure levels is different between species.

Glucuronidation rates of MPA in *in vitro* systems have been shown to vary up to ten fold between species, and also genders of rats but differences in toxicity have not been observed across rat strains (Miles et al., 2005; Miles et al., 2006; Stern et al., 2007). MPAG formation rates have been shown to be higher in male Sprague Dawley rats and male rats have also been more resistant to MPA induced GI toxicity than females (Stern et al., 2007). Ugt1a deficient Gunn rats and AV_{Ugt} treated Gunn rats whose rUgt expression is restored within the liver, exhibit lacrimation, malaise and diarrhea after MPA administration (Miles et al., 2006). While Gunn rats and AV_{Ugt} treated Gunn rats exhibit no intestinal Ugt1a activity, Wistar and male Sprague Dawley rats expressing high levels of rUgt1a activity are resistant to MPA induced GI toxicity (Miles et al., 2006; Stern et al., 2007). Furthermore, MPA administration to AV_{Ugt} treated Gunn rats that lacked intestinal Ugt activity resulted in an elevated level of intestinal toxicity when compared to control Wistar rats which were resistant to MPA induced GI toxicity (Miles et al., 2006). This indicates that intestinal glucuronidation activity may help prevent GI toxicity due to decreased enterocyte MPA exposure which could be due to either increased metabolism or enhanced efflux. As in humans, glucuronidation activity in rats is likely to be the primary source of detoxification of MPA and a key factor in the prevention of MPA related toxicological effects.

F. Rationale for the Proposed Project

Glucuronidation has repeatedly been demonstrated as a determining factor of toxicity and disposition of numerous endogenous and exogenous

compounds (Bock and Lilebaum, 1994; Tukey and Strassburg, 2000). However, the fate of some acyl glucuronide metabolites within body systems remains a contested debate. MPA represents an excellent model compound for study due to its ability to form the nontoxic and inactive MPAG, in addition to the labile and potentially reactive acMPAG metabolite, while remaining a well-tolerated treatment for transplant patients. While many papers have been published establishing assays to quantify proteins of interest within *in vivo* systems there have been no attempts to link enzyme expression levels assayed using quantitative proteomics via LC-MS/MS with their biological significance. The methods developed through this proposed project, coupled with pharmacokinetic and acMPAG stability studies examine the relationship between MPA disposition and altered Ugt and transporter levels within the rat. The overall hypothesis of this dissertation project is that variable glucuronidation formation and efflux within the liver and gastrointestinal tract results in differential MPAG formation rates and thus modulates MPA toxicity. To evaluate the potential effect of glucuronidation on MPA toxicity, the stability, reactivity and disposition of the MPA glucuronide metabolites will be examined in the following aims:

AIM 1: Differences in toxicity of mycophenolic acid will be examined through evaluation of glucuronide disposition. There are conflicting reports on acMPAG stability and reactivity. These experiments on acMPAG stability and reactivity will help determine if acMPAG is a reactive metabolite that could be a factor in MPA GI toxicity. In addition, a series of pharmacokinetic studies

evaluating MPA, acMPAG and MPAG disposition will be conducted for future studies comparing enzyme expression with metabolite disposition:

a. A method to assay the acyl glucuronide metabolite of mycophenolic acid will be established and used to evaluate the stability of acMPAG *in vitro* and measure it within biological matrices.

b. Acyl glucuronide reactivity will be examined through covalent binding studies

c. MPAG and acMPAG will be administered intravenously to rats to examine the fate of the glucuronides and to determine hepatic uptake from the systemic circulation.

AIM 2: The differences in UGT enzyme expression levels will be quantified *in vivo* across human tissues involved with drug disposition. To properly evaluate metabolite disposition with enzyme and transporter expression, methods to quantify UGT enzymes will be established. It is important to first evaluate and validate our quantitative proteomic methods against established assays for hUGT quantification in the following experiments:

a. A quantitative proteomic LC-MS/MS method to measure hUGT1A1 and hUGT1A6 levels within human liver and intestine will be established to validate the proposed methodology.

b. The quantitative proteomic method will then be optimized to quantify enzyme levels of the hUGT1A gene family using nano-LC MS/MS instrumentation.

c. The expanded and optimized hUGT1A assay will be used to compare UGT enzyme expression levels in human liver, kidney and intestinal microsomes.

AIM 3: The association between varying rUGT and transporter expression levels and the disposition of MPA will be determined. Once the utility and accuracy of hUGT quantitative assays have been evaluated, the effect of altered enzyme and transporter expression on MPA metabolism and disposition will be examined. Experiments examining the relationship between rUgt and membrane transporter expression with the metabolism, disposition and toxicity of MPA are outlined below:

a. An LC-MS/MS quantitative proteomic method for quantifying rUGT1A1, rUGT1A6 and rUGT1A7 within the liver and gastrointestinal tract will be established.

b. Biliary excretion of MPA and its glucuronides administered to bile cannulated Wistar rats will be examined with respect to rUGT expression levels and *in vitro* glucuronidation rates.

c. Ugt 1a1, 1a6, 1a7, Mrp2, Mrp3 and Bcrp expression levels will be compared between Wistar, AV_{Ugt} and TR- rats to examine the effect of the altered Ugt or Mrp2 protein on Bcrp, Mrp3 and UGT enzyme levels and MPA disposition.

Figure 1.1 Structure of Mycophenolic Acid and its two primary glucuronide metabolites formed through the action of rUgts (Miles et al., 2005; Picard et al., 2005; Young and Sollinger, 1994)

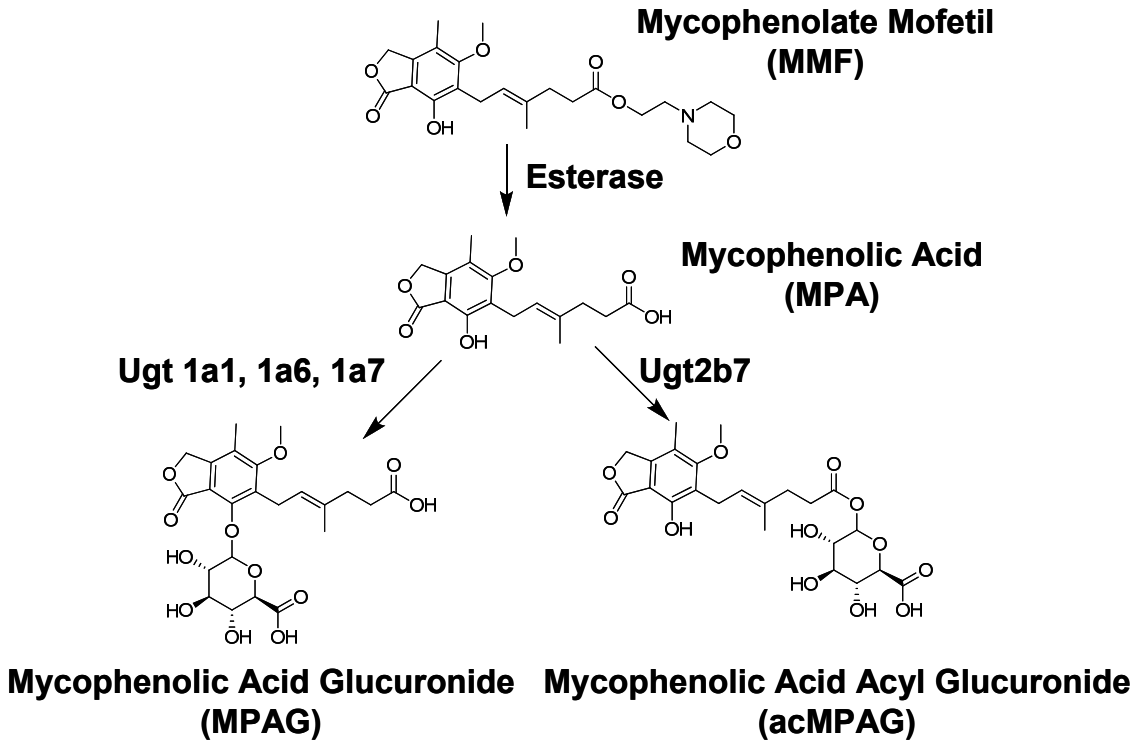

Table 1.1 Localization of UGT1A mRNA in human and rat tissues with isoforms in **bold** responsible for MPA glucuronidation

Enzyme	Species	Localization
Ugt1a1	Rat	Liver, kidney, intestinal tract, brain, lung, testis
Ugt1a2	Rat	Small intestine, large intestine, colon, stomach
Ugt1a3	Rat	Small intestine, large intestine
Ugt1a5	Rat	Liver
Ugt1a6	Rat	Large and small intestine, kidney, stomach, liver, lung, brain, esophagus
Ugt1a7	Rat	Small and large intestine, kidney, lung, ovary, spleen, stomach
Ugt1a8	Rat	Liver and kidney
UGT1A1	Human	Liver, biliary tract, colon, duodenum, jejunum, ileum
UGT1A3	Human	Liver, biliary tract, colon, gastric lining, small intestine
UGT1A4	Human	Liver, biliary tract, colon and small intestine
UGT1A6	Human	Liver, biliary tract, stomach, colon, small intestine
UGT1A7	Human	Stomach, esophagus
UGT1A8	Human	Colon, esophagus
UGT1A9	Human	Liver, colon, esophagus
UGT1A10	Human	Biliary, gastric lining, colon, esophagus, small intestine

*Isoforms in **bold** indicate capability for MPA glucuronidation, table above includes only functional encoded proteins within UGT1A locus. List does not include the isoforms rUgt1a4, rUgt1a9, UGT1A2, UGT1A11, UGT1A12 and UGT1A13 which encode nonfunctional pseudogenes (Mackenzie, 2000; Miles et al., 2006; Miles et al., 2006; Shelby et al., 2003; Strassburg et al., 1997; Strassburg et al., 1998; Strassburg et al., 1999; Strassburg et al., 2000).

Table 1.2 Estimates of MPA and MPAG pharmacokinetic parameters following a single oral dose of 1.5 g of MMF in healthy human volunteers (n=6) (Bullingham et al., 1996; Bullingham et al., 1998; Hofmann-La Roche; Parker et al., 1996). Data are presented as mean values +/- SD.

Pharmacokinetic Parameter	MPA	MPAG
Cmax (mg/L)	34.0±7.1	43.1±6.8
Tmax (h)	1.0±0.1	1.8±0.5
Terminal $t_{1/2}$	17.9±6.5	16.1±5.2
$AUC_{0-\infty}$ (mg/L*h)	101.1±23.4	480.1±105.2
CL_{Renal} (mL/min)	1.2 (0-4.6)	33.7 (7.4)
Exposure due to EHC	40%	N/A
Therapeutic Range	1-60 mg/L	N/A
%Dose recovered in urine	0.6%	96.3%
%Dose recovered in feces	0.5%	5.5%
%Dose excreted into bile	0.1%	18.0%

* Cmax (Maxicum concentration), Tmax (Time to reach maximum concentration), AUC (Area under the curve)

G. References

Allison AC and Eugui EM. Preferential Suppression of Lymphocyte Proliferation by Mycophenolic Acid and Predicted Long Term Effects of Mycophenoliate Mofetil in Transplantation. *Transpl Proc.* **1994**, 26(6), 3205-3210.

Auyeung DJ, Kessler FK and Ritter JK. Differential regulation of alternate UDP-glucuronosyltransferase 1A6 gene promoters by hepatic nuclear factor 1. *Toxicol Appl Pharm.* **2003,** 191, 156-166.

Barbier O and Bellanger A. The cynomolgus monkey (Macaca fascicularis) is the best animal model for the study of steroid glucuronidation. *J Steroid Biochem Mol Biol.* **2003,** 85(2-5), 235-45.

Barnidge DR, Goodmanson MK, Klee GG, Muddiman DC. Absolute quantification of the model biomarker prostate-specific antigen in serum by LC-Ms/MS using protein cleavage and isotope dilution mass spectrometry. *J Prot Res*. **2004,** 3(3), 644-52.

Barr JR, Maggio VL, Patterson DG Jr, Cooper GR, Henderson LO, Turner WE, Smith SJ, Hannon WH, Needham LL, Sampson EJ. Isotope dilution--mass spectrometric quantification of specific proteins: model application with apolipoprotein A-I. *Clin Chem.* **1996,** 42(10):1676-82.

Bailey MJ, Worrall S, Jersey J and Dickinson RG. Zomepirac acyl glucuronide covalently modifies tubulin in vitro and in vivo and inhibits its assembly in an in vitro system. *Chem Biol Interact.* **1998,** 115, 153-166.

Beynon RJ, Doherty MK, Pratt JM, Gaskell SJ. Multiplexed absolute quantification in proteomics using artificial QCAT proteins of concatenated signature peptides. *Nat Meth.* **2005,** 2(8), 587-9.

Beynon RJ, Pratt JM. Metabolic labeling of proteins for proteomics. *Mol Cell Prot*. **2005,** 4(7), 857-72.

Bier DM. The use of stable isotopes in metabolic investigation. *Baillieres Clinical Endocrinology and Metabolism*. **1987,** 1(4), 817-36.

Bock KW and Lilienblum W. Roles of Uridine Diphosphate Glucuronosyltransferases in Chemical Carcinogenesis, in *Conjugation-Deconjugation Reactions in Drug Metabolism and Toxicity* (Kauffamn F ed) , Springer-Verlag, Berlin. **1994,** 391-428.

Bock KW and Kohle C. Topological aspects of oligomeric UDP-glucuronosyltransferases in endoplasmic reticulum membranes: Advances and open questions. *Biochem Pharm* **2009,** 77, 1458-1465.

Boelsterli UA. Diclofenac-induced liver injury: a paradigm of idiosyncratic drug toxicity. *Toxicol Appl Pharmacol.* **1998,** 192, 307-322.

Bullingham RE, Nicholls AJ, Kamm BR. Clinical pharmacokinetics of mycophenolate mofetil. *Clin Pharmacokinet.* **1998,** 34(6), 429-55.

Bullingham R, Monroe S, Nicholls A, Hale M. Pharmacokinetics and bioavailability of mycophenolate mofetil in healthy subjects after single-dose oral and intravenous administration. *J Clin Pharmacol.* **1996,** (4), 315-24.

Burchell B, Ebner T, Baird S, Bin Senafi S, Clarke D, Brierley C, Sutherland L. Use of cloned and expressed human liver UDP-glucuronosyltransferases for analysis of drug glucuronide formation and assessment of drug toxicity. *Environ Health Perspect*. **1994,** 102 Suppl 9, 19-23.

Cañas B, López-Ferrer D, Ramos-Fernández A, Camafeita E, Calvo E. Mass spectrometry technologies for proteomics. *Brief Funct Genomic Proteomic.* **2006,** 4(4), 295-320.

Carr SF, Papp E, Wu JC and Natsumeda Y. Characterization of Human Type I and Type II IMP Dehydrogenases. *J. Biol Chem.* **1998,** 268(36), 27286-272890.

Cattaneo D, Perico N and Remuzzi G. From Pharmacokinetics to Pharmacogenomics: A New Approach to Tailor Immunosuppressive Therapy. *Am J Transpl*. **2004,** 4, 299-310.

Chowdhury JR, Kondapalli R and Chowdhury NR. Gunn Rat: a model for inherited deficiency of bilirubin glucuronidation. *Adv vet sci comp med.* **1993,** 37, 149-73.

Clutterbuck PW and Raistrick H. The Molecular Constitution of the Metabolic Products of *Penicillium Brevi-Compactum* Dierckx and Related Species. *Studies in the Biochemistry of Microorganisms.* **1933.**

Cohen MB, Maybaum J and Sadee W. Guanine Nucleotide Depletion and Toxicity in Mouse T Lymphoma (S-49) Cells. *J Biol Chem.* **1981,** 256(16), 8713-8717.

Coleman M. Drug Biotransformation Systems: Orgins and Aims in *Human Drug Metabolism: An Introduction.* Wiley, London. **2005,** 13-19, 23-56, 101-157.

Cooper GS, Makris SL, Nietert PJ, Jinot J. Evidence of autoimmune-related effects of trichloroethylene exposure from studies in mice and humans. *Environ Health Perspect*. **2009,** 117(5), 696-702.

Court MH. Isoform-Selective Probe Substrates for *in Vitro* Studies of Human UDP-Glucuronosyltranferases. *Meth Enzymology.* **2005,** 400,104-116.

Cussoneau X, Bolon-Lager M, Prunet-Spano C, Bastien O and Boulieu R. Relationship between MPA free fraction and free MPAG concentrations in heart transplant recipients based on simultaneous HPLC quantification of the target compounds in human plasma. *J Chrom B.* **2007.**

Dass C, Fridland GH, Tinsley PW, Killmar JT, Desiderio DM. Characterization of beta-endorphin in human pituitary by fast atom bombardment mass spectrometry of trypsin-generated fragments. *Intl J Pep Prot Res*. **1989,** 34(2), 81-7.

Dickinson RG and Bailey MJ. Acyl Glucuronide reactivity in perspective: biological consequences. *Chem Biol Interact.* **2003,**145, 117-137.

Dickinson RG and King AR. Studies on the reactivity of acyl glucuronides----v. glucuronide-derived covalent binding of diflunisal to bladder tissue of rats and its modulation by urinary pH and β-glucuronidase. *Biochem Pharm.* **1993,** 46(7), 1175-1182.

Djebi N, Picard N, Rerolle JP, Meur YL and Marquet P. Influence of the UGT2B7 promoter region and exon 2 polymorphisms and comedications on Acyl-MPAG production *in vitro* and in adult renal transplant patients. *Pharmacogen Gen*. **2007,** 17, 321-330.

Domon B, Aebersold R. Mass spectrometry and protein analysis. *Science.* **2006,** 312(5771), 212-7.

Faed EM. Properties of acyl glucuronides: implications for studies of the pharmacokinetics and metabolism of acidic drugs. *Drug Metab Rev***. 1984,** 15, 1213-1249.

Fisher MB, VandenBranden M, Findlay K, Burchell B, Thummel KE, Hall SD and Wrighton SA. Tissue distribution and interindividual variation in human UDP-Glucuronosyltransferase activity: relationship between UGT1A1 promoter genotype and variability in a liver bank. *Pharmacogenetics*. **2000,** 10, 727-739.

Gerber SA, Rush J, Stemman O, Kirschner MW, Gygi SP. Absolute quantification of proteins and phosphoproteins from cell lysates by tandem MS. *Proc Natl Acad Sci USA*. **2003,** 100(12), 6940-5.

Gonazalez-Roncero FM, Govantes MAG, Chaves VC, Palomo PP and Serra MB. Influence of Renal Insufficiency on Pharmacokinetics of ACYL-Glucuronide Metabolite of Mycophenolic Acid in Renal Transplant Patients. *Transpl Proc.* **2007,** 39, 2176-2178.

Görg A, Weiss W, Dunn MJ. Current two-dimensional electrophoresis technology for proteomics. *Proteomics.* **2004,** 4(12), 3665-85.

Gregory PA, Lewinsky RH, Gardner-Stephen DA and Mackenzie PI. Regulation of UDP glucuronosyltransferases in the gastrointestinal tract. *Toxicol Appl Pharmacol.* **2004,** 199, 354-363.

Gstaiger M, Aebersold R. Applying mass spectrometry-based proteomics to genetics, genomics and network biology. *Nat Rev Genet.* **2009,** 10(9), 617-27.

Guillemette C. Pharmacogenomics of human UDP-glucuronosyltransferase enzymes. *Pharmacogenomics J.* **2003,** 3(3), 136-58.

Hancock WS, Wu SL, Shieh P. The challenges of developing a sound proteomics strategy. *Proteomics*. **2002,** 2(4), 352-9.

Hebert MF, Ascher NL, Lake JR, Emond J, Nikolai B, Linna TJ and Roberts JP. Four-year follow-up of mycophenolate mofetil for graft rescue in liver allograft recipients. *Transplantation.* **1999**, 67, 707–712.

Hesselink DA, van Hest R, Mathot RAA, Bonthuis F, Weimer W, Bruin RWF and Gelder T. Cyclosporine Interacts with Mycophenolic Acid by Inhibiting the Multidrug Resistance-Associated Protein 2. *Am J of Transpl.* **2005,** 5, 987-994.

Hofmann-La Roche, Basle, Switzerland, data on file

Hoofnagle AN, Wener MH. The fundamental flaws of immunoassays and potential solutions using tandem mass spectrometry. *J Immunol Meth.* **2009,** 347(1-2), 3-11.

Ionescu C and Caira MR. Drug Metabolism in Context and Pathways of Biotransformation: Phase II Reactions, in *Drug Metabolism Current Concepts*, Springer, Dordrecht, The Netherlands. **2005,** 1-37, 129-139.

Jaggi R, Addison RS, King AR, Suthers BD and Dickinson RG. Conjugation of Desmethylnaproxen in the rat-A novel acyl glucuronide-sulfate diconjugate as a major biliary metabolite. *Drug Metab Dispos.* **2002,** 30:161-166.

Javitt NB. Ethereal and acyl glucuronide formation in the homozygous Gunn rat. *Am J of Physiol.* **1966,** 211(2), 424-8.

Jenkins RE, Kitteringham NR, Hunter CL, Webb S, Hunt TJ, Elsby R, Watson RB, Williams D, Pennington SR, Park BK. Relative and absolute quantitative expression profiling of cytochromes P450 using isotope-coded affinity tags. *Proteomics.* **2006,** 6(6),1934-47.

Kamiie J, Ohtsuki S, Iwase R, Ohmine K, Katsukura Y, Yanai K, Sekine Y, Uchida Y, Ito S, Terasaki T. Quantitative atlas of membrane transporter proteins: development and application of a highly sensitive simultaneous LC/MS/MS method combined with novel in-silico peptide selection criteria. *Pharm Res.* **2008,** 25(6),1469-83.

King AR and Dickinson RG. The Utility of the Bile-Exteriorized Rat as a Source of Reactive Acyl Glucuronides: Studies with Zomepirac. *J Pharm Toxicol Meth.* **1996,** 36, 131-136.

King CD, Green MD, Rios GR, Coffman BL, Owens IS, Bishop WP and Tephly TR. The Glucuronidation of Exogenous and Endogenous Compounds by Stably Expressed Rat and Human UDP-Glucuronosyltransferase 1.1. *Arc Biochem Biophys.* **1996,** 332(1), 92-100.

Kobayashi M, Saitoh H, Koboyashi M, Tadano K, Takahashi Y and Hirano T. Cyclosporin A, but not Tacrolimus, Inhibits the Biliary Excretion of Mycophenolic Acid Glucuronide Possibly Mediated by Multidrug Resistance-Associated Protein 2 in Rats. *J Pharm Exp Therap.* **2004,** 309 (3), 1029-1035.

Kuhn E, Wu J, Karl J, Liao H, Zolg W, Guild B. Quantification of C-reactive protein in the serum of patients with rheumatoid arthritis using multiple reaction monitoring mass spectrometry and 13C-labeled peptide standards. *Proteomics*. **2004,** 4(4),1175-86.

Kypers DRJ, Vanrenterghem Y, Squifflet JP, Mourad M, Abramowicz D, Oellerich M, Armstrong V, Shipkova M and Daems J. Twelve Month Evaluation of the Clinical Pharmacokinetics of Total and Free Mycophenolic Acid and Its Glucuronide Metabolites in Renal Allograft Recipients on Low Dose Tacrolimus in Combination with Mycophenolate Mofetil. *Ther Drug Monit.* **2003,** 25, 609-622.

Li N, Nemirovskiy OV, Zhang Y, Yuan H, Mo J, Ji C, Zhang B, Brayman TG, Lepsy C, Heath TG, Lai Y. Absolute quantification of multidrug resistance-associated protein 2 (MRP2/ABCC2) using liquid chromatography tandem mass spectrometry. *Anal Biochem.* **2008,** 380(2), 211-22.

Levesque E, Girard H, Journault K, Lepine J and Guillemette C. "Regulation of the UGT1A1 Bilirubin-Conjugating Pathway: Role of a new Splicing Event at the UGT1A Locus. *Hepatology.* **2007,** 128-138.

Luukkanen L, Mikkola J, Forsman T, Taavitsainen P, Taskinen J and Elovaara E. Glucuronidation of 1-Hydroxypyrene by Human Liver Microsomes and Human UDP-Glucuronosyltransferases UGT1A6, UGT1A7 and UGT1A9: Development of a High-Sensitivity Glucuronidation Assay for Human Tissue. *Drug Metab Dispos.* **2001,** 29, 1096-1101.

Mackenzie PI. Identification of uridine diphosphate glucuronosyltransferases involved in the metabolism and clearance of mycophenolic acid. *Ther Drug Monit.* **2000,** 22(1), 10-3.

Mackenzie PI, Owens IS, Burchell B, Bock KW, Bairoch A, Bélanger A, Fournel-Gigleux S, Green M, Hum DW, Iyanagi T, Lancet D, Louisot P, Magdalou J, Chowdhury JR, Ritter JK, Schachter H, Tephly TR, Tipton KF, Nebert DW. The UDP glycosyltransferase gene superfamily: recommended nomenclature update based on evolutionary divergence. *Pharmacogenetics.* **1997,** 7(4), 255-69.

Meech R and Mackenzie PI. UDP-Glucuronosyltransferase, the Role of the Amino Terminus in Dimerization. *J Biol Chem.* **1997,** 272(43), 26913-26917.

Meech R and Mackenzie PI. Structure and Function of Uridine Diphosphate Glucuronosyltransferases. *Clin Exp Pharm Phys.* **1997,** 24 (12), 907-915.

Melethil S and Conway WD. Urinary excretion of probenecid and its metabolites in humans as a function of dose. *J Pharm Sci.* **1976,** 65 (6), 861-865.

McDiarmid SV. Mycophenolate mofetil in liver transplantation. *Clin. Transplant.* **1996,** 10(1), 140-145

Miles KK, Kessler FK, Webb LJ, Smith PC and Ritter JK. Adenovirus-Mediated Gene Therapy to Restore Expression and Functionality of Multiple UDP-Glucuronosyltransferase 1A Enzymes in the Gunn Rat Liver. *J Pharmaco Exp Therap.* **2006,** 318, 1240-1247.

Miles KK, Stern ST, Smith PC, Kessler FK, Ali S and Ritter JK. An Investigation of Human and Rat Liver Microsomal Mycophenolic Acid Glucuronidation: Evidence for a Principle Role of UGT1A Enzymes and Species Differences in UGT1A Specificity. *Drug Metab Dispos.* **2005,** 33, 1513-1520.

Miners JO. The glucuronidation of mycophenolic acid by human liver, kidney and jejunum microsomes. *J Clin Pharm.* **2001,** 52, 605-609.

Miura M, Kagaya H, Satoh S, Inoue K, Saito M, Habuchi T, Suzuki T. Influence of Drug Transporters and UGT Polymorphisms on Pharmacokinetics of Phenolic glucuronide Metabolite of Mycophenolic Acid in Japanese Renal Transplant Recipients. *Ther Drug Monit.* **2008.**

Mizuma T, Benet LZ and Lin ET. Interaction of Human Serum Albumin with Furosemide Glucuronide: a Role of Albumin in Isomerization, Hydrolysis, Reversible Binding and Irreversible Binding of a 1-O-Acyl Glucuronide Metabolite. *Biopharm Drug Dispos.* **1999,** 20, 131-136.

Monaghan G, Clarke DJ, Povey S, See CG, Boxer M, Burchell B. Isolation of a human YAC contig encompassing a cluster of UGT2 genes and its regional localization to chromosome 4q13. *Genomics.* **1994,** 23(2), 496-9.

Naderer OJ, Dupuis RE, Heinzen EL, Wiwattanawongsa K, Johnson MW, Smith PC. The influence of norfloxacin and metronidazole on the disposition of mycophenolate mofetil. *J Clin Pharmacol.* **2005,** 45(2), 219-26.

Naesens M, Kuypers DRJ, Verbeke K and Vanrenterghen Y. Multidrug Resistance Protein 2 Genetic Polymorphisms Influence Mycophenolic Acid Exposure in Renal Allograft Recipients. *Transplantation*. **2006,** 82(8).

Nagai F, Satoh H, Mori S, Sato H, Koiwai O, Homma H, Matsui M. Mapping of rat bilirubin UDP-glucuronosyl-transferase gene (Ugt1a1) to chromosome region 9q35-->q36. *Cytogenet Cell Genet.* **1995,** 69(3-4),185-6.

Nagar S and Remmel RP. Uridine diphophoglucuronosyltransferase pharmacogenetics and cancer. *Oncogene.* **2006,** 25, 1659-1672.

Neerman MF, Boothe DM. A possible mechanism of gastrointestinal toxicity posed by mycophenolic acid. *Pharmacol Res*. **2003,** 47(6), 523-6.

O'Farrell PH. High resolution two-dimensional electrophoresis of proteins. *J Bioll Chem.* **1975,** 250(10), 4007-21.

Owens IS, Ritter JK. Gene structure at the human UGT1 locus creates diversity in isozyme structure, substrate specificity, and regulation. *Prog Nucleic Acid Res Mol Biol*. **1995,** 51, 305-38.

Paoluzzi L, Singh AS, Price DK, Danesi R, Mathijssen RHJ, Verweij J, Figg WD and Sparreboom A. Influence of Genetic Variants in UGT1A1 and UGT1A9 on the In Vivo Glucuronidation of SN-38. *J Clin Pharm.* **2004,** 44, 854-860.

Parker G, Bullingham R, Kamm B, Hale M. Pharmacokinetics of oral mycophenolate mofetil in volunteer subjects with varying degrees of hepatic oxidative impairment. *J Clin Pharmacol.* **1996,** 36(4), 332-44.

Picard N, Ratanasavanh D, Premaud A, Le Meur Y, and Marquet P. Identification of the UDP-glucuronosyltransferase isoforms involved in mycophenolic acid phase 2 metabolism. *Drug Metab Dispos.* **2005,** 33, 139-146

Ritter JK. Roles of glucuronidation and UDP-glucuronosyltransferases in xenobiotic bioactivation reactions. *Chem Biol Interact.* **2000,** 129(1-2), 171-93.

Ritter JK, Chen F, Sheen YY, Tran HM, Kimura S, Yeatman MT, Owens IS. A novel complex locus UGT1 encodes human bilirubin, phenol, and other UDP-

glucuronosyltransferase isozymes with identical carboxyl termini. *J Biol Chem*. **1992,** 267(5), 3257-61.

Ritter JK, Crawford JM, Owens IS. Cloning of two human liver bilirubin UDP-glucuronosyltransferase cDNAs with expression in COS-1 cells. *J Biol Chem*. **1991,** 266(2), 1043-7.

Ritter JK, Yeatman MT, Ferreira P, Owens IS. Identification of a genetic alteration in the code for bilirubin UDP-glucuronosyltransferase in the UGT1 gene complex of a Crigler-Najjar type I patient. *J Clin Invest.* **1992,** 90(1), 150-5.

Saitoh H, Kobayashi M, Oda M, Nakasato K, Kobayashi M and Tadano K. Characterization of Intestinal Absorption and Enterohepatic Circulation of Mycophenolic Acid and Its 7-O-Glucuronide in Rats. *Drug Metab Pharmacokinet.* **2006,** 21(5), 406-413.

Sallustio BC, Sabordo L, Evans AM and Nation RL. Hepatic Disposition of Electrophilic Acyl Glucuronide Conjugates. *Curr Drug Metab.* **2000,** 1, 163-180.

Sechi S, Oda Y. Quantitative proteomics using mass spectrometry. *Curr Op Chem Biol.* **2003,** 7(1), 70-7.

Senafi SB, Clarke DJ, Burchell B. Investigation of the substrate specificity of a cloned expressed human bilirubin UDP-glucuronosyltransferase: UDP-sugar specificity and involvement in steroid and xenobiotic glucuronidation. *Biochem J.* **1994,** 303(Pt 1), 233-40.

Shaw LM, Nowak I. Mycophenolic acid: measurement and relationship to pharmacologic effects. *Ther Drug Monit.* **1995,** 17(6), 685-9.

Shipkova M, Armstron VW, Scheneider T, Neidmann PD, Schutz E, Wieland E and Oellerich M. Stability of Mycophenolic Acid and Mycophenolic Acid Glucuronide in Human Plasma. *Clin Chem.* **1999,** 45(1).

Shipkova M, Armstrong VW, Oellerich M and Wieland E. Mycophenolate mofetil in organ transplantation: focus on metabolism, safety and tolerability. *Exp Op Drug Metab Tox.* **2005,** 1(3), 505-526.

Shipkova M, Armstrong VW, Weber L, Niedmann PD, Wieland E, Haley J, Tonshoff B and Oellerich M. Pharmacokinetics and Protein Adduct Formation of the Pharmacologically Active Acyl Glucuronide Metabolite of Mycophenolic Acid in Pediatric Renal Transplant Patients. *Ther Drug Monit.* **2004.**

Shipkova M, Armstrong VW, Oellerich M and Wieland E. Acyl Glucuronide Drug Metabolites: Toxicological and Analytical Implications. *Ther Drug Monit.* **2003,** 25, 1-16.

Shipkova M, Beck H, Voland A, Armstrong VW, Grone HJ, Oellerich M and Wieland E. Identification of protein targets for mycophenolic acid acyl glucuronide in rat liver and colon tissue. *Proteomics.* **2004,** 4, 2728-2738.

Shipkova M, Strassburg CP, Braun F, Streit F, Grone HJ, Armstrong VW, Tukey RH, Oellerich M and Wieland E. Glucuronide and glucoside conjugation of mycophenolic acid by human liver, kidney and intestinal microsomes. *Brit J Pharm.* **2001,** 132, 1027-1034.

Shipkova M, Wieland E, Schutz E, Wiese C, Niedmann PD, Oellerich M and Armstrong VW. The Acyl Glucuronide Metabolite of Mycophenolic Acid Inhibits the Proliferation of Human Mononuclear Leukocytes. *Transplantation Proceedings.* **2001,** 33, 1080-1081.

Sollinger H. "Enteric-Coated Mycophenolate Sodium: Therapeutic Equivalence to Mycophenolate Mofetil in De Novo Renal Transplant Patients." *Transplantation Proceedings.* 36 (suppl 2S), 517S-520S 2004.
Sollinger HW. From mice to man: the preclinical history of mycophenolate mofetil. *Clin Transpl.* **1996,** 10, 85-92.

Staatz CE, Tett SE. Clinical pharmacokinetics and pharmacodynamics of mycophenolate in solid organ transplant recipients. *Clin Pharmacokin.* **2007,** 46(1), 13-58.

Stern ST, Tallman MN, Miles KK, Ritter JK, Dupuis RE, Smith PC. Gender-related differences in mycophenolate mofetil-induced gastrointestinal toxicity in rats. *Drug Metab Dispos.* **2007,** 35(3), 449-54.

Strassburg CP, Manns MP, and Tukey RH. Expression of UDP-Glucuronosyltransferase 1A locus in the human colon. Identification and characterization of the novel extrahepatic UGT1A8. *J Biol Chem* **1998,** 273, 8719-8726.

Strassburg CP, Nguyen N, Manns MP, Tukey RH. UDP-glucuronosyltransferases in the human liver and colon. *Gastroenterology.* **1999,** 116(1), 149-160.

Strassburg CP, Oldhafer K, Manns MP and Tukey RH. Differential expression of the UGT1A locus in human liver, biliary and gastric tissue: identification of UGT1A7 and UGT1A10 transcripts in extrahepatic tissue. *Mol Pharmacol* **1997,** 52, 212-220.

Strassburg CP, Strassburg A, Nguyen N, Li Q, Manns MP and Tukey RH. Regulation and function of family 1 and family 2 UDP-glucuronosyltransferase

genes (UGT1A, UGT2B) in human oesophagus. *Biochem J* **1999,** 338(Pt 2), 489-498.

Strassburg CP, Vogel A, Kneip S, Tukey RH and Manns MP. Polymorphisms of the human UDP-glucuronosyltransferase (UGT) 1A7 gene in colorectal cancer. *Gut.* **2002,** 50, 581-856.

Sweeney MJ, Hoffman DH and Esterman MA. Metabolism and Biochemistry of Mycophenolic Acid. *Cancer Research.* **1972,** 32, 1803-1809.

Sweeney MJ, Gerzon K, Harris PN, Holmes RE, Poore GA and Williams RH. Experimental Antitumor Activity and Preclinical Toxicology of Mycophenolic Acid. *Cancer Research* **1972,** 32, 1795-1802.

Tallman MN, Miles KK, Kessler FK, Nielsen JN, Tian X, Ritter JK, Smith PC. The contribution of intestinal UDP-glucuronosyltransferases in modulating 7-ethyl-10-hydroxy-camptothecin (SN-38)-induced gastrointestinal toxicity in rats. *J Pharmacol Exp Ther*. **2007,** 320(1), 29-37.

Tang W. The Metabolism of Diclofenac- Enzymology and Toxicology Perspectives. *Curr Drug Metab.* **2003,** 4(1), 319-329.

Takekuma Y, Kakiuchi H, Yamazaki K, Miyauchi S, Kikukawa T, Kamo N Ganapathy V and Sugawara M. Difference between Pharmacokinetics of Mycophenolic acid (MPA) in Rats and that in Humans is caused by Different affinities of MRP2 in glucuronized form. *J Pharm Pharmaceut Sci.* **2007,** 10(1), 71-85.

Tukey RH and Strassburg CP. Genetic Mobility of the Human UDP-Glucuronosyltransferases and Regulation in the Gastrointestinal Tract. *Mol Pharmacol.* **2001,** 59, 405-414.

Tukey RH and Strassburg CP. Human UDP-Glucuronosyltransferases: Metabolism, Expression and Disease. *Ann Rev of Pharmacol and Tox.* **2000,** 40, 581-616.

UDP Glucuronosyltransferase Homepage. Department of Clinical Pharmacology, Flinders University. <http://som.flinders.edu.au/FUSA/ClinPharm/UGT/>

Wang M and Dickinson RG. Bile duct ligation promotes covalent drug-protein adduct formation in the plasma but not in liver of rats given zomepirac. *Life Sci.* **2000,** 68, 525-537.

Wang MZ, Wu JQ, Dennison JB, Bridges AS, Hall SD, Kornbluth S, Tidwell RR, Smith PC, Voyksner RD, Paine MF, Hall JE. A gel-free MS-based quantitative

proteomic approach accurately measures cytochrome P450 protein concentrations in human liver microsomes. *Proteomics.* **2008,** 8(20), 4186-96.

Wang K, Zhang H, Li Y, Wei Q, Li H, Yang Y and Lu Y. Safety of mycophenolate mofetil versus azathioprine in renal transplantation: a systemic review. *Transplant Proc.* **2004,** 36, 2608-2070.

Westley IS, Brogan LR, Morris RG, Evans AM, Sallustio BC. Role of Mrp2 in the hepatic disposition of mycophenolic acid and its glucuronide metabolites: effect of cyclosporine. *Drug Metab Dispos.* **2006,** 34(2), 261-6.

Westley IS, Morris RG, Evans AM and Sallustio BC. Glucuronidation of mycophenolica acid by Wistar and Mrp2 deficient TR- rat liver microsomes. *Drug Metab Dispos.* **2007.**

Whitehouse CM, Dreyer RN, Yamashita M and Fenn JB, Electrospray interface for liquid chromatographs and mass spectrometers. *Anal. Chem.* **1985,** 57**,** 675-679.

Wieland E, Shipkova M, Schellhaas U, Schutz E, Neidmann PD, Armstrong VW, Oellerich M. Induction of Cytokine Release by the Acyl Glucuronide of Mycophenolic Acid: A Link to Side Effects? *Clin Biochem.* **2000,** 33, 2, 107-113.

Wiwattanawongsa K, Heinzen E, Kemp DC, Dupuis RE and Smith PC. Determination of mycophenolic acid and its phenol glucuronide metabolite in human plasma and urine by high performance liquid chromatography. *J Chrom B.* **2001,** 763, 35-45.

Wolff NA, Burckhardt BC, Burckhardt G, Oellerich M and Armstrong VW. Mycophenolic acid (MPA) and its glucuronide metabolites interact with transport systems responsible for excretion of organic anions in the basolateral membrane of the human kidney. *Neph Dialysis Transpl*. **2007.**

Wu SL, Amato H, Biringer R, Choudhary G, Shieh P, Hancock WS. Targeted proteomics of low-level proteins in human plasma by LC/MSn: using human growth hormone as a model system. *J Prot Res*. **2002,** 1(5), 459-65.

Wu WW, Wang G, Baek SJ and Shen RF. Comparative Study of Three Proteomic Quantitative Methods, DIGE, cICAT, and iTRAQ, using 2D Gel- or LC-MALDI TOF/TOF. *J Prot Res.* **2006,** 5, 651-658.

Young CJ and Sollinger HW. RS-61443: A new Immunosuppressive Agent. *Transpl Proc.* **1994,** 26(8), 3144-3146.

Zhou J, Zhang J and Xie W. Xenobiotic Nuclear Receptor-Mediated Regulations of UDP-Glucuronosyltransferases. *Curr Drug Metab.* **2005,** 6, 289-298.

CHAPTER 2

STABILITY OF MYCOPHENOLIC ACID ACYL GLUCURONIDE AND ITS POTENTIAL BIOLOGICAL CONSEQUENCES

A. INTRODUCTION

Mycophenolic acid (MPA) is used as an adjuvant immunosuppressive agent for prevention of renal and liver allograft rejection. It is also used to treat several autoimmune disorders. MPA is a selective and reversible inhibitor of the inosine monophosphate dehydrogenase type II enzyme, which is primarily responsible for the conversion of xanthine monophosphate to guanine monophosphate in the *de novo* purine biosynthesis pathway (Young and Sollinger, 1994). This enzyme is particularly important for B and T lymphocytes that are unable to undergo the salvage pathway for purine biosynthesis and proliferation (Young and Sollinger, 1994). Because the type II enzyme is found primarily in lymphocytes, MPA makes an ideal agent for immunosuppressive therapy.

MPA is administered as either an ester prodrug, mycofenolate mofetil, (MMF) or an enteric coated sodium salt (MPA-Na^+) in IV or oral formulations. Following administration, MMF is rapidly converted to MPA and subsequently conjugated to form the inactive phenolic glucuronide (MPAG) or the putative reactive acyl glucuronide (acMPAG). These glucuronide metabolites can then be excreted into the biliary tract by the canalicular multidrug resistance-associated protein 2 (MRP2) transporter (Kobayashi et al., 2004). Enterohepatic cycling is responsible for approximately forty percent of MPA exposure in humans, which is visible through the presence of a secondary peak of MPA between 8-12 hours following dosing (Bullingham et al., 1996; Staatz et al., 2007).

While MMF and MPA-Na^+ are generally well tolerated, side effects such as leucopenia, increased infection rate and diarrhea are observed in 20-30% of patients (Davies et al., 2007). Diarrhea usually develops between one and three months into MPA therapy and in severe cases can require dosage reduction or cessation of therapy, increasing the chance of allograft rejection (Davies et al., 2007). Numerous potential causes of delayed onset diarrhea due to MMF therapy have been examined and investigated, but the precise origin remains unknown. Due to the reactivity of acyl glucuronides, attempts have been made to link the acMPAG metabolite to the gastrointestinal side effects of MPA in humans. (Oellerich et al., 2000; Bailey and Dickinson, 2003; Heller et al., 2007). Indeed, *in vitro* studies conducted with acMPAG indicate that it has the potential to elevate cytokine levels, inhibit lymphocyte proliferation and form drug-protein adducts with plasma and liver proteins (Wieland et al., 2000; Shipkova et al., 2001; Shipkova et al., 2002). All of these findings could conceivably contribute to toxicities or affect efficacy.

The purpose of this investigation was to evaluate acMPAG stability under various conditions and to assess its covalent binding potential. The *in vitro* $t_{1/2}$ of the acMPAG metabolite and its relative stability as compared to other common acyl glucuronide metabolites was investigated. Furthermore, the effects of plasma proteins and liver microsomes on acMPAG stability were evaluated. Using *in vivo* studies in male rats, we estimated the systemic clearance and the fraction of acMPAG metabolite that is converted to MPA following direct acMPAG administration. The ability of acMPAG to covalently bind with albumin *in vitro*

was examined to evaluate its stability and reactivity. This investigation of acMPAG stability coupled with *in vivo* and covalent binding studies, provides insight into whether the presence of drug-protein adducts could be a factor in adverse reactions to MPA.

B. METHODS

Materials

AcMPAG (reported >95% pure) was generously donated in separate batches by Roche Pharmaceuticals (Metby, NJ) and Novartis Pharmaceuticals. MMF (CellCept©) was purchased from Roche Pharmaceuticals (Nutley, NJ). Analytical grade acetonitrile (ACN), methyl alcohol (anhydrous) and glacial acetic acid (HOAc) were purchased from Fisher Scientific Co. (Pittsburgh, PA). β-Glucuronidase (Type β-1 from Bovine Liver), formic acid (FA), suprofen, diethyl ether, human serum albumin fraction V (HSA), alamethicin, magnesium chloride ($MgCl_2$), phenylmethylsulfonyl fluoride (PMSF), D-saccharic acid 1, 4-lactone (D-SL), dextrose, carboxyl methyl cellulose (CM-cellulose) and TRIZMA® hydrochloride were purchased from Sigma-Aldrich Co. (St. Louis, MO). Potassium phosphate monobasic, dibasic and sodium acetate (anhydrous) were obtained from Mallinckrodt Baker, Inc. (Paris, Kentucky). Tris base was purchased from Bio-Rad Laboratories (Hercules, CA). Protein concentrations were determined using the Pierce BCA Protein Assay Kit with bovine serum albumin (BSA) as the reference standard. Bond Elut solid phase extraction cartridges (SPE, RP-C18) were obtained from Varian Inc (Palo Alto, CA). Human liver microsomes (HLMs) (20 mg/mL) were purchased from BD

Biosciences (Franklin Lakes, NJ) (pools of 33), and human plasma (K_2-EDTA treated) was obtained from Valley Biomedical, Inc (Winchester, Virginia).

HPLC-UV Analysis

Analysis by reversed phase HPLC utilized a HP 1050 LC equipped with a autosampler and an Axxiom (Moorpark, CA) C18 (15cm length, 4.6 mm diameter, 5 µ particle size, 100 Å pore size) column, with an HP 1100 series UV detector set at 250 nm. Data analysis was performed with a Chemstation (A.05.01, Agilent Technologies, Santa Clara, CA). The HPLC method was adopted from an earlier protocol with some modifications (Wiwattanawongsa et al., 2001). The mobile phase was 52% methanol/48% (0.1% formic acid (FA)) under isocratic conditions at a 1.0 mL/min flow rate over 24 minutes. Stability experiments and pharmacokinetic analyses were conducted several different times over a period of weeks with small variations (<20%) in both standard error and stability calculations.

LC-MS Conditions

Analysis by reversed phase LC-MS was adopted from a previous method using an HP 1100 series LC system and autosampler coupled to a single quadrapole mass spectrometer (Sciex API 100, MDS Sciex, Concord, CA) (Stern et al., 2007). A Zorbax RX-C8 column (Agilent Technologies, Palo Alto, CA) (15 cm, 2.1 mm, 5 µ particle size) was run under gradient conditions utilizing acetonitrile (sovent B) and 0.1% HOAc (solvent A) mobile phase. Linear gradient

conditions used were, 0 minutes, 20%B; 7 minutes, 90% B; 10 minutes, 90% B; 11 minutes, 20% B; 15 minutes, 20% B. Data analysis was performed by Analyst 1.4.2 (build 1236) (Applied Biosystems, Foster City, CA).

Stability Experiments in Phosphate Buffer

Concentrations of sodium phosphate monobasic and dibasic solutions (0.1 M) were used for pH 4, pH 7.4 and pH 9 buffers. AcMPAG (Roche) was added to 50:50 ACN/0.1% HOAc (pH 3) to provide a 1 mg/mL stock and stored at -20ºC prior to analysis. AcMPAG solution (75 µL, 0.1 mg/mL) was first diluted from the 1 mg/mL stock using HPLC water then added to microcentrifuge tubes and brought to 0.2 mL with 150 mM phosphate buffer and incubated at 37ºC in duplicate. At 0, 30, 60, 120, 240, 480, 720 and 1440 minutes, a 10µL aliquot was extracted and, either quenched with 800 µL of acidified acetonitrile (0.5% FA, pH 3.2), or hydrolyzed with 10 µL of β-glucuronidase solution (final dilution of 100 U/µL in pH 5 acetate buffer) for four hours. Following quenching of either the incubated or hydrolyzed acMPAG, samples were centrifuged at 15,000*g* for 10 minutes at 4ºC and dried under nitrogen. Samples were then reconstituted with 0.15mL of MeOH/0.1% FA (25:75) and suprofen internal standard (2 µg/mL final concentration) and injected for HPLC analysis.

AcMPAG Stability in Plasma

Stability studies in plasma were processed using the same sample preparation protocol described in the previous section. AcMPAG diluted stock

(0.1 mg/mL) was added to either human plasma (K_2-EDTA treated) at physiological pH or plasma acidified with HOAc (pH 4), providing a final concentration of 40 µg/mL. During incubation, samples (in duplicate) were obtained and prepared as indicated in the buffer experiments. Samples were centrifuged again at 15,000*g* for 15 minutes at 4ºC, and the supernatant was extracted and dried under nitrogen gas. After evaporation to dryness, samples were reconstituted with MeOH/0.1% FA (25:75) and injected onto the HPLC-UV.

Stability in Human Liver Microsomes

HLMs (1 mg/mL) were prepared in 100 mM Tris buffer (pH 7.7) and incubated on ice for 10 minutes with 100 mM $MgCl_2$ and alamethicin (20 µg/mL) and either tris buffer (control), PMSF (2 µM), D-SL (0.8 mM) or both PMSF and DS-L in duplicate in buffer. The reaction was initiated with an aliquot of acMPAG (40 µg/mL final concentration, Roche) and incubated at 37°C in duplicate. At 0, 15, 30, 60 and 120 minutes, a 10µL aliquot was extracted and either hydrolyzed with β-glucuronidase (100 U/µL) or quenched with acidified ACN. Following quenching, samples were then centrifuged, dried and reconstituted prior to HPLC-UV analysis.

Covalent Binding of acMPAG in HSA

Covalent binding experiments were carried out under protocols that have been previously reported (Smith et al., 1993; Liu et al., 1996). HSA fraction V was dissolved in phosphate buffer (pH 7.4, 150 mM) to 30 mg/mL and then

combined with acMPAG to obtain 50 µg/mL for incubation. The mixture was incubated at 37ºC for 24 hours, and 0.1 mL aliquots were obtained in triplicate at 0, 30, 60, 120, 240, 480, 720 and 1440 minutes and immediately quenched with 1 mL isopropanol/43% phosphoric acid (50:1). MPA was similarly incubated in duplicate in HSA fraction V to serve as a control. Samples were centrifuged and the precipitated protein pellet was washed 10X with methanol/diethyl ether (3:1). After washing, the pellets were spiked with suprofen internal standard (0.4 mg/mL in solution) and dissolved in 1 mL 0.2 M NaOH, followed by three hour incubation at 37ºC to hydrolyze and release covalently-bound acMPAG to form MPA. To confirm MPA stability against extreme acidic or basic treatment, MPA was incubated with aqueous 0.1 M NaOH or 0.1 M HCl over 8 hours and its content monitored by HPLC. Following hydrolysis, concentrated phosphoric acid was added to adjust the pH to approximately 2. Samples were then purified by SPE. Following conditioning, samples were added to SPE tubes, followed by a wash with MeOH/0.1% FA (20:80), and then eluted with of ACN/0.1% FA (80:20). The eluents were dried under nitrogen, reconstituted in MeOH/0.1% FA (25:75), and injected for HPLC analysis. Chromatographic conditions were the same as previously described with the exception of the mobile phase (60% MeOH/40% 0.1% FA). Run time was ten minutes with retention times of 5.5 and 7.5 minutes for suprofen and MPA, respectively.

Animals

Male Wistar rats (250-300 g) were purchased from Charles River laboratories (Wilmington, MA) and housed under a 12 hour-light dark cycle. Experimental methods were approved by the Institutional Animal Care and Use Committee (IACUC) and the Division of Lab Animal Medicine (UNC-Chapel Hill). Animals were acclimated for one week prior to experimentation. Male rats (n=3) were administered a single bolus 2.5 mg/kg AcMPAG (in MPA equivalents) dose intravenously in 5% isotonic dextrose solution or IV with 50 mg/kg MMF in a 5% isotonic dextrose solution (6 mg/mL). Blood was collected from the tail vein in 0.1-0.2 mL aliquots into microcentrifuge tubes at 2, 5, 10, 15, 20, 30, 60, 120, 180, 240, 360 and 480 minutes post IV dosing and 0, 15, 30, 60, 120, 180, 240, 360 and 480 minutes post MMF dosing, placed on ice, and centrifuged at 15,000*g* for 10 minutes. Following centrifugation, plasma was transferred into microcentrifuge tubes containing acetic acid (HOAc) (pH 3, 5μL/mL) to stabilize acMPAG at pH~4 and stored at -20ºC until analysis. For quantitative analysis, 50 μL of plasma was precipitated with 300 μL of acetonitrile containing 5 μL of 0.1mg/mL suprofen internal standard and centrifuged, dried under nitrogen and reconstituted in methanol/0.1% formic acid (25:75) for HPLC injection. Noncompartmental pharmacokinetic estimates were obtained using WinNonlin 5.0.1 (Pharsight, Cary, NC). Individual pharmacokinetic estimates for each rat were calculated based on plasma concentration data using noncompartmental pharmacokinetics on WinNonline and averaged (n=3) to generate parameter estimates.

C. RESULTS

AcMPAG Purity

Initial HPLC analysis of both the Novartis and Roche acMPAG products revealed an additional peak eluting as a shoulder just prior to the acMPAG peak (Figure 2.1). After β-glucuronidase treatment, the first peak remained and was later confirmed through mass spectrometry (Figure 2.2) to be a putative isomeric conjugate impurity of the initial acMPAG sample. This peak was consistently seen throughout all stability testing and indicated that the initial samples provided by both the Roche and Novartis pharmaceutical companies consisted of 82% β-1 acMPAG and 18% isomeric conjugates that are resistant to β-glucuronidase.

Isomeric Conjugate Content

Prior to stability testing, the time dependant β-glucuronidase (1000 U/mL) treatment was evaluated at 2, 4 and 6 hours to determine the optimal duration of hydrolysis. At two hours, there was still a significant fraction of β-1 conjugate that was not cleaved by β-glucuronidase, but at four and six hours, there was no detectable β-1 conjugate present at R_t=10.2 minutes. Furthermore, there was no difference in isomeric conjugate impurity seen at R_t=9.4 minutes between the four and six hour treatments (18.2% at four hours, 18.5% at six hours, p=0.88, data not shown). Based on these results, four hours of β-glucuronidase treatment was used for the subsequent stability testing in phosphate buffer and biological matrices.

Stability Experiments

The buffer stability experiments with acMPAG consistently showed a pH dependant acyl migration and hydrolysis. While acMPAG was very stable through 24 hours at pH 4, all three pH conditions demonstrated a noticeable product loss following the first hour of incubation (Figure 2.3). This pattern was seen most dramatically at pH 7.4 which demonstrated a much steeper rate of decline in the first 120 minutes of incubation compared to the remaining incubation time period up to 24 hours. The $t_{1/2}$ of 18.1 hours (Table 2.1) indicates that acMPAG is a moderately stable acyl glucuronide in protein free buffer under physiological conditions. Comparatively, acyl glucuronides from drugs removed from the market such as zomepirac ($t_{1/2}$ 0.5 hours) and benoxaprofen acyl glucuronide ($t_{1/2}$ 1.4 hours) are much less stable under similar conditions (Hasegawa et al., 1982; Dong et al., 2005).

Relative to buffer, acMPAG demonstrated a similar yet more rapid pattern of decline in human plasma under both physiological (pH 7.4) and acidic (pH 4) conditions (Figure 2.4). The mildly acidic condition stabilized acMPAG compared to physiological pH through 24 hours, but continued to display the biphasic decline seen in the phosphate buffer experiments (Figure 2.3). In human plasma, the $t_{1/2}$ was 6.7 hours, but there were no significant differences in isomeric rearrangement. It is likely that the presence of esterases within the human plasma caused acMPAG hydrolysis to increase dramatically as compared with protein free phosphate buffer.

Within HLMs, the initial β-1 acyl glucuronide of acMPAG maintained a similar pattern of degradation as seen in both the buffer and plasma experiments (Figure 2.5). After an initial period of rearrangement and hydrolysis, acMPAG was somewhat stabilized with the inhibitors PMSF and D-SL but continued its decline more rapidly compared to both the buffer and plasma experiments. Interestingly, while the decline of the β-1 conjugate was more rapid in HLM than occurs with the addition of one or two protease inhibitors, the relative concentration of isomeric conjugates remained steady throughout the incubation period in all four conditions employed with HLM (Figure 2.5). Since HLMs have high concentrations of esterases, cleavage back to the parent aglycone was more extensive in the control HLM samples compared to HLM samples with a thirty minute pre-incubation period with inhibitors. As expected, the $t_{1/2}$ associated with the HLM incubation (2.6 h) was the shortest of the three physiological *in vitro* conditions tested (Table 2.1).

Covalent Binding of acMPAG to HSA

Covalent binding in HSA *in vitro* was examined to evaluate the reactivity of acMPAG and its potential to form drug-protein adducts *in vivo*. Hydrolysis of MPA bound (either as MPA or via isomeric acMPAG) was performed with 0.2 M NaOH at 37ºC. Preliminary experiments indicated <4% loss of MPA over an 8 hour incubation in 0.2 M NaOH (data not shown). Covalent binding to HSA levels was below detection limits (<0.35 ng/mg HSA) through the first hour of incubation. During the incubation period, the formation of acMPAG dependent

HSA adducts was minimal and lower than that reported for ibuprofen acyl glucuronide and almost ten fold lower than that reported for reactive ibufenac acyl glucuronide under the same experimental conditions (Figure 2.6, Castillo et al. 1995). These data indicates that acMPAG is a fairly nonreactive acyl glucuronide with a low propensity for rapid accumulation of drug-protein adducts within the systemic circulation and tissues *in vivo*.

AcMPAG Disposition in a Rat

Three male Wistar rats were dosed intravenously with 2.5 mg/kg acMPAG to obtain AUC and Cl estimates. The plasma concentration profile demonstrated that the metabolite is rapidly cleared after IV administration, with hydrolysis being the primary route of loss for acMPAG. After a 2.5 mg/kg dose (based on MPA equivalents), the average $AUC_{(acMPAG)0-\infty}$ was 1.4 mg*min/mL with the average parent aglycone $AUC_{(MPA)0-\infty}$ is 0.2 mg*min/mL (Table 2.2). IV dosing of MMF 50 mg/kg (based on MPA equivalents) resulted in an $AUC_{(MPA)0-\infty}$ of 2.9 mg/mL*min. Data from the IV MMF and IV acMPAG dosing to rats were used to estimate the MPA fraction converted from acMPAG ($F_{acMPAG \rightarrow MPA}$) as 0.88. This extent of hydrolytic conversion indicates extensive cleavage of acMPAG back to the MPA aglycone, with the remaining metabolite excreted likely through the urine or bile. None of the rats administered a single dose of acMPAG demonstrated any signs of overt toxicity during the course of the experiments.

D. DISCUSSION

A few attempts have been made previously to study the stability of the acMPAG metabolite of MPA. The results of these reports were ambiguous (Wieland et al., 2000; Shipkova et al., 1999; Shipkova et al., 2000; de Loor et al., 2008). We therefore sought to provide a comprehensive investigation into acMPAG stability using various physiological conditions that may be responsible for the previously reported results that were inconsistent. Our first observation was that the chromatographs from both the HPLC-UV and LC-MS experiments indicate a significant amount of impurity is present within the samples of acMPAG obtained from both pharmaceutical companies prior to stability testing, indicating the presence of the isomeric conjugates. It is likely that, during the overnight incubation process of liver microsomes with MPA used to generate the acMPAG metabolites, the samples underwent significant acyl migration (Kittelmann et al., 2003). In each of our stability experiments, there was an immediate loss of initial β-1 acyl glucuronide (prior to the terminal phase degradation period) that existed under all conditions tested. It has been previously reported that while acMPAG metabolites are stable when stored in acidic conditions at -20ºC, this metabolite undergoes hydrolysis and rearrangement under some experimental settings (Shipkova et al., 1999; Shipkova et al., 2000, de Loor et al., 2008). These setting include incubations in both plasma and phosphate buffer at both room temperature and under refridgeration (Shipkova et al., 2000, de Loor et al., 2008). Our studies here confirm these findings and show that the primary differences in acMPAG stability

is that it decreases when progressing from protein-free conditions to an intact *in vivo* system.

The decreases in stability of acMPAG demonstrated from the physiological phosphate buffer incubations compared to human plasma indicate that the plasma protein matrix itself destabilizes the acyl glucuronide. While the rates of isomeric rearrangement remain consistent between the two matrices, the rate of hydrolysis increases dramatically in human plasma and is responsible for the reduced $t_{1/2s}$ calculated using the concentration time plots (Figures 2.3 and 2.4). Esterase cleavage of acMPAG responsible for increased MPA concentration could also be a source for the efficacy of the acMPAG metabolite reported by Shipkova et al. for an *in vitro* assay (Shipkova et al., 2001). Esterases are readily present within mononuclear leukocytes and an incubation period of 96 hours at 37ºC could cause a significant contamination of the parent MPA aglycone, resulting in inhibited leukocyte proliferation (Shipkova et al., 2001).

Of the three *in vitro* matrices chosen for this study (buffer, plasma, HLM), the acMPAG metabolite was found to be the least stable within the HLM matrix. This is likely due to not only the presence of a significant amount of esterase activity within the HLM but also because of β-glucuronidase enzymes within the liver microsomes. The actions of these enzymes was confirmed following the addition of the two different inhibitors to the HLM cocktail, which decreased the degradation rate with the HLMs individually, but were most effective when combined. PMSF is a nonspecific protease inhibitor that can be used for liver or

intestinal microsome preparations to prevent loss of enzyme activity (Dutton, 1980).

The putative toxicity of acyl glucuronides has continued to be a source of investigation primarily due to the large number of nonsteroidal anti-inflammatory drugs (NSAIDs) forming acyl glucuronide metabolites that have been removed from the market because of adverse drug reactions (ADRs) (Dickinson, 1993; Bailey and Dickinson, 2003). Acyl glucuronide metabolites are unique when compared to other glucuronides because they undergo esterase cleavage back to the parent aglycone and they also form isomeric conjugates through acyl migration (Faed, 1984). Acyl migration results from the intraconversion of the 1-O-β acyl glucuronide into 2-O-β, 3-O-β, 4-O-β or α isomeric conjugates and unlike the parent 1-O-β conjugate, they are resistant to β-glucuronidase hydrolysis (Sinclair, 1982; Faed, 1984). Isomeric conjugates observed for numerous NSAIDs have shown the ability to bind to both plasma and liver proteins such as tubulin and albumin; primarily through the nucleophilic displacement or Schiff base mechanisms, leading to the formation of drug-protein adducts (Smith et al., 1990; Smith et al., 1992). It has been hypothesized that these drug-protein adducts could disrupt cellular function such as seen in dipeptidyl peptidase IV (DPP-IV) adducts with diflunisal (King and Dickinson, 1993; Bailey and Dickinson, 2003). In addition, the binding of tubulin with the acyl glucuronides of zomepirac, tolmetin and valproic acid (VPA) may lead to the inhibition of hepatocyte function and subsequent liver toxicity (Bailey et al., 1998; Bailey and Dickinson, 2003; Cannell et al., 2003). Many NSAIDs that form

unstable acyl glucuronides undergoing rapid acyl migration in phosphate buffer under physiological conditions have been removed from the market primarily because of extensive hypersensitivity reactions or hepatotoxicity (Bailey and Dickinson, 2003). However, other drugs such as VPA form very stable glucuronide metabolites and continue to enjoy a steady market share despite being blamed for over 100 deaths from adverse drug reactions.

A common comparison of acyl glucuronide stability is the half life of the glucuronide in pH 7.4 phosphate buffer (100 or 150 mM) at 37°C. Drugs forming unstable glucuronides including zomepirac ($t_{1/2}$ 0.5 hours) and suprofen ($t_{1/2}$ 0.7 hours) not only have been removed from the market due to not only hepatotoxicity but also have shown the ability to form drug-protein adducts with both liver and plasma proteins (Spahn-Langguth et al., 1992; Smith et al., 1993; Bailey et al., 1998). Even for these compounds, it has become difficult to directly link the formation of these adducts with either hypersensitivity reactions or as sources of drug toxicity, but it is possible that a rapid buildup in drug-protein adducts *in vivo* could disrupt cellular function in either the liver or result in lymphocyte sensitization as seen with diflunisal-albumin adducts in rats (King and Dickinson, 1993; Worrall and Dickinson, 1995).

While stability in phosphate buffer is seen as the standard means of comparison for acyl glucuronide reactivity, the ability to bind and form covalent drug-protein adducts is more physiologically relevant. One consistent pattern seen with acyl glucuronides is the inverse relationship between acyl glucuronide $t_{1/2}$ in phosphate buffer and the number of covalent adducts (mol carboxylate/mol

protein) formed by these same conjugates (Spahn-Langguth et al., 1992). This pattern is seen with reactive glucuronides (zomepirac/tolmetin), as well as stable acyl glucuronides (beclobric acid and VPA), for two reasons. The first is that unstable acyl glucuronides are more likely to form isomeric conjugates that are more readily able to form drug-protein adducts through both the imine mechanism and the transacylation mechanism (Smith et al., 1990, Spahn-Langguth et al., 1992). However, the parent O-β-1 acyl glucuronide can only form these same adducts through the transacylation mechanism (Spahn-Langguth et al., 1992). Furthermore, isomeric conjugates are resistant to cleavage by β-glucuronidase enzymes, which can lengthen their *in vivo* residence time, along with their exposure to liver and plasma proteins (Faed, 1984; Spahn-Langguth et al., 1992). The $t_{1/2}$ of acMPAG of 18.1 hours within phosphate buffer indicates that it is a fairly stable acyl glucuronide, which would be unlikely to rapidly form isomeric conjugates and drug-protein adducts *in vivo*. This was supported by the covalent binding studies where the highest level of drug-protein adduct formation (1.2 mmol MPA/mol protein, Figure 2.6) was a fraction of that seen in a similar incubations of ibuprofen (IBP) (6 mmol IBP/mol HSA), which is considered a stable and less reactive acyl glucuronide (Castillo et al., 1995). However, even though beclobric acid is moderately stable in phosphate buffer and may be classified as a fairly unreactive acyl glucuronide, it was still removed from the market in 1992 due to extensive hepatotoxicity (Spahn-Langguth et al., 1992; Mayer et al., 1993).

While it has been shown that plasma protein adducts formed by diflusinal are readily immunogenic when administered to rats, this same reaction was not seen with naproxen, an NSAID that is still available as an over-the-counter medication (King and Dickinson, 1993; Worrall and Dickinson, 1995). This variety of potential immunogenic and hepatotoxic reactions to these drug protein adducts remains a contentious debate today because it encompasses not only reactive acyl glucuronides but also reactive acyl-CoA metabolites among other reactive intermediates that could lead to drug toxicity of carboxylic acids (Boelsterli, 2002). Because of this, it is difficult to classify whether the drug-protein adducts formed by acMPAG that have been found in both the liver and colonic tissue could be a pattern of toxicity or a harmless secondary effect also seen with aspirin and ibuprofen (Dickinson, 1993; Dickinson et al., 1994; Castillo et al., 1995). However, due to the stability of acMPAG under standard *in vitro* conditions, coupled with its low levels of covalent binding *in* vitro, indicate that the reactivity of acMPAG is probably an insignificant factor in MPA side effects.

One potential effect of these adducts and of unstable acyl glucuronides is the presence of either immunogenic reactions or hepatoxicity. Outside of a small amount of isolated cases where a brief elevation of serum transaminases were seen in the reported clinical chemistry of two tested patients administered MMF for treatment of atopic dermatitis, there have been no literature reports of significant MMF related hepatotoxicity (Hantash and Fiorentino, 2006; Morath et al., 2006; Zwerner and Fiorentino, 2007). In addition, while elevated cytokines have been seen with *in vitro* incubations of acMPAG, MPA continues to be a

primary standard used for preventing immunogenic reactions along with prevention of renal allograft and hepatic allograft rejection (Davies et al., 2007; Heller et al., 2007; Staatz and Tett, 2007; Zwerner et al., 2007). As of this report, no renal toxicity or autoimmune disorders have developed as a consequence to MPA administration, either on a short-term or long-term dosing regimen.

The primary side effect of MMF administration besides an increased infection rate, which is commonly seen in patients on any form of long-term immunosuppressive therapy, is the presence of delayed-onset diarrhea (Hantash and Fiorentino, 2006; Morath et al., 2006; Zwerner and Fiorentino, 2007). A recent attempt at linking these side effects with either a direct increase or decrease in acMPAG blood levels was inconclusive (Heller et al., 2007). An alternative theory for the mechanism of delayed onset diarrhea could be due to the actions of MPA itself. MPA is designed to inhibit the IMPDH enzyme type II to prevent purine synthesis, leading to lymphocyte proliferation, and thus modify the response to either an extensive autoimmune reaction or allograft rejection (Young and Sollinger, 1994). However, because lymphocytes rely on the *de novo* purine synthesis pathway utilizing the IMPDH enzyme to synthesize purine nucleotides as opposed to the salvage pathway, lymphocyte proliferation is inhibited in patients on MPA therapy. Lymphocyte cytotoxicity is also seen in *in vitro* cultures of lymphocytes treated with MPA because of this same mechanism (Allison and Eugui, 1994). Numerous other cell types, including enterocytes, rely on this pathway for proliferation through the IMPDH type I enzyme. Prolonged exposure to MPA seen in transplant patients on extended MMF/MPA therapy

could result in a consistent exposure to high local concentrations of MPA within the intestinal lumen through the actions of the gut flora producing β-glucuronidase enzymes. The fraction of acMPAG cleaved to MPA in the systemic circulation of rats, to 0.88, indicates that a large portion of acMPAG formed and effluxed into the blood is hydrolyzed back into the parent aglycone. Efficient hydrolysis *in vivo* is supported by the large amount of β-glucuronidase and esterase hydrolysis displayed in the HLM incubations along with the significant hydrolysis within the plasma (Figure 2.4 and 2.5). AcMPAG could serve as a secondary source of MPA within the systemic circulation and intestinal lumen, which over time could be a factor in MPA intestinal toxicity, even if the metabolite itself is not proven to be the source of drug toxicity.

In conclusion, the data presented here indicate that acMPAG is a fairly stable acyl glucuronide with low relative reactivity compared to other metabolites of this type. It is a labile metabolite in the systemic circulation and minor metabolite in plasma and bile, thus there is little evidence to support this metabolite as a likely reactive metabolite to be associated with the adverse drug reactions of MPA.

E. ACKNOWLEDGEMENTS

I would like to thank Dr. Melanie Joy along with Novartis and Roche Pharmaceuticals for providing the acMPAG. I would also like to thank the NIH Training Grant T32-ES007126 for providing funding.

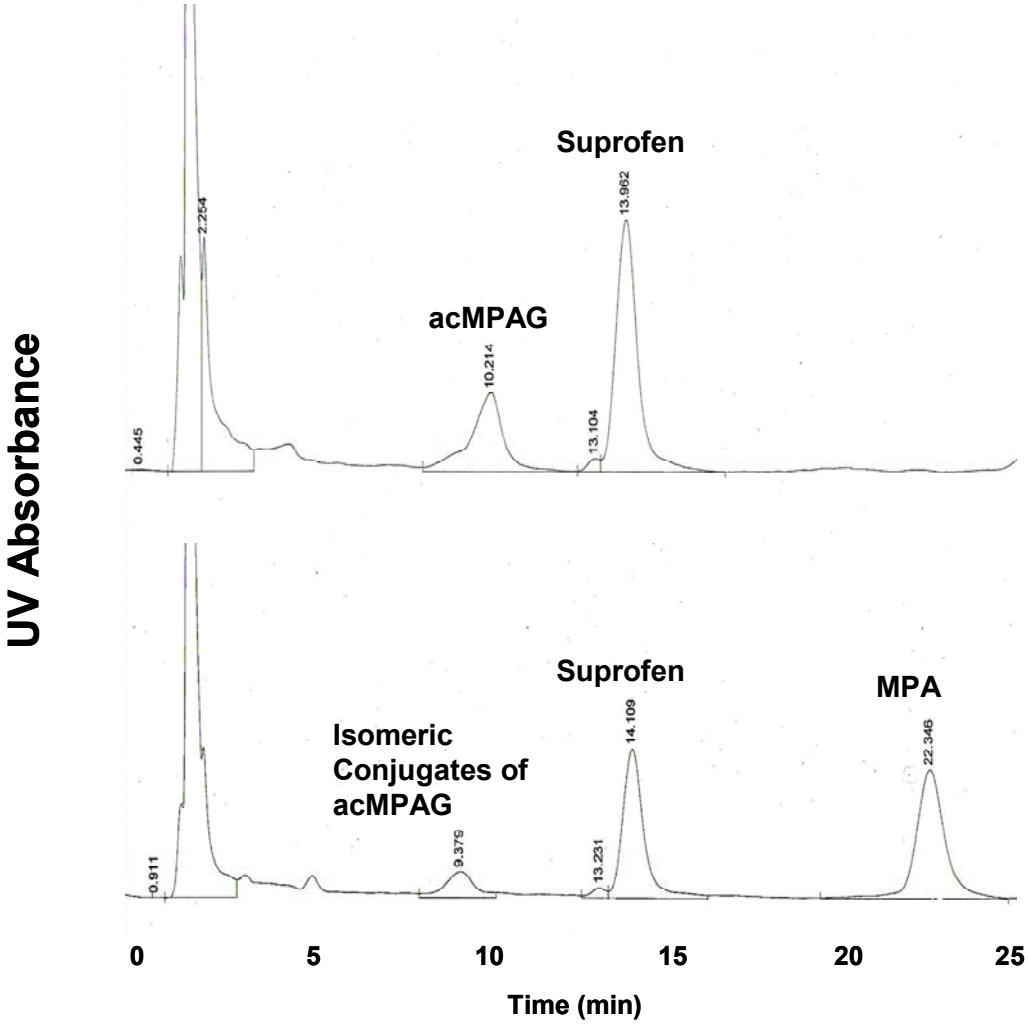

Figure 2.1. HPLC-UV chromatogram of 0.1 mg/mL acMPAG solution before (top) and after (bottom) β-glucuronidase treatment. Retention times as indicated for isomeric conjugates (9 min), AcMPAG (10 min), suprofen (14 min), and MPA (22.5 min).

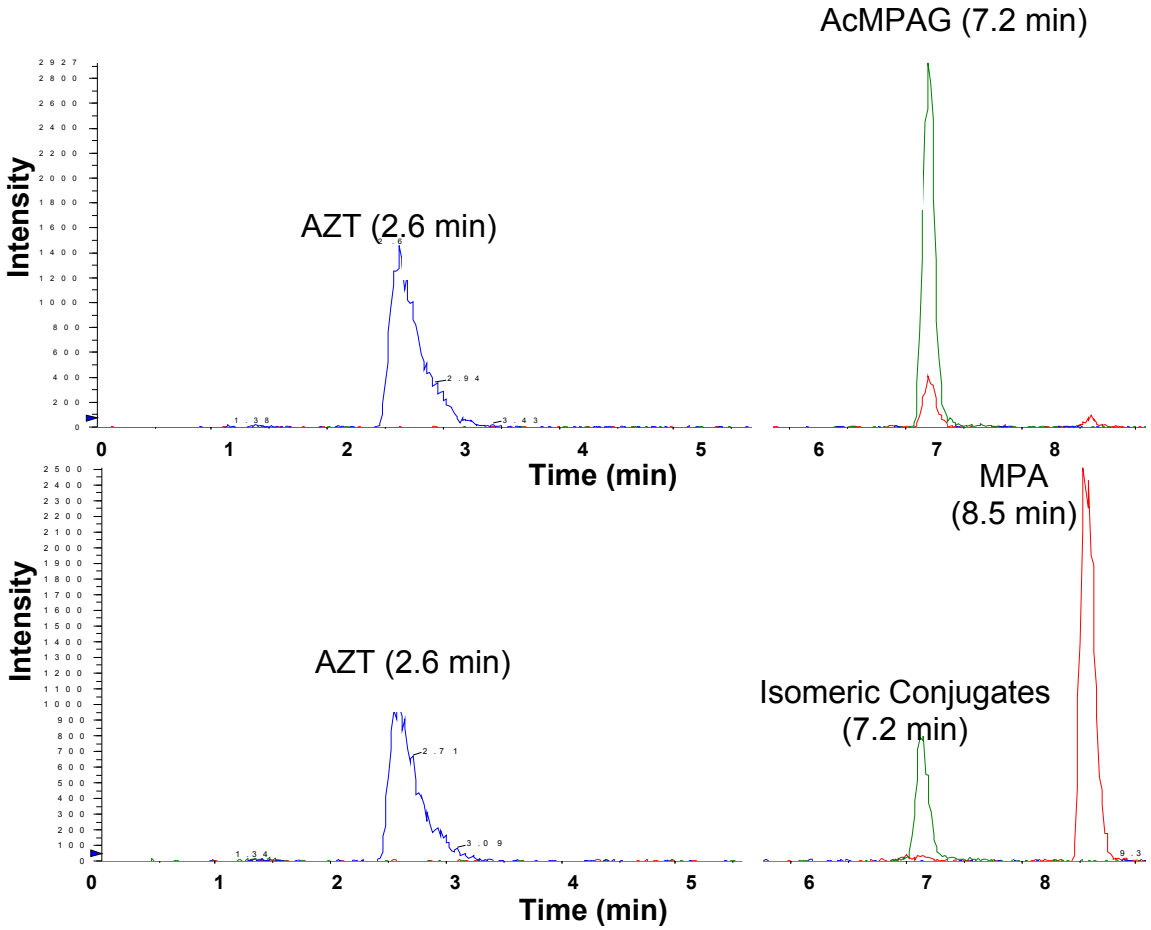

Figure 2.2. LC-MS selected ion chromatogram of AZT (266 m/z, 2.6 min), Isomeric Conjugates (495 m/z, 7.2 min), AcMPAG (495 m/z, 7.2 min) and MPA (319 m/z, 8.5 min) both before (top) and after (bottom) β-glucuronidase treatment for four hours.

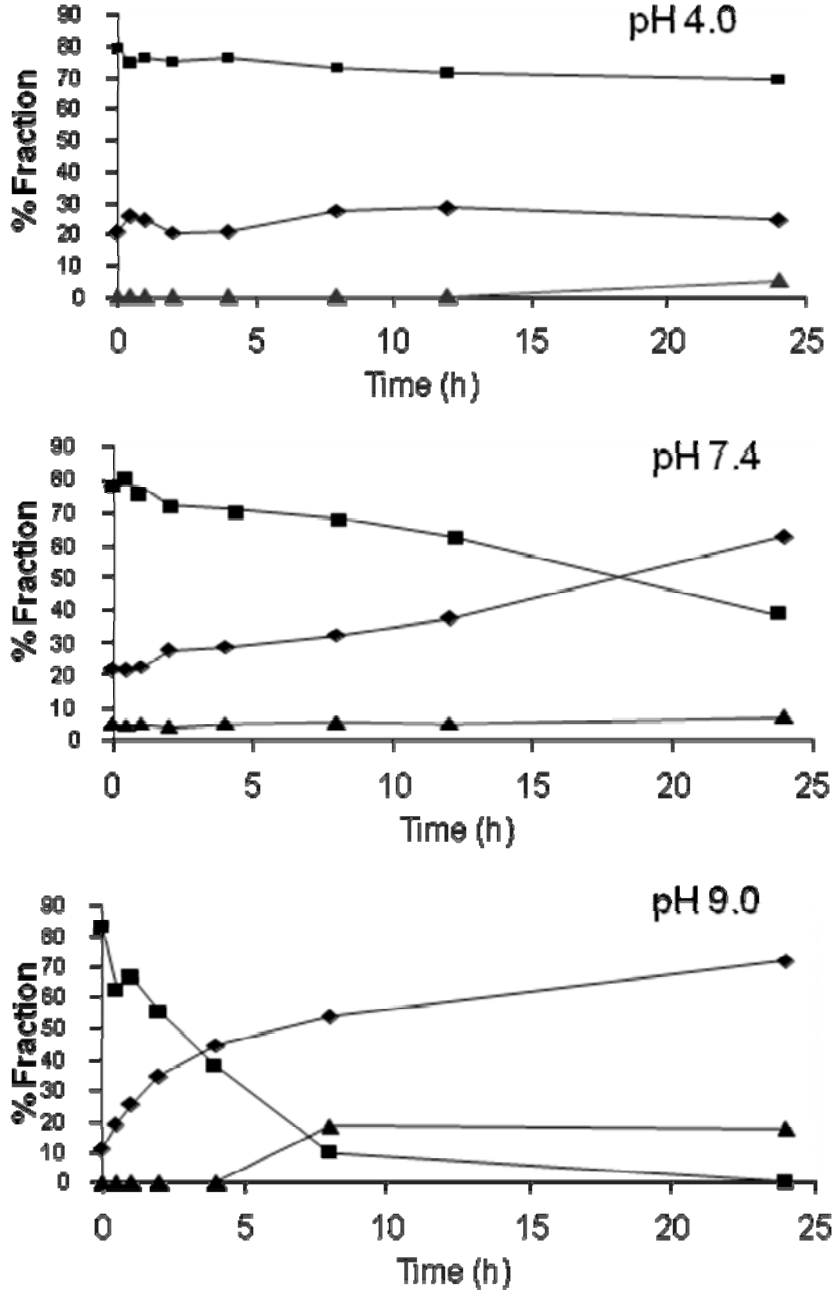

Figure 2.3. Stability of acMPAG (■) in aqueous buffer performed at pH 4 (top), pH 7.4 (middle) and pH 9 (bottom). Fractions were averaged from experiments run in duplicate (variation between samples <25%). Degradation to isomeric conjugates of acMPAG (◆) and MPA (▲) are shown.

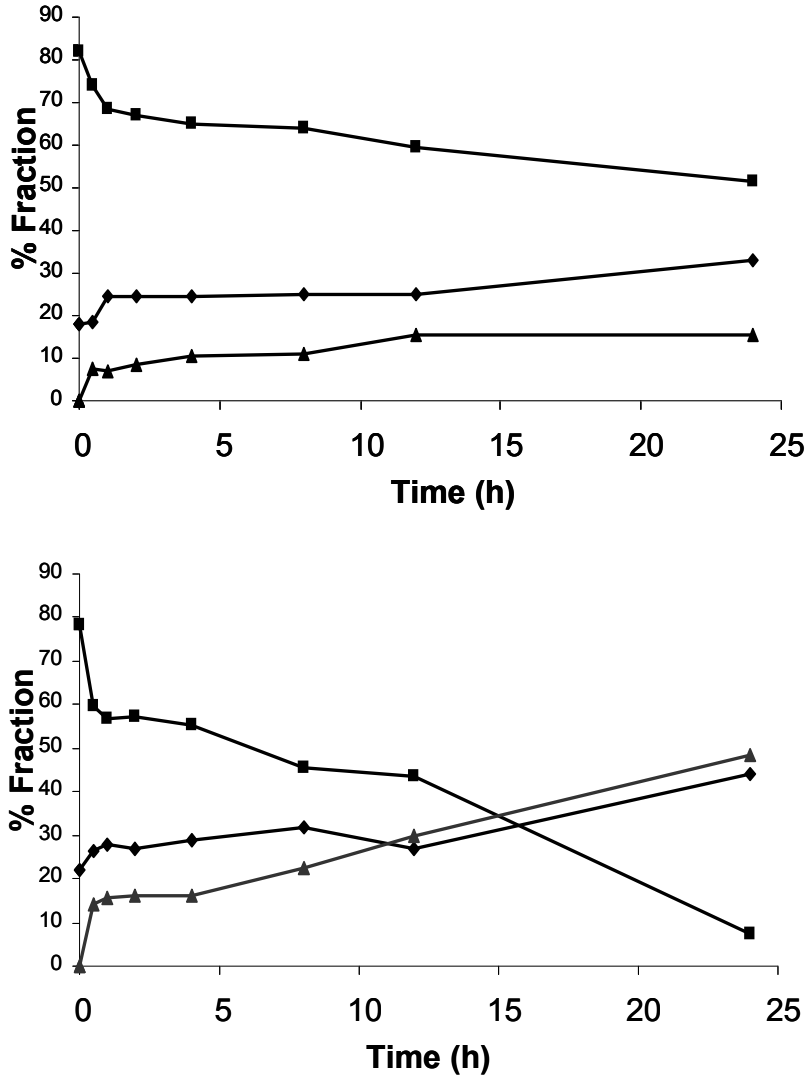

Figure 2.4. Stability and degradation of acMPAG (■) to isomeric conjugates (◆) and MPA (▲) is shown in human plasma at pH 4 (top) and physiological pH (bottom) for 0.1 mg/mL acMPAG. Fractions were averaged from experiments run in duplicate (variation <25%).

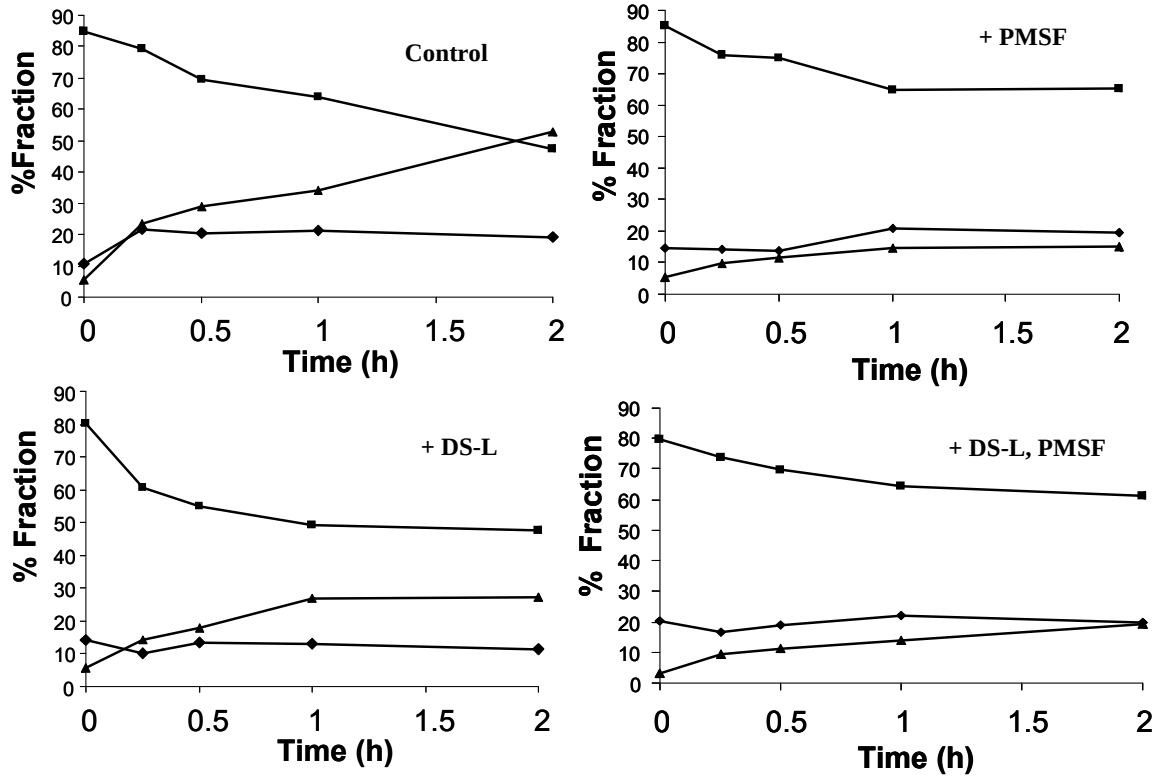

Figure 2.5. AcMPAG (■) stability in HLM when incubated under control conditions (top left), HLM with DS-L inhibitor (0.8 mM, bottom left), HLM with PMSF (2 mM, top right) and HLM with both inhibitors added (bottom right). Fractions were averaged from experiments run in duplicate (variation <30%). Degradation to isomeric conjugates of acMPAG (◆) and MPA (▲) are shown.

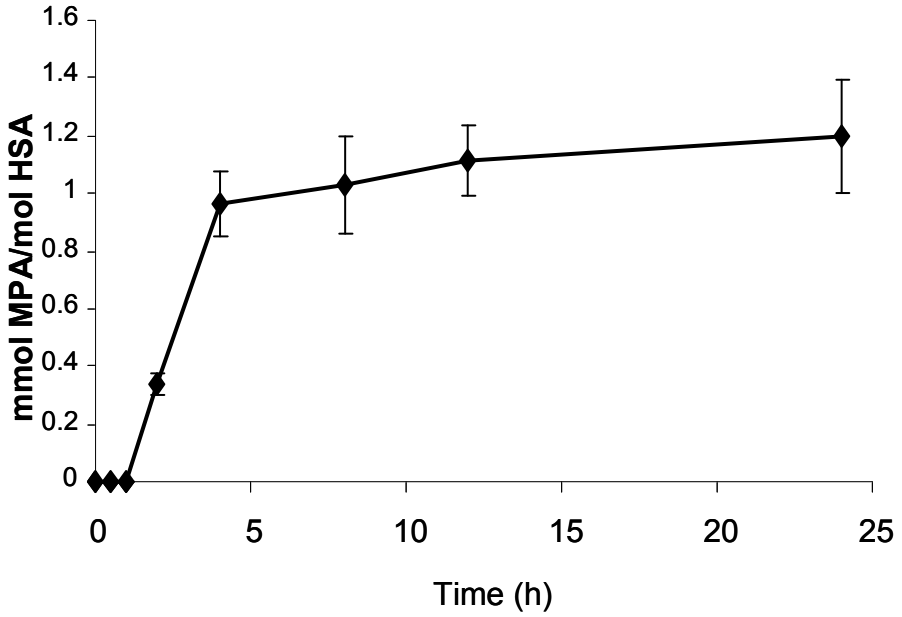

Figure 2.6. Covalent binding of acMPAG to HSA over a 24 hour incubation period when incubated with 0.67 mM acMPAG. Binding was measured following cleavage of bound acMPAG to MPA. Data is presented as mean ± SD (n=3).

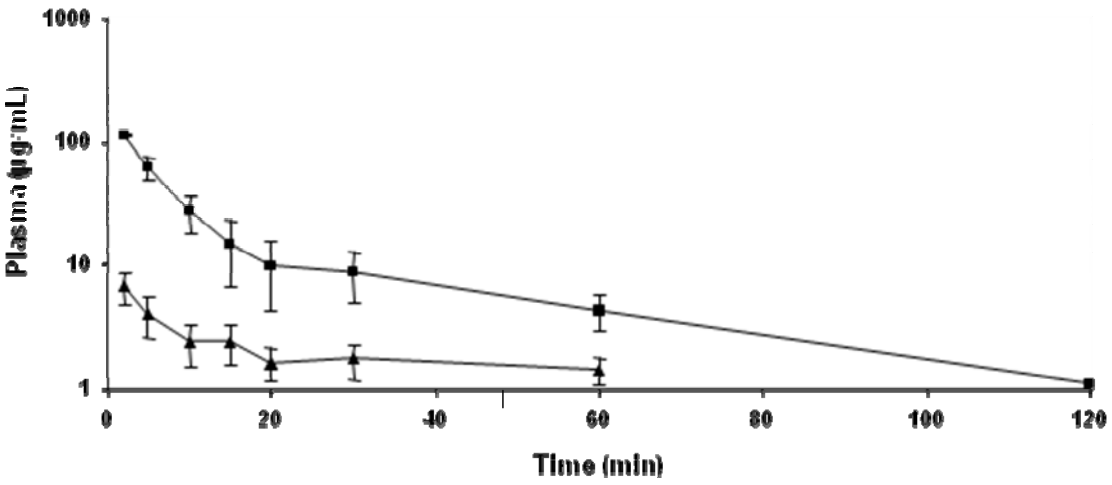

Figure 2.7. Mean plasma concentrations of acMPAG (■) and MPA (▲) (in MPA equivalents of µg/mL) for male Wistar rats (n=3) following a 2.5 mg/kg IV dose of acMPAG (Roche). Data is presented as mean ± SD.

Table 2.1. Half life values of acMPAG in various matrices.

Condition	k (h^{-1})	$t_{1/2}$ (h)
pH 4 Buffer	0.01	>100[b]
pH 7.4 Buffer	0.04	18.1
pH 9 Buffer	0.18	3.8
Human Plasma	0.10	6.7
Human Liver Microsomes	0.27	2.6
In vivo IV injection [c]	1.37	0.5

[a]First order half-life estimated by terminal log-linear decline (>3 data points)
[b]Listed as >100 hours due to insufficient terminal end phase data through 24 hours.
[c]Value in male Wistar rats

Table 2.2 Noncompartmental pharmacokinetic estimates obtained following 2.5 mg/kg IV injection of acMPAG (in MPA equivalents) in a 5% dextrose solution in male Wistar rats (n=3).

$AUC_{acMPAG0-\infty}$ (mg/mL*min)	1.3 ±0.2
$AUC_{MPA0-\infty}$ (mg/mL*min)	0.28 ± 0.03
$F_{acMPAG \longrightarrow MPA}$	0.88
CL_{acMPAG} (ml/min)	2.0 ± 0.3
Terminal $t_{1/2}$ (min)	26.1
$V_{ss\text{-}acMPAG}$ (mL)	19.6 ± 2.5
***V_{MPA} (mL)**	254.3 ± 31.3

*V_{MPA} was obtained following administration of 50 mg/kg MMF IV to male Wistar rats (n=3) (See Chapter 4)

F. References

Allison AC and Eugui EM. "Preferential Suppression of Lymphocyte Proliferation by Mycophenolic Acid and Predicted Long Term Effects of Mycophenoliate Mofetil in Transplantation." *Transplant Proc.* **1994,** 26(6), 3205-3210.

Bailey MJ, Dickinson RG. Acyl glucuronide reactivity in perspective: biological consequences. *Chem Biol Interact.* **2003,** 145, 117-137.

Bailey MJ, Worrall S, de Jersey J, Dickinson RG Zomepirac acyl glucuronide covalently modifies tubulin in vitro and in vivo and inhibits its assembly in an in vitro system. *Chem Biol Interact*. **1998,** 115, 153-166.

Boelsterli UA. Diclofenac-induced liver injury: a paradigm of idiosyncratic drug toxicity. *Toxicol Appl Pharmacol.* **2003,** 192, 307-322.

Boelsterli UA. Xenobiotic acyl glucuronides and acyl CoA thioesters as protein-reactive metabolites with the potential to cause idiosyncratic drug reactions. *Curr Drug Metab.* **2002,** 3, 439-450.

Cannell GR, Bailey MJ, Dickinson RG. Inhibition of tubulin assembly and covalent binding to microtubular protein by valproic acid glucuronide in vitro. *Life Sci.* **2002,** 71, 2633-2643.

Cannell GR, Vesey DA, Dickinson RG. Inhibition of proliferation of HT-29 colon adenocarcinoma cells by carboxylate NSAIDs and their acyl glucuronides. *Life Sci.* **2001,** 70, 37-48.

Castillo M, Smith PC. Disposition and reactivity of ibuprofen and ibufenac acyl glucuronides in vivo in the rhesus monkey and in vitro with human serum albumin. *Drug Metab Dispos.* **1995,** 23, 566-572.

Chiou YJ, Tomer KB, Smith PC. Effect of nonenzymatic glycation of albumin and superoxide dismutase by glucuronic acid and suprofen acyl glucuronide on their functions in vitro. *Chem Biol Interact.* **1999,** 121, 141-159.

Davies NM, Grinyó J, Heading R, Maes B, Meier-Kriesche HU, Oellerich M. Gastrointestinal side effects of mycophenolic acid in renal transplant patients: a reappraisal. *Nephrol Dial Transplant.* **2007,** 22, 2440-2448.

de Loor H, Naesens M, Verbeke K, Vanrenterghem Y, Kuypers DR. Stability of mycophenolic acid and glucuronide metabolites in human plasma and the impact of deproteinization methodology. *Clin Chim Acta.* **2008,** 389, 87-92.

Dickinson RG. Acyl glucuronide conjugates: reactive metabolites of non-steroidal anti-inflammatory drugs. *Proc West Pharmacol Soc.* **1993,** 36, 157-162.

Dickinson RG, Baker PV, King AR. Studies on the reactivity of acyl glucuronides--VII. Salicyl acyl glucuronide reactivity in vitro and covalent binding of salicylic acid to plasma protein of humans taking aspirin. *Biochem Pharmacol.* **1994,** 47, 469-476.

Dickinson RG, King AR. Studies on the reactivity of acyl glucuronides--V. Glucuronide-derived covalent binding of diflunisal to bladder tissue of rats and its modulation by urinary pH and beta-glucuronidase. *Biochem Pharmacol.* **1993,** 46, 1175-1182.

Djebli N, Picard N, Rérolle JP, Le Meur Y, Marquet P. Influence of the UGT2B7 promoter region and exon 2 polymorphisms and comedications on Acyl-MPAG production in vitro and in adult renal transplant patients. *Pharmacogenet Genomics*. **2007,**17, 321-330.

Dong JQ, Liu J, Smith PC. Role of benoxaprofen and flunoxaprofen acyl glucuronides in covalent binding to rat plasma and liver proteins in vivo. *Biochem Pharmacol.* **2005,** 70, 937-48.

Dutton GJ. *Glucuronidation of Drugs and Other Compounds.* CRC Press, Baco Raton, FL. 1980.

Faed EM. Properties of acyl glucuronides: implications for studies of the pharmacokinetics and metabolism of acidic drugs. *Drug Metab Rev*. **1984,** 15, 1213-1249.

González-Roncero FM, Govantes MA, Chaves VC, Palomo PP, Serra MB. Influence of renal insufficiency on pharmacokinetics of ACYL-glucuronide metabolite of mycophenolic acid in renal transplant patients. *Transplant Proc.* **2007,** 39, 2176-2178.

Hantash B, Fiorentino D. Liver enzyme abnormalities in patients with atopic dermatitis treated with mycophenolate mofetil. *Arch Dermatol*. **2006,** 142, 109-110.

Hasegawa J, Smith PC, Benet LZ. Apparent intramolecular acyl migration of zomepirac glucuronide. *Drug Metab Dispos*. **1982,** 10, 469-473.

Heller T, van Gelder T, Budde K, de Fijter JW, Kuypers D, Arns W, Schmidt J, Rostaing L, Powis SH, Claesson K, Macphee IA, Pohanka E, Engelmayer J, Brandhorst G, Oellerich M, Armstrong VW. Plasma concentrations of mycophenolic acid acyl glucuronide are not associated with diarrhea in renal transplant recipients. *Am J Transplant.* **2007,** 7, 1822-1831.

Jaggi R, Addison RS, King AR, Suthers BD, Dickinson RG. Conjugation of desmethylnaproxen in the rat--a novel acyl glucuronide-sulfate diconjugate as a major biliary metabolite. *Drug Metab Dispos.* **2002,** 30, 161-166.

King AR, Dickinson RG. Studies on the reactivity of acyl glucuronides--IV. Covalent binding of diflunisal to tissues of the rat. *Biochem Pharmacol.* **1993,** 45, 1043-1047.

King AR, Dickinson RG. The utility of the bile-exteriorized rat as a source of reactive acyl glucuronides: studies with zomepirac. *J Pharmacol Toxicol Methods*. **1996,** 36, 131-136.

Kittlemann M., Rheinegger U., Espigat A., Oberer L., Aichholz R., Francotte E., Ghisalba O. Preparative enzymatic synthesis of the acyl glucuronide of mycophenolic acid. *Ad*V *Synth Catal.* **2003,** 345, 825-829.

Kobayashi M, Saitoh H, Kobayashi M, Tadano K, Takahashi Y, Hirano T. Cyclosporin A, but not tacrolimus, inhibits the biliary excretion of mycophenolic acid glucuronide possibly mediated by multidrug resistance-associated protein 2 in rats. *J Pharmacol Exp Ther.* **2004,** 309, 1029-1035.

Kuypers DR, Vanrenterghem Y, Squifflet JP, Mourad M, Abramowicz D, Oellerich M, Armstrong V, Shipkova M, Daems J. Twelve-month evaluation of the clinical pharmacokinetics of total and free mycophenolic acid and its glucuronide metabolites in renal allograft recipients on low dose tacrolimus in combination with mycophenolate mofetil. *Ther Drug Monit.* **2003,** 25, 609-622.

Liu JH, Malone RS, Stallings H and Smith PC. Influence of Renal Failure in Rats on the Disposition of Salicyl Acyl Glucuronide and Covalent Binding of Salicylate to Plasma Proteins. *J Pharmacol Exp Ther.* **1996,** 278, 277-283.

Mayer S, Mutschler E, Benet LZ, Sphahn-Langguth H. In vitro and in vivo irreversible plasma protein binding of beclobric acid enantiomers. *Chirality.* **1993,** 5, 120-125.

Miles KK, Kessler FK, Smith PC, Ritter JK. Characterization of rat intestinal microsomal UDP-glucuronosyltransferase activity toward mycophenolic acid. *Drug Metab Dispos*. **2006,** 34, 1632-1639.

Mizuma T, Benet LZ, Lin ET. Interaction of human serum albumin with furosemide glucuronide: a role of albumin in isomerization, hydrolysis, reversible binding and irreversible binding of a 1-O-acyl glucuronide metabolite. *Biopharm Drug Dispos.* **1999,** 20, 131-136.

Morath C, Schwenger V, Beimler J, Mehrabi A, Schmidt J, Zeier M, Muranyi W. Antifibrotic actions of mycophenolic acid. *Clin Transplant*. **2006,** 20 Suppl 17, 25-29.

Oellerich M, Shipkova M, Schütz E, Wieland E, Weber L, Tönshoff B, Armstrong VW. Pharmacokinetic and metabolic investigations of mycophenolic acid in pediatric patients after renal transplantation: implications for therapeutic drug monitoring. *Ther Drug Monit*. **2000,** 22, 20-26. Erratum in: *Ther Drug Monit.* **2000,** 22, 500.

Ritter JK. Intestinal UGTs as potential modifiers of pharmacokinetics and biological responses to drugs and xenobiotics. *Expert Opin Drug Metab Toxicol.* **2007,** 3, 93-107.

Shipkova M, Armstrong VW, Oellerich M, Wieland E. Acyl glucuronide drug metabolites: toxicological and analytical implications. *Ther Drug Monit.* **2003,** 25, 1-16.

Shipkova M, Armstrong VW, Schneider T, Niedmann PD, Schütz E, Wieland E, Oellerich M. Stability of mycophenolic acid and mycophenolic acid glucuronide in human plasma. *Clin Chem*. **1999,** 45, 127-129.

Shipkova M, Armstrong VW, Weber L, Niedmann PD, Wieland E, Haley J, Tönshoff B, Oellerich M. Pharmacokinetics and protein adduct formation of the pharmacologically active acyl glucuronide metabolite of mycophenolic acid in pediatric renal transplant recipients. *Ther Drug Monit.* **2002,** 24, 390-399.

Shipkova M, Beck H, Voland A, Armstrong VW, Gröne HJ, Oellerich M, Wieland E. Identification of protein targets for mycophenolic acid acyl glucuronide in rat liver and colon tissue. *Proteomics.* **2004,** 4, 2728-2738.

Shipkova M, Schütz E, Armstrong VW, Niedmann PD, Oellerich M, Wieland E. Determination of the acyl glucuronide metabolite of mycophenolic acid in human plasma by HPLC and Emit. *Clin Chem.* **2000,** 46, 365-372.

Shipkova M, Wieland E, Schütz E, Wiese C, Niedmann PD, Oellerich M, Armstrong VW. The acyl glucuronide metabolite of mycophenolic acid inhibits the proliferation of human mononuclear leukocytes. *Transplant Proc.* **2001,** 33, 1080-1081.

Schütz E, Shipkova M, Armstrong VW, Wieland E, Oellerich M. Identification of a pharmacologically active metabolite of mycophenolic acid in plasma of transplant recipients treated with mycophenolate mofetil. *Clin Chem.* **1999,** 45, 419-422.

Sinclair KA, Caldwell J. The formation of beta-glucuronidase resistant glucuronides by the intramolecular rearrangement of glucuronic acid conjugates at mild alkaline pH. *Biochem Pharmacol*. **1982,** 31, 953-957.

Smith PC, Benet LZ, McDonagh AF. Covalent binding of zomepirac glucuronide to proteins: evidence for a Schiff base mechanism. *Drug Metab Dispos.* **1990,** 18, 639-644.

Smith PC and Liu JH. Covalent binding of suprofen acyl glucuronide to albumin in vitro. *Xenobiotica.* **1993,** 23, 337-348.

Smith PC, McDonagh AF, Benet LZ. Irreversible binding of zomepirac to plasma protein in vitro and in vivo. *J Clin Invest.* **1986,** 77, 934-9

Smith PC, Wang C. Nonenzymic glycation of albumin by acyl glucuronides in vitro. Comparison of reactions with reducing sugars. *Biochem Pharmacol.* **1992,** 44, 1661-8.

Spahn-Langguth H, Dahms M, Hermening A. Acyl glucuronides: covalent binding and its potential relevance. *Adv Exp Med Biol.* **1992,** 387, 313-328.

Staatz CE, Tett SE. Clinical pharmacokinetics and pharmacodynamics of mycophenolate in solid organ transplant recipients. *Clin Pharmacokinet.* **2007,** 46, 13-58.

Stern ST, Tallman MN, Miles KK, Ritter JK, Dupuis RE, Smith PC. Gender-related differences in mycophenolate mofetil-induced gastrointestinal toxicity in rats. *Drug Metab Dispos.* **2007,** 35, 449-454.

Treinen-Moslen M, Kanz MF. Intestinal tract injury by drugs: Importance of metabolite delivery by yellow bile road. *Pharmacol Ther*. **2006,** 112, 649-667.

Wade LT, Kenna JG, Caldwell J. Immunochemical identification of mouse hepatic protein adducts derived from the nonsteroidal anti-inflammatory drugs diclofenac, sulindac, and ibuprofen. *Chem Res Toxicol.* **1997,** 10, 546-555.

Wang M, Dickinson RG. Bile duct ligation promotes covalent drug-protein adduct formation in plasma but not in liver of rats given zomepirac. *Life Sci.* **2000,** 68, 525-537.

Wieland E, Shipkova M, Schellhaas U, Schütz E, Niedmann PD, Armstrong VW, Oellerich M (2000) Induction of cytokine release by the acyl glucuronide of mycophenolic acid: a link to side effects? *Clin Biochem.* **33**: 107-113.

Williams AM, Dickinson RG. Studies on the reactivity of acyl glucuronides--VI. Modulation of reversible and covalent interaction of diflunisal acyl glucuronide

and its isomers with human plasma protein in vitro. *Biochem Pharmacol.* **1994,** 47, 457-467.

Williams AM, Worrall S, De Jersey J, Dickinson RG. Studies on the reactivity of acyl glucuronides--VIII. Generation of an antiserum for the detection of diflunisal-modified proteins in diflunisal-dosed rats. *Biochem Pharmacol.* **1995,** 49, 209-217.

Wiwattanawongsa K, Heinzen EL, Kemp DC, Dupuis RE, Smith PC. Determination of mycophenolic acid and its phenol glucuronide metabolite in human plasma and urine by high-performance liquid chromatography. *J Chromatogr B Biomed Sci Appl*. **2001,** 763, 35-45.

Worrall S, Dickinson RG. Rat serum albumin modified by diflunisal acyl glucuronide is immunogenic in rats. *Life Sci.* **1995***,* 56, 1921-1930.

Young CJ and Sollinger HW. RS-61443: A New Immunosuppressive Agent. *Transplant Proc.* **1994***,* 26, 3144-3146.

Zwerner J, Fiorentino D, Mycophenolate mofetil. *Dermatol Ther*. **2007,** 20, 229-238.

CHAPTER 3

QUANTIFICATION OF UDP-GLUCURONOSYLTRANSFERASE ENZYME EXPRESSION LEVELS WITHIN HUMAN LIVER, INTESTINAL AND KIDNEY MICROSOMES USING nanoLC TANDEM MASS SPECTROMETRY

A. INTRODUCTION

UGT enzymes catalyze the formation of glucuronide conjugates of Phase II metabolism. Through the actions of the cofactor uridine disphosphate glucuronide acid (UDPGa) and UGT enzymes, glucuronidation encompasses the most common and clinically important of the Phase II metabolic pathways. In humans, the UGT genome consists of two families and three subfamilies. The UGT1A locus found on chromosome 2q37 encodes for nine functional enzymes located throughout the body and is responsible for converting a large number of endogenous and exogenous compounds to more hydrophilic conjugates, ultimately for excretion outside the body (Owens and Ritter, 1995). Traditional quantification methods have been used to evaluate relative hUGT levels including Western blots, ELISA and RT-PCR studies, but these methods lack the sensitivity, reproducibility and dynamic range to properly examine expression. Furthermore, the correlation between mRNA levels measured using RT-PCR and protein expression is often poor, making these methods unreliable for evaluation of protein expression in biological systems (Izukawa et al., 2009). In addition, the high degree of sequence homology between hUGT enzymes (as high as 94% in some isoforms) prevents the raising of antibodies against specific UGT isoforms, with few exceptions (Tukey et al., 2000).

Traditional approaches to protein quantification include differential gel electrophoresis (DIGE) which involves separation through 2D-gel electrophoresis followed by fluorescent tagging of lysine side chains (Bantscheff et al., 2007). While multiple proteins may be monitored through the DIGE technique through

the use of alternate fluorescent tags, it is often difficult to distinguish high and low molecular weight proteins, and DIGE often lacks the sensitivity to detect low abundant proteins (Wu et al., 2006). In recent years, advances in electrospray ionization (ESI), coupled with sensitive tandem mass spectrometry (MS/MS), has allowed for the development of several different approaches at relative quantification of proteins. Methods for relative protein quantification within cells include *in vivo* metabolic labeling within enriched media (C^{13}, N^{15}, O^{18}), followed by digestion and quantification of labeled peptides to evaluate changing expression of proteins of interest (Beynon et al., 2005; Gu et al., 2004; Hsu et al., 2005; Huttlin et al., 2009). These methods have been used to determine expression changes in myoglobins, immune response, HIV levels, glycoproteins and mitochondrial proteins. Recently, label-free techniques have also been used that can evaluate global expression changes, but these methods are not commonly employed due to variability across instrumentation platforms and ion suppression from complex matrices (Bantscheff et al., 2007).

Along with the use of capillary LC-MS/MS for relative quantification for global proteomics, stable isotope internal standards also have been developed for targeted absolute quantitative proteomics. Labeling techniques such as ICAT and iTRAQ can be utilized for relative quantification or for absolute quantification if a known amount of targeted peptide is added during sample preparation (Gygi et al., 1999; Hardt et al., 2005; Jenkins et al., 2006; Zieske et al., 2006). However, because ICAT reagents only target peptide with cysteine groups, the number of potential targeted peptides is limited (Wu et al., 2006). Furthermore,

iTRAQ methods can encounter difficulties in precursor ion selection in complex matrices (Wu et al., 2006). Although both ICAT and iTRAQ methods have greatly increased sensitivity and selectivity of peptide/protein analysis when compared with gel based methods further improvement and more general approaches are being developed (Wu et al., 2006).

Other approaches using stable isotope labels have had more recent success with quantifying proteins and peptides. Barr et al. were able to accurately quantify apolipoprotein A-1 using unique heavy-labeled peptides (Barr et al., 1996). Following these initial experiments, both C-reactive protein (CRP) and PSA were quantified within human plasma by preselecting heavy isotope-labeled internal standards added prior to a tryptic protein digestion (Barnidge et al., 2004; Kuhn et al., 2004). Using sensitive capillary LC coupled with MS/MS, it was found that using isotope dilution mass spectrometry, the concentration levels of PSA and CRP were comparable to immunoassay with lower detection limits (Barnidge et al., 2004; Kuhn et al., 2004). These methods fostered the development of stable isotope labeling with amino acids in cell culture (SILAC), absolute quantification (AQUA) and Quantitative Concatamer (QCAT) stable isotope standards and have been applied more recently for determining gonadotropin releasing hormone (GnRH) across different MS platforms (Thomas et al., 2008). While QCAT standards require development of recombinant protein expression in cell lines to produce heavy labeled internal standard proteins for quantification, heavy isotope-labeled peptides can be

readily prepared following preselection using standard peptide synthesis methods.

The continued development of quantitative proteomics is significant for biological scientists interested in understanding precise levels of protein expression. By being able to precisely quantify enzymes involved in drug metabolism, scientists will be better able to describe differences between species to evaluate the effects of induction and inhibition, and to provide more accurate *in vitro* and *in vivo* predictions of drug elimination. Furthermore, the use of targeted absolute quantitative proteomics also may be used for quantification of enzymes for which specific antibodies are unavailable and for proteins yet to be discovered. These techniques will continue to open new avenues for drug metabolism studies that will now be able to directly establish relationships between enzymes and metabolite levels.

While capillary LC connected to triple quadrupole tandem MS is common instrumentation for MRM quantification, other platforms have been successfully implemented for these purposes. LC-MS/MS has been applied using quadrupole time of flight mass spectrometry (Q-TOF) for both metabolite detection and peptide quantification (Jeanville et al., 2000; Spaulding et al., 2006). In addition, a new MS platform that couples capillary LC to a linear ion trap time of flight mass spectrometer (LIT-TOF) from Hitachi Hi-Technologies has been utilized for both qualitative and quantitative mass spectrometry (Deguchi et al., 2007; Ito H et al., 2006; Ito S et al., 2008). Most recently, Ito et al. were able to successfully quantify a novel glycosylated phospholipid and demonstrate that the LIT-TOF

platform was not only very sensitive, but also has a dynamic range approaching three orders of magnitude (Ito S et al., 2008).

We have previously demonstrated the utility of quantifying hUGTs using stable isotope standards and tandem MS (Fallon et al., 2008). While this method was successfully applied for quantification of two of the nine active human UGT isoforms, it is necessary to extend this method for the remaining hUGT1A isoforms to not only better examine the relationship within and across species, but to also be able to quantify other UGT1A isoforms that lack a specific antibodies. By taking advantage of the increased sensitivity offered by capillary LC compared to standard bore HPLC and extending the LC gradient for better separation of labeled and unlabeled peptides, we will be able to selectively quantify all hUGT1As in a single chromatographic run. Here we present a method to quantify the entire hUGT1A proteome of nine active UGTs using capillary LC coupled to a LIT-TOF mass spectrometer using the extracted MRM mode.

B. METHODS

Materials

Analytical grade acetonitrile and methyl alcohol (anhydrous) were purchased from Fisher Scientific Co. (Pittsburg, PA). Ammonium bicarbonate, dithiothreitol, iodoacetamide, ammonium hydroxide, formic acid, 2,2,2-trifluoroethanol (TFE) and TPCK (L-1-tosylamido-2-phenylethyl chloromethyl ketone) treated trypsin from bovine pancreas (≥ 10,000 BAEE units/mg protein) were purchased from Sigma-Aldrich Co. (St. Louis, MO). Bond Elut solid phase

extraction cartridges (C18 100mg, 1mL) were purchased from Varian, Inc. Recombinant UGTs 1A1, 1A3, 1A4, 1A6, 1A7, 1A8, 1A9, 1A10 and control supersomes were purchased from BD Biosciences (San Jose, CA). Human liver microsomes (HLMs) (20 mg/mL) were purchased from BD Biosciences (pool of 33) and Xenotech LLC (Lenexa, KA) (pool of 50). A human liver microsome library of individual donors (n=10, 20 mg/mL) was purchased from Human Biologics International (Scottsdale, AZ). Human kidney microsomes were purchased from BD Biosciences (pool of 33, 20 mg/mL) and a human intestinal microsome library of individual donors (n=3, mixed gender) were graciously donated by Dr. Mary Paine (UNC-Chapel Hill, Chapel Hill, NC) (Paine et al., 2006). Pooled human intestinal microsomes (HIMs) were obtained from Xenotech LLC (Lenexa, KA) (8 donors, mixed gender). Protein concentrations were determined using the Pierce BCA Protein assay Kit, in which bovine serum albumin is used as the standard.

Instrumentation

Samples were analyzed using capillary LC attached to a linear ion trap time of flight (LIT-TOF) mass spectrometer (Hitachi High-Technologies, Tokyo, Japan). The LC column was a monolithic C-18 column (GL Sciences, Tokyo, Japan, 150 mm, 0.075 mm ID). The instrument was operated in positive ion mode for multiple reaction monitoring (MRM) analysis. Data analysis was performed using NanoFrontier LD-ECD Data Processing software (Hitachi High Technologies, Tokyo, Japan)

Stable Isotope Labeled Internal Standards

Synthetic peptide standards (8-15 mer), each containing one amino acid heavy labeled with ^{13}C [98%] and ^{15}N [95%], were purchased from Thermo Electron (Thermo Scientific, Waltham, MA) using methods and selection criteria as previously reported (Fallon et al., 2008). For each UGT isoform, two unique peptides were purchased for analysis and validation. The peptides were selected according to manufacturer recommendations and previously published guidelines (Beynon et al., 2005; Gerber et al., 2003). Amino acid sequences for the nine UGT1A isoforms were obtained using the Universal Protein Resource Knowledge Base (UniProtKB). Peptide uniqueness of tryptic fragments was verified by NCBI Blast (National Center for Biotechnology Information Basic Local Alignment Search Tool). Amino acid analysis on each peptide to determine sample purity which was conducted at the Center for Structural Biology, Wake Forest University School of Medicine, Winston-Salem, NC. Some amino acids were excluded from the analysis because of known acid hydrolysis effects (e.g., bonds between isoleucine and valine [peptide 3] are not easily broken) and the possible cyclization and isomerization of aspartic acid adjacent to glycine or isoleucine (peptides 2 and 3).

Known variable single nucleotide polymorphisms (SNPs) were also considered during peptide selection. While at the time of purchase there were no known interferences with SNPs along the targeted protein sequence, reports

indicate that there are potential conflicts due to polymorphisms for UGT1A1 (Peptide 2, frequency <1%), UGT1A6 (Peptide 4, frequency ~4% in Caucasians) and UGT1A7 (Peptide 11, frequency ~2% in African Americans) (Kadakol et al., 2000; Krishnaswamy et al., 2006; Villeneuve et al., 2007). Furthermore, while it is initially intended to obtain two unique peptides per isoform, the dearth of unique peptides for UGT1A8 and UGT1A9 that are amendable to the LC-MS approach only provided one unique peptide for these isoforms along with one peptide that is shared between the two enzymes.

Sample Preparation

Aliquots of 50 µg of microsomal protein, recombinant enzyme or UGT control supersomes were denatured and digested as previously reported with some modifications (Fallon et al., 2008). Samples of digested protein matrix with heavy labeled peptides added as internal standards, 10 pmol for each peptide, excluding peptide 16 and 17, (Table 3.1) and the residual acetonitrile was removed by evaporation under nitrogen for ~5 min were then denatured and reduced by heating at 95 ºC for 10 min in 5 mM dithiothreitol (sample volume 90 µL; buffer 50 mM ammonium bicarbonate). This was followed by alkylation with 100 mM iodoacetamide stock for 20 min in the dark. Samples were dissolved in 150 µL 50 mM ammonium bicarbonate (volume brought to 150 µL with HPLC water); with trypsin enzyme/protein ratio = 1:50; for 4 h at 37 ºC. The reaction was then quenched by addition of 50 µL acetonitrile. Following centrifugation at 1000*g* for 10 min, the organic content was removed by evaporation under nitrogen for ~10 min. An aliquot of 0.9 mL of 50 mM ammonium bicarbonate was

then added in preparation for solid phase extraction. SPE cartridges were conditioned with methanol and distilled water. Samples were then added and the cartridges were washed with 1 mL 10 mM ammonium acetate (pH 3) then eluted with acetonitrile/25 mM formic acid (40:60). The eluate was evaporated to dryness under nitrogen at 42ºC in a water bath, and samples were reconstituted with 250 µL (80:20) acetonitrile/25 mM formic acid at pH 3 (pH was adjusted to 3 by drop wise addition of ammonium hydroxide) to minimize sample loss from glass tubes. Following initial reconstitution, samples were transferred and dried under nitrogen at 42 ºC, then reconstituted in 50 µL (15:85) acetonitrile/25 mM formic acid at pH 3. Samples were stored at -20 ºC until analyzed by LC-MS/MS.

MRM Selection

All peptide heavy labeled standards were directly infused into the LIT-TOF mass spectrometer at a rate of 2 µL/min for MRM and MS optimization. Upon infusion, a vast majority of the peptide standards were doubly charged. Peptide 5, 16 and 17, were found to be triply charged or greater and were ultimately excluded because of inadequate MRM selection. For each peptide, two MRMs above 500 m/z were selected to be used for quantification. MRM selections were then confirmed following an optimized LC gradient elution of a solution of 10 pmole aliquots of each selected peptide. These peptides were then subject to MRM spectrum analysis using the LIT-TOF in scanning mode.

LC/MS Conditions

The mobile phase used for analysis consisted of 25 mM formic acid in water (solvent A) and acetonitrile (solvent B). A NanoFrontier L series (Hitachi-High Technologies, Tokyo, Japan) using a nano-flow HPLC was coupled to an AT10PV nano-flow gradient generator and connected to a LIT-TOF instrument with an electrospray ion source (Deguchi et al., 2004). An Upchurch M-435 microinjection valve (Upchurch Scientific, Oak Harbor, WA) was used as the sample injector (Ito et al. 2008). A 1 µL injection (approximately 0.5 µg of digested protein) was loaded onto a 5 cm trap column (C18, 2.1 mm ID, 5 µ particle size) at a rate of 10 µL /min for 4 minutes. The sample was then transferred onto the analytical column and analyzed under the following linear gradient conditions, 0 min, 5% B; 30 min, 55% B; 30.1 min, 100% B; 40 min, 100% B; 40.1 min, 5% B and then equilibrated until 65 min. The gradient pump maintained a 100 µL/min flow rate while the nanoflow pump was run at 200 nL/min during analysis. MS conditions were similar to a previous report by Ito et al. (Ito et al., 2008) except the AP1 temperature was set a 120ºC, with an isolation time of 50 ms.

Calibration Curves

Recombinant enzymes of all UGT1A isoforms excluding 1A5 (not commercially available) were used to establish recombinant enzyme calibration curve points representative of 0.19 µg, 0.75 µg, 1.5 µg, 3.0 µg and 6.0 µg of recombinant microsomal protein. To keep volumes consistent for the tryptic

digests, each recombinant enzyme was taken through a series of serial dilutions using tris buffer, pH 7.4. Prior to the tryptic digestion, 10 pmol of each heavy labeled peptide standard was added and the response ratio between the labeled and unlabeled peptides was used to establish a calibration curve and to verify linearity. Equality of response between the labeled and unlabeled peptides along with complete tryptic digestion was assumed in the creation of the calibration curves. Calibration curves were constructed by comparing response of unlabeled peak area to labeled peak area for each MRM selected. These MRMs standard curves were calculated in units of pmol/mg protein (microsomal protein) and used the response ratio between unlabeled and labeled peptides in the unknown microsomal protein fitted to the calibration curves to calculate enzyme concentrations.

Ion Suppression/Matrix Effects

Aliquots containing 25 µg of each recombinant enzyme microsomes were digested as described earlier in two separate groups in triplicate. The internal standard of heavy labeled peptides was added at either before the tryptic digest or following reconstitution. The internal standard solution was also added to a 0.1 mL aliquot of the reconstitution buffer, in triplicate, with peak areas of the heavy peptides serving as a baseline.

Interday and Intraday Variability

To examine intraday variability, five replicate calibration curves along with human liver, intestinal and kidney microsomes (n=5) were digested within the same day and analyzed on the nanoLC LIT-TOF instrumentation. Individual peptide measurements for four of the UGT1A isoforms using two peptides for quantification were averaged to obtain final enzyme expression levels (Table 3.5). Interday variability experiments were carried out in a similar manner with five replicate standard curves along with digests of human liver microsomes analyzed over five separate analyses and days.

Human Liver and Intestinal Microsomal Library

To compare the newly established method to the initial method established by Fallon et al., a library of ten individual liver microsomal donors were digested and analyzed in duplicate (Fallon et al., 2008). Individual donors of intestinal microsomes (n=3) were also digested and analyzed in duplicate using the response ratios generated to compare against calibration curves analyzed in duplicate and prepared within the same day. For the human liver microsomal library, the enzyme expression levels of hUGT1A1 and hUGT1A6 were compared against those results obtained by the previous assay (Fallon et al., 2008).

C. RESULTS

MRM Scheduling

Following initial scouting gradient runs and MRM optimization on the LIT-TOF, it was found that peptides of interest eluted between 17 and 32 minutes. Further increases in the %B at the beginning of the LC gradient or increases in slope of the gradient to decrease run times resulted in band broadening or loss of signal. Peptides eluted consistently with six separate time windows (T_1 0-17 min, T_2 17-19.5 min, T_3 19.5-22.0 min, T_4 22.1-26.4 min and T_5 26.5-28 min, T_6 28.1-32 min) and were optimized using MRM scheduling with NanoFrontier LD-ECD software. Extraction of selected MRMs from a single chromatographic run is shown in Figure 3.1. Peptide 5 and 14 were not consistently detectable using the LC gradient due to insufficient singly charged MRMs and were excluded from sample analysis. MRM time segments assigned are listed in Table 3.2 and were used for the remaining analyses.

Calibration Curves

Calibrants for each of the hUGT isoforms were quantified using procedures described in METHODS. Initial curves were converted to pmol/mg protein units for enzyme concentration calculations. Each peptide produced two MRM calibration curves resulting in as many as four curves per UGT isoform. For each interday enzyme measurement, curves performed in duplicate produced replicate expression data which was then averaged between the two MRMs per peptide to obtain final enzyme concentration levels. Calibration

curves produced a linear range between 0.19 µg and 6.0 µg of recombinant microsomal matrix with a LOD approximately one third of the lowest concentration on the calibration curve (approximately 1 pmol enzyme/mg protein). Calibration curves were generally similar between MRMs for each peptide, and MRM ratios between labeled standards and unlabeled peptide were averaged to generate expression ratios (Table 3.5). Any peptides that did not generate quality product ion scans, stable and reproducible LC retention times or sufficient sensitivity or precise quantification (%C.V. <25% with repeat sampling) were excluded from all hUGT enzymatic analyses. All R^2 values for calibration curves were between 0.96 and 0.99 including the hUGT1A9 intraday calibration curve indicated in Fig (3.3).

Ion Suppression

Ion suppression varied between time segments, but was most evident for segment 4 and 6. While peptide 1 demonstrated significant ion suppression (92% for both MRMs), most ions eluting during segment 4 and 6 demonstrated >75% ion suppression and ion some cases ion suppression was >90% (Table 3.2). Peptides eluting early benefited from minimal ion suppression and recovery of these peptides was generally >75%, which is similar to our previous assay validation studies (Fallon et al., 2008). While ion suppression levels were slightly lower in the 25 µg recombinant microsomal protein samples, compared to the human liver microsomal protein samples, the recombinant microsomal protein ion suppression studies are presented due to the limitations in linearity

discovered in the calibration curves. Because the linear range of the method was established using the calibrations curves constructed with digests of recombinant microsomal protein, the recombinant microsomal protein matrix was used to determine loss of signal due to ion suppression.

Intraday and Interday Variability

Intraday variability measurements (n=5) for the hUGTs provided reproducible results with minimal variation (<25%) between samples. hUGT1A1 enzyme levels were 22.7 pmol/mg protein in human liver microsomes (Table 3.3) which is similar to what we reported earlier (Fallon et al., 2008). hUGT1A6 levels were 8.5 pmol/mg protein (Table 3.3). However, hUGT1A6 demonstrated less variability (16.7% C.V. compared to 19.9% of hUGT1A1, (Table 3.3)) but was not as reproducible as the other isoforms found in the liver. Peptides for isoforms hUGT1A7, hUGT1A8 and hUGT1A10 were below detection limits in the liver, which agree with previous reports of their lack of UGT liver expression based on mRNA (Ohno et al., 2009; Strassburg et al., 1997; Tukey et al., 2000). In addition, UGT1A3, UGT1A4 and UGT1A5 were below detection limits in the intestine (Ohno et al., 2009; Tukey et al., 2000). In contrast, UGT1A3 and UGT1A5 were the only isoforms below detection limits in the kidney. With few exceptions, all C.V. values were below 20% for each of the UGT enzymes (Table 3.4). Intraday variability studies produced similar results both with regards to variability and expression (Table 3.3).

Human Liver, Intestine and Kidney UGT Expression

The data from liver microsomes indicated that hUGT1A1, hUGT1A9 and UGT1A5 consistently had the highest enzyme levels among the UGTs. While UGT1A3, UGT1A4 and UGT1A6 were readily detectable, their expression levels (3.2 pmol/mg protein for 1A3 to 8.5 pmol/mg protein for 1A6, (Table 3.3) were generally 50-75% lower when compared to the other three enzymes. UGT1A1 expression was the highest within the liver along with UGT1A3, UGT1A5 and UGT1A6. UGT1A8 was found at its highest levels within the intestine while UGT1A7, UGT1A9 and UGT1A10 were most extensively expressed in the kidney.

Human Liver and Intestinal Libraries

Expression studies from the human liver and intestinal libraries are shown in Table (3.4). UGT1A1 expression varied five fold (7.0 pmol/mg protein to 32.6 pmol/mg protein) which was the general trend for liver expression of the other measurable isoforms. An exception was UGT1A9, where variation was more than ten fold in the liver (9.0 pmol/mg protein to 96.4 pmol/mg protein in liver). Unlike in the liver library, the intestinal library enzyme expression data indicated less variability between patients. Most isoforms demonstrated between 1.5 to 3 fold variability between the lowest and highest concentration (Table 3.4). One exception was UGT1A8 which demonstrated five fold variability (1.9 pmol/mg

protein to 9.4 pmol/mg protein) in the intestine. Isoforms that were determined to be below detection limits within the pooled microsomal studies were also not detected within any of the individual library specimens.

To further validate the LIT-TOF based assay for UGT expression, UGT1A1 and UGT1A6 enzyme rank orders and enzymatic levels were compared between the current assay and the UGT1A1/1A6 assay previously developed on the ABI 3000 (Fallon et al., 2008). Both correlation plots indicated a strong correlation (r=.92 for UGT1A1, r=.75 for UGT1A6, Fig. (3.4). Furthermore, the rank orders for each isoform within the library specimens were very similar and most of the enzyme levels validated in the previous method varied <20% from the values of the current assay (Fallon et al., 2008).

Recombinant UGT Enzyme Concentrations

Using the calibration curves generated following digestion of recombinant microsomal protein, calibration curves were extrapolated to obtain UGT isoform expression levels in the recombinants. Based on the calibration curves, isoform concentration levels ranged from 0.83 nmol/mg protein to 2.74 nmol/mg protein indicating that recombinant microsomal protein stocks contained approximately 5-20% recombinant UGT protein (Table 3.7). Generally, isoforms expressed at high levels within the tested microsomal samples were found in high concentrations in the recombinants with the exception of UGT1A4 whose concentration in the recombinant microsomal protein stocks (2.23 nmol/mg

protein) ranked third among the recombinant UGT1A isoforms despite low expression levels in the liver, kidney and intestine (Table 3.5).

D. DISCUSSION

In recent years, the use of stable isotope internal standards with tandem MS methods to quantify biologically active proteins has become more common. The goal of this report was to develop a method that could successfully quantify all of the human UGT1A enzymes within a single chromatographic run using capillary LC-MS/MS, which is the preferred platform within the proteomics community (Bantscheff et al., 2007; Domon et al., 2006; Thomas et al., 2008). While triple quadrupole mass spectrometry has been applied for quantification in many investigations of quantitative proteomics via isotope dilution, hybrid instruments including the LIT-TOF used in this report have been applied for similar investigations and displayed the selectivity and sensitivity desired to quantify biological enzymes within complex matrices. Thus a range of MS platforms can be successfully employed for targeted quantitative proteomics.

The UGT1A protein sequence is 530 amino acids in length and consists of five exons, of which amino acids residing in the C terminus (exons 2-5) are shared between each 1A isoform (Tukey et al., 2000). The N terminal region is subject to individual enzyme splicing, resulting in the 9 unique active isoforms and 4 pseudogenes in humans (Owens and Ritter, 1995; Tukey and Strassburg, 2000). Because of this, amino acid sequences unique to each isoform are often a small list, making peptide selection limited. It is desired in targeted quantitative

proteomics to select two unique peptides and at least two MRMs over 500 m/z for optimal sensitivity and selectivity (Anderson and Hunter, 2006). However, the limited selection window for UGT1A8 and UGT1A9 resulted in the selection of only one unique peptide for each isoform along the peptide and the sequence TYSTSYT**L***EDLDR, which was shared between the two isoforms. Furthermore, peptides containing reactive/unstable amino acids such as methionine and cysteine, which are normally excluded based on selection criteria, were selected and employed due to a lack of unique peptides for some UGT1A isoforms.

Peptide 15 (FFTLTAYA**V***PWTQK), an internal standard for UGT1A4 that contains a tryptophan residue, would normally be excluded based on selection criteria, yet the peptide produced consistently linear standard curves (r^2>0.97, data not shown) and low C.V. values on interday and intraday variability testing (Table 3.4). Reproducible product ions could not be obtained for peptide 16 (VTLGYTQG**F***FETEHLLK) and peptide 17 (GHQVVV**L***TLEVNMYIK) because the parent ions from these peptides were from the +3 to +5 charge states, making both MRM analysis and chromatography cumbersome and often unresolvable. In addition, one peptide that was not successful was peptide 5 from UGT1A3 (HVLGHTQ**L***YFETEHFLK). This peptide was also beset by a quadruply charged parent ion as a result of multiple histidine residues within the sequence. Along with peptide 5, 16 and 17, peptide 10 (TYSTSYT**L***EDLDR) was excluded from UGT analysis due to lack of specificity for a particular isoform since its peptide sequence was shared by both UGT1A8 and UGT1A9. Often the best peptides of those employed for UGT analysis contained single or multiple

proline residues that exhibit the well documented “proline effect” that is responsible for favorable cleavage near proline sites under collision induced dissociation (CID) MS conditions (Vaisar and Urban, 1996). Based on our experience, optimal peptide selection is of the utmost importance for accurate quantification of proteins digested to peptides. While guidelines recommend that peptides as large as 16mer may be selected, it is often smaller peptides between 8-10mer in length containing proline and no reactive residues (C, M, W) that perform better for high sensitivity MRM based peptide quantification (Beynon et al., 2005; Gerber et al., 2003; Kamiie et al., 2008).

Initial analysis was performed with an extended gradient of 2-60% B over sixty minutes. Assay length (95 minute run time) and lack of signal intensity resulted in several alterations, including a higher starting %B, but this was again inadequate due to peak splitting and band broadening with the stable isotope standards. Following further modification, a 5-55% B gradient over thirty minutes provided both the highest signal intensity and shortest run time on the instrumentation. Peptides eluted between 17 and 32 minutes over five distinct time segments. To maximize MRM collections, eight to sixteen transitions were monitored over the five primary segments, enabling quantification of all UGT1As within a single chromatographic run. While the current LIT-TOF has a limit of monitoring 100 MRM transitions within a single chromatographic run, it proved useful to monitor the 66 MRM transitions needed to measure all of the peptides of interest within this study and could be applied for other proteomic investigations.

With the exception peptide 5, 16 and 18, all peptides generated calibration curves that were linear between 0.19 and 6.0 µg of recombinant microsomal protein. When the stable isotope calibrants were incorporated, this represented a range of 1 pmole to 140 pmole per mg protein. Because variability was <30% between the peptide MRMs monitored, MRM values for each UGT1A isoform were averaged to generate expression datasets. For peptides with only one unique peptide, two MRM measurements were averaged from the single peptide. The highest detected UGT concentration was 96.4 pmol/mg protein of UGT1A9 within the kidney; however, even this concentration was well within the linear range of the assay. Wang demonstrated that some CYP isoforms are expressed in much higher concentration than UGT enzymes (>300 pmol/mg protein), indicating that the digested protein levels may need to be adjusted between assays to remain within the linear range of some instruments (Wang et al., 2008).

Enzyme expression data generated for the liver, intestine and kidney generally agree with previous reports for both mRNA expression and *in vitro* glucuronidation profiles (Izukawa et al., 2009; Nakamura et al., 2008; Tukey and Strassburg, 2000; Wen et al., 2007). Within the liver, UGT1A1, 1A5 and 1A9 were consistently expressed at a higher level than 1A3, 1A4 and 1A6 (Table 3.3, 3.4 and Figure 3.5). While there have been conflicting reports of the predominately extrahepatic UGTs 1A7, 1A8 and 1A10 being present in the liver, none of these enzymes were detected in either pooled or individual HLMs (Strassburg et al., 1997; Strassburg et al., 1998; Li et al., 2008). Of particular note was the high level of expression for UGT1A5 (Figure 3.5), which has been

difficult to characterize and not successfully detected until recently (Finel et al., 2005). Within the liver, the highest variability in individual donor specimens was found with UGT1A1 and UGT1A9 isoforms, both which are polymorphic (Kadakol et al., 2000; Strassburg et al., 1997; Tukey et al., 2000; Villeneuve et al., 2007).

Within the intestinal tract, expression of UGT1A1 and 1A6 was approximately 35% of expression seen in livers, which concurs with our previous investigation into these isoforms (Fallon et al., 2008). Furthermore, previous studies by Wen et al. with etoposide, a UGT1A1 and 1A8 probe substrate indicated that the V_{max} of etoposide glucuronidation in the intestine was approximately 30% of liver levels (Wen et al., 2007). However, the low levels of UGT1A enzymes found within the recombinant microsomal protein stocks coupled with the difficulties in *in vitro/in vivo* activity extrapolations indicate that protein concentration may not always correlate well with protein activity when using recombinant microsomal protein in probe substrate and *in vitro* glucuronidation studies (Table 3.7) (Miners et al., 2006). While UGT1A1, 1A6, 1A7, 1A8, 1A9 and 1A10 were all detected within the intestine, levels were appreciably lower than liver hepatic enzyme levels, and only UGT1A8 was expressed at a higher level within the intestine than the other two tissues using microsomes. Individual patient levels of UGT1A8 were highly variable within the intestine, yet there have been few UGT1A8 polymorphisms reported with appreciable effects on glucuronidation (Lévesque et al., 2007). An additional mechanism or unreported polymorphism could be responsible for this large variation.

Expression levels within the kidney microsomes were much higher than the intestine and sometimes higher than seen in the liver. Particularly, UGT1A9 was expressed (81.4 pmol/mg protein, Figure 3.5) at a level nearly four fold that of the liver. While mRNA and protein correlation is often poor, recent reports characterizing UGT mRNA expression indicated UGT1A9 was highly expressed within the human kidney (Nakamura et al., 2008; Ohno and Nakajin, 2009). However, it is important to note that when making comparisons between mRNA assays and with the hUGT assay, one must take into account the numerous polymorphisms within the hUGT gene family that result in high expression variability in the tissue populations. Altered protein expression affected by SNPs or other polymorphisms in human tissues could account for the low level discrepancies in 1A3 expression within the intestine and kidney in both the UGT assay and mRNA values. In addition, some isoforms including 1A1 and 1A4 expressed at low levels within the kidney may benefit from the increased sensitivity using targeted proteomics (Nakamura et al., 2008; Ohno et al., 2009). Despite some differences in mRNA expression, UGT expression within the kidney coincides with MPA glucuronidation levels that are also three fold higher in the kidney compared to the liver and fifteen fold higher than those seen in the intestinal tract (Picard et al., 2005). Not only were enzyme levels highest in the kidney for UGT1A4, 1A7, 1A9 and 1A10, but only UGT1A3 and UGT1A5 were not detected, making the kidney a potentially important organ for clearance via glucuronidation in the body.

By combining the advantages of capillary LC coupled with the new LIT-TOF instrumentation, we developed and applied a method to detect all of the active human UGT1A isoforms within a single chromatographic assay. Our assay demonstrates acceptable variability (<25%) with comparable sensitivity relative to our earlier method performed using older triple quadrupole (ABI 3000) instrumentation. The use of capillary LC allowed for a dramatic reduction of protein needed for the assay without a loss of sensitivity. Furthermore, we are now able to compare absolute expression levels of UGTs within different tissues in humans that are comparable with previous reports of relative mRNA expression and RT-PCR studies. The significant levels of UGT expression within the kidney demonstrate that this organ could have a potentially important role in glucuronide disposition within the body. Liver expression was generally higher than levels seen within the intestine, but more UGT1A isoforms were detected in kidney compared with the liver. The data obtained here confirms previous reports of UGT1A5 expression in the liver (Nakamura et al., 2008; Ohno et al., 2009).

While the liver is seen as the primary organ involved in metabolite disposition, the importance of other organ systems within the body should not be underestimated. The emergence of novel targeted quantitative proteomic methods based upon LC-MS/MS will allow the explosion of protein expression studies, especially for the many proteins not amenable to developing specific antibodies. The ability to quantify specific proteins within and between species without a reliance on specific antibodies not only opens many new avenues of

research into xenobioltic metabolism but also within the areas of protein-protein interactions, enzyme regulation and induction/inhibition studies with proteins that were not previously amenable to antibody based assays.

E. ACKNOWLEDGEMENTS

This work was made possible through the NIH Training Grant T32-ES007126 and with the technical assistance of Takashi Baba, Shinya Ito and Dr. Gary Glish.

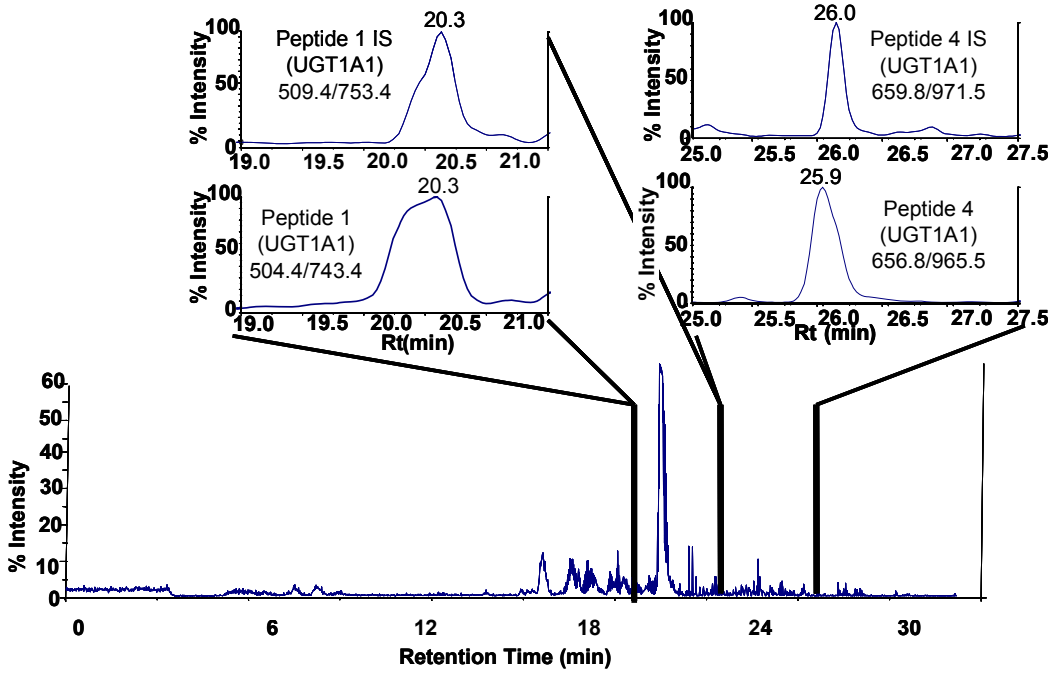

Figure 3.1. UGT isoforms and stable isotope standards were separated using segmented MRMs in the base peak chromatogram of a human liver microsomal digest. Five time segments (17-19.5 min, 19.6-22.5 min, 22.6-26 min, 26-28 min, and 28.1-32 min) were used for MRM scheduling. First extracted ion chromatogram (XIC) shows peptide 1 from UGT1A1, eluting at 20.3 min in segment 2 representing 22.7 pmol/mg protein. Labeled and unlabeled MRMs for the second XIC representing peptide 4 from UGT1A6 from segment 3 representing 8.5 pmol/mg protein.

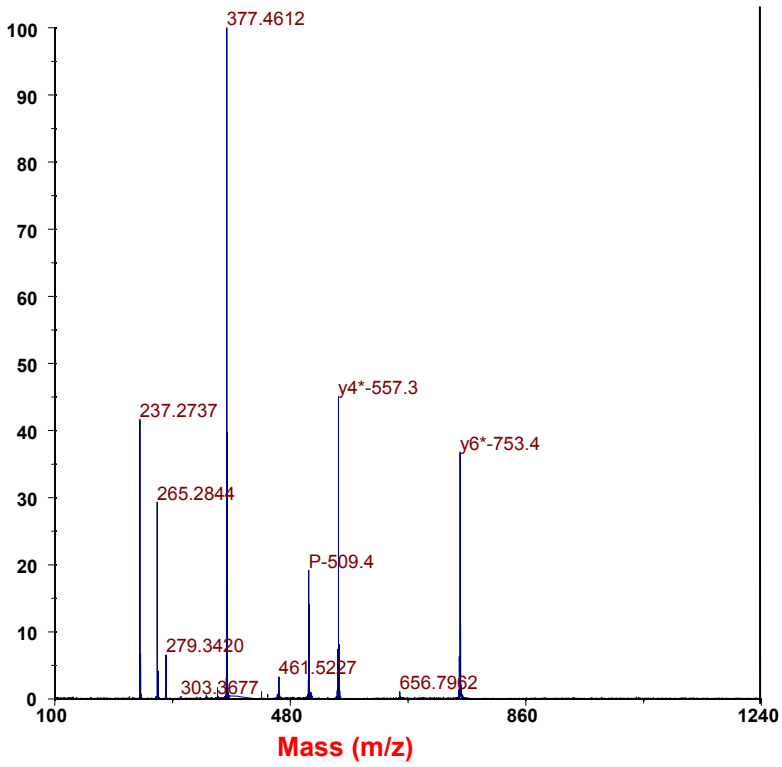

Figure 3.2. TOF spectrum analysis of peptide 1 (Table 3.1) following injection of 10 pmol of peptide on LC-MS/MS to confirm MRM optimization of 557.3 (y4) and 753.4 (y6) ions used for quantification.

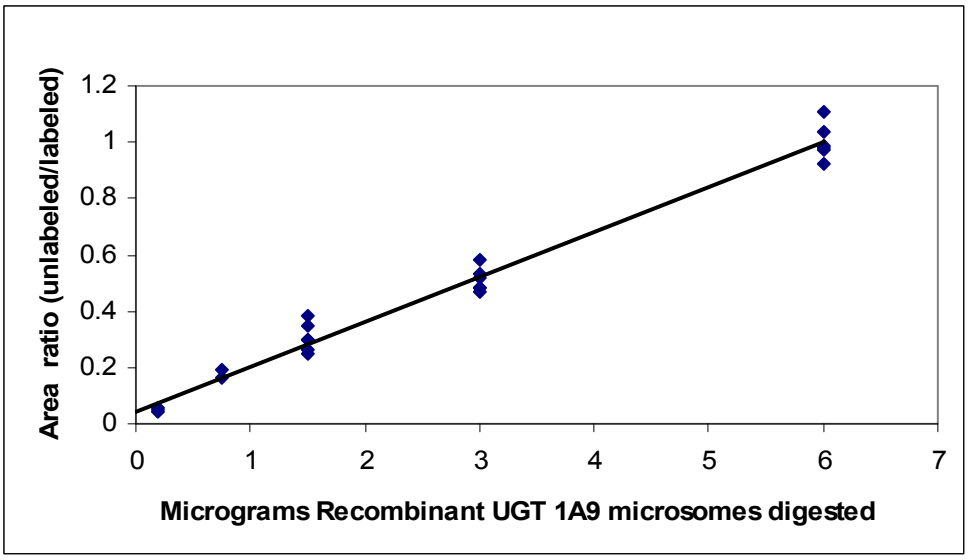

Figure 3.3. Standard curve of MRM 2 of peptide 12 (Table 3.1) representative of UGT1A9 obtained from five intraday measurements of recombinant digests (r^2=.99). A 1 µg aliquot of 6.0 µg of digested microsomal protein was injected on column, with a peak area ratio (PAR) of unity equivalent to 132 pmol/mg protein in the prepared sample.

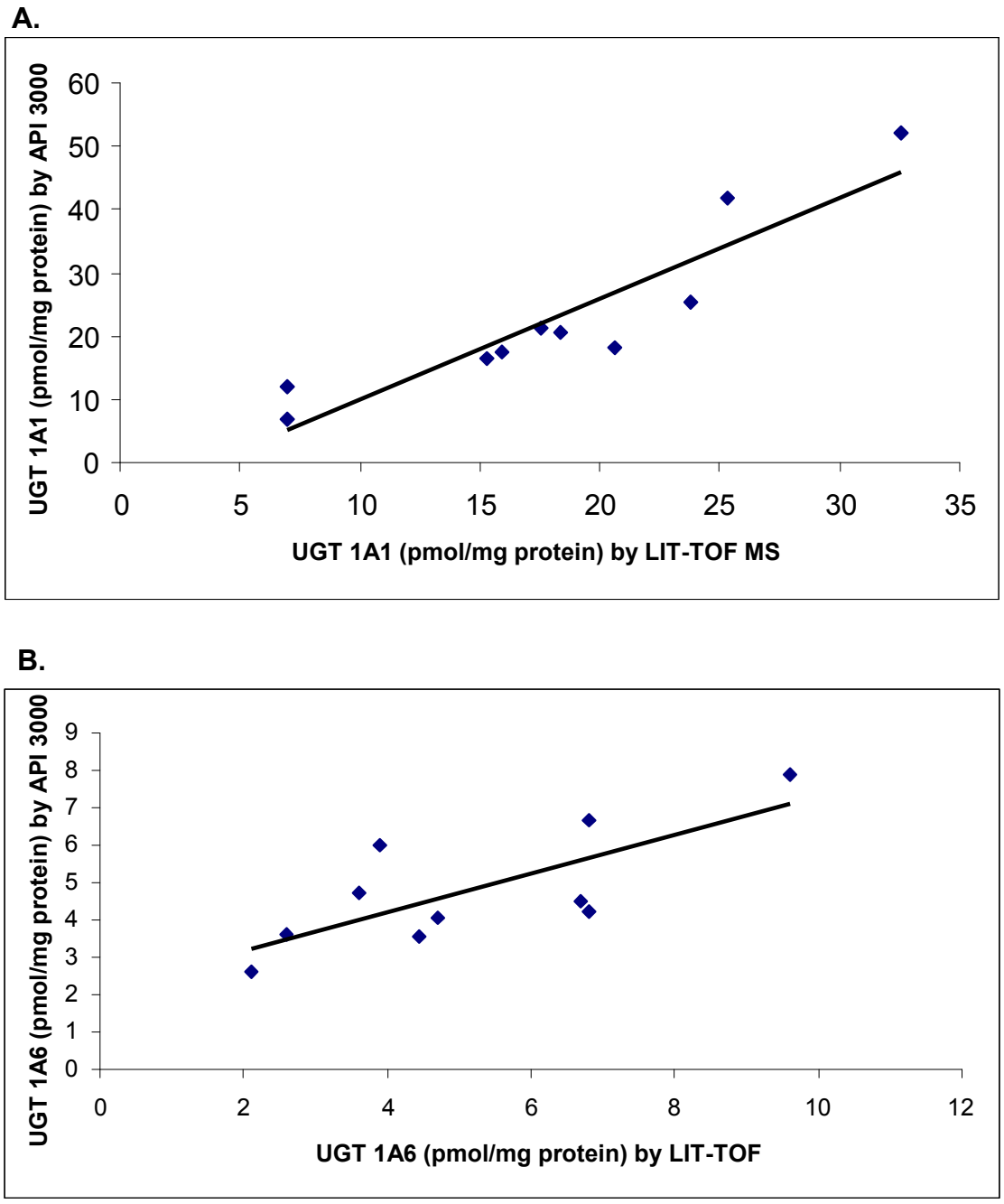

Figure 3.4. Correlation analysis between UGT1A1 (A) and UGT1A6 (B) enzyme expression levels obtained by the LIT-TOF and the ABI 3000 (r=.92). UGT1A1 analysis was performed on ten human liver microsomal samples performed in duplicate using the nano LC LIT-TOF MS system.

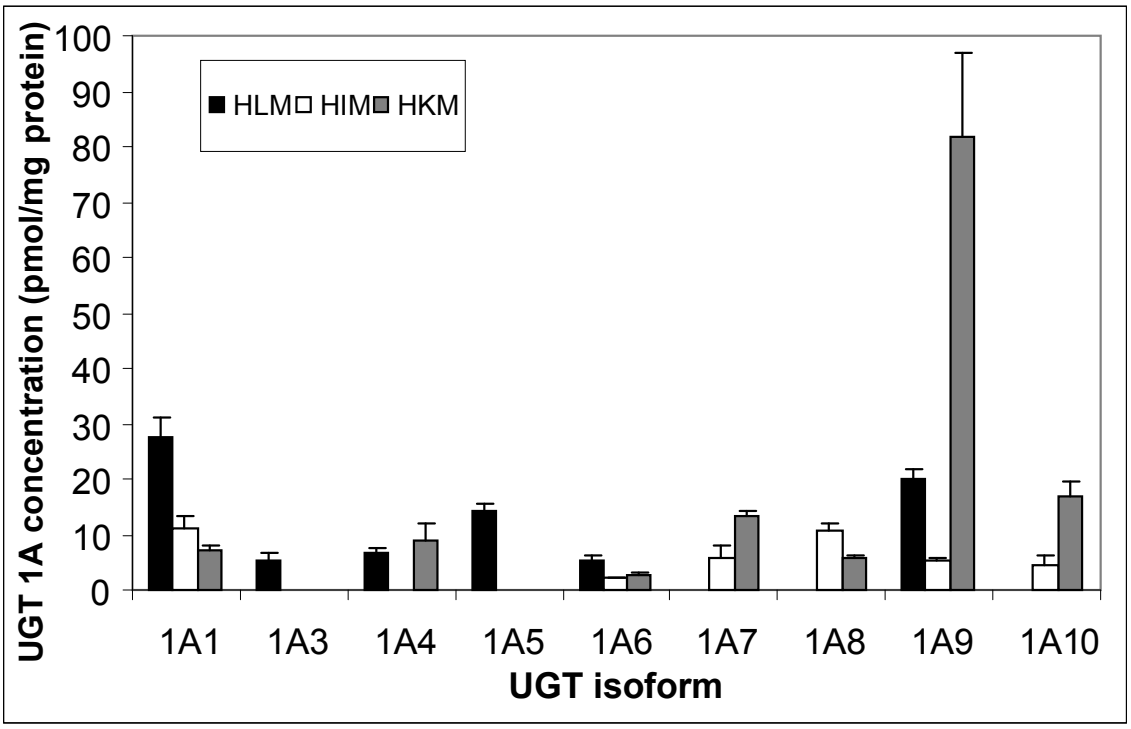

Figure 3.5. Comparison of human UGT enzyme expression from five replicate measurements of digests of pooled human liver, intestinal and kidney microsomes. Data are presented as mean values with standard deviation error bars of each enzyme obtained from averages of two MRMs from one or two peptides as detailed in Methods.

Table 3.1. Peptide standards for the UGT isoforms measured using LIT-TOF with their sequence and optimized MRMs used for UGT analysis.

UGT Isoform	Sequence	IS MRMs (labeled)	Unknown MRMs (Unlabeled)	Rt (min)
1A1 (peptide1)	TYPVP**F***QR	509.4/557.3 509.4/753.4	504.4/547.3 504.4/743.4	20
1A1 (peptide 2)	DGA**F***YTLK	462.7/526.3 462.7/681.4	457.7/526.3 457.7/671.4	18.50
1A1 (peptide 3)	DIVE**V***LSDR	526.5/724.6 526.5/823.6	523.5/718.6 523.5/817.6	21
1A3 (peptide 5)	HVLGHTQ**L***YFETEHFLK	**	**	**
1A3 (peptide 6)	YLSI**P***TVFFLR	681.3/885.5 681.3/1085.6	678.3/879.5 678.3/1079.6	30.1
1A4 (peptide 15)	FFTLTAYA**V***PWTQK	839.9/764.4 839.6/1020.5	836.9/758.4 836.9/1014.5	27.5
1A4 (peptide 16)	VTLGYTQG**F***FETEHLLK	**	**	**
1A5 (peptide 17)	GHQVVV**L***TLEVNMYIK	**	**	**
1A5 (peptide 18)	YLSIPA**V***FFLR	666.3/855.4 666.3/1055.6	663.3/849.4 663.3/1049.6	29.8
1A6 (peptide 4)	SFLTA**P***QTEYR	659.8/799.3 659.8/971.4	656.8/793.3 656.8/965.4	26.0
1A6 (peptide 7)	IYPV**P***YDQEELK	750.5/1027.5 750.5/1223.8	747.5/1021.5 747.5/1217.8	30.5
1A7 (peptide 8)	TYSTSYT**L***EDQDR	793.8/1046.4 793.8/883.4	790.3/1039.4 790.3/876.4	18.5
1A7 (peptide 9)	ESCFDAV**F***LDPFDR	835.9/649.3 835.9/919.4	830.9/649.3 830.9/909.4	24.5
1A8/1A9 (peptide 10)	TYSTSYT**L***EDLDR	786.3/518.3 786.3/647.3	786.3/518.3 786.3/647.3	18.8
1A8 (peptide 11)	EFMD**F***ADAQWK	699.3/990.4 699.3/875.4	694.3/980.4 694.3/865.4	24.1
1A9 (peptide 12)	AFAH**A***QWK	481.7/536.2 481.7/744.3	479.7/532.2 479.7/740.3	18.1
1A10 (peptide 13)	TYSTSYT**L***EDQNR	792.8/661.2 792.8/882.4	789.3/661.2 789.3/875.4	20.2
1A10 (peptide 14)	EFMV**F***AHAQWK	702.8/740.3 702.8/897.4	699.3/740.3 699.3/897.4	24.3

** Indicates that MRM analysis aborted due to insufficient product ion sensitivity following infusion of pure peptide.
a: MRM values were obtained following infusion and LC analysis of stable isotope internal standards.
b: **Bold*** amino acid indicates presence of C13, N15 heavy label to generate a mass difference between four and ten daltons.

Table 3.2. Ion suppression and matrix effect determination following tryptic digestion of recombinant enzyme represented with % intensity of signals from selected stable isotope internal standards.

MRM Segment	I	II	III	III/IV	V
MRM	**481.7/536.2**	**509.4/557.5**	**699.3/990.4**	**659.8/971.5**	**666.3/855.4**
*%Signal	64.8	7.7	90.5	91.9	6.9
MRM	**481.7/744.3**	**509.4/753.4**	**699.3/875.4**	**659.8/799.3**	**666.3/1055.6**
*%Signal	96.9	7.9	28.4	74.3	34.9
MRM	**793.8/883.4**	**792.8/661.2**	**835.9/919.4**	**839.9/1020.5**	**681.3/855.5**
*%Signal	89.5	100.9	73.1	25.1	10
MRM	**793.8/1046.4**	**792.8/882.4**	**835.9/649.3**	**839.9/764.4**	**681.3/1085.6**
*%Signal	83.3	61.7	73.1	22	11.8

*Compares % signal relative to stable isotope standard signal intensities in solution of reconstitution buffer (ACN/0.1% FA pH 3.0 (15:85)) relative to the addition of internal standard after reconstitution following SPE at the end of sample preparation. %C.V. varied between 2.8% and 27.6% but was generally <15% for all standards

Table 3.3. Comparison of UGT Expression through intraday variability measurements that were averaged following five replicate digestions of human liver, intestinal and kidney microsomes. Data are presented as averages of two MRMs from one or two peptide representatives for each UGT.

	hUGT Isoform								
Tissue	**1A1**	**1A3**	**1A4**	**1A5[a]**	**1A6**	**1A7**	**1A8**	**1A9**	**1A10**
HLM[d] (pmol/mg protein)	22.7	3.2	7.4	19.5	8.5	*	*	22.4	*
% C.V.	19.9	12.6	8.4	11.8	16.7	*	*	15.5	*
HIM[e] (pmol/mg protein)	9.7	*	*	*	3.5	7.3	18.2	8.8	5.5
%C.V.	5.7	*	*	*	35.0	17.0	28.0	9.8	32.4
HKM (pmol/mg protein)	7.0	*	9.1	*	2.5	13.4	5.6	81.9	16.7
%C.V.	14.4	*	32.5	*	17.3	6.9	9.1	18.1	16.0

* Denotes enzyme levels were below detection limits (0.5 pmol/mg protein)
[a] Denotes quantification based on one point calibration curve due to lack of recombinant enzyme
[b] Experiments were run in duplicate with 100 µg liver microsomal protein, 100 µg of kidney microsomal protein and 50 µg intestinal microsomal protein
[c] Data are average of 2 MRMs per peptide.
[d] Indicates sample pooled human microsomal protein purchased from Xenotech LLC

**Samples were analyzed on the Hitachi NanoFrontier L/LIT-TOF instrument with a monolithic column (75 µm X 150 mm) at 250 nL/min using a linear gradient conducted as follows: 0 min, 5% B; 5 min, 5% B; 30 min, 55% B; 30.1 min, 100%B; 40 min, 100% B; 40.1 min, 5% B; reequilibration until 65 minutes. LIT-TOF was operated in positive mode using Scheduled MRMs optimized as indicated in Methods.

Table 3.4. Comparison of UGT Expression through interday variability measurements that were averaged following five between day replicate digestions of human liver from two separate pools and pooled intestinal microsomes. Data are presented as averages of two MRMs from one or two peptide representatives for each UGT.

	hUGT Isoform								
Tissue	**1A1**	**1A3**	**1A4**	**1A5[a]**	**1A6**	**1A7**	**1A8**	**1A9**	**1A10**
HLM[d] (pmol/mg protein)	27.6	5.3	6.6	14.1	5.3	*	*	19.9	*
%C.V.	13.1	23.8	16.0	9.3	15.4	*	*	9.0	*
HLM[e] (pmol/mg protein)	29.1	3.3	6.2	17.6	6.4	*	*	22.2	*
%C.V.	16.2	27.7	14.0	7.6	8.3	*	*	9.8	*
HIM[d] (pmol/mg protein)	11.2	*	*	*	2.0	6.0	10.5	5.2	4.6
%C.V.	18.2	*	*	*	18.3	30.9	15.0	13.1	38.3

* Denotes enzyme levels were below detection limits (0.5 pmol/mg protein)
[a] Denotes quantification based on one point calibration curve due to lack of recombinant enzyme
[b] Experiments were run in duplicate with 100 µg liver microsomal protein and 50 µg intestinal microsomal protein
[c] Data are average of 2 MRMs per peptide.
[d] Indicates sample pooled human microsomal protein was purchased from Xenotech LLC (X)
[e] Microsomal protein which was purchased from Becton Dickinson (B&D)

**Samples were analyzed on the Hitachi NanoFrontier L/LIT-TOF instrument with a monolithic column (75 µm X 150 mm) at 250 nL/min using a linear gradient conducted as follows: 0 min, 5% B; 5 min, 5% B; 30 min, 55% B; 30.1 min, 100%B; 40 min, 100% B; 40.1 min, 5% B; reequilibration until 65 minutes. LIT-TOF was operated in positive mode using Scheduled MRMs optimized as indicated in Methods.

Table 3.5. Peptide hUGT measurements using the LIT-TOF. Enzyme concentrations were obtained following calibration curve generation and all enzyme isoform concentrations calculated by combining peptides are shown. Enzyme concentrations from individual peptides were obtained following replicate digests of pooled human intestinal microsomes (n=5). UGT isoforms not included on the table (UGT1A3, 1A4, 1A5, 1A8, 1A9) were determined by averaging two MRMs from one peptide due to the rejection of the secondary peptide based on selection criteria.

	hUGT Isoform							
	1A1		**1A6**		**1A7**		**1A10**	
Peptide	**1**	**3**	**4**	**7**	**8**	**9**	**13**	**14**
UGT concentration (pmol/mg protein)	13.30	9.76	4.63	3.40	8.97	8.78	5.95	6.10
(%C.V.)	(15.0)	(4.9)	(15.9)	(22.4)	(5.3)	(6.7)	(11.8)	(19.3)

*Samples were analyzed on the Hitachi NanoFrontier L/LIT-TOF instrument with a monlithic column (75 μm X 150 mm) at 250 nL/min using a linear gradient conducted as follows: 0 min, 5% B; 5 min, 5% B; 30 min, 55% B; 30.1 min, 100%B; 40 min, 100% B; 40.1 min, 5% B; reequilibration until 65 minutes. LIT-TOF was operated in positive mode using scheduled MRMs optimized as indicated in Methods.
**Peptide Selection Rules for Quantification: 1) If recombinant protein available, must produce a linear standard curve with a %C.V. <25% at the base of the calibration curve, 2) must produce a %C.V. <25% on both interday/intraday validation, 3) if two peptides are used for protein quantification average protein concentrations must be within 50% of each other.

Table 3.6. UGT concentrations obtained from three individual intestinal microsomal donors (HIM) and ten individual donors of liver microsomal protein (HLM) performed on the LIT-TOF in duplicate.

	hUGT Isoform								
Specimen	**1A1**	**1A3**	**1A4**	**1A5**	**1A6**	**1A7**	**1A8**	**1A9**	**1A10**
HIM-1	9.9	*	*	*	3.2	10.8	9.4	8.2	7.8
HIM-21	3.0	*	5.8	*	1.5	6.1	1.9	5.6	3.9
HIM-27	8.7	*	4.8	*	*	8.4	7.0	5.9	2.4
AVG±SD	7.2±3.7	*	5.3±0.7	*	2.3±1.2	8.4±2.4	6.1±3.8	6.6±1.4	4.7±2.8
%C.V.	51.3	*	13.4	*	49.8	28.0	62.8	21.7	59.3
HLM-216	23.8	8.9	4.7	15.6	4.7	*	*	16.9	*
HLM-218	15.3	8.1	7.7	17.7	2.1	*	*	9.0	*
HLM-219	20.6	2.9	1.8	14.2	6.8	*	*	23.5	*
HLM-222	32.6	10.5	4.4	11.6	6.8	*	*	17.3	*
HLM-224	17.5	3.4	4.9	22.4	4.5	*	*	11.6	*
HLM-225	25.3	6.1	1.5	18.0	6.7	*	*	17.9	*
HLM-228	7.0	27.5	4.4	10.9	3.6	*	*	96.4	*
HLM-230	15.9	7.4	4.7	16.2	3.9	*	*	16.1	*
HLM-233	18.4	*	7.8	12.1	9.6	*	*	36.4	*
AVG±SD	18.3±7.8	9.9±7.4	4.6±2.0	15.3±3.5	5.2±2.3	*	*	26.7±25.6	*
%C.V.	43.0	75.2	44.9	22.9	43.4	*	*	95.7	*

Variability between enzyme measurements was generally <25%.
Sections marked with an * indicate enzyme concentrations that were below detection limits (0.5 pmol/mg protein).

**Samples were analyzed on the Hitachi NanoFrontier L/LIT-TOF instrument with a monolithic column (75 µm X 150 mm) at 250 nL/min using a linear gradient conducted as follows: 0 min, 5% B; 5 min, 5% B; 30 min, 55% B; 30.1 min, 100%B; 40 min, 100% B; 40.1 min, 5% B; reequilibration until 65 minutes. LIT-TOF was operated in positive mode using Scheduled MRMs optimized as indicated in Methods.

Table 3.7. Recombinant hUGT enzyme isoform concentrations using the LIT-TOF. Enzyme concentrations were obtained following calibration curve generation.

	hUGT Isoform							
	1A1	**1A3**	**1A4**	**1A6**	**1A7**	**1A8**	**1A9**	**1A10**
Lot Number[a]	73760	93819	92773	70201	30991	36867	18663	96097
hUGT Isoform Concentration (nmol/mg protein)	1.31	0.80	2.23	1.10	2.25	0.83	2.74	0.75

[a] Gentest hUGT1A5 was not available for calibration curve generation. UGT1A2, UGT1A11, UGT1A12 and UGT1A13 are pseudogenes that do not produce active proteins in humans.
*Samples were analyzed on the Hitachi NanoFrontier L/LIT-TOF instrument with a monlithic column (75 µm X 150 mm) at 250 nL/min using a linear gradient conducted as follows: 0 min, 5% B; 5 min, 5% B; 30 min, 55% B; 30.1 min, 100%B;40 min, 100% B; 40.1 min, 5% B; reequilibration until 65 minutes. LIT-TOF was operated in positive mode using scheduled MRMs optimized as indicated in Methods.
**Peptide Selection Rules for Quantification: 1) If recombinant protein available, must produce a linear standard curve with a %C.V. <25% at the base of the calibration curve, 2) must produce a %C.V. <25% on both interday/intraday validation, 3) if two peptides are used for protein quantification average protein concentrations must be within 50% of each other.

F. References

Alterman MA, Kornilayev B, Duzhak T, Yakovlev D. Quantitative analysis of cytochrome p450 isozymes by means of unique isozyme-specific tryptic peptides: a proteomic approach. *Drug Metab Dispos.* **2005,** 33(9), 1399-1407.

Anderson NL, Anderson NG, Haines LR, Hardie DB, Olafson RW, Pearson TW. Mass spectrometric quantitation of peptides and proteins using Stable Isotope Standards and Capture by Anti-Peptide Antibodies (SISCAPA). *J Proteome Res.* **2004,** 3(2), 235-244.

Anderson L, Hunter CL. Quantitative mass spectrometric multiple reaction monitoring assays for major plasma proteins. *Mol Cell Proteomics.* **2006,** 5(4), 573-88.

Bantscheff M, Schirle M, Sweetman G, Rick J, Kuster B. Quantitative mass spectrometry in proteomics: a critical review. *Anal Bioanal Chem.* **2007,** 389(4), 1017-31.

Barnidge DR, Goodmanson MK, Klee GG, Muddiman DC. Absolute quantification of the model biomarker prostate-specific antigen in serum by LC-Ms/MS using protein cleavage and isotope dilution mass spectrometry. *J Proteome Res.* **2004,** 3(3), 644-52.

Barr JR, Maggio VL, Patterson DG Jr, Cooper GR, Henderson LO, Turner WE, Smith SJ, Hannon WH, Needham LL, Sampson EJ. Isotope dilution--mass spectrometric quantification of specific proteins: model application with apolipoprotein A-I. *Clin Chem.* **1996,** 42(10), 1676-82.

Beynon RJ, Doherty MK, Pratt JM, Gaskell SJ. Multiplexed absolute quantification in proteomics using artificial QCAT proteins of concatenated signature peptides. *Nat Methods.* **2005,** 2(8), 587-9.

Beynon RJ, Pratt JM. Metabolic Labeling of Proteins for Proteomics. *Mol. Cell. Proteomics.* **2005,** 4, 857-872.

Bock KW and Kohle C. Topological aspects of oligomeric UDP-glucuronosyltransferases in endoplasmic reticulum membranes: Advances and open questions. *Biochem Pharm.* **2009,** 77, 1458-1465.

Cañas B, López-Ferrer D, Ramos-Fernández A, Camafeita E, Calvo E. Mass spectrometry technologies for proteomics. *Brief Funct Genomic Proteomic.* **2006,** 4(4), 295-320.

Deguchi K, Ito H, Baba T, Hirabayashi A, Nakagawa H, Fumoto M, Hinou H, and Nishimura S. Structural analysis of O-glycopeptides employing negative- and

positive-ion multi-stage mass spectra obtained by collision-induced and electron-capture dissociations in linear ion trap time-of-flight mass spectrometry. *Rapid Commun Mass Spectrom.* **2007,** 21(5), 691-8.

Deguchi K, Ito S, Yoshioka S, Ogata I, and Takeda A. Nanoflow gradient generator for capillary high-performance liquid chromatography-nanoelectrospray mass spectrometry. *J Chromatogr A.* **2004,** 1051(1-2), 19-23.

Doherty MK, McLean L, Hayter JR, Pratt JM, Robertson DH, El-Shafei A, Gaskell SJ, Beynon RJ. The proteome of chicken skeletal muscle: changes in soluble protein expression during growth in a layer strain. *Proteomics.* **2004,** 4(7), 2082-93.

Domon B, Aebersold R. Mass spectrometry and protein analysis, *Science.* **2006,** 312(5771), 212-7.

Fallon JK, Harbourt DE, Maleki SH, Kessler FK, Ritter JK and Smith PC. Absolute Quantification of Human Uridine-Diphosphate Glucuronosyl Transferase (UGT) Enzyme Isoforms 1A1 and 1A6 By Tandem LC MS, *Drug Metabolism Letters.* **2008,** 2, 210-222.

Finel M, Li X, Gardner-Stephen D, Bratton S, Mackenzie PI. Radominska-Pandya A. Human UDP-glucuronosyltransferase 1A5: identification, expression, and activity. *J Pharmacol Exp Ther.* **2005,** 315, 1143-9.

Gerber SA, Rush J, Stemman O, Kirschner MW, Gygi SP. Absolute quantification of proteins and phosphoproteins from cell lysates by tandem MS. *Proc Natl Acad Sci U S A.* **2003,** 100(12), 6940-5.

Gregory PA, Lewinsky RH, Gardener-Stephen DA, and Mackenzie PI. Regulation of UDP glucuronosyltransferases in the gastrointestinal tract, *Tox. and App. Pharmacol*. **2004,** 199, 354-363.

Goshe MB, Smith RD. Stable isotope-coded proteomic mass spectrometry. *Curr Opin Biotechnol.* **2003,** 14(1), 101-9.

Gu S, Liu Z, Pan S, Jiang Z, Lu H, Amit O, Bradbury EM, Hu CA, Chen X. Global investigation of p53-induced apoptosis through quantitative proteomic profiling using comparative amino acid-coded tagging. *Mol Cell Proteomics.* **2004,** 3(10), 998-1008.

Gygi SP, Rist B, Gerber SA, Turecek F, Gelb MH, Aebersold R. Quantitative analysis of complex protein mixtures using isotope-coded affinity tags. *Nat Biotechnol.* **1999,** 17(10), 994-9.

Hardt M, Witkowska HE, Webb S, Thomas LR, Dixon SE, Hall SC, Fisher SJ. Assessing the effects of diurnal variation on the composition of human parotid saliva: quantitative analysis of native peptides using iTRAQ reagents. *Anal Chem.* **2005,** 77(15), 4947-54.

Hoofnagle AN, Becker JO, Wener MH, Heinecke JW. Quantification of thyroglobulin, a low-abundance serum protein, by immunoaffinity peptide enrichment and tandem mass spectrometry. *Clin Chem.* **2008,** 54(11), 1796-804.

Hsu JL, Huang SY, Shiea JT, Huang WY, Chen SH. Beyond quantitative proteomics: signal enhancement of the a1 ion as a mass tag for peptide sequencing using dimethyl labeling. *J Proteome Res.* **2005,** 4(1), 101-8.

Huttlin EL, Chen X, Barrett-Wilt GA, Hegeman AD, Halberg RB, Harms AC, Newton MA, Dove WF, Sussman MR. Discovery and validation of colonic tumor-associated proteins via metabolic labeling and stable isotopic dilution. *Proc Natl Acad Sci U S A.* **2009,** 106, 17235-17240.

Ito H, Takegawa Y, Deguchi K, Nagal S, Nakagawa H, Shinohara Y, and Nishimura S, Direct structural assignment of neutral and sialylated N-glycans of glycopeptides using collision-induced dissociation MSn spectral matching. *Rapid Commun Mass Spectrom.* **2006,** 20(23), 3557-65.

Ito H, Yamada K, Deguchi K, Nakagawa H, and Nishimura S, Structural assignment of disialylated biantennary N-glycan isomers derivatized with 2-aminopyridine using negative-ion multistage tandem mass spectral matching. *Rapid Commun Mass Spectrom.* **2007,** 21(2), 212-8.

Ito S, Nabetani T, Shinoda Y, Nagatsuka Y, Hirabayashi Y, Quantitative analysis of a noval glucosylated phospholipid by liquid chromatography-mass spectrometry, *Anal. Biochem.* **2008,** 376, 252–257.

Ito S, Yoshioka S, Ogata I, Yamashita E, Nagai S, Okumoto T, Ishii K, Ito M, Kaji H, Takao K, Deguchi K, Capillary high-performance liquid chromatography/electrospray ion trap time-of-flight mass spectrometry using a novel nanoflow gradient generator. *J Chromatogr A*. **2005,** 1090(1-2), 178-83.

Izukawa T, Nakajima M, Fujiwara R, Yamanaka H, Fukami T, Takamiya M, Aoki Y, Ikushiro S, Sakaki T, Yokoi T. Quantitative analysis of UDP-glucuronosyltransferase (UGT) 1A and UGT2B expression levels in human livers. *Drug Metab. Dispos.* **2009,** 37, 1759-68.

Jeanville PM, Woods JH, Baird TJ 3rd, Estapé ES. Direct determination of ecgonine methyl ester and cocaine in rat plasma, utilizing on-line sample

extraction coupled with rapid chromatography/quadrupole orthogonal acceleration time-of-flight detection. *J Pharm Biomed Anal.* **2000,** 23(5), 897-907

Jenkins RE, Kitteringham NR, Hunter CL, Webb S, Hunt TJ, Elsby R, Watson RB, Williams D, Pennington SR, Park BK. Relative and absolute quantitative expression profiling of cytochromes P450 using isotope-coded affinity tags. *Proteomics.* **2006,** 6(6), 1934-47.

Kadakol A, Ghosh SS, Sappal BS, Sharma G, Chowdhury JR, Chowdhury NR. Genetic lesions of bilirubin uridine-diphosphoglucuronate glucuronosyltransferase (UGT1A1) causing Crigler-Najjar and Gilbert syndromes: correlation of genotype to phenotype. *Hum Mutat.* **2000,** 16(4), 297-306.

Kamiie J, Ohtsuki S, Iwase R, Ohmine K, Katsukura Y, Yanai K, Sekine Y, Uchida Y, Ito S, Terasaki T. Quantitative atlas of membrane transporter proteins: development and application of a highly sensitive simultaneous LC/MS/MS method combined with novel in-silico peptide selection criteria. *Pharm Res.* **2008,** 25(6), 1469-83.

Kirkpatrick DS, Gerber SA, Gygi SP. The absolute quantification strategy: a general procedure for the quantification of proteins and post-translational modifications. *Nat. Methods.* **2005,** 35(3), 265-73.

Kirkpatrick DS, Weldon SF, Tsaprailis G, Liebler DC, Gandolfi AJ. Proteomic identification of ubiquitinated proteins from human cells expressing His-tagged ubiquitin. *Proteomics.* **2005,** 5(8), 2104-11.

Krishnaswamy S, Hao Q, Al-Rohaimi A, Hesse LM, von Moltke LL, Greenblatt DJ, Court MH. UDP glucuronosyltransferase (UGT) 1A6 pharmacogenetics: I. Identification of polymorphisms in the 5'-regulatory and exon 1 regions, and association with human liver UGT1A6 gene expression and glucuronidation. *J Pharmacol Exp Ther.* **2005,** 313(3), 1331-9.

Kuhn E, Wu J, Karl J, Liao H, Zolg W, Guild B. Quantification of C-reactive protein in the serum of patients with rheumatoid arthritis using multiple reaction monitoring mass spectrometry and 13C-labeled peptide standards. *Proteomics.* **2004,** 4(4), 1175-86.

Lévesque E, Delage R, Benoit-Biancamano MO, Caron P, Bernard O, Couture F, Guillemette C. The impact of UGT1A8, UGT1A9, and UGT2B7 genetic polymorphisms on the pharmacokinetic profile of mycophenolic acid after a single oral dose in healthy volunteers. *Clin Pharmacol Ther.* **2007,** 81(3), 392-400.

Li M, Yuan H, Li N, Song G, Zheng Y, Baratta M, Hua F, Thurston A, Wang J, Lai Y. Identification of interspecies difference in efflux transporters of hepatocytes from dog, rat, monkey and human., *Eur J Pharm Sci.* **2008,** 35, 114-26.

Li N, Nemirovskiy OV, Zhang Y, Yuan H, Mo J, Ji C, Zhang B, Brayman TG, Lepsy C, Heath TG, Lai Y. Absolute quantification of multidrug resistance-associated protein 2 (MRP2/ABCC2) using liquid chromatography tandem mass spectrometry. *Anal Biochem.* **2008,** 380, 211-22.

Li N, Zhang Y, Hua F, Lai Y. Absolute difference of hepatobiliary transporter multidrug resistance-associated protein (MRP2/Mrp2) in liver tissues and isolated hepatocytes from rat, dog, monkey, and human. *Drug Metab Dispos.* **2009,** 37, 66-73.

Little JL, Wempe MF, Buchanan CM. Liquid chromatography-mass spectrometry/mass spectrometry method development for drug metabolism studies: Examining lipid matrix ionization effects in plasma. *J Chromatogr B Analyt Technol Biomed Life Sci.* **2006,** 833(2), 219-30.

Li X, Bratton S, and Radominska-Pandya A, Human UGT1A8 and UGT1A10 mRNA are expressed in primary human hepatocytes. *Drug Metab Pharmacokinet.* **2007,** 22(3), 152-61.

Marley K, Mooney DT, Clark-Scannell G, Tong TT, Watson J, Hagen TM, Stevens JF, Maier CS. Mass tagging approach for mitochondrial thiol proteins. *J Proteome Res.* **2005,** 4(4), 1403-12.

Mayya V, Rezual K, Wu L, Fong MB, Han DK. Absolute quantification of multisite phosphorylation by selective reaction monitoring mass spectrometry: determination of inhibitory phosphorylation status of cyclin-dependent kinases. *Mol Cell Proteomics.* **2006,** 5(6), 1146-57.

Miners JO, Knights KM, Houston JB, Mackenzie PI. In vitro-in vivo correlation for drugs and other compounds eliminated by glucuronidation in humans: pitfalls and promises. *Biochem Pharmacol.* **2006,** 71(11), 1531-9.

Nakamura A, Nakamura M, Yamanaka H, Fujiwara R, Yokoi T, Expression of UGT1A and UGT2B mRNA in Human Normal Tissues and Various Cell Lines, *Drug Metab Dispos*. **2008,** 36, 1461-1464.

Ohno S, Nakajin S**.** Determination of mRNA expression of human UDP-glucuronosyltransferases and application for localization in various human tissues by real-time reverse transcriptase-polymerase chain reaction. *Drug Metab Dispos.* **2009,** 37(1), 32-40.

Owens IS, Ritter JK. Gene structure at the human UGT1 locus creates diversity in isozyme structure, substrate specificity, and regulation. *Prog Nucleic Acid Res Mol Biol.* **1995,** 51, 305-38.

Paine MF, Hart HL, Ludington SS, Haining RL, Rettie AE, Zeldin DC. The human intestinal cytochrome P450 "pie". *Drug Metab Dispos*. **2006,** 34(5), 880-6.

Picard N, Ratanasavanh D, Premaud A, Le Meur Y, and Marquet P, Identification of the UDP-Glucuronosyltransferase Isoforms Involved in Mycophenolic Acid Phase II Metabolism, *Drug Metab. Dispos.* **2005,** 33, 139-146.

Ross PL, Huang YN, Marchese JN, Williamson B, Parker K, Hattan S, Khainovski N, Pillai S, Dey S, Daniels S, Purkayastha S, Juhasz P, Martin S, Bartlet-Jones M, He F, Jacobson A, Pappin DJ. Multiplexed protein quantitation in Saccharomyces cerevisiae using amine-reactive isobaric tagging reagents. *Mol Cell Proteomics.* **2004,** 3(12), 1154-69.

Saeki M, Saito Y, Jinno H, Sai K, Kaniwa N, Ozawa S, Komamura K, Kotake T, Morishita H, Kamakura S, Kitakaze M, Tomoike H, Shirao K, Minami H, Ohtsu A, Yoshida T, Saijo N, Kamatani N, Sawada J. Genetic polymorphisms of UGT1A6 in a Japanese population. *Drug Metab Pharmacokinet.* **2005,** 20(1), 85-90.

Souchelnytskyi S, Proteomics in studies of signal transduction in epithelial cells. *J Mammary Gland Biol Neoplasia.* **2002,** 7(4), 359-71.

Spaulding RS, George KM, Thompson CM. Analysis and sequencing of the active-site peptide from native and organophosphate-inactivated acetylcholinesterase by electrospray ionization, quadrupole/time-of-flight (QTOF) mass spectrometry. *J Chromatogr B Analyt Technol Biomed Life Sci.* **2006,** 830(1), 105-13.

Strassburg CP, Manns MP, Tukey RH, Expression of the UDP-glucuronosyltransferase 1A locus in human colon. Identification and characterization of the novel extrahepatic UGT1A8. *J Biol Chem.* **1998,** 273(15), 8719-26.

Strassburg CP, Nguyen N, Manns M and Tukey RH, Polymorphic expression of the UDP-glucuronosyltransferase UGT1A gene locus in human gastric epithelium. *Mol Pharmacol.* **1998,** 54(4), 647-54.

Strassburg CP, Nguyen N, Manns MP, and Tukey RH, UDP-glucuronosyltransferase activity in human liver and colon. *Gastroenterology.* **1999,** 116(1), 149-60.

Strassburg CP, Oldhafer K, Manns MN, and Tukey RH, Differential expression of the UGT1A locus in human liver, biliary, and gastric tissue: identification of UGT1A7 and UGT1A10 transcripts in extrahepatic tissue. *Mol Pharmacol.* **1997,** 52, 212-20.

Thomas A, Geyer H, Kamber M, Schänzer W, Thevis M. Mass spectrometric determination of gonadotrophin-releasing hormone (GnRH) in human urine for doping control purposes by means of LC-ESI-MS/MS. *J Mass Spectrom.* **2008,** 43(7), 908-15.

Tukey RH, and Strassburg CP. Genetic multiplicity of the human UDP-glucuronosyltransferases and regulation in the gastrointestinal tract. Mol Pharmacol. **2001,** 59(3), 405-14.

Tukey RH, Strassburg CP. Human UDP-Glucuronosyltransferases: Metabolism, Expression and Disease, *Annu. Rev. Pharmacol. Toxicol.* **2000,** 40, 581-616.

Vaisar T and Urban J. Probing the Proline Effect in CID of Protonated Peptides, *J. Mass Spectrom.* **1996,** 31, 1185-1187.

Villeneuve L, Girard H, Fortier LC, Gagné JF, Guillemette C. Novel functional polymorphisms in the UGT1A7 and UGT1A9 glucuronidating enzymes in Caucasian and African-American subjects and their impact on the metabolism of 7-ethyl-10-hydroxycamptothecin and flavopiridol anticancer drugs. *J Pharmacol Exp Ther.* **2003,** 307(1), 117-28.

Wang H, Qian WJ, Mottaz HM, Clauss TR, Anderson DJ, Moore RJ, Camp DG 2nd, Khan AH, Sforza DM, Pallavicini M, Smith DJ, Smith RD. Development and evaluation of a micro- and nanoscale proteomic sample preparation method. *J Proteome Res.* **2005,** 4(6), 2397-403.

Wang MZ, Wu JQ, Dennison JB, Bridges AS, Hall SD, Kornbluth S, Tidwell RR, Smith PC, Voyksner RD, Paine MF, Hall JE. A gel-free MS-based quantitative proteomic approach accurately measures cytochrome P450 protein concentrations in human liver microsomes. *Proteomics.* **2008,** 8(20), 4186-4196.

Wang T, Gu S, Ronni T, Du YC, Chen X. In vivo dual-tagging proteomic approach in studying signaling pathways in immune response. *J Proteome Res.* **2005,** 4(3), 941-9.

Wen Z, Tallman MN, Ali SY, Smith PC. UDP-glucuronosyltransferase 1A1 is the principal enzyme responsible for etoposide glucuronidation in human liver and intestinal microsomes: structural characterization of phenolic and alcoholic glucuronides of etoposide and estimation of enzyme kinetics. *Drug Metab Dispos.* **2007,** 35(3), 371-80.

Williams JG, Tomer KB, Hioe CE, Zolla-Pazner S, Norris PJ. The antigenic determinants on HIV p24 for CD4+ T cell inhibiting antibodies as determined by limited proteolysis, chemical modification, and mass spectrometry. *J Am Soc Mass Spectrom.* **2006,** 17(11), 1560-9.

Wu SL, Amato H, Biringer R, Choudhary G, Shieh P, Hancock WS. Targeted proteomics of low-level proteins in human plasma by LC/MSn: using human growth hormone as a model system. *J Proteome Res.* **2002,** 1(5), 459-65.

Wu WW, Wang G, Baek SJ, Shen RF. Comparative study of three proteomic quantitative methods, DIGE, cICAT, and iTRAQ, using 2D gel- or LC-MALDI TOF/TOF. *J Proteome Res.* **2006,** 5(3), 651-8.

Zieske LR, A perspective on the use of iTRAQ reagent technology for protein complex and profiling studies, *J Exp Bot.* **2006,** 57(7), 1501-8.

CHAPTER 4

QUANTITATIVE RELATIONSHIP BETWEEN RAT UDP-GLUCURONOSYLTRANSFERASE ENZYMES AND TRANSPORTERS WITH METABOLISM AND ELIMINATION OF MYCOPHENOLIC ACID

A. INTRODUCTION

Glucuronidation is a phase II metabolism process that involves the conjugation of glucuronic acid by uridine disphosphate glucuronosyl transferase (UGT) enzymes to many exogenous and endogenous lipophilic compounds to yield a polar, anionic product for urinary or biliary excretion. Glucuronidation enzymes in mammals are composed of two families and three subfamilies and are present throughout the body (Shelby et al., 2003). One of the primary sites for glucuronidation activity is the liver, where compounds are subsequently excreted into either the bile or the sinusoid following conjugation. The process of biliary or sinusoidal excretion of glucuronide conjugates is aided by a number of transporters from the ATP binding cassette (ABC) family, including the multidrug resistance-associated protein 2 and 3 (Abcc2/Abcc3, Mrp2/Mrp3) and the breast cancer resistance protein (Abcg2/Bcrp) (Westley et al., 2006). The actions of these glucuronidation enzymes and transporters facilitate the elimination of many compounds.

Mycophenolic acid (MPA) is used primarily as part of first line adjuvant immunosuppressive therapy following renal or hepatic transplantation. MPA selectively inhibits the ionosine monophosphate dehydrogenase enzyme type II (IMPDH II) enzyme that inhibits the *de novo* purine biosynthesis pathway in lymphocytes (Platz et al., 1991). Following administration, MPA is conjugated by UGT enzymes within the liver to either the pharmacologically inactive phenolic glucuronide (MPAG) or its potentially labile acyl glucuronide (acMPAG). MPAG and acMPAG are subsequently excreted into the bile and intestinal tract via

MRP2/Mrp2 or BCRP/Bcrp, either for elimination through the feces or cleavage by β-glucuronidase enzymes back to MPA and subsequent reuptake through the portal vein back into the liver (Bullingham et al., 1998; Staatz et al., 2007). Enterohepatic cycling is common in MPA dosing both in rats and humans, and in humans, it is responsible for 10-61% of MPA exposure (Bullingham et al., 1998; Naderer et al., 2005; Staatz et al., 2007). While MPA is generally well tolerated, side effects including leucopenia, an increased infection rate and delayed onset diarrhea in 20-30% of patients can sometimes result in dosage reduction or cessation of therapy with potential life threatening complications (Davies et al., 2007).

The field of quantitative proteomics rapidly advanced following the development of electrospray ionization (ESI) in 1985 that allowed for analysis of intact proteins and peptides (Cañas B et al., 2006; Whitehouse et al., 1985). In addition to the development of ESI, several types of stable isotope standards have allowed for precise quantification of several proteins, including apo A-I (Barr et al., 1996), thyroglobulin (Hoofnagle et al., 2006), C-reactive protein (Kuhn et al., 2004), prostate specific antigen (Barnidge et al., 2003), yeast regulatory proteins and phosphoproteins (Gerber et al., 2003) and gonadotropin releasing hormone (Thomas et al., 2008). More recently, the development of absolute quantification strategies to evaluate expression levels of CYP enzymes, membrane transporters and UGT enzymes has become particularly important to biologists and the pharmaceutical industry due to their ability to relate expression levels and metabolite profiles, i.e. *in vitro/in vivo* predictions, or to evaluate the

induction/inhibition ability of particular compounds of interest (Alterman et al., 2005; Fallon et al., 2008; Jenkins et al., 2006; Kamiie et al., 2008.; Li et al., 2009; Wang et al., 2008).

Previously, our lab has explored quantification of hUGT enzymes within liver, kidney and intestinal segments using both standard bore LC coupled with triple quardrupole instrumentation and nanoLC linked to an LIT-TOF mass spectrometer (Fallon et al., 2008). While these experiments were successful in quantifying all of the enzymes of interest, they lacked sufficient sensitivity or throughput capability to quantify extremely low abundant proteins on a larger scale. Moreover, to apply quantitative proteomics when an experiment is sample limited, such as with cell culture or biopsy samples, more sensitive methods are needed. Li et al. and Kamiie et al. indicated that some particular membrane proteins of interest are expressed at levels below the 1 pmol/mg protein limit of quantification of our previous assays (Li et al., 2008; Kamiie et al., 2008). By combining the advantages of nano-UPLC chromatography with the new ABI 5500 QTRAP mass spectrometer, we are now able to use the advantages in sensitivity and spray efficiency provided by capillary LC and increase throughput with UPLC particle technology.

We present a method for quantification of rUgt 1a1, 1a6 and 1a7 and the membrane efflux transporters Mrp2, Mrp3 and Bcrp in rat tissues. In addition, through *in vitro* incubations and pharmacokinetic experiments the enzyme expression in separate strains of male rats were related to the disposition of MPA and its glucuronide conjugates. This experimental approach also allowed

determination if particular strains of rats may be sensitive to MPA induced delayed onset diarrhea due to MPA exposure within the intestinal tract.

B. METHODS

Materials

Analytical grade acetonitrile, methyl alcohol (anhydrous), potassium hydroxide, ammonium acetate, ethyl acetate and glacial acetic acid (HOAc) were purchased from Fisher Scientific Co. (Pittsburgh, PA). Ammonium bicarbonate, dithiothreitol, iodoacetamide, ammonium hydroxide, formic acid, TPCK treated trypsin from bovine pancreas (= 10,000 BAEE units/mg protein) alamethicin, magnesium chloride ($MgCl_2$), phenylmethylsulfonyl fluoride (PMSF), D-saccharic acid 1, 4-lactone (D-SL), dextrose, carboxyl methyl cellulose (CM-cellulose), chymostatin (catalog no. C-7268), leupeptin (L-2023), aprotinin (A-1153), antipain (A-6191), pepstatin A (P-5318), methyl (tri-O-acetyl-α-D -glucopyranosyl bromide)-uronate, β-casein and TRIZMA® hydrochloride were purchased from Sigma-Aldrich Co. (St. Louis, MO). Tris base was purchased from Bio-Rad Laboratories (Hercules, CA). Bond Elut solid phase extraction cartridges (C18 100mg, 1mL) were purchased from Varian, Inc. Rat Ugt 1a1, 1a6 and 1a7 recombinant enzyme and control supersomes were obtained from transfected HepG2 cells out of the lab of Joe Ritter (VCU Medical Center, Richmond, Va). Human liver microsomes (20 mg/mL) were purchased from Xenotech LLC (Lenexa, KA) (Lot 1037, pool of 50). Rat liver microsomes (RLMs) and membrane protein fractions from Wistar, TR- and Gunn (j+/-) rats were prepared

rats were prepared using standard methods (Miles et al. 2006; Stern et al. 2007). Protein concentrations were determined using the Pierce BCA Protein assay Kit, in which bovine serum albumin is used as the standard.

Animals

Male Wistar rats (250-300 g) and Mrp2 deficient TR- rats (250-300 g) were purchased from Charles River laboratories (Wilmington, MA) and housed under a 12 hour-light dark cycle. Male adenovirus treated Gunn rat livers were obtained from the lab of J. Ritter at Virginia Commonwealth University (Richmond, VA) following AV_{Ugt} restoration using previously established methods (Miles et al., 2006). Experimental methods were approved by the Institutional Animal Care and Use Committee (IACUC) and the Division of Lab Animal Medicine (UNC-Chapel Hill). Animals were acclimated for one week prior to experimentation. Male rats (n=5) were administered either a single oral 50 mg/kg MMF suspension in 1% CMC (10 mg/mL) or a 50 mg/kg MMF IV infusion dissolved in 5% dextrose at pH 4 over a thirty minute time period. Following anesthesia using ketamine/xylezine, the bile ducts were cannulated, and blood was collected from the tail vein in 0.1-0.2 mL aliquots into microcentrifuge tubes. Time points for blood and bile collection were 15, 20, 30, 60, 120, 180, 240, 360 and 480 post dosing. Blood samples were placed on ice and centrifuged at 10,000*g* for 12 minutes, and plasma was transferred into vials acidified with HOAc (pH~4, 5µL/mL) and kept at -20°C until analysis. Bile samples were collected in microcentrifuge tubes containing acetic acid (HOAc) (final pH 4, 5µL/mL) and stored at -20ºC until analysis. For quantitative analysis, 0.050 mL of plasma was

precipitated with 0.3 mL acetonitrile containing suprofen internal standard and centrifuged, dried under nitrogen and reconstituted in methanol/0.1% formic acid (25:75) for HPLC injection. Pharmacokinetic measures were obtained by noncompartmental methods using WinNonlin 5.0.1 (Pharsight, Cary, NC). Statistical analysis was performed using a one way ANOVA to separate parameters across different rat strains (p=0.05). MPA exposure from enterohepatic cycling was determined from the equation:

$$\text{MPA Exposure} = \frac{AUC(MPA_{(0 \rightarrow \text{inf})})_{(Intact)} - AUC(MPA_{(0 \rightarrow \text{inf})})_{(Cannulated)}}{AUC(MPA_{(0 \rightarrow \text{inf})})_{(Cannulated)}}$$

HPLC-UV Analysis

Analysis by reversed phase HPLC utilized a HP 1050 LC equipped with a autosampler and an Axxiom (Moorpark, CA) C18 (15cm length, 4.6 mm diameter, 5 µ particle size, 100 Å pore size) column, with an HP 1100 series UV detector set at 250 nm. Data analysis was performed with a Chemstation (A.09.01, Agilent Technologies, Palo Alto, CA). The HPLC method was adopted from an earlier protocol with the some modifications (Wiwattanawongsa et al., 2001). The mobile phase was 52% methanol/48% (0.1% formic acid (FA)) under isocratic conditions at a 1.0 mL/min flow rate over 15 minutes.

MPAG Biliary Elimination

MPAG was synthesized as previously indicated following isolation of MMF from Cellcept© tablets (Roche Pharmaceuticals, Nutly, NJ) at pH 10 and extracted using ethyl acetate (Wiwattanawongsa et al., 2001). After extraction,

the solution was evaporated and the residue was dried overnight prior to NMR analysis. Once MMF purity was confirmed, one gram of purified MMF was added to a solution of pyridine, 0.6 g of silver carbonate and one gram of methyl (tri-O-acetyl-α-D -glucopyranosyl bromide)-uronate under gentle stirring overnight. Briefly, the reaction was then diluted with toluene and filtered then washed with HCl, 0.3 M KOH and water, dried with $MgSO_4$ and rotary evaporated. The crude product was then subject to saponification in acetone with 0.1 M NaOH followed by the addition of Amberlite IR-120 (H+ form) and filtering with toluene washing. The product was dried and obtained through the addition of heated ethanol (~80ºC) in minimal amounts and petroleum ether dropwise. The yellowish solution was placed in -20ºC overnight and product identity was confirmed through HPLC, LC-MS and NMR.

Purified MPAG was solubilized in 5% dextrose solution (5 mg/mL) and administered IV to male Wistar rats following bile cannulation. Blood (0.25 mL) and bile (0.5 mL) was collected at 5, 15, 30, 60, 120, 180, 240, 360 and 480 minutes. Blood samples were centrifuged for plasma collection and bile was placed in -20ºC prior to analysis.

Tissue Collection and Microsome Preparation

At the conclusion of the pharmacokinetic studies, rats were euthanized via thoracotomy and the livers, kidneys and the entire intestinal tract from the pylorus to the distal colon was removed and placed on a bed of ice. Livers and kidneys were collected and snap frozen in liquid nitrogen and placed at -80ºC prior to

microsome and membrane protein fraction collection. Intestine segments were taken in 10 cm fractions according to protocols previously indicated by Miles et. al (Miles et al., 2006).

In vitro MPA Glucuronidation Studies

In vitro glucuronidation rates were based upon previous studies using 1 mM MPA and 1 mg/mL microsomal protein with minor modifications (Stern et al., 2007). Reactions were terminated at 15 and 30 minutes with 1 mL of acetonitrile with suprofen as internal standard. Following centrifugation, drying and reconstitution, 50 µL was injected onto an HP1050 system with the UV detector set at 250nm.

Stable Isotope Labeled Internal Standards

Peptide standards (7mer-15mer), each containing one amino acid heavy labeled with ^{13}C [98%] and ^{15}N [95%], selected according to previous methods (Fallon et al., 2008) were purchased from Thermo Electron (Thermo Scientific, Waltham, MA). For each rUGT isoform, two synthetic peptide standards were purchased but three synthetic standards were purchased as representatives for each transporter of interest. The peptides were purchased for rUgt1a1, 1a6 and 1a7, along with the canalicular transporters rMrp2 and rBcrp and the basolateral transporter rMrp3 due to their principle effect on MPA metabolism and distribution within rats. The peptides were selected according to manufacturer recommendations and previously published guidelines (Beynon et al., 2005;

Fallon et al., 2008; Kamiie et al., 2008). The selection criteria along with previous guidelines established within our lab were used in all peptide selections.

Amino acid analysis and LC-MS was conducted on each peptide to determine exact amount present as previously described (Fallon et al., 2008). Amino acid analysis was conducted at the Center for Structural Biology, Wake Forest University School of Medicine, Winston-Salem, NC. While some peptides exhibited purity levels of 90%, many peptide purity levels were between 75-85%. The peptides purchased are listed in Table 4.1 together with optimal MRM transitions for quantitation.

Sample Preparation and Tryptic Digestion

Calibration curves were generated containing 0.075, 0.19, 0.75, 1.5, 3.0 and 6.0 µg of microsomes for recombinant rat Ugts 1a1, 1a6 and 1a7 with protein normalized to 25 µg by the addition of HLMs. A blank containing 25 µg of rUGT control supersomes, with protein normalized in the same way was prepared for each calibration curve. Rat liver, intestinal or kidney microsomal protein or membrane protein fractions prepared from the same rat tissues using the Novagen Native Membrane Protein Extraction Kit (EMD Chemicals, Gibbstown, NJ) were prepared prior to digestion. Samples were denatured and digested as previously described with slight modifications (Fallon et al., 2008). Samples were denatured by heating at 95 ºC for 11 min after the addition of 5 mM dithiothreitol (sample volume 90 µL), followed by alkylation by iodoacetimide (IAA, 10 µL of 100 mM solution added) for 20 under darkness. Heavy labeled peptides were

then added as internal standards (1 pmol of peptides 1-15, Table 4.1) and the residual acetonitrile (< 5 µL) was removed by evaporation under nitrogen. Samples were then digested with trypsin in 50 mM ammonium bicarbonate; enzyme/protein ratio = 1:50; overnight at 37ºC. The reaction was then quenched by acetonitrile, centrifuged at 1000*g* for 10 min and the organic content was then removed by evaporation under nitrogen for ~10 min. Ammonium bicarbonate (0.9 mL, 50 mM solution) was then added in preparation for solid phase extraction. SPE cartridges were conditioned with methanol and HPLC water. Samples were then added and the cartridges were washed with ammonium acetate (10 mM, pH3), then with acetonitrile/0.1% FA in water solution (10:90). Peptides were eluted from SPE with a 1 mL 65:35 solution of acetonitrile/0.1%FA. The eluate was evaporated to dryness under nitrogen at 42ºC in a water bath and samples were reconstituted with 200 µL of 15% acetonitrile/0.1% formic acid at pH 3 (pH was adjusted to 3 by drop wise addition of ammonium hydroxide). Samples were stored at -20 ºC until analyzed by LC-MS/MS.

LC Conditions

Following tryptic digestion and sample preparation, peptides from tissue samples were injected onto a Waters nanoACQUITY UPLC system (Waters Corporation, Milford, MA) with a Waters Symmetry® loading column (length, 2cm; internal diameter, 180 µm; particle size, 5µ). Samples were loaded onto the loading column for 3 minutes using 95% Solvent A at 5 µL/min followed by gradient elution through a bridged ethylene hybrid (BEH) column (length, 10cm;

internal diameter, 150 µm; particle size, 1.7µ; pore size, 100Å). The mobile phase consisted of 98% HPLC water and 2% acetonitrile with 0.1% formic acid (Solvent A) coupled with 98% acetonitrile and 2% HPLC water with 0.1% formic acid (Solvent B). Injection volume was 2 µL and the flow rate was held constant at 2.0 µL/min. Gradient; 15% B from 0 to 5 min, 15% to 65% B at 25 min, to 99% at 25.1 min, hold at 99% until 30 min, then to 15%B at 30.1 min with equilibration until 40 minutes.

MS/MS Analysis

MS instrumentation consisted of an ABI QTRAP 5500 system with a Nanospray III ion source operated in positive ion mode (Applied Biosystems, Foster City, CA). All data acquisition and method development was carried out using Analyst Software (version 1.5, build 3655, Applied Biosystems, Foster City, CA). A majority of the heavy labeled peptides were found to be doubly charged when infused into the mass spectrometer in 1 µg/mL concentrations in mobile phase (50:50). Two MRM transitions, with product ions that were generally >500amu (and precursor ion as doubly charged ion, except for peptide 9 which was triply charged), were chosen for each heavy labeled peptide following optimization as shown in Table 4.1, i.e. 30 MRMs for monitoring the heavy labeled standards. Two additional MRM transitions were chosen for the corresponding unlabeled peptides from digested recombinant enzyme and microsomal samples with adjustment based on the masses of the unlabeled peptides. Thus, there were four MRM transitions monitored per peptide, giving a

total of 60 MRMs, which were acquired between the rat UGT enzymes of interest and the three transporters potentially involved in MPA glucuronide efflux. Due to the similar nature of many of the peptides, there were several distinct time windows of peptide elution, allowing for the development of a scheduled MRM method. Following optimization, total scan time per MRM was set to 100 msec using an 80 sec scan window for each MRM. MS ion voltage was set at 4000V, curtain gas 30 L/min, entrance potential 10V, source temperature set at 160ºC, nebulizer gas set at were maintained 14 L/min while the declustering potential (DP), collision energy (CE) and collision cell exit potential (CXP) were optimized for each MRM. A majority of MRM product ions were y ions with some b ions used for quantification. The MRM transitions acquired are listed in Table 4.1.

C. RESULTS

Rat MPA Pharmacokinetics

After administration of MMF to bile cannulated Wistar rats via either the oral or intravenous routes, the exposure to MPA was essentially the same (11.6 vs 10.3 mg/ml*min, respectively) which indicates that oral bioavailability of MPA via the prodrug was essentially complete (Table 4.2, Figures 4.1, A, B). Thus, CL/F and CL were similar and not statistically different (Table 4.2). The terminal half-lives were also not statistically different following these two routes of input into bile cannulated Wistar rats (Table 4.2). The peak concentrations of both MPA and MPAG were within 60 min following oral dosing. Systemic exposure to the primary metabolite, MPAG, was also not measurably different between the

oral and intravenous dose of MMF, which resulted in ratios of MPAG/MPA to be similar as well with values below 1.0, reflecting less relative systemic exposure in rats to MPAG relative to humans where the ratio is often above five in healthy volunteers.

Biliary excretion in cannulated Wistar rats provided estimates of apparent biliary clearance. The apparent biliary clearance is defined as “apparent” due to it measuring amounts of glucuronides in bile relative to parent, MPA, in plasma. The apparent biliary clearance thus reflects metabolism and then excretion of the glucuronide(s) into bile. Mean values for apparent biliary clearance were 1.1 and 0.8 mL/min the bile cannulated Wistar rats after the intravenous and oral doses of MPA, respectively. These were not statistically different and represent biliary clearance following metabolism as major route of elimination with approximately 60% of the dose excreted in bile when the rats were cannulated and enteroheptatic recycling was not permitted.

MPA and MPAG disposition in Wistar rats, without bile duct cannulation, after an intravenous dose allowed an estimate of enterohepatic recycling. The mean AUC for MPA was 14.3 mg/ml*min following IV dosing of MMF to Wistar rats and 12.3 mg/ml*min following oral dosing which was much higher than obtained with cannulation (Table 4.2, Figure 4.2B) and a secondary peak was noted. From the AUC differences, an estimate for the fraction of dose that is subject to enterohepatic recycling in the Wistar rat is between 20-39% using both IV and oral formulations (Table 4.2).

When TR- rats were administered MMF orally with bile duct cannulation, the systemic exposure to MPA was reduced to a mean AUC of 6.1 mg/ml*min from 11.6 in Wistar rats (Table 4.2). The TR- rats did have substantially elevated systemic exposure to MPAG (Figure 4.1C) relative to normal Wistar rats, resulting in an MPAG/MPA level of 6.7 compared with MPAG/MPA values of 0.63 and 0.53 in the Wistar oral and IV dosing groups (Table 4.2)

MPAG in Bile

Within five minutes following a 2.5 mg/kg dose of MPAG (in MPA equivalents), between 40-50% of the original dose is excreted within the bile. A significant secondary fraction (~30%) is present within the blood and remained detectable up to three hours post dosing (Figure 4.4). While there was initially a large fraction of the MPAG dose excreted into the bile, MPAG elimination through the bile dropped off dramatically after five minutes to levels below detection limits for four hours, when a small fraction was detected until the end of the study. At the end of the collection period (0-8 hr), 53% of the original MPAG dose was eliminated in bile with the remaining fraction eliminated in the urine and a small amount undergoing hydrolysis and subsequent hydrolysis *in vivo* followed by conjugation and elimination.

***In Vitro* Glucuronidation Studies**

Following incubation periods of 15 and 30 minutes with 1 mM MPA, hepatic and intestinal microsomes obtained from TR- rats generally exhibited

higher glucuronidation formation rates (nmol/min/mg protein) than the Wistar rat tissue specimens, although the difference was not significant (ANOVA one way, p=0.45). Furthermore, glucuronidation rates were generally lower in the middle segments of the gastrointestinal tract in both the TR- and Wistar rats (Figure 4.5) which is consistent with previous reports (Miles et al., 2006). MPA conjugation rates were the highest within the liver microsomes of both animal strains, and our findings on TR- and Wistar rats generally agreed with previously reported glucuronidation rates (Westley et al., 2006; Miles et al., 2006).

Stable Isotope Standards

Upon infusion into the MS with electrospray ionization, all heavy labeled peptides produced doubly charged parent ions with the exception of Peptide 6 and Peptide 9 (Table 4.1). However, following inconsistent retention times and inadequate sensitivity of Peptide 6 during method development, it was infused again for optimization of the doubly charged parent ion that ultimately yielded better sensitivity and reproducible retention times on the LC-MS/MS. While our previous experiments relied on peptides with product ions >500 m/z, inadequate sensitivity of the product ions of peptide 2 and peptide 13 made it necessary to expand product ion selections beyond this window (Fallon et al., 2008). Due to the increased size of the protein sequences for the transporters of interest relative to the rUgts, coupled with the need for accurate quantification at the base of the calibration curves, three stable isotope standards were utilized for MRM quantification. However, due to %C.V. values >25% for peptide 12 (Mrp3) at

levels below 1 pmol/mg protein, this peptide was not used for quantification (Table 4.3).

Calibration Curves

Recombinant microsomal protein was serially diluted to generate a six point calibration curve for each rUgt enzyme and to establish lower limit of detection (LLOD) values of the LC-MS/MS instrument. Calibration curves were constructed following five replicate digests and averaged for each calibrant to obtain %C.V. values used to evaluate accuracy and precision. All peptide MRMs generated calibration curves with R^2 values >0.98; however, both MRMs of peptide 1, peptide 3 and peptide 4 also demonstrated %C.V. values of <10% at the base of their respective calibration curves (Figure 8). While peptides 2, 5 and 6 had slightly higher %C.V. values for rUgt quantification, all %C.V. were <20% for the analytical procedures.

Validation

Efficiency of tryptic digestion was evaluated by monitoring the ratios of missed cleavages following a timed digest of 50 µg of β-casein. Missed cleavages were monitored through two MRMs from the peptides DERFFSDK (522.4/496.2, 522.4/481.1) and **FFSDK** (643.4/625.2, 643.4/349.2) along with IAKYIPIQYVLSR (782.3/764.3, 782.3/782.4) and **YIPIQYVLSR** (626.4/975.6, 626.4/488.2) representing incomplete and **complete** digestion. Complete digestion efficiency was observed when only MRMs from FFSDK and YIPIQYVLSR were observed following overnight digestion (Figure 4.9). Interday

and intraday precision was obtained following five replicate digestions of pooled RLMs or membrane fractions prepared from frozen Wistar rat livers. All %C.V. values for each of the casein digests were <20% while the difference in enzyme expression between the tissue and casein sample sets was minimal (Table 4.3).

Calibration curves were generated for each of the peptide MRMs representative of the three rUgts (peptides 1-6). All calibration curves were linear between 0.075-6.0 µg of microsomal protein (R^2>0.98) (Figure 4.8). The lower limit of detection (LLOD) was established at 15 fmol/mg protein by monitoring the signal: noise ratio at the lowest end of the calibration curves. Enzyme expression measured in microsomes were obtained by averaging converted peak area ratios (unlabeled/labeled) of each peptide MRM with %C.V. <20% at the lowest end of the calibration curves. The low end of the calibration curve was used to indicate optimal linear range for the tested peptides. Values for %C.V. for transporters were determined through interday and intraday testing of Wistar liver membrane fractions. Peptide 12 was eliminated for quantitative purposes because %C.V. values were >25% in both interday and intraday samples (Table 4.3).

Rat Microsomes

Microsomal digests of Wistar, TR- and adenovirus treated (AV_{Ugt}) rat tissues (Miles et al. 2006) were examined for rUgt expression following validation of the quantitative proteomic method. It has been previously reported that TR- rUgt levels are upregulated using a general rUgt1a antibody in a Western Blot

when compared with Wistar rat expression levels; however, this was not seen across all tissues (Johnson et al., 2006). Using our specific quantitative proteomic method, while rUgt 1a1 was significantly upregulated in the TR- rat livers no other significant differences according to one way ANOVA analysis in rUgt expression of rUgt 1a1, 1a6 and 1a7 for any of the other tested tissues (Figure 4.10). There was a general increase in rUgt1a1 and rUgt1a7 expression both between the Wistar and TR- rat tissues and proceeding down the segments of the GI tract within both sets of rat intestines (Figure 4.10). Of the three isoforms, rUgt1a7 expression was often lower than rUgt1a1 and rUgt1a6 across all tissues with the exception of the S3 and S4 segments within the TR- rat GI tract. Often expression levels of this isoform were below 1 pmol/mg protein, which would have been <LOD in our previous hUGT targeted proteomic assays established (Fallon et al., 2008).

Rat Membrane Fractions

Rat membrane fractions were isolated using the Novagen Membrane Extraction Kit from tissues following pharmacokinetic analysis and euthanasia. In the Wistar rat tissue samples, rBcrp was the most abundant of the three transporters expressed, between 0.9 and 2.0 pmol/mg protein. In the liver and kidney, there were no significant differences in transporter expression, and rBcrp expression was relatively unchanged between intestinal segments. Expression of rMrp3 was generally higher in the liver and kidney as opposed to the GI tract and also was present in higher levels descending into the colonic segment (S4).

Expression levels of rMrp3 and rMrp2 were highest within the colonic segments of the intestine while rBcrp expression was minimal (Figure 4.11).

In the TR- rats, as expected, rMrp2 was below detection limits in all samples, while both rMrp3 and rBcrp were dramatically upregulated in the liver and kidney. In the liver, rMrp3 was the most abundant of the two transporters, which has been previously reported; however, rBcrp was expressed in a higher amount than rMrp3 in the kidney (Johnson et al., 2006). In the intestine, there was a reversal of transporter expression, where rMrp3 was highest in S1 and S4 of the GI tract while rBcrp expression was more abundant in segments S3 and S4 (Figure 4.11). AV_{Ugt} rat liver expression of rMrp2 was not statiscally different compared with Wistar rat livers but both rMrp3 and rBcrp expression was significantly lower compared to Wistar rats (Figure 4.11).

Correlation Analysis

Correlation results were obtained following evaluation of both *in vitro* glucuronidation levels and enzyme and transporter expression across liver, kidney and intestinal segments from Wistar, TR- and AV_{Ugt} treated Gunn rats. A strong correlation was seen between rUgt1a1 and rMrp2 (R^2=0.75, Figure 4.14) but no correlations were observed between any other rUgt enzymes or transporters (R^2<0.20, data not shown). However, *in vitro* glucuronidation rates were found to correlate strongly with rMrp2 expression values across all species and tissues (Figure 4.12, 4.13). In addition, a strong correlation (R^2=0.76) was found between *in vitro* glucuronidation rates and rUgt1a1 across all tissue types;

however, there was no correlation between rUgt1a6 and glucuronidation rates (R^2=0.18, Figure 4.12). While it has been previously reported that *in vitro* MPA metabolism correlates with rUgt1a7 expression, initially correlation tests between the two conditions did not correlate across all tested liver, kidney and intestinal samples (Miles et al. 2006) (R^2=0.21, data not shown). When liver and kidney samples were removed from the dataset, the correlation improved (Figure 4.12) and supports previous reports that indicate *in vitro* glucuronidation rates depend on rUgt1a7 expression within the gastrointestinal tract (Miles et al., 2006).

D. DISCUSSION

The field of targeted quantitative proteomics has rapidly advanced over the last decade; however, many studies have not been able to link protein quantification with physiological effects. In particular, drug metabolizing enzymes and protein biomarkers are of interest to many scientists due to the need to understand metabolism endpoints in preclinical testing and to increase to the likelihood of early detection of disease biomarkers for patients in the clinic. Here we have attempted to examine the differential expression levels of both rUgt enzymes and transporters using *in vitro* and *in vivo* glucuronidation of MPA as a probe substrate.

While MPA total clearance values varied slightly between Wistar and TR- rats (1.7 mL/min vs. 2.5 mL/min, Table 4.2), there was great variability in biliary clearances (1.1 mL/min vs. 0.09 mL/min, Table 4.2). Initial pharmacokinetic

studies centered on determining any differences in AUC or clearance levels between oral and IV dosing in Wistar rats. Even though initial plasma MPA/MPAG plasma concentrations differed slightly due to first pass metabolism observed upon oral dosing of MMF compared with IV dosing, none of the pharmacokinetic parameters were significantly different between the Wistar rats (Table 4.2). Furthermore, MPA/MPAG plasma concentration time curves were virtually identical after sixty minutes in both cannulated and Wistar rats after oral and IV dosing with intact bile ducts. Both the oral and IV dosed Wistar rats demonstrated an increase in MPA plasma concentration between four and six hours post dosing, an indicator of enterohepatic cycling, which is typically seen between six and eight hours post dosing in humans and responsible for a significant fraction of overall MPA exposure in humans. Using the IV and oral dose studies both the bile cannulated rats and control animals with intact bile flow, it was found that approximately between 20-39% of overall MPA exposure results from enterohepatic cycling. Enterohepatic cycling is important for both rats and humans because it represents not only an increase in mean residence time and overall exposure to the parent compound, but can also increase efficacy and potential side effects, especially if intestinal metabolism or exposure to the parent drug is associated with toxicity.

Previous experiments (Chapter 2) demonstrated that rats rapidly excrete acMPAG that is not cleaved by esterases within the body following IV administration of the pre-formed acyl glucuronide metabolite. While previous experiments have indicated that acyl glucuronides can be taken back into the

liver following IV administration, it is also important to consider the possibility of rapid cleavage of the acyl glucuronide back to the parent aglycone, which may then be available for hepatic uptake and metabolism within the liver. MPAG, which is resistant to esterase cleavage, was also administered intravenously to Wistar rats to evaluate the potential for reuptake and excretion of the intact glucuronide. Following IV administration, MPAG is excreted rapidly into the bile within five minutes, but plasma levels of MPAG decrease rapidly to below detection limits within three hours. Of the original IV dose of MPAG, 53% is ultimately excreted within the bile, indicating that glucuronide metabolites may be taken back up into the liver intact (Figure 4.4). This could possibly serve as a tertiary source of parent aglycone exposure following potential β-glucuronidase cleavage within the liver, in addition to the initial dose and parent aglycone that is reabsorbed during enterohepatic cycling.

The side effects of MPA are well documented, but of particular concern is the 20-30% fraction of the patient population that suffers from debilitating delayed onset diarrhea (Davies et al., 2007). This particular side effect is troubling not only because of lifestyle factors, but also because many patients that exhibit this symptom must either alter MPA dosing levels or resort to second line therapy. Second line therapy can result in allograft rejection, leading to not only life threatening complications for the patients but also substantial increases in patient care costs for the individuals. Within the body, MPA is detoxified through the actions of UGT enzymes in the liver and gastrointestinal tract, leading to the formation of two glucuronides, MPAG and acMPAG, which are then excreted in

bile and urine. Even though many attempts have been made to link acMPAG exposure levels with the GI toxicity of MPA, no distinct correlations have been found and *in vitro* studies of the acMPAG metabolite indicate that compared with many acyl glucuronide metabolites, it is a fairly stable and unreactive metabolite (Chapter 2; Shipkova et al., 2003). Therefore, our lab in collaboration with Miles and Ritter (VCU Medical Center, Richmond, VA) investigated different rat strains that exhibit variable rUgt and transporter expression, then modulated rUgt expression through the use of AV_{Ugt} Gunn rats (Miles et. al 2006). MPA exposure in plasma varied, thus MPA toxicity also varied.

While TR- rats demonstrated much lower MPA biliary clearance values during the pharmacokinetic experiments, CL_{total} was generally higher than Wistar rats tested under the same conditions with bile collection. Biliary clearance of 0.1 mL/min and Fe_{bile} below 10% in TR- rats were consistent with what has been previously reported (Westley et al., 2006). The retention of some biliary efflux of MPAG in TR- rats indicates that glucuronide efflux into the bile involves additional canicular transporters besides Mrp2. While BCRP single nucleotide polymorphisms have been linked to altered MPA exposure levels in humans, Bcrp is likely a minor factor in rat MPAG elimination due to the low biliary clearance levels observed in TR- rats (Miura et al., 2008).

Analysis of *in vitro* glucuronidation demonstrated no statistically significant differences between Wistar and TR- rat tissue samples. Generally, there was a modest increase in MPA glucuronidation rates between Wistar and TR- rat liver and kidney samples (Figure 4.5). Westey et al. reported a modest increase in

TR- rat liver glucuronidation rates and attributed this as being due to increases in rUgt1a enzymes (Johnson et al., 2006; Westley et al., 2008). However, because a general antibody for all rUgt1a isoforms was used in determining changes in rUgt expression levels, it has been difficult to determine if the increase in rUgt expression can be related to increased MPA glucuronidation capacity. In order to more precisely examine this relationship, it was beneficial to develop an assay to quantify rUgt1a1, 1a6 and 1a7, which are primarily responsible for MPA glucuronidation within rats (Miles et al., 2005).

Targeted quantitative proteomic assays were performed on the nanoACQUITY UPLC system connected to the QTRAP 5500 using 15 stable isotope (C^{13}, N^{15}) internal standards. Standards were selected and purchased following *in silico* digest of each respective protein of interest following selection rules (avoid extensive hydrophilicity/hydrophobicity, 8mer-16mer in length, no D-G N terminus, no C or W residues) that we have previously outlined (Fallon et al., 2008). In addition, peptide selections were based on previous experience with peptides used in hUGT quantification, where it was found that multiply charged peptides are much more common with multiple histidine residues and proline residues generate preferential MRM product ions (Fallon et al., 2008; Vaisar and Urban, 1996). Only two peptides were selected for quantification of each of the three rUgts studied due to their shorter protein sequences, which resulted in a lack of ideal stable isotope peptide standards. Upon infusion, all peptides were doubly charged with the exception of peptide 6 (TVS**V***SHTSQEDQEDLNR) and peptide 9 (LIHDLLVL**F***LNPQLLK), which were

triply charged. While peptide 9 demonstrated excellent reproducibility on the LC-MS/MS system, peptide 6 lacked consistent reproducible LC retention times. Peptide 6 was then optimized again on the MS/MS system following infusion. Even though the triply charged state was approximately ten fold more abundant than the doubly charged state, peptide 6 was optimized using the doubly charged ion and subsequently produced consistent and reliable LC retention times and adequate MS/MS sensitivity. Despite careful evaluation during the peptide selection process, peptide 12 (Y**P***GLELVLK, rMrp3) was ultimately excluded from the analysis due to excessive variability when applied to assays for the analysis of membrane fractions. Unlike previous experiments (Chapter 3), all peptides produced strong MRM product ion spectra and were easily resolvable on the nano-UPLC MS/MS system.

The LC properties of the stable isotope standards and their corresponding unlabeled peptides from the digested proteins produced several distinct windows of peptide retention times (Figure 4.7). This was addressed by the development of a scheduled MRM method to optimize instrument dwell times and ensure that enough data points are collected across a peak. While previous experiments with scheduled MRMs were based on peak widths between 60-90 seconds allowing for generous dwell times (Fallon et al., 2008), the advantages of UPLC often resulted in peak widths as small as 10 seconds for particular peptides (Figure 4.7). Because of this, it became necessary to shorten dwell times from 60ms employed on the API 3000 to approximately 3-5ms using scheduled MRMs

on the QTRAP 5500 to acquire sufficient points across a particular MRM peak for all 60 MRMs analyzed within a single LC run.

Calibration curves for each peptide representing a rUgt enzyme were established to validate the lower limit of quantification (LLOQ) and linear range of the assay with injection of approximately 0.2 µg of digested protein on column. At the low end of the calibration curve (75 fmol/mg protein) the signal to noise ratio (S:N) was approximately 25:1 for each peptide, resulting in a 30 fmol/mg protein LLOQ value. To validate the effectiveness of peptides used for quantification of membrane transporters, the %C.V. values from the interday and intraday analysis were evaluated since recombinant transporters were not available to determine linear ranges of the assays. Any targeted peptides with %C.V. values >25% were excluded from the analysis. Peptide 12 was excluded from all transporter analyses because %C.V. values were >25% for both MRMs in both the interday and intraday validations. All other peptide %C.V. values were below 20% during validation and the MRM measurements for each peptide were averaged to generate the transporter expression data. Transporter expression levels not only agreed between peptide MRMs on the QTRAP 5500 but also between the three peptides employed for quantification of rMrp2 and rBcrp and the two peptides used for quantification of rMrp3 (Table 4.5; Table 4.6). Compared to our previous targeted proteomic assays for human UGTs using the LIT-TOF with capillary LC (Chpater 3), the %C.V. values obtained on the ABI 5500 were generally lower but no significant differences in assay precision have been observed across any of the three instrument platforms

evaluated to date (Fallon et al., 2008). However, the limit of detection of the ABI 5500 (rUgt 1a1, 1a6, 1a7 and transporters) was fifty fold lower (0.01 pmol/mg protein vs. 0.5 pmol/mg protein) compared to both the ABI 3000 (for hUGT1A1 and 1A6) and the LIT-TOF (for all active hUGT1A isoforms).

After assay development and validation, Ugt enzymes between Wistar, TR- and AV_{Ugt} rats were analyzed on the LC-MS/MS system. Previous experiments using Western Blots have indicated that rUgt1a enzymes increase in concentration from the duodenum section of the GI tract descending into the colon (Miles et al., 2006; Shelby et al., 2003). In addition, mRNA analysis indicates that rUgt1a1 is the most prevalent isoform of the rUgt enzymes followed by rUgt1a6 and rUgt1a7 (Miles et al., 2006; Shelby et al., 2003). Current RT-PCR assays lack consistent sensitivity to detect rUgt1a7 within the liver, and these same studies detected this isoform within each section of the intestinal tract. Using the LC-MS/MS analytical procedure, we were able to detect rUgt1a7 in the liver, kidney and intestinal tracts in both Wistar and TR- rats.

Consistent with previous reports, rUgt1a1 was the most prominent enzyme within the liver in across all rat strains (Figure 4.10). Ugt1a7 was expressed at the highest levels within the colon in both Wistar and TR- rats with a general trend of increasing expression from the duodenum to the colon of the GI tract. Despite altered expression levels of rUgt1a1 and rUgt1a7 across tissue segments of the GI tract, expression of rUgt1a6 remained relatively unchanged. MPA glucuronidation within the kidney was approximately 40% of the levels within the liver, which was supported by both *in vitro* glucuronidation studies, but

also by previous experiments using selective antibodies with Western Blots showing that rUgt1a1 and rUgt1a7 levels were approximately half of those seen in the liver (Stern et al., 2007). Miles et al. reported that rUgt1a7 preferentially glucuronidates MPA compared to rUgt1a6 and rUgt1a1 in rats, which suggests that MPA glucuronidation rates should be higher within liver and colon compared to other tissues (Miles et al., 2005; Miles et al., 2006). While MPA toxicity is minimal within the liver, MPA toxicity within the colon is one of the primary sources of delayed onset diarrhea. The higher levels of rUgt1a7 and MPA glucuronidation capacity likely help protect Wistar rats, which are resistant to MPA toxicity, while Gunn rats, which lack all rUgt1a activity within all organs, are susceptible to MPA induced side effects (Miles et al., 2006).

While there were no statistically significant differences in rUgt1a6 and rUgt1a7 expression between Wistar and TR- rats, rUgt1a1 was significantly upregulated in TR- rat livers (Figure 4.10). Previous reports of glucuronidation in TR- rat livers indicate a slight increase in glucuronidation catalysis, but significant upregulation of rUgt expression when measured using Western Blots and RT-PCR (Johnson et. al 2006; Westley et al. 2006). The expression studies presented here using targeted quantitative proteomics indicate that while rUgt1a1 expression significantly increases in TR- rats, it is likely that alterations in transporter expression also factor in overall differences in MPA exposure between TR- rats and Wistar rats. This is because previous studies have indicated that rUgt1a1 is not the primary rUgt isoform involved in MPA

glucuronidation in the rat due to its higher Km and Vmax compared with rUgt1a7 (Miles et al., 2006).

Many previous experiments with membrane transporters have indicated that rMrp2 is highly expressed within the liver, kidney and brush border of the intestinal tract (Johnson et al., 2006). In addition, rBcrp and rMrp3 are also both highly expressed within the liver with variable expression within the intestinal tract. The experiments presented here have indicated that rMrp2 is highly expressed within the liver, kidney, duodenum and colon and found at lower levels within the jejunum and ileum. In Wistar rats, rMrp3 is present at lower levels than both rMrp2 and rBcrp except within the colon, and rMrp3 lacks any discernible pattern of expression within the intestinal tract. Compared to previous reports in the literature, levels of rMrp2 in Wistar rats found here by quantitative proteomics were approximately three fold lower than those reported in Sprague Dawley rats (Li et al., 2008). Because of the lack of genetic homogeneity within the outbred Sprague Dawley rat strains, along with differences in methodology, it is difficult to directly compare transporter expression levels between labs and species. Miles et al. noted that Sprague Dawley rats have approximately three fold higher *in vitro* MPA glucuronidation rates compared with Wistar rats (20.7 nmol/min/mg vs 6.0 nmol/min/mg) (Miles et al., 2006). The data presented in Figure 4.13 show that rMrp2 expression and *in vitro* glucuronidation rates correlate strongly, and enhanced rMrp2 expression could be a compensatory effect of increased glucuronidation capacity that varies with rat strain.

Unlike rMrp2, rBcrp was highly expressed within the liver and kidney but expression drops off within the intestinal tract. rBcrp levels within the liver and kidney (1.8 pmol/mg protein, Figure 4.11) were slightly higher than those reported by Li et al. within Sprague Dawley rats (Li et al., 2009). Using absolute quantitative proteomics, it is possible to compare values between labs, which were not feasible when using relative measurements with Western Blots to evaluate protein expression. Expression of rBcrp within the intestinal tract of rats was largely unchanged descending from the duodenum to the colon and was the least prominent of the three tested transporters in the colon. While the three efflux transporters within the Wistar and AV_{Ugt} strains were moderately expressed, tissue levels of the transporters changed substantially when compared with TR- rats (Figure 4.11).

There was a significant difference in rMrp3 levels within the tissues of the TR- rats with rMrp3 expression increasing five fold in both the liver and kidney relative to Wistar rats (Figure 4.11). Alterations in transporter expression were more modest between Wistar and TR- rats within the intestinal tract with minor decreases in rBcrp expression and increases in expression of rMrp3 primarily within the duodenum and colon. Previous reports with Western Blots of Wistar and TR- rats indicated a 500% increase in rMrp3 expression in TR- rat livers with minor decreases between TR- rats and Wistar rats across the intestinal tract in both rMrp3 and rBcrp expression (Johnson et al., 2006). The data presented here supports those earlier studies with some exceptions for rBcrp within the liver and rMrp3 within the intestinal tract. While Figure 4.11 shows slight increases in

rMrp3 levels in both the duodenum and colon, previous studies using Western Blot studies reported decreases in expression of both transporters of interest in rats (Johnson et al., 2006). It is likely that differences in sample preparation (cellular homogenate vs. membrane fractions) and tissue handling (homogenizing buffers, tissue extract conditions) contribute to this variability in discernible expression levels. In addition, the differences in assay methodology and lack of linearity of relative quantification with a Western Blot compared with targeted quantitative proteomics also contribute to variability in membrane transporter expression levels seen between the quantitative proteomics and the Western Blot method (Hoofnagle and Werner, 2009). The combination of increased levels of rMrp3 and rUgt1a1 enzymes, together with the decrease in efflux to bile by loss of rMrp2 contributes to the increased MPAG levels seen within the TR- rat plasma, while the maintenance of 10% of MPAG bilary excretion in TR- rats compared with Wistar rats within the bile indicate that rBcrp is likely a minor factor in the biliary excretion of MPAG in control Wistar rats.

Levels of both rMrp3 and rBcrp in AV_{Ugt} rats were largely unchanged with slight but not statistically significant increases in rMrp2 expression (Figure 4.11). Liver transporter levels in AV_{Ugt} rats were lower than the control Wistar strains and significantly lower than TR- rat livers ($p<0.05$). Gunn rats, the rUgt1a deficient background strain of the AV_{Ugt} rats, have been reported to possess upregulated rMrp3 transporter expression compared to Sprague Dawley rats (Higuchi et al., 2004). Interestingly, this was not seen within our experiments, although it should be noted that mRNA expression of rMrp3 is actually decreased

in Gunn rats and it is possible that nuclear receptor cofactors could be altered by enhanced rUgt expression (Higuchi K et al., 2004). In addition, compensatory changes in transporter expression in AV_{Ugt} rats may not be linear since it takes four days for the adenovirus vector to restore rUgt expression within the liver after IV administration to Gunn rats (Miles et al., 2006). This delayed response in transporter expression following rUgt restoration in Gunn rats could explain the lack of changes in tranporter expression levels.

While the experiments performed here were able to correlate rUgt1a1 expression with rMrp2, no other relationships were established between rUgt isoforms and tested transporters. Correlating expression levels of each tested rUgt isoform with each individual transporter generated very poor correlations (R^2<0.20, Figure 4.12, 13, 14), indicating that large scale coordinate up or down regulation of rUgt enzymes and transporters is unlikely. While many nuclear factors are shared between the two types of proteins (pregnane X receptor (PXR), constitutive androstane receptor (CAR), aryl hydrocarbon receptor (AhR)) there are many different regulatory sequences within the genome and protein sequences of each protein affecting expression at different levels (Wong et al., 2005). In humans, many primary transcription factors involved in UGT expression such as the cdx2 domain within the intestine, hepatocyte nuclear factor 1-alpha (HNF-1α) and the TATA box have not been linked to altered transporter expression (Strassburg et al., 1997; Tukey and Strassburg, 2000). The large differences in the type and behavior of the regulatory sequences

between the two types of proteins may explain their lack of coordinate and compensatory expression between subtypes and isoforms.

While there was no observed coordinate expression between the three efflux membrane transporters and the three rUgt enzymes of interest, there were strong correlations observed between MPAG formation levels with some of the membrane transporters and rUgts. A very strong correlation was observed between rMrp2 and MPA glucuronidation activity across all tissues, potentially indicating that while individual compensatory regulation is unlikely between rUgts and transporters, overall glucuronidation capacity could factor in efflux transporter expression (Figure 4.12-14). This is also seen in TR- rat livers, where rMrp2 expression is absent yet rUgt1a enzymes and rMrp3 are both upregulated, resulting in increased glucuronide conjugate concentrations within the blood due to increased efflux into the sinusoid of hepatocytes (Figure 4.1) (Johnson et al., 2006). Miles et al. have previously established a strong correlation between rUgt1a7 expression and MPA glucuronidation activity levels in rats (Miles et al., 2006). Initially, this relationship was not seen in our experiments; however, once the data from the intestinal tract was isolated from the liver and kidney rUgt studies, a strong correlation was observed between rUgt1a7 levels and MPA glucuronidation (Figure 4.12). The higher levels of rUgt1a1 within the liver and kidney likely contributed to the nonlinear relationship between rUgt1a7 levels and MPA glucuronidation activity.

This research successfully developed a targeted quantitative proteomic method to analyze the primary rUgt1a isoforms and membrane transporters

involved in MPA metabolism and hepatic efflux in rats. While coordinate regulation between individual rUgt isoforms and membrane transporters is unlikely due to the high degree of sequence homology between UGT enzymes, resulting in a number of similarities in substrate specificity between isoforms, glucuronidation activity could potentially result in higher expression levels of membrane transporters involved in glucuronide efflux (Meech and Mackenzie, 1997; Tukey and Strassburg, 2000). Previous experiments have suggested that acMPAG is not reactive enough to be a primary factor in MPA induced toxicity, so the increased expression of rUgt enzymes within the intestinal tract of both the Wistar and TR- rat livers could potentially limit MPA exposure to intestinal epithelial cells and toxicity within the gastrointestinal tract (Arns, 2007; Saitoh et al., 2005; Stern et al., 2007). The likely combination of rMrp3 and rUgt1a1 upregulation within the liver of TR- rats contributes with the loss of rMrp2 to elevated levels of MPAG and decreased levels of MPA within the blood while markedly decreased biliary clearance indicates that rBcrp is not a primary transporter involved in MPAG efflux in the rat. The continued development of targeted quantitative proteomics will continue to advance our understanding of the relationship between protein expression and metabolite disposition, providing investigators with an improved ability to properly evaluate the inter relationships of transporter protein and enzyme activity levels in tissues.

E. ACKNOWLEDGEMENTS

This work was made possible by funding through Cambridge Theranostics (U.K.) and the NIH along with Dr. Yurong Lai and Dr. Brigitte Simons who provided technical assistance.

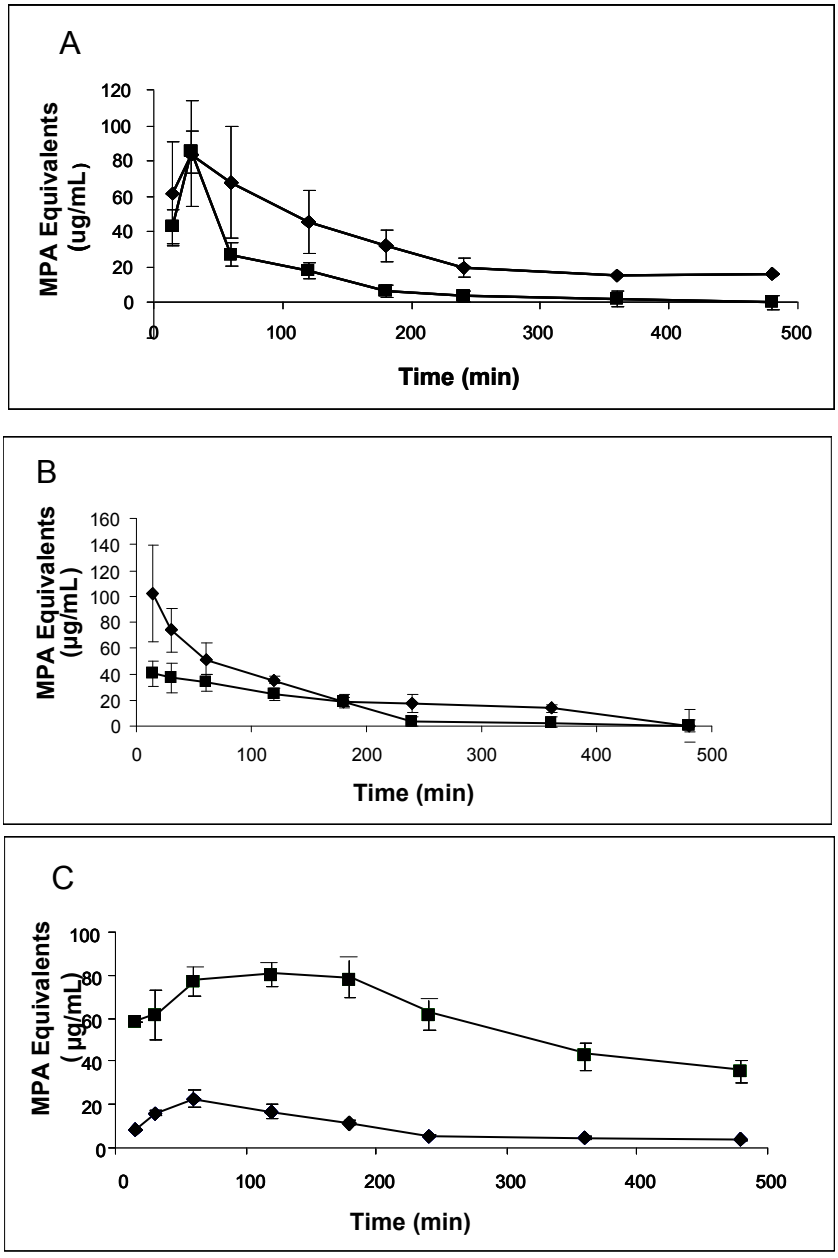

Figure 4.1. The disposition of MPA (◆) and MPAG (■) in plasma of bile cannulated rats after administration of 50 mg/kg MMF (33 mg/kg MPA equivalents) to Wistar rats (oral dosing, **A** and IV dosing, **B**) and oral dosing (**C**) to TR-rats. Data are presented as Mean±SE, n=5.

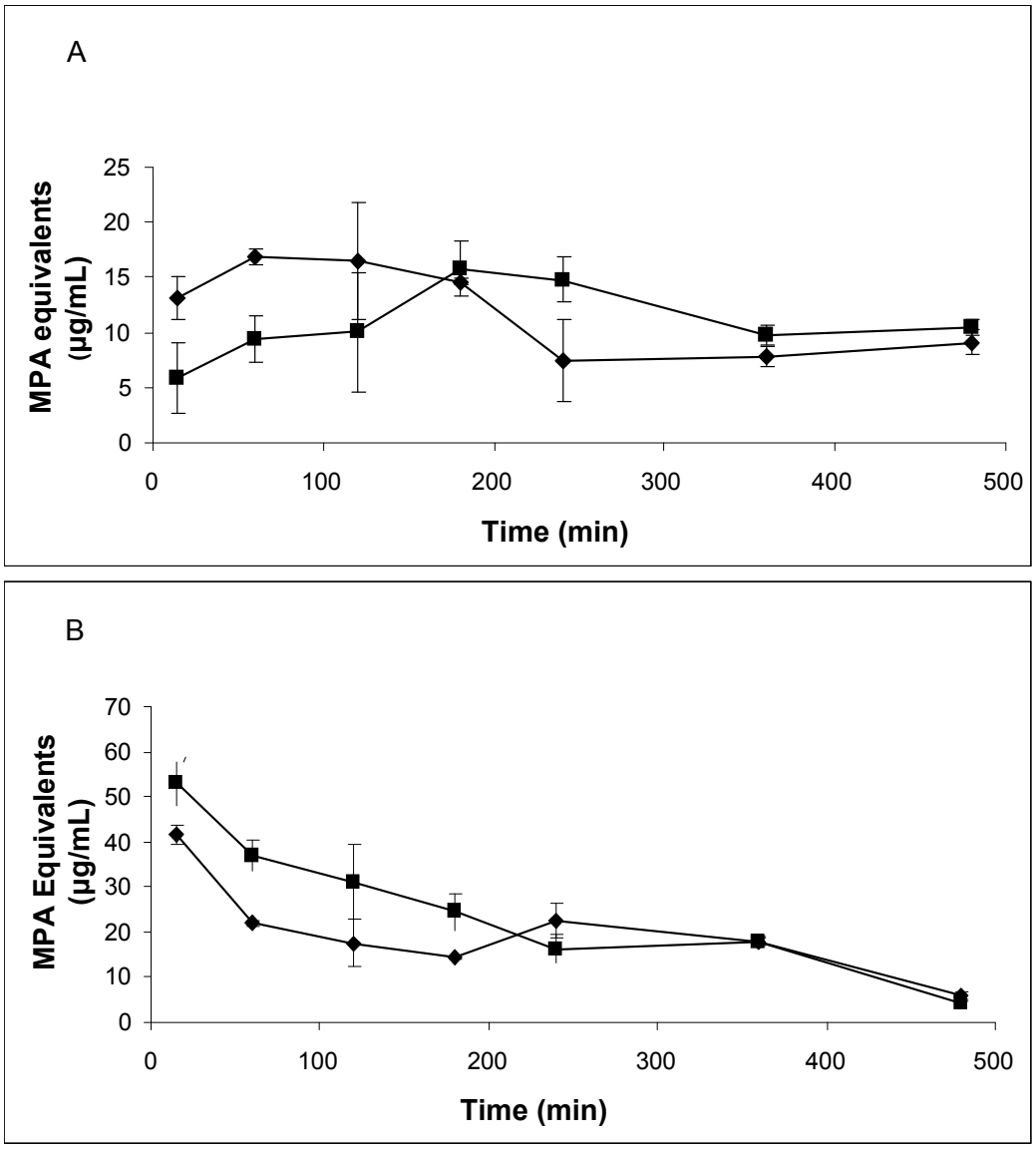

Figure 4.2. The disposition of MPA (◆) and MPAG (■) in plasma of Wistar rats without bile duct cannulation is shown after administration of 50 mg/kg MMF (33 mg/kg in MPA equivalents). **A**, oral dose; **B**, intravenous dose. Data is presented as Mean±SE, n=5.

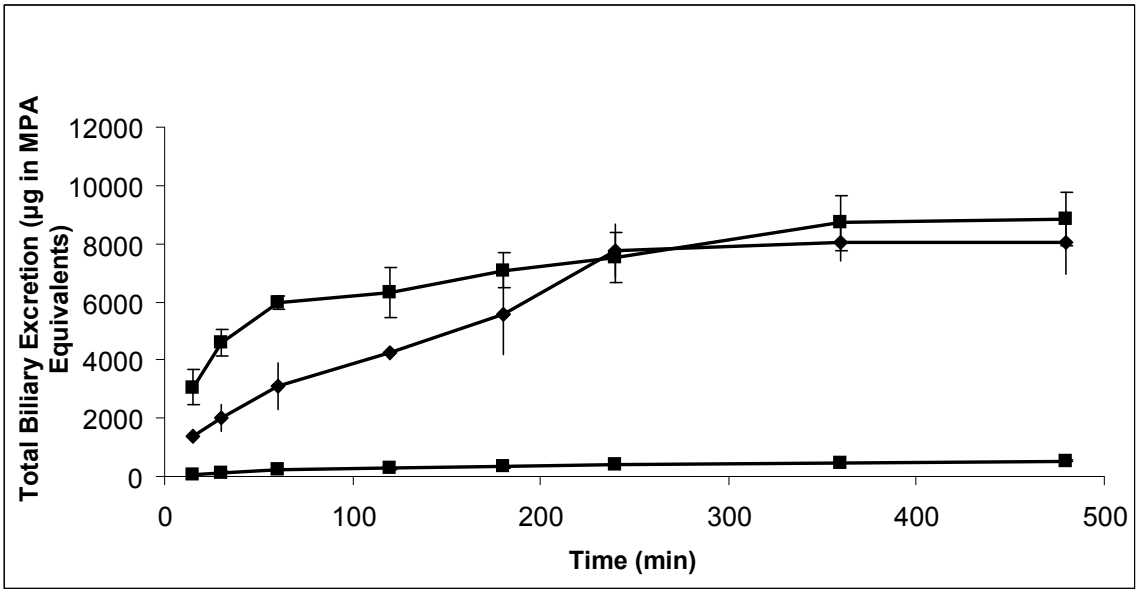

Figure 4.3. Total biliary excretion of combined acMPAG and MPAG in Wistar and TR- rats after a single 50 mg/kg dose of MMF (33 mg/kg in MPA equivalents). Biliary excretion values are shown for oral (■, top) and IV (◆) dosing to Wistar rats and oral dosing to TR- (■, bottom) rats. Data represents mean ±SE of biliary excretion values (n=5). In all cases acMPAG was a minor component of bile representing ~5% of MPA equivalents in bile. MPA was not measureable in bile.

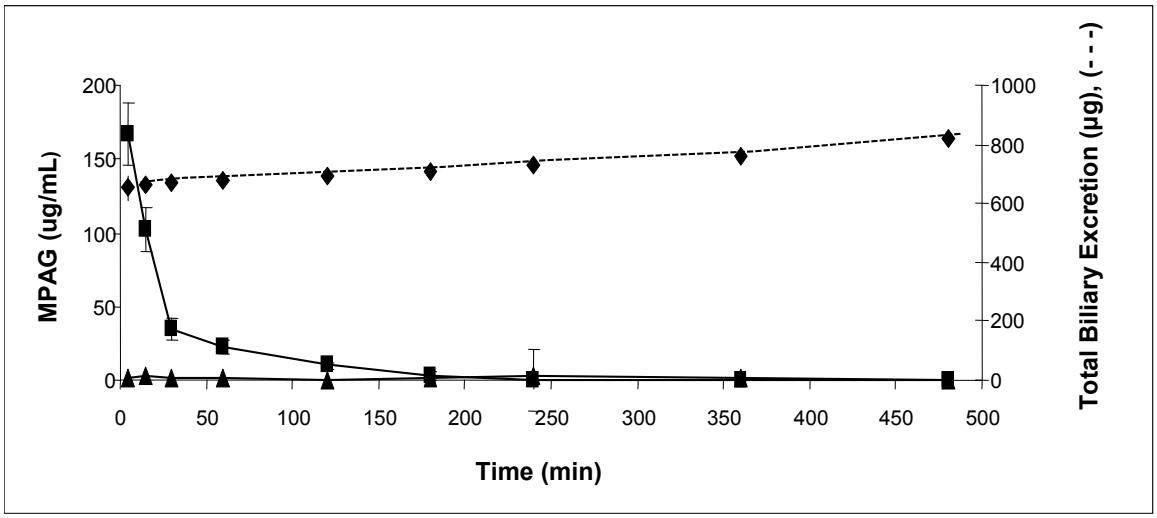

Figure 4.4. MPAG bile and plasma levels following 2.5 mg/kg IV MPAG (in MPA equivalents) administration to male Wistar rats with bile cannulation. Solid lines indicate plasma concentration data while total biliary excretion levels are demarcated by dashed lines. Symbols indicate mean values (n=3) for MPAG in bile (◆), MPAG in plasma (■) and MPA in plasma (▲). Data are presented as mean±SE (n=3).

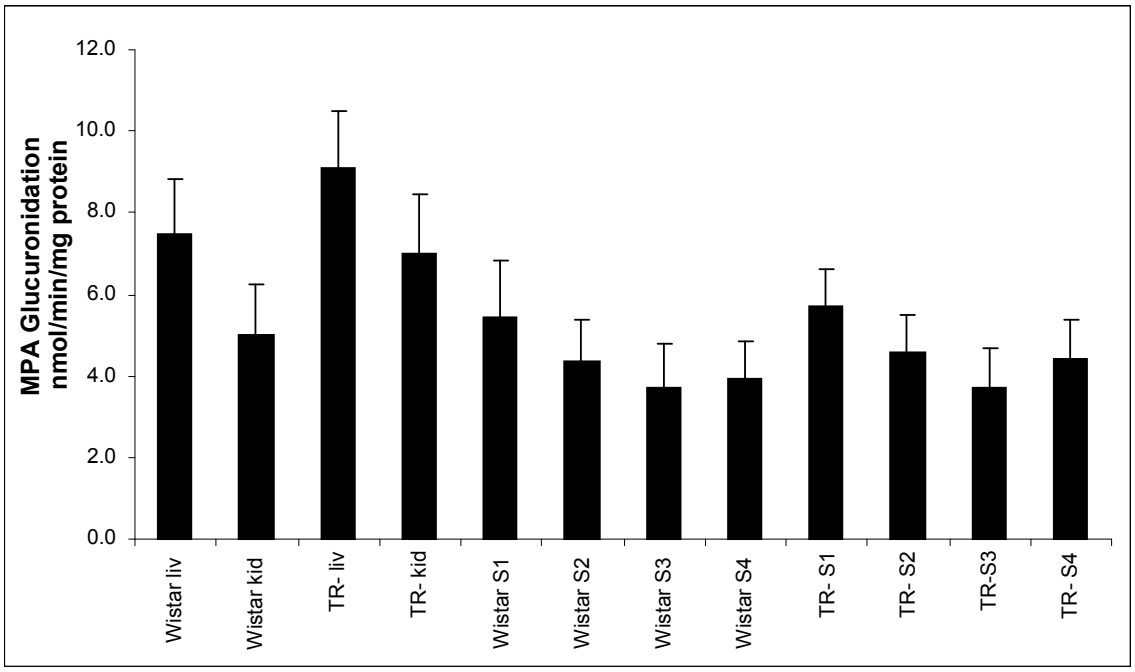

Figure 4.5. *In vitro* MPA glucuronidation rates for tissues from Wistar and TR- rats extracted following pharmacokinetic studies. MPA (1mM) incubations were stopped at 15 and 30 minutes and the obtained MPAG concentrations were averaged between the separate time periods to generate glucuronidation profiles. Data are presented as mean+SE (n=4).
*S1-S4 refers to intestinal segments obtained following rat euthanasia (S1-duodenum, S2-10cm segment of jejunum, S3-10 cm distal to caecum, S4-colon)

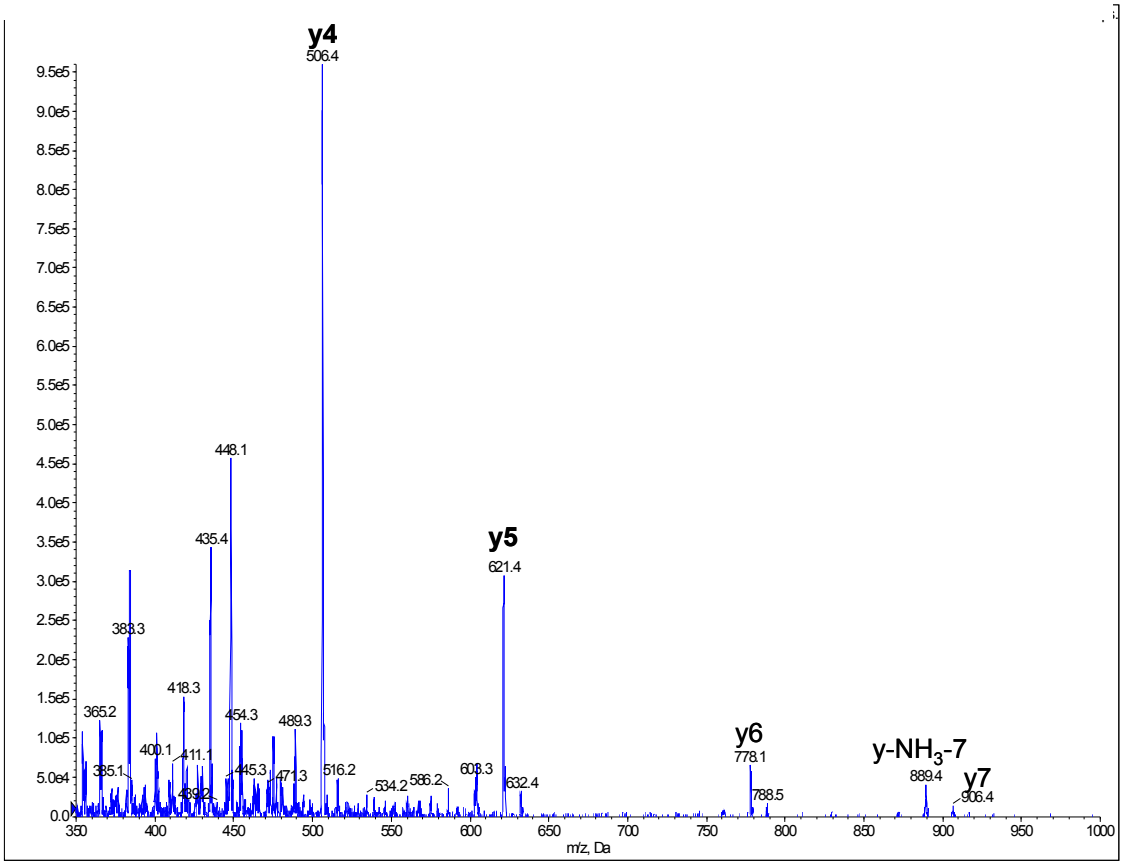

Figure 4.6. Representative product ion scan of 1 µg/mL infusion of peptide 3 heavy labeled standard (ENQF*DALFR, parent ion 575.4) on the QTRAP 5500 system yielding product ions for MRM quantification of peptide 3 representing rUgt1a6. Product ions **y4** and **y5** were selected for quantification based on signal intensities.

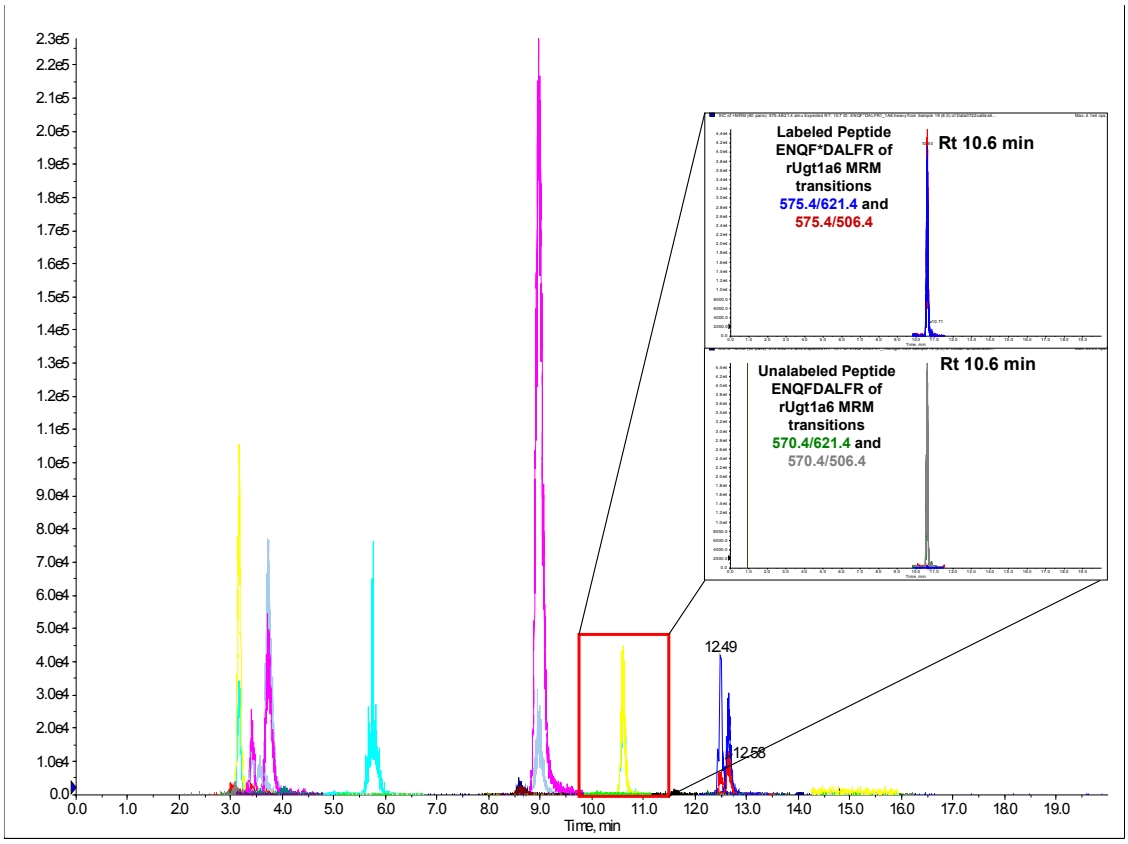

Figure 4.7. MRM chromatogram of 1.5 µg recombinant rUgt microsomal protein digest (containing rUgt1a1, 1a6 and 1a7) equivalent to 1.6 pmol/mg protein analyzed on the nanoACQUITY UPLC/QTRAP 5500 system. Extracted ion chromatograms from two MRMs of heavy labeled peptide 3 (ENQF*DALFR) and its corresponding unlabeled peptide representative of rUgt1a6 MRMs are enlarged.

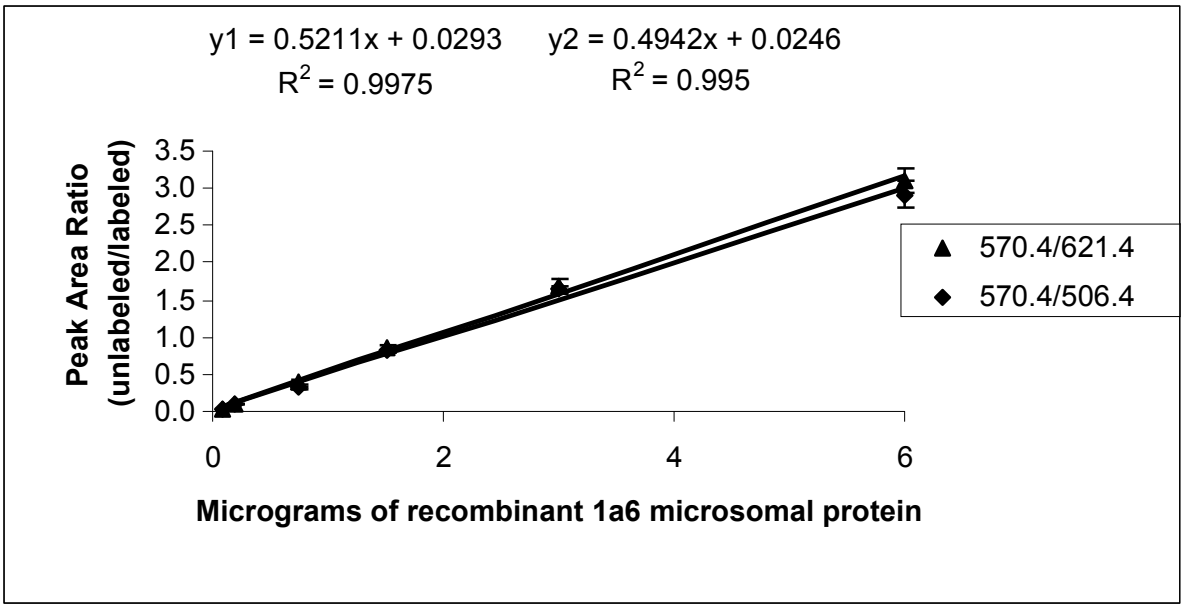

Figure 4.8. Calibration curves constructed from 5 replicate digests for two MRMs (y1 570.4/621.4, y2 570.4/506.4) of peptide 3 representative of rUgt1a6. Data is presented as mean ± SE.

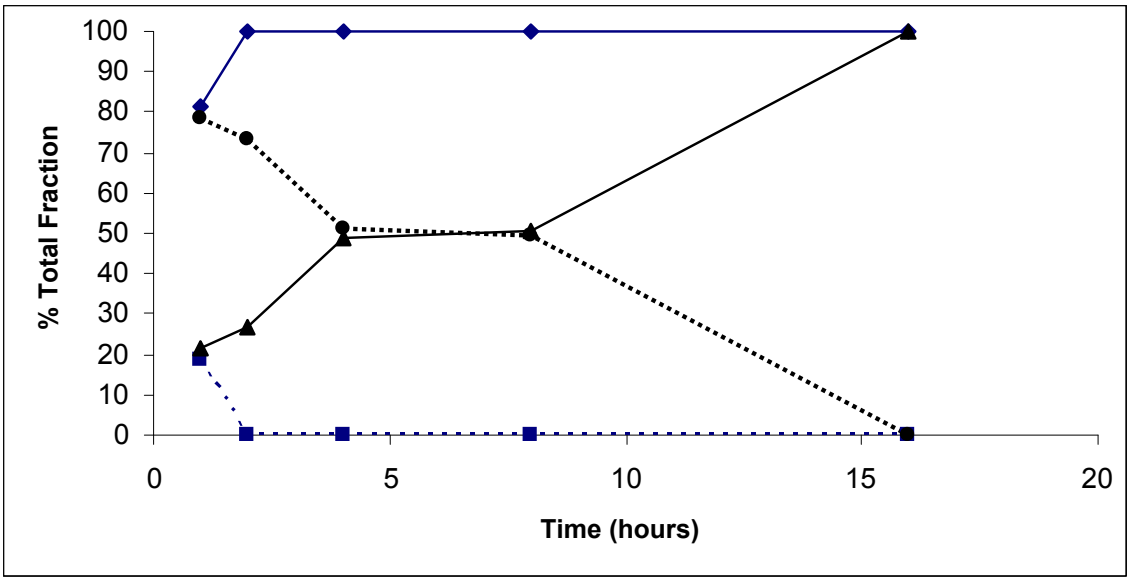

Figure 4.9. Time dependant tryptic digestion of β-casein protein using specific MRMs from two peptides monitoring missed cleavages sites performed in triplicate. Peptide MRMs representing complete (solid line) digestion obtained from peptides FFSDK (◆) and YIPIQYVLSR (▼) and incomplete digestion (dotted line) from DERFFSDK (■) and IAKYIPIQYVLSR (●). Peak areas ratios were obtained from the peptide MRMs using peptide 4 (ENQF*DALFR) as the internal standard. Measured area ratios were then compared between missed cleavage peptides to generate time dependant digestion curve.

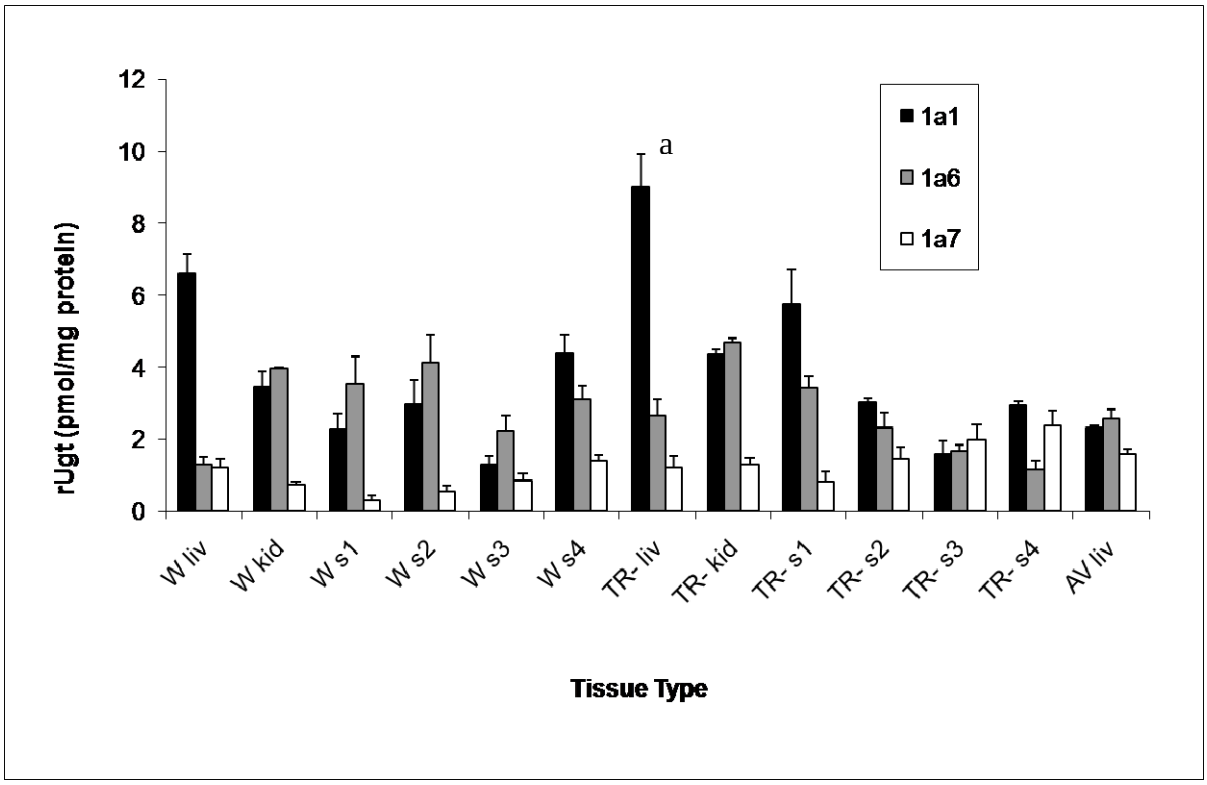

Figure 4.10. Graph indicates mean+SE (n=3 animals in duplicate) rUgt expression levels in tested rat tissues obtained following pharmacokinetic studies. One way ANOVA statistical analyses were used to evaluate potential significant differences in expression between each enzyme isoform across all tested tissues along with evaluating strain differences in rUgt expression.

*W refers to Wistar rat samples while TR- refers to TR- rats samples AV tissues indicates livers that were obtained from Dr. Ritter representing adenovirus (AV_{Ugt}) treatment of native Gunn rats to restore glucuronidation capacity

**S1-S4 refer to different segments of the GI tract extracted following euthanasia of rats with S1 containing the duodenum and S4 the distal colon as detailed in METHODS

[a] Significantly different between other tissue samples (rUgt1a1) ($p<0.05$)

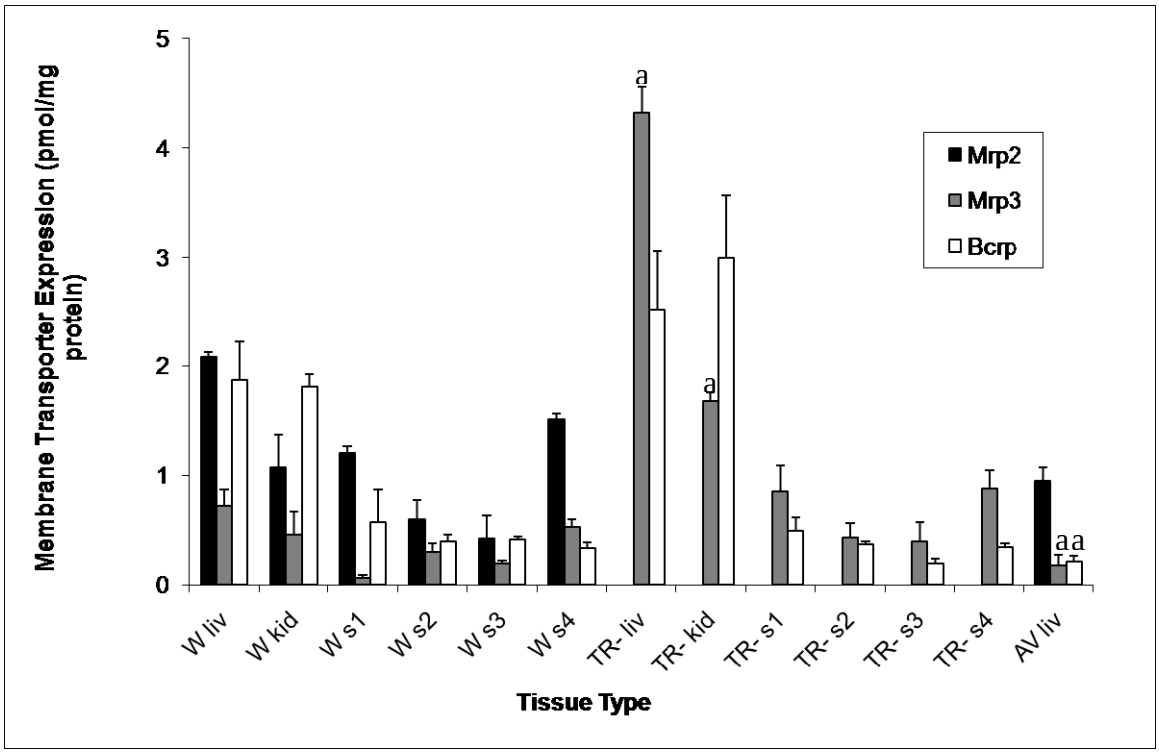

Figure 4.11. Graph indicates mean+SE (n=3) rat transporter expression levels in rat tissues following pharmacokinetic studies. Representative transporters evaluated were rMrp2 (Abcc2), rMrp3 (Abcc3) and rBcrp (Abcg2). One way ANOVA statistical analyses were used to evaluate potential significant differences in expression between each transporter across all tested tissues along with evaluating strain differences in rat transporter expression.

*All rMrp2 measurements were <LOD (0.01 pmol/mg protein) in TR- rat tissues

**W refers to Wistar rat samples while TR- refers to TR- rats samples AV tissues were obtained from Dr. Ritter representing AV_{Ugt} treatment of native Gunn rats to restore glucuronidation capacity.

***S1-S4 refer to different segments of the GI tract extracted following euthanasia of rats with S1 containing the duodenum and S4 the distal colon

[a] rMrp3 significantly different between other tissue samples across all tested rat strains ($p<0.05$)

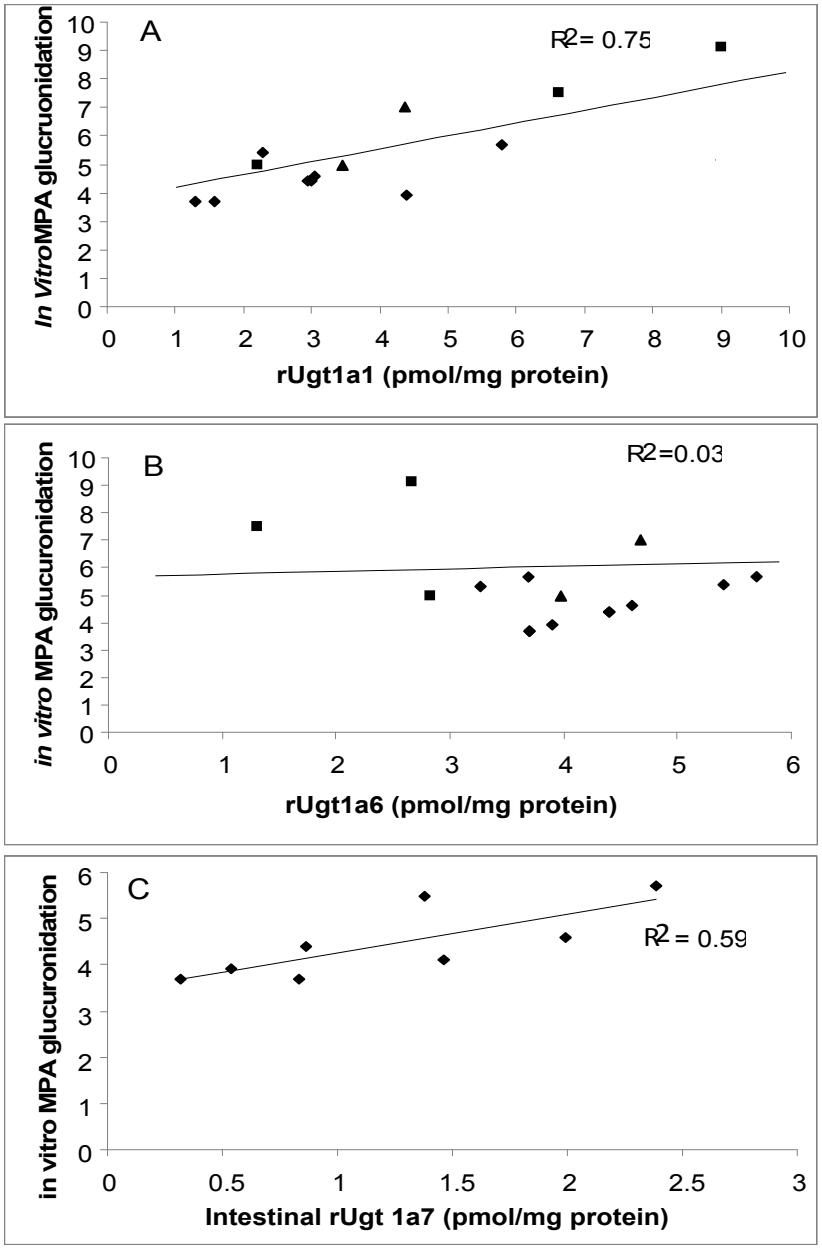

Figure 4.12. Correlation analysis relating glucuronidation activity (MPA catalysis) levels in rat liver (■), intestine (◆) and kidney (▲) (averaged, n=3 animals) to protein expression data obtained using quantitative proteomics. Correlation analysis was performed for glucuronidation rate vs. rUgt1a1 (A), glucuronidation rate vs. rUgt1a6 (B), glucuronidation rate vs. intestinal rUgt1a7 (C). Data points are averaged (n=3) from tissue measurements from microsomal protein or membrane fractions in Wistar, TR- and AV_{Ugt} rats (liver only). *In vitro* rates were matched with enzyme expression for each strain and tissue type to obtain R^2 values.

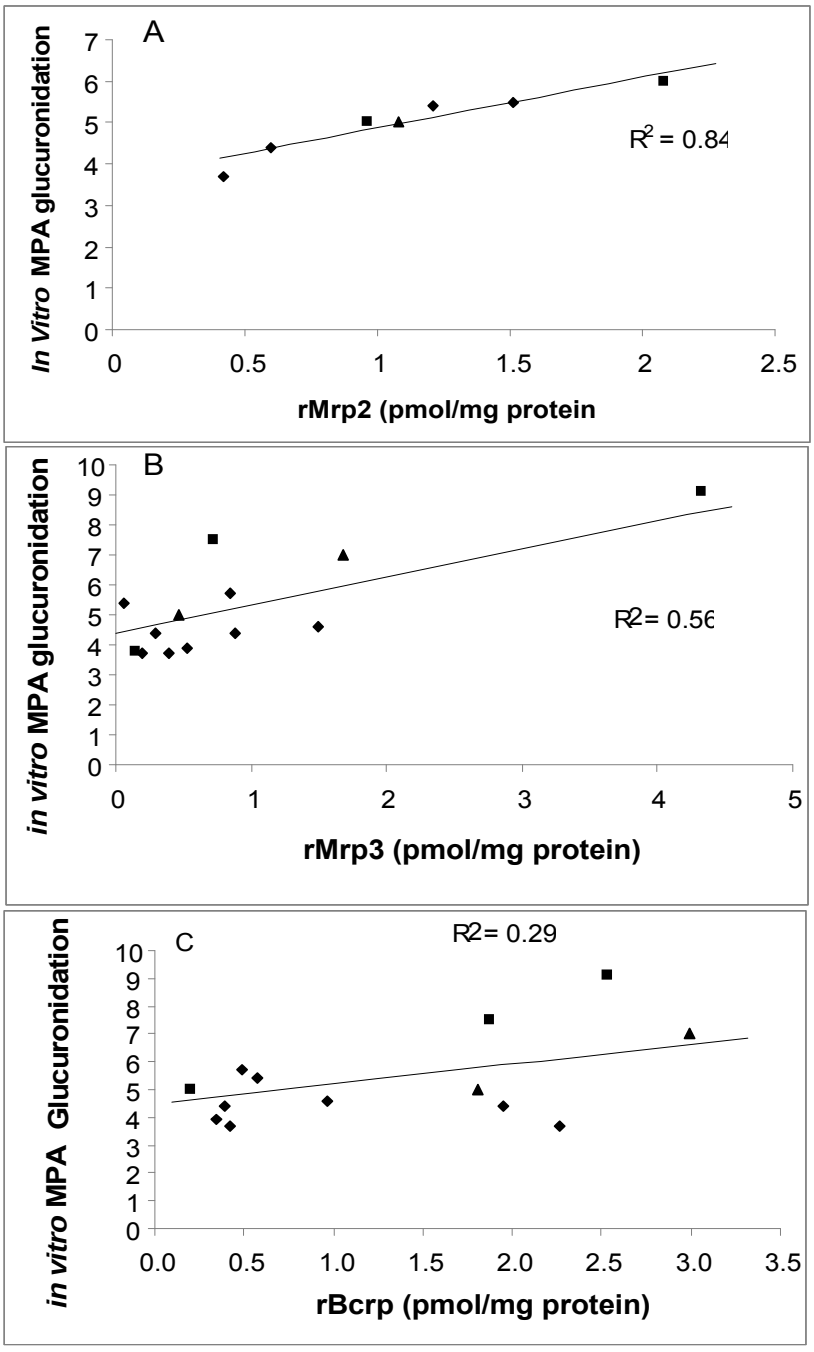

Figure 4.13. Correlation analysis relating glucuronidation activity (MPA catalysis) levels in rat liver (■), intestine (◆) and kidney (▲) (averaged, n=3 animals) to protein expression data obtained using quantitative proteomics. Correlation analysis was performed for glucuronidation rate vs. rMrp2 (A), glucuronidation rate vs. rMrp3 (B), glucuronidation rate vs. intestinal rBcrp (C). Data points are averaged (n=3) from tissue measurements from microsomal protein or membrane fractions in Wistar, TR- and AV_{Ugt} rats (liver only). *In vitro* rates were matched with enzyme expression for each strain and tissue type to obtain R^2 values.

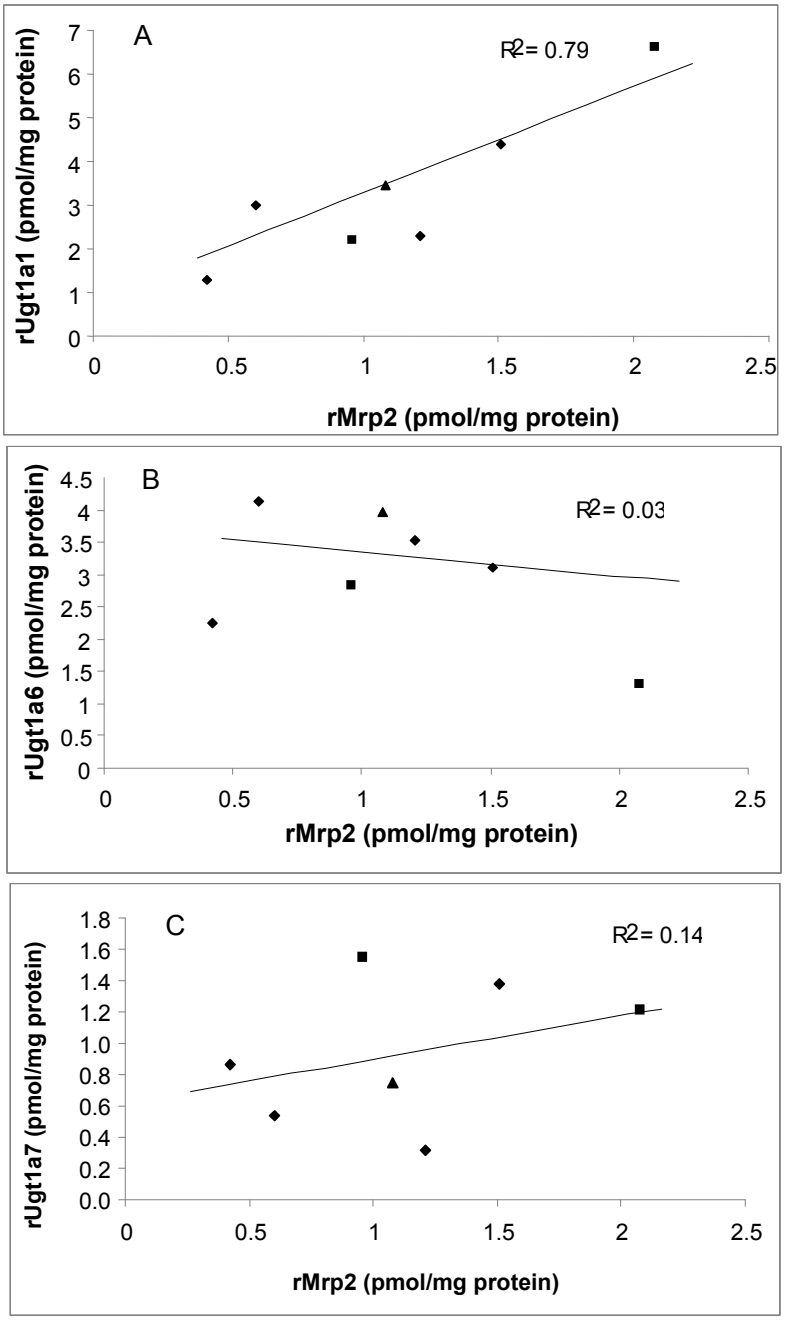

Figure 4.14. Correlation analysis relating rUgt expression levels in rat liver (■), intestine (◆) and kidney (▲) (averaged, n=3 animals) to protein expression data obtained using quantitative proteomics. Correlation analysis was performed for glucuronidation rate vs. rUgt1a1 (A), glucuronidation rate vs. rUgt1a6 (B), glucuronidation rate vs. intestinal rUgt1a7 (C). Data points are averaged (n=3) from tissue measurements from microsomal protein or membrane fractions in Wistar, TR- and AV_{Ugt} rats (liver only). Expression levels of rUgt enzymes were matched with rMrp2 levels for each strain and tissue type to obtain R^2 values.

Table 4.1. Rat Ugt/Transporter stable isotope labeled peptide standards and MRM transitions used for rat enzyme expression studies with QTRAP 5500 system. Optimal MRM transitions were obtained following direct infusion of heavy labeled standards (1 µg/mL).

Peptide Number	***Protein of Interest***	***Peptide Sequence***	***MRM Transitions***
Peptide 1	rUgt1a1	SVFP(^{13}C5,^{15}N)QDPFLLR	663.0/651.5 663.0/634.5
Peptide 2	rUgt1a1	EGSF(^{13}C9,^{15}N)YTMR	500.9/407.1 500.9/570.4
Peptide 3	rUgt1a6	ENQF(^{13}C9,^{15}N)DALFR	575.4/621.4 575.4/506.4
Peptide 4	rUgt1a6	SVFP(^{13}C5,^{15}N)VPYNLEELR	735.5/773.3 735.5/936.4
Peptide 5	rUgt1a7	YFSLP(^{13}C5,^{15}N)SVVFSR	654.5/797.5 654.5/997.5
Peptide 6	rUgt1a7	TYSV(^{13}C5,^{15}N)SHTSQEDQEDLNR	778.2/875.4 778.2/774.3
Peptide 7	rMrp2	ALTL(^{13}C6,^{15}N)SNLAR	483.5/560.1 483.5/656.0
Peptide 8	rMrp2	AFTSITL(^{13}C6,^{15}N)FNLLR	701.9/883.5 701.9/662.3
Peptide 9	rMrp2	LIHDLLVF(^{13}C9,^{15}N)LNPQLLK	596.1/479.2[a] 596.1/592.3[a]
Peptide 10	rMrp3	TAII(^{13}C5,^{15}N)GVLYR	506.4/613.0 506.4/726.6
Peptide 11	rMrp3	TTYP(^{13}C5,^{15}N)YIASNR	596.4/723.4 596.4/826.3
Peptide 12	rMrp3	YP(^{13}C5,^{15}N)GLELVLK	519.8/612.3 519.8/723.2
Peptide 13	rBcrp	VGTQF(^{13}C9,^{15}N)TR	409.8/276.2 409.8/240.1[a]
Peptide 14	rBcrp	AELDQLP(^{13}C5,^{15}N)VAQK	609.4/548.1 609.4/661.6
Peptide 15	rBcrp	TIIF (^{13}C9,^{15}N)SIHQPR	663.5/551.4 663.5/663.2

a: Transitions were b ions. All other transitions represent y ions.

Table 4.2. MPA pharmacokinetic estimates in rats were obtained using Noncompartmental pharmacokinetic endpoints after 50 mg/kg single dose of MMF (33 mg/kg in MPA equivalents). AUC and clearance values were measured for individual rats then averaged. Numbers in **bold** indicate significant difference ($p<0.05$) using one way ANOVA. Values not available are denoted with an * while MPA exposure levels were calculated as indicated in the footnotes below.

Pharmacokinetic Parameter	IV BD[a] Cannulated Wistar rats (n=5)	PO BD[a] Cannulated Wistar rats (n=5)	PO BD[a] Cannulated TR- rats (n=4)	IV BD[a] Intact Wistar rats (n=4)	PO BD[a] Intact Wistar rats (n=4)
Tmax (min)	*	36.0±13.4	75.0±30.0	*	220.0±34.6
Cmax (µg/mL)	145.4±40.3	89.1±21.6	20.1±3.4	50.8±12.6	34.9±10.7
$t_{1/2}$ (hr)	2.5±0.7	3.0±0.7	2.9±0.5	2.0±0.6	2.2±0.8
$AUC_{(MPA_{0-inf})}$ (mg/mL*min)	10.3±1.7	11.6±1.2	6.1±1.2	14.3±3.3	12.3±4.6
$AUC_{(MPAG_{0-inf})}$ (mg/mL*min)	6.7±2.8	6.0±1.7	**42.1±3.9**	16.1±2.5	14.2±2.5
AUC_{MPAG}/AUC_{MPA}	0.63±0.28	0.53±0.15	**6.94±2.13**	1.24±0.28	1.21±0.34
$CL_{biliary}$ (mL/min)[e]	1.1±0.3	0.81±0.23	**0.09±0.03**	*	*
Total Clearance (mL/min)	1.7±0.3	1.2±0.1[b]	2.5±0.4[b]	1.9±0.3	1.8±0.5
Fe_{bile}[c]	0.64±0.14	0.68±0.09	**0.031±0.009**	*	*
MPA exposure derived from EHC[d]	*	*	*	0.39	0.20

Data are presented as mean±SD.
a: BD= bile duct
b: CL/F for oral dosing
c: Sum of MPAG and acMPAG in bile collected over 8 hours
d: %EHC= $\frac{AUC(MPA_{(0 \rightarrow \text{inf})})_{(Intact)} - AUC(MPA_{(0 \rightarrow \text{inf})})_{(Cannulated)}}{AUC(MPA_{(0 \rightarrow \text{inf})})_{(Cannulated)}}$
e: Apparent $CL_{biliary}$= $\frac{\sum (MPAG_{bile} + acMPAG_{bile})}{AUC_{(MPA0 \rightarrow \text{inf})}}$

Table 4.3. Assay method validation of intraday variability of rUgt enzymes and membrane transporter expression levels were averaged from five replicate measurements. Units are expressed as pmol/mg microsomal protein (n=5)

Sample	rUgt1a1	rUgt1a6	rUgt1a7	rMrp2	rMrp3	rBcrp
[a]Wistar Liver	8.3	2.1	0.8	*	*	*
(%C.V.)	(6.3)	(16.0)	(6.6)	*	*	*
[c]Wistar Liver Membrane	*	*	*	1.9	0.7	1.9
(%C.V.)	*	*	*	(5.7)	(19.1)	(15.6)

* Indicates samples were below limit of detection (<0.01 pmol/mg protein)
[a] Denotes intraday rUgt measurements from Wistar liver microsomes
[b]Denotes intraday transporter measurements from Wistar liver membrane fractions

**Samples were analyzed on the nanoACQUITY UPLC-QTRAP 5500 instrument with a BEH column (150 µm X 100 mm X 1.7 µ) at 2 µL/min using a linear gradient conducted as follows: 0 min, 15% B; 5 min, 15% B; 25 min, 65% B; 25.1 min, 99%B; 30 min, 15% B; reequilibration until 40 minutes. QTRAP5500 was operated in positive mode with the Nanospray III source using Scheduled MRMs optimized as indicated in METHODS.

Table 4.4. Interday Variability of rUgt enzymes and membrane transporter expression levels were averaged from five replicate measurements in pmol/mg protein

Sample	rUgt1a1	rUgt1a6	rUgt1a7	rMrp2	rMrp3	rBcrp
[a]Wistar Liver	8.1	1.9	1.0	*	*	*
(%C.V.)	(7.9)	(11.0)	(15.6)	*	*	*
[b]Wistar Liver Membrane	*	*	*	1.7	0.7	1.4
(%C.V.)	*	*	*	(18.6)	(12.6)	(8.8)

* Indicates samples were below limit of detection (<0.01 pmol/mg protein)
[a] Denotes interday rUgt measurements from Wistar liver microsomes
[b] Denotes interday transporter measurements from Wistar liver membrane
**Samples were analyzed on the nanoACQUITY UPLC-QTRAP 5500 instrument with a BEH column (150 µm X 100 mm X 1.7 µ) at 2 µL/min using a linear gradient conducted as follows: 0 min, 15% B; 5 min, 15% B; 25 min, 65% B; 25.1 min, 99%B; 30 min, 15% B; reequilibration until 40 minutes. QTRAP5500 was operated in positive mode with the Nanospray III source using Scheduled MRMs optimized as indicated in METHODS.

Table 4.5. Individual peptide measurements of rUgt enzyme expression levels were averaged from five replicate measurements. Two MRMs from each peptide were selected (Table 4.1) and averaged between each individual sample.

Sample	rUgt1a1	rUgt1a1	rUgt1a6	rUgt1a6	rUgt1a7	rUgt1a7
Peptide	1	2	3	4	5	6
rUgt (pmol/mg protein)	5.53	7.25	1.47	1.08	1.31	1.10
(%C.V.)	(8.7)	(16.1)	(8.6)	(12.3)	(20.8)	(6.3)

*Samples were analyzed on the nanoACQUITY UPLC-QTRAP 5500 instrument with a BEH column (150 µm X 100 mm X 1.7 µ) at 2 µL/min using a linear gradient conducted as follows: 0 min, 15% B; 5 min, 15% B; 25 min, 65% B; 25.1 min, 99%B; 30 min, 15% B; reequilibration until 40 minutes. QTRAP5500 was operated in positive mode with the Nanospray III source using Scheduled MRMs optimized as indicated in METHODS.
**Peptide Selection Rules for Quantification: 1) If recombinant protein available, must produce a linear standard curve with a %C.V. <25% at the base of the calibration curve, 2) must produce a %C.V. <25% on both interday/intraday validation, 3) if two peptides are used for protein quantification average protein concentrations must be within 50% of each other.

Table 4.6. Individual peptide measurements of rat transporter expression levels were averaged from five replicate measurements. Two MRMs from each peptide were selected (Table 4.1) and averaged between each individual sample. For each transporter three peptides were selected for quantification with the exception of rMrp3 due to the elimination of peptide 12 based on selection rules.

Sample	**rMrp2**	**rMrp2**	**rMrp2**	**rMrp3**	**rMrp3**	**rBcrp**	**rBcrp**	**rBcrp**
Peptide	**7**	**8**	**9**	**10**	**11**	**13**	**14**	**15**
Rat Transporter (pmol/mg protein)	1.53	2.13	1.71	0.54	0.44	1.61	1.39	2.09
(%C.V.)	(14.5)	(23.9)	(11.9)_	(20.2)	(19.2)	(17.1)	(17.6)	(7.8)

*Samples were analyzed on the nanoACQUITY UPLC-QTRAP 5500 instrument with a BEH column (150 µm X 100 mm X 1.7 µ) at 2 µL/min using a linear gradient conducted as follows: 0 min, 15% B; 5 min, 15% B; 25 min, 65% B; 25.1 min, 99%B; 30 min, 15% B; reequilibration until 40 minutes. QTRAP5500 was operated in positive mode with the Nanospray III source using Scheduled MRMs optimized as indicated in METHODS.

**Peptide Selection Rules for Quantification: 1) If recombinant protein available, must produce a linear standard curve with a %C.V. <25% at the base of the calibration curve, 2) must produce a %C.V. <25% on both interday/intraday validation, 3) if two peptides are used for protein quantification average protein concentrations must be within 50% of each other.

F. References

Alterman MA, Kornilayev B, Duzhak T, Yakovlev D. Quantitative analysis of cytochrome p450 isozymes by means of unique isozyme-specific tryptic peptides: a proteomic approach. *Drug Metab Dispos.* **2005,** 33(9),1399-407.

Arns W. Noninfectious gastrointestinal (GI) complications of mycophenolic acid therapy: a consequence of local GI toxicity? *Transplant Proc.* **2007**, 39(1), 88-93.

Barnidge DR, Goodmanson MK, Klee GG, Muddiman DC. Absolute quantification of the model biomarker prostate-specific antigen in serum by LC-Ms/MS using protein cleavage and isotope dilution mass spectrometry. J *Proteome Res.* **2004,** 3(3), 644-52.

Barr JR, Maggio VL, Patterson DG Jr, Cooper GR, Henderson LO, Turner WE, Smith SJ, Hannon WH, Needham LL, Sampson EJ. Isotope dilution--mass spectrometric quantification of specific proteins: model application with apolipoprotein A-I. *Clin Chem.* **1996,** 42(10), 1676-82.

Beynon RJ, Doherty MK, Pratt JM, Gaskell SJ. Multiplexed absolute quantification in proteomics using artificial QCAT proteins of concatenated signature peptides. *Nat Methods.* **2005,** 2(8), 587-9.

Brun V, Dupuis A, Adrait A, Marcellin M, Thomas D, Court M, Vandenesch F, Garin J. Isotope-labeled protein standards: toward absolute quantitative proteomics. *Mol Cell Proteomics.* **2007,** 6(12), 2139-49.

Cañas B, López-Ferrer D, Ramos-Fernández A, Camafeita E, Calvo E. "Mass spectrometry technologies for proteomics." *Brief Funct Genomic Proteomic.* **2006,** 4(4), 295-320.

Catania VA, Luquita MG, Sánchez Pozzi EJ, Ikushiro S, Emi Y, Iyanagi T, Mottino AD. Effect of spironolactone on the expression of rat hepatic UDP-glucuronosyltransferase. *Biochem Pharmacol.* **2003,** 66(1), 171-7.

Davies NM, Grinyó J, Heading R, Maes B, Meier-Kriesche HU, Oellerich M. Gastrointestinal side effects of mycophenolic acid in renal transplant patients: a reappraisal. *Nephrol Dial Transplant.* **2007,** 22, 2440-2448.

Emi Y, Ikushiro S, Kato Y. Thyroxine-metabolizing rat uridine diphosphate-glucuronosyltransferase 1A7 is regulated by thyroid hormone receptor. *Endocrinology.* **2007,** 148(12), 6124-33.

Fallon JK, Harbourt DE, Maleki SH, Kessler FK, Ritter JK and Smith PC, Absolute Quantification of Human Uridine-Diphosphate Glucuronosyl Transferase (UGT) Enzyme Isoforms 1A1 and 1A6 By Tandem LC MS, *Drug Metabolism Letters.* **2008,** 2, 210-222.

Gerber SA, Rush J, Stemman O, Kirschner MW, Gygi SP.Absolute quantification of proteins and phosphoproteins from cell lysates by tandem MS. *Proc Natl Acad Sci U S A.* **2003,** 100(12), 6940-5.

Goshe MB, Smith RD. Stable isotope-coded proteomic mass spectrometry. *Curr Opin Biotechnol.* **2003,** 14(1), 101-9.

Gregory PA, Lewinsky RH, Gardner-Stephen DA, Mackenzie PI. Regulation of UDP glucuronosyltransferases in the gastrointestinal tract. *Toxicol Appl Pharmacol.* **2004,** 199(3), 354-63.

Higuchi K, Kobayashi Y, Kuroda M, Tanaka Y, Itani T, Araki J, Mifuji R, Kaito M, Adachi Y. Modulation of organic anion transporting polypeptide 1 and multidrug resistance protein 3 expression in the liver and kidney of Gunn rats. *Hepatol Res.* **2004,** 29(1), 60-66.

Hoofnagle AN, Becker JO, Wener MH, Heinecke JW. Quantification of thyroglobulin, a low-abundance serum protein, by immunoaffinity peptide enrichment and tandem mass spectrometry. *Clin Chem.* **2008,** 54(11), 1796-804.

Hoofnagle AN, Wener MH. The fundamental flaws of immunoassays and potential solutions using tandem mass spectrometry. *J Immunol Met.* **2009,** 347(1-2), 3-11.

Huttlin EL, Chen X, Barrett-Wilt GA, Hegeman AD, Halberg RB, Harms AC, Newton MA, Dove WF, Sussman MR. Discovery and validation of colonic tumor-associated proteins via metabolic labeling and stable isotopic dilution. *Proc Natl Acad Sci U S A.* **2009,** 106(40), 17235-40.

Jenkins RE, Kitteringham NR, Hunter CL, Webb S, Hunt TJ, Elsby R, Watson RB, Williams D, Pennington SR, Park BK. Relative and absolute quantitative expression profiling of cytochromes P450 using isotope-coded affinity tags. *Proteomics.* **2006,** 6(6), 1934-47.

Johnson BM, Zhang P, Schuetz JD, Brouwer KL. Characterization of transport protein expression in multidrug resistance-associated protein (Mrp) 2-deficient rats. *Drug Metab Dispos.* **2006,** 34(4), 556-62.

Kamiie J, Ohtsuki S, Iwase R, Ohmine K, Katsukura Y, Yanai K, Sekine Y, Uchida Y, Ito S, Terasaki T. Quantitative atlas of membrane transporter proteins:

development and application of a highly sensitive simultaneous LC/MS/MS method combined with novel in-silico peptide selection criteria. *Pharm Res.* **2008,** 25(6), 1469-83.

Kirkpatrick DS, Gerber SA, Gygi SP. The absolute quantification strategy: a general procedure for the quantification of proteins and post-translational modifications. *Methods.* **2005,** 35(3), 265-73.

Kuhn E, Wu J, Karl J, Liao H, Zolg W, Guild B. Quantification of C-reactive protein in the serum of patients with rheumatoid arthritis using multiple reaction monitoring mass spectrometry and 13C-labeled peptide standards. *Proteomics.* **2004,** 4(4), 1175-86.

Li N, Nemirovskiy OV, Zhang Y, Yuan H, Mo J, Ji C, Zhang B, Brayman TG, Lepsy C, Heath TG, Lai Y. Absolute quantification of multidrug resistance-associated protein 2 (MRP2/ABCC2) using liquid chromatography tandem mass spectrometry. *Anal Biochem.* **2008,** 380(2), 211-22.

Li N, Palandra J, Nemirovskiy OV, Lai Y. LC-MS/MS Mediated Absolute Quantification and Comparison of Bile Salt Export Pump and Breast Cancer Resistance Protein in Livers and Hepatocytes across Species. *Anal Chem.* **2009.**

Li N, Zhang Y, Hua F, Lai Y. Absolute difference of hepatobiliary transporter multidrug resistance-associated protein (MRP2/Mrp2) in liver tissues and isolated hepatocytes from rat, dog, monkey, and human. *Drug Metab Dispos.* **2009,** 37(1), 66-73.

Meech R and Mackenzie PI. UDP-Glucuronosyltransferase, the Role of the Amino Terminus in Dimerization. *J Biol Chem.* **1997,** 272(43), 26913-26917.

Miles KK, Kessler FK, Smith PC, Ritter JK. Characterization of rat intestinal microsomal UDP-glucuronosyltransferase activity toward mycophenolic acid. *Drug Metab Dispos.* **2006,** 34(9), 1632-9.

Miles KK, Kessler FK, Webb LJ, Smith PC, Ritter JK. Adenovirus-mediated gene therapy to restore expression and functionality of multiple UDP-glucuronosyltransferase 1A enzymes in Gunn rat liver. *J Pharmacol Exp Ther.* **2006,** 318(3), 1240-7.

Miles KK, Stern ST, Smith PC, Kessler FK, Ali S, Ritter JK. An investigation of human and rat liver microsomal mycophenolic acid glucuronidation: evidence for a principal role of UGT1A enzymes and species differences in UGT1A specificity. *Drug Metab Dispos.* **2005,** 33(10), 1513-20.

Miura M, Satoh S, Inoue K, Kagaya H, Saito M, Inoue T, Suzuki T, Habuchi T. Influence of SLCO1B1, 1B3, 2B1 and ABCC2 genetic polymorphisms on mycophenolic acid pharmacokinetics in Japanese renal transplant recipients. *Eur J Clin Pharmacol.* **2007,** 63(12), 1161-9.

Miura M, Kagaya H, Satoh S, Inoue K, Saito M, Habuchi T, Suzuki T. Influence of Drug Transporters and UGT Polymorphisms on Pharmacokinetics of Phenolic glucuronide Metabolite of Mycophenolic Acid in Japanese Renal Transplant Recipients. *Ther Drug Monit.* **2008.**

Naderer OJ, Dupuis RE, Heinzen EL, Wiwattanawongsa K, Johnson MW, Smith PC. The influence of norfloxacin and metronidazole on the disposition of mycophenolate mofetil. *J Clin Pharmacol.* **2005**, 45(2), 219-26.

Nagai F, Satoh H, Mori S, Sato H, Koiwai O, Homma H, Matsui M. Mapping of rat bilirubin UDP-glucuronosyl-transferase gene (Ugt1a1) to chromosome region 9q35-->q36. *Cytogenet Cell Genet.* **1995,** 69(3-4), 185-6.

Nagaraj N, Lu A, Mann M, Wiśniewski JR. Detergent-based but gel-free method allows identification of several hundred membrane proteins in single LC-MS runs. *J Proteome Res.* **2008,** 7(11), 5028-32.

Owens IS, Basu NK, Banerjee R. UDP-glucuronosyltransferases: gene structures of UGT1 and UGT2 families. *Methods Enzymol.* **2005,** 400, 1-22.

Picard N, Ratanasavanh D, Prémaud A, Le Meur Y, Marquet P. Identification of the UDP-glucuronosyltransferase isoforms involved in mycophenolic acid phase II metabolism. *Drug Metab Dispos.* **2005,** 33(1), 139-46.

Platz KP, Sollinger HW, Hullett DA, Eckhoff DE, Eugui EM, Allison AC. RS-61443--a new, potent immunosuppressive agent. *Transplantation*. **1991,** 51(1), 27-31.

Ros JE, Roskams TA, Geuken M, Havinga R, Splinter PL, Petersen BE, LaRusso NF, van der Kolk DM, Kuipers F, Faber KN, Müller M, Jansen PL. ATP binding cassette transporter gene expression in rat liver progenitor cells. *Gut.* **2003,** 52(7), 1060-7.

Saitoh H, Kobayashi M, Oda M, Nakasato K, Kobayashi M, Tadano K. Characterization of intestinal absorption and enterohepatic circulation of mycophenolic Acid and its 7-O-glucuronide in rats. *Drug Metab Pharmacokinet.* **2006**, 21(5), 406-13.

Shelby MK, Cherrington NJ, Vansell NR, Klaassen CD. Tissue mRNA expression of the rat UDP-glucuronosyltransferase gene family. *Drug Metab Dispos.* **2003,** 31(3), 326-33.

Shipkova M, Armstrong VW, Oellerich M, Wieland E. Acyl glucuronide drug metabolites: toxicological and analytical implications. *Ther Drug Monit.* **2003,** 25, 1-16.

Stern ST, Tallman MN, Miles KK, Ritter JK, Dupuis RE, Smith PC. Gender-related differences in mycophenolate mofetil-induced gastrointestinal toxicity in rats. *Drug Metab Dispos.* **2007,** 35(3), 449-54.

Strassburg CP, Nguyen N, Manns MP, Tukey RH. Polymorphic expression of the UDP-glucuronosyltransferase UGT1A gene locus in human gastric epithelium. *Mol Pharmacol.* **1998,** 54(4), 647-54.

Strassburg CP, Oldhafer K, Manns MP, Tukey RH. Differential expression of the UGT1A locus in human liver, biliary, and gastric tissue: identification of UGT1A7 and UGT1A10 transcripts in extrahepatic tissue. *Mol Pharmacol.* **1997**, 52(2), 212-20.

Staatz CE, Tett SE. Clinical pharmacokinetics and pharmacodynamics of mycophenolate in solid organ transplant recipients. *Clin Pharmacokinet.* **2007,** 46, 13-58.

Takano M, Yumoto R, Murakami T. Expression and function of efflux drug transporters in the intestine. *Pharmacol Ther.* 2006, 109(1-2), 137-61.

Thomas A, Geyer H, Kamber M, Schänzer W, Thevis M. Mass spectrometric determination of gonadotrophin-releasing hormone (GnRH) in human urine for doping control purposes by means of LC-ESI-MS/MS. *J Mass Spectrom.* **2008,** 43(7), 908-15.

Tukey RH, Strassburg CP. Human UDP-glucuronosyltransferases: metabolism, expression, and disease. *Annu Rev Pharmacol Toxicol.* **2000,** 40, 581-616.

Vaisar T, Urban J. Probing the proline effect in CID of protonated peptides. *J Mass Spectrom.* **1996,** 31(10), 1185-7.

Vansell NR, Klaassen CD. Increase in rat liver UDP-glucuronosyltransferase mRNA by microsomal enzyme inducers that enhance thyroid hormone glucuronidation. *Drug Metab Dispos.* **2002,** 30(3), 240-6.

Wang MZ, Wu JQ, Dennison JB, Bridges AS, Hall SD, Kornbluth S, Tidwell RR, Smith PC, Voyksner RD, Paine MF, Hall JE. A gel-free MS-based quantitative proteomic approach accurately measures cytochrome P450 protein concentrations in human liver microsomes. *Proteomics.* **2008,** 8(20), 4186-96.

Webb LJ, Miles KK, Auyeung DJ, Kessler FK, Ritter JK. Analysis of substrate specificities and tissue expression of rat UDP-glucuronosyltransferases UGT1A7 and UGT1A8. *Drug Metab Dispos.* **2005,** 33(1), 77-82

Westley IS, Brogan LR, Morris RG, Evans AM, Sallustio BC. Role of Mrp2 in the hepatic disposition of mycophenolic acid and its glucuronide metabolites: effect of cyclosporine. *Drug Metab Dispos.* **2006,** 34(2), 261-6.

Westley IS, Morris RG, Evans AM, Sallustio BC. Glucuronidation of mycophenolic acid by Wistar and Mrp2-deficient TR- rat liver microsomes. *Drug Metab Dispos.* **2008,** 36(1), 46-50.

Whitehouse CM, Dreyer RN, Yamashita M and Fenn JB, Electrospray interface for liquid chromatographs and mass spectrometers. *Anal. Chem.* **1985,** 57**,** 675-679.

Wong H, Lehman-McKeeman LD, Grubb MF, Grossman SJ, Bhaskaran VM, Solon EG, Shen HS, Gerson RJ, Car BD, Zhao B, Gemzik B. Increased hepatobiliary clearance of unconjugated thyroxine determines DMP 904-induced alterations in thyroid hormone homeostasis in rats. *Toxicol Sci.* **2005**, 84(2), 232-42.

Wu SL, Amato H, Biringer R, Choudhary G, Shieh P, Hancock WS. Targeted proteomics of low-level proteins in human plasma by LC/MSn: using human growth hormone as a model system. *J Proteome Res.* **2002,** 1(5), 459-65.

Wu WW, Wang G, Baek SJ, Shen RF. Comparative study of three proteomic quantitative methods, DIGE, cICAT, and iTRAQ, using 2D gel- or LC-MALDI TOF/TOF. *J Proteome Res.* **2006,** 5(3), 651-8.

Zamek-Gliszczynski MJ, Hoffmaster KA, Humphreys JE, Tian X, Nezasa K, Brouwer KL. Differential involvement of Mrp2 (Abcc2) and Bcrp (Abcg2) in biliary excretion of 4-methylumbelliferyl glucuronide and sulfate in the rat. *J Pharmacol Exp Ther.* **2006,** 319(1), 459-67.

CHAPTER 5

CONCLUSIONS

The experiments presented here utilizing novel methods for the quantitative analysis of UGTs and transporters have increased our understanding of MPA metabolism and disposition while beginning to establish relationships between quantitative expression of drug metabolizing enzymes and metabolic profiles. MPA is metabolized and detoxified through the actions of UGT enzymes almost exclusively, making it an excellent compound for studying effects of varying expression levels of UGTs and membrane transporters on MPA exposure. Because MPA is metabolized into two forms of glucuronide conjugates, an inactive phenolic and the labile acyl, it is also imperative to examine any potential toxicity resulting from excessive acMPAG exposure. Potential toxicity resulting from acyl glucuronide exposure has been reported since the 1970s, and despite conflicting reports, acMPAG had been postulated as a potential factor in MPA based GI toxicity (Bailey and Dickinson, 2003; Faed, 1984; Shipkova et al., 2003). It was important to evaluate acMPAG stability and reactivity in order to validate that glucuronidation activity is beneficial within the GI tract, and subjects with moderate or elevated UGT activity within the intestine are likely less susceptible to MPA toxicity due to lower levels of MPA regional tissue exposure compared with subjects deficient in UGT enzymes within the intestinal tract.

Our experiments indicated that acMPAG is neither highly reactive nor highly unstable. When these experiments are coupled with previous *in vivo* evidence that found no correlations between acMPAG exposure and GI toxicity, it supports the argument that acMPAG is not a primary factor to consider in MPA

toxicity. With acMPAG discounted as a primary factor in MPA toxicity, glucuronidation within the GI tract can be viewed as a detoxification process that is beneficial to enterocytes and also a secondary parameter when evaluating MPA toxicity in patients.

Pharmacogenomics is a rapidly growing field with respect to understanding the effect of altered enzyme expression and drug toxicity. The recent modification of adding Gilbert's Syndrome (UGT1A1*28 polymorphism), which results in a reduction of UGT1A1 activity in humans by 70%, warnings to labels on irinotecan products is a prime example of how genetic variations in enzyme expression can affect drug safety in the clinical setting (Guillemette, 2003; Nagar et al., 2006). Yet one primary problem with developing drug warnings based on polymorphisms is that it is difficult to accurately quantify the precise changes in enzyme expression using traditional antibody assays commonly employed. In humans, there are over thirty known polymorphisms affecting UGT1A1 expression alone and numerous others affecting expression of the remaining UGT1As (Guillemette, 2003; Tukey and Strassburg, 2000; <http://som.flinders.edu.au/FUSA/ClinPharm/UGT/>). Without the development of more sensitive or reliable testing, scientists have had to rely on mRNA expression studies, which may correlate poorly with protein expression or Western Blots, which are difficult to correlate between labs, lack specific antibodies for numerous enzymes, and have limited sensitivity and dynamic ranges.

Quantitative proteomics can be employed for both preclinical and clinical samples of interest based on the results using reliable methods for evaluating UGT expression in both humans and rats, along with membrane transporters in the rat kidney, liver and intestine. A significant component of this dissertation project involved the development of these methods due to the need to overcome numerous hurdles during this process of methods development on several LC-MS/MS platforms. One of the primary obstacles during the method development process throughout this project was the selection of the proper internal standards. The first 18 peptides selected for analysis of the hUGTs were beset by some difficulties in MRM product ion selection and inconsistent retention times on the LC-MS/MS. Primarily, peptides in these experiments longer than 13 amino acids containing a number of histidine residues were prone to excessive charge states resulting in inadequate sensitivity for reliable quantification. A secondary problem with peptide selection, both during these experiments and for future studies, is that some proteins may only generate one or two acceptable tryptic fragments. In this case, it may become necessary to examine alternative enzymes for proteolytic digests such as chymotrypsin or Lys-C or to combine proteases to expand the sequence coverage of each enzyme in hopes of generating more suitable peptides for quantification.

Another issue to examine in future studies concerns flow rates and column selection for future applications. While our lab performed the rat enzyme studies using a 150 µm ID column, we have also evaluated the utility of 100 µm and 300 µm ID columns. Compared to the 150 µm columns, the other two formats were

between two and five fold less sensitive on the 5500 QTRAP, indicating that the current column generates the best data for all current applications and is the best current compromise between sensitivity and robustness (data not shown). However, it should be noted that larger ID columns could be applied for future studies where absolute sensitivity can be sacrificed for increased throughput and column lifetime.

Even though targeted quantitative proteomics produces a number of advantages for scientists, there are still drawbacks. One of the primary criticisms of quantitative proteomics continues to be the upfront cost in both LC-MS/MS instrumentation along with annual maintenance. An additional problem is that even though several new software packages have been recently produced by a number of companies attempting to make LC-MS/MS more user friendly, there is a still a steep learning curve. While the development of multiple protease digests has generated an increasing amount of potential stable isotope standards, there will still be proteins that are not amenable to the current methods in quantitative proteomics due to insufficient peptide candidates that lend themselves to high sensitivity LC-MS/MS detection.

What the development of targeted quantitative proteomics allows for is to precisely evaluate altered expression of proteins of interest with their biological significance. In particular, these experiments can highlight sources of potential differences in metabolite exposure using quantitative proteomics compared with either mRNA expression or *in vitro* metabolism studies. One example that can be highlighted in this project involves evaluating differences in MPAG levels seen

in TR- rat plasma compared with Wistar rats. Following MPA administration and bile cannulation, there was a significant difference in MPAG exposure seen in TR- rats, while there were no differences in *in vitro* glucuronidation rates between TR- rats and Wistar rats. However, when transporter and rUgt levels are compared between the two strains, there was a significant increase in rUgt1a1 and rMrp3 expression within the liver in TR- rats. Because rUgt1a1 and rMrp3 are two of the primary proteins responsible for MPAG formation and efflux, respectively, into the blood, it is likely that the upregulation of these two proteins coupled with the absence of Mrp2 for biliary excretion in TR- rats results in increased MPAG plasma levels. This illustrates that quantitative proteomics can be a powerful tool in explaining differences in metabolism, elimination and toxicity that may be irresolvable using more traditional methods.

One of the more frustrating aspects within the field of quantitative proteomics is the lack of applications directly linking protein expression with clinical outcomes. Recently, there have been a number of published reports for quantifying a number of biologically significant drug metabolizing enzymes and biomarkers including CYPs, membrane transporters, C-reactive protein and prostate specific antigen (Barnidge et al., 2004; Jenkins et al., 2006; Kuhn et al., 2004; Li et al., 2008; Wang et al., 2008). Yet despite the wealth of knowledge and resources, scientists have been unable to apply these methods to evaluate potential differences in enzyme expression with any events of biological significance. One of the primary goals of this project was to begin to bridge the

gap between proteomic experiments performed primarily by analytical chemists and clinicians lacking the tools needed for applications in quantitative proteomics.

A secondary goal of this project was to begin to set up preliminary methods to be able to analyze large numbers of samples for targeted quantitative proteomic analysis. One primary advantage that the AQUA^{TM} peptide selection rules provide is that the resulting peptides will retain similar chromatographic profiles due to size and residue restrictions. Because of this, method alterations to accommodate the analysis of different proteins will likely be minor, enabling faster method development and minimal variations in LC gradients. The advantages of rapid method development, faster LC runs and precise and sensitive quantification provided will make targeted quantitative proteomics more accessible to biologists and clinicians than ever before.

Within the areas of UGTs and transporters, there are several different avenues where this research may be applied. One of the primary interests to scientists is the effect of genetic polymorphisms on protein expression. As noted earlier, there are over thirty polymorphisms within the UGT1A1 isoform alone (Guillemette, 2003; Nagar et al., 2006; Tukey and Strassburg, 2000). One potential benefit could be gained by evaluating different expression levels of UGT enzymes across a number of microsomal donors and correlating these levels with any SNPs discovered during genotyping. Using both of these methods will help evaluate whether the polymorphisms of interest significantly affect isoform expression, resulting in decreased UGT activity. An additional area of interest to clinicians could be in evaluating patients undergoing either irinotecan or MPA

therapy for UGT levels to help determine patient susceptibility to GI toxicity. Patients on either treatment regimen may undergo colonic biopsies that may be analyzed for UGT expression with our current protein requirements (~10 µg per assay). Susceptible patients displaying diminished UGT levels might be carefully monitored over the course of treatment and may open other areas of adjuvant therapy, including coadministration with potential UGT inducers to help improve therapeutic outcomes.

In summary, the work presented within this project has advanced our understanding of acMPAG stability and reactivity relating to MPA toxicity, along with the development and application of targeted quantitative proteomics to evaluate enzyme expression in both rats and humans. Most importantly, through the use of proteomics and *in vitro/in vivo* models, we have begun to establish relationships between tissue expression and xenobiotic metabolism and elimination. Furthermore, these relationships open up a number of areas of research into possible coregulation of enzymes and transporters and relating metabolite profiles using both Phase II and Phase III metabolism. In addition, because of the low protein requirements of our current methods, clinical applications evaluating drug metabolism and toxicity are also possible. Finally, we hope that this research eventually helps clinicians and scientists tailor treatment regimens to susceptible populations resulting in improved therapeutic outcomes with less adverse reactions and toxicity.

References

Allison AC and Eugui EM. "Preferential Suppression of Lymphocyte Proliferation by Mycophenolic Acid and Predicted Long Term Effects of Mycophenoliate Mofetil in Transplantation." *Transplant Proc.* **1994,** 26(6), 3205-3210.

Barnidge DR, Goodmanson MK, Klee GG, Muddiman DC. "Absolute quantification of the model biomarker prostate-specific antigen in serum by LC-Ms/MS using protein cleavage and isotope dilution mass spectrometry." *J Proteome Res*. **2004,** 3(3), 644-52.

Bock KW and Kohle C. Topological aspects of oligomeric UDP-glucuronosyltransferases in endoplasmic reticulum membranes: Advances and open questions. *Biochem Pharm.* **2009,** 77, 1458-1465.

Bullingham RE, Nicholls AJ, Kamm BR. Clinical pharmacokinetics of mycophenolate mofetil. *Clin Pharmacokinet.* **1998,** 34(6), 429-55.

Cañas B, López-Ferrer D, Ramos-Fernández A, Camafeita E, Calvo E. "Mass spectrometry technologies for proteomics." *Brief Funct Genomic Proteomic.* **2006,** 4(4), 295-320.

Cattaneo D, Perico N and Remuzzi G. "From Pharmacokinetics to Pharmacogenomics: A New Approach to Tailor Immunosuppressive Therapy." *Am J Transplant*. **2004,** 4, 299-310.

Dickinson RG and Bailey MJ. "Acyl Glucuronide reactivity in perspective: biological consequences." *Chem Biol Interact.* **2003,** 145, 117-137.

Faed EM. Properties of acyl glucuronides: implications for studies of the pharmacokinetics and metabolism of acidic drugs. *Drug Metab Rev*. **1984,** 15, 1213-1249.

Guillemette C. Pharmacogenomics of human UDP-glucuronosyltransferase enzymes. *Pharmacogenomics J.* **2003,** 3(3), 136-58.

Jenkins RE, Kitteringham NR, Hunter CL, Webb S, Hunt TJ, Elsby R, Watson RB, Williams D, Pennington SR, Park BK. Relative and absolute quantitative expression profiling of cytochromes P450 using isotope-coded affinity tags. *Proteomics.* **2006,** 6(6), 1934-47.

Kamiie J, Ohtsuki S, Iwase R, Ohmine K, Katsukura Y, Yanai K, Sekine Y, Uchida Y, Ito S, Terasaki T. Quantitative atlas of membrane transporter proteins: development and application of a highly sensitive simultaneous LC/MS/MS method combined with novel in-silico peptide selection criteria. *Pharm Res.* **2008,** 25(6), 1469-83.

Kuhn E, Wu J, Karl J, Liao H, Zolg W, Guild B. Quantification of C-reactive protein in the serum of patients with rheumatoid arthritis using multiple reaction monitoring mass spectrometry and 13C-labeled peptide standards. *Proteomics.* **2004,** 4(4), 1175-86.

Kypers DRJ, Vanrenterghem Y, Squifflet JP, Mourad M, Abramowicz D, Oellerich M, Armstrong V, Shipkova M and Daems J. Twelve Month Evaluation of the Clinical Pharmacokinetics of Total and Free Mycophenolic Acid and Its Glucuronide Metabolites in Renal Allograft Recipients on Low Dose Tacrolimus in Combination with Mycophenolate Mofetil. *Ther Drug Monit.* **2003,** 25, 609-622.

Li N, Nemirovskiy OV, Zhang Y, Yuan H, Mo J, Ji C, Zhang B, Brayman TG, Lepsy C, Heath TG, Lai Y. Absolute quantification of multidrug resistance-associated protein 2 (MRP2/ABCC2) using liquid chromatography tandem mass spectrometry. *Anal Biochem.* **2008,** 380(2), 211-22.

Nagar S and Remmel RP. "Uridine diphophoglucuronosyltransferase pharmacogenetics and cancer." *Oncogene.* (2006) 25, 1659-1672.

Shipkova M, Armstrong VW, Oellerich M, Wieland E. Acyl glucuronide drug metabolites: toxicological and analytical implications. *Ther Drug Monit.* **2003,** 25, 1-16.

Tukey RH and Strassburg CP. "Human UDP-Glucuronosyltransferases: Metabolism, Expression and Disease." *Ann Rev Pharmacol Toxicol.* **2000,** 40, 581-616.

UDP Glucuronosyltransferase Homepage. Department of Clinical Pharmacology, Flinders University. <http://som.flinders.edu.au/FUSA/ClinPharm/UGT/>

Wang MZ, Wu JQ, Dennison JB, Bridges AS, Hall SD, Kornbluth S, Tidwell RR, Smith PC, Voyksner RD, Paine MF, Hall JE. A gel-free MS-based quantitative proteomic approach accurately measures cytochrome P450 protein concentrations in human liver microsomes. *Proteomics.* **2008,** 8(20), 4186-96.

APPENDIX

ABSOLUTE QUANTIFICATION OF HUMAN URIDINE-DIPHOSPHATE GLUCURONOSYL TRANSFERASE (UGT) ENZYME ISOFORMS 1A1 AND 1A6 BY TANDEM LC-MS

This section was published in *Drug Metablism Letters*. 2, 210-222. 2008

A. INTRODUCTION

UGT enzymes catalyze the formation of glucuronic acid conjugates of Phase II metabolism. Glucuronidation is the most important Phase II metabolic pathway for drugs [Evans and Relling 1999] and is also a primary elimination route for other xenobiotics and endogenous compounds [Meech and Mackenzie 1997, Tukey and Strassburg 2000, Guillemette 2003, Wells et al. 2004]. Quantification of UGTs in biological matrices has traditionally been done by immunometric methods such as Western blots and ELISA. These methods can be time consuming and cumbersome, and require the raising of antibodies, which are often unsuccessful in achieving specificity. Indeed, there is a high degree of sequence identity among the UGT1A subfamily of enzymes, and antibodies have been found to be cross reactive between isoforms. Quantitative measurements by Western blot can be highly variable, with very limited dynamic range, and often provide imprecise quantification results, even if done relative to a control experiment. The ELISA method is more sensitive, and linearity can be greater, but considerable effort is needed to validate an ELISA assay, even when a specific antibody is available.

Other techniques for quantitative analysis of proteins have been developed in recent years. These include the Difference Gel Electrophoresis (DIGE) method [Friedman et al. 2007, Tonge et al. 2001] which employs fluorescent tags and gel electrophoresis for separation and relative quantification, and antibody arrays [Wellmann et al. 2002]. Methods based on isotopic labeling have also been developed. These include stable isotope labeling

with amino acids in cell culture (SILAC) [Ong et al. 2002], Isotope Coated Affinity Tags (ICAT) [Gygi et al. 1999, Jenkins et al. 2006, Smolka et al. 2001, Turecek 2002], and iTRAQ reagents [Ross et al. 2004, Skalnikova et al. 2007]. ICAT targets a specific amino acid, cysteine, on the protein sequence, while iTRAQ enables coverage of an entire peptide sequence by N-terminal labeling of all peptides. Many of these techniques can at best only be described as semi-quantitative because they establish relative differences in protein expression between samples. iTRAQ and ICAT can be used for absolute quantification when employed with standards of known concentration as calibrants.

The approach of using heavy isotope labeling for absolute quantification has previously been established [Barnidge et al. 2003, Barr et al. 1996, Gerber et al. 2003, Kuhn et al. 2004] and has become increasingly popular with the ongoing development of higher sensitivity analytical instrumentation [Kamiie et al. 2008, Kirsch et al. 2007, Lin et al. 2006]. The determination of absolute concentration enables better interpretation of metabolic studies by, for example, allowing transfer of data between laboratories without needing to normalize to different controls. It also enables better comparison of data between biological tissue types. Barr et al. [Barr et al. 1996] used heavy labeled peptides, unique to the protein, to quantify apoliproprotein A-I. They found the concentration obtained to be in good agreement with the known concentration of the Apo A-I standard. Gerber et al. [Gerber et al. 2003] used the technique, with tandem MS (including selected reaction monitoring), to quantify proteins and phosphoproteins from cell lysates, and introduced the term AQUA (absolute quantification). Myoglobin was

measured in the presence of whole yeast and was found to equal the known amount of myoglobin added. Kuhn et al. [Kuhn et al. 2004] quantified C-reactive protein in serum using ^{13}C-labeled peptide standards. They cautioned against claims of absolute quantification due to possible peptide losses during sample preparation or incomplete trypsin digestion. Their sample preparation procedure was complex (size exclusion chromatography and SDS-PAGE analysis) and heavy labeled peptides were added after trypsinization. Barnidge et al. [Barnidge et al. 2003] quantified prostate specific antigen in serum using a synthetic peptide containing two glycine atoms each labeled with two ^{13}C atoms and one ^{15}N atom. Although they found values determined to be lower than those obtained by immunoassay, the method was deemed worth pursuing as a possible means of standardizing commercially available immunoassays performed in serum. The inclusion of the reactive amino acids cysteine and tryptophan in their heavy labeled peptide may have contributed to the lower values obtained. Lin et al. [Lin et al. 2006] used a single quadrupole ion trap for isotope labeling determinations and found it sufficient for their purposes of quantifying intermediate abundance proteins in human serum. Kirsch et al. [Kirsch et al. 2007] quantified two human growth hormone serum biomarkers in samples containing approximately 8 mg of serum protein (100 µL volume) by tandem LC-MS. They considered their isotope dilution method to be easily adaptable to other proteins and possibly to other species. More recently Kamiie et al. [Kamiie et al. 2008] used stable isotope labeled peptides as internal standards for quantification of 34 transporter proteins in liver, kidney and blood-

brain barrier of mouse. They used one representative peptide per protein and the average of three MRM product ions per peptide for quantification. A long LC (liquid chromatography) run time of 50 min was used to enable the assay of many analytes.

An alternative, but related, method has recently been reported by Beynon et al. (Beynon et al. 2005), where the formation of a concatenation of tryptic peptides (a QCAT protein) encoded from an artificial gene was employed. The peptides in the QCAT protein are present in strict 1:1 stoichiometry and each is derived from a naturally occurring tryptic peptide in the parent protein of interest. A single cysteine containing extension is added at the C terminus and used for calibration of the QCAT protein. Although effort is required to construct the artificial gene, repeated expression of the QCAT is facile, and there is no need for individual peptides to be quantified before use. The QCAT can also be heavy labeled by being expressed in medium containing $^{15}NH_4Cl$ to afford internal standard for calibration.

The use of stable isotope labeled peptides as internal standards for the assay of digested proteins is a logical development based on the earlier reported methods. This has led to the commercial availability of custom labeled peptides. Here we present a tandem mass spectrometry method, using such labeled peptides, for the absolute quantification of human UGT enzyme isoforms 1A1 and 1A6 in microsomal tissue preparations. The method reported here provides a basis for extension of the assay to the entire UGT family of proteins, many of which do not have adequate antibodies available due to high sequence identity.

B. METHODS

Materials

Analytical grade acetonitrile and methyl alcohol (anhydrous) were purchased from Fisher Scientific Co. (Pittsburg, PA). Ammonium bicarbonate, dithiothreitol, iodoacetamide, ammonium hydroxide, formic acid, 2,2,2-trifluoroethanol (TFE) and TPCK (L-1-tosylamide
-2-phenylethyl chloromethyl ketone) treated trypsin from bovine pancreas (≥ 10,000 BAEE units/mg protein) were purchased from Sigma-Aldrich Co. (St. Louis, MO). Bond Elut solid phase extraction cartridges (C18 100 mg, 1 mL) were purchased from Varian, Inc. Recombinant UGTs 1A1, 1A6 and control supersomes were purchased from BD Biosciences (San Jose, CA). Human liver microsomes (HLMs)(20 mg/mL) were purchased from BD Biosciences (pool of 33; 15 female, 18 male) and Xenotech LLC (Lenexa, KA) (pool of 50; 26 female, 24 male). A human liver microsome library of individual donors (n=10, 3 female, 7 male, 20 mg/mL) was purchased from Human Biologics International (Scottsdale, AZ). Rat liver microsomes (RLMs), for normalizing total protein content of samples, were prepared from male and female Sprague-Dawley rats using standard methods. Protein concentrations were determined using the Pierce BCA Protein assay Kit, in which bovine serum albumin is used as the standard. Human intestinal microsomes (HIMs) (duodenum and jejunum derived) were obtained from Xenotech LLC (Lenexa, KA) (pool of 8 donors, 5 female, 3 male).

Instrumentation

Analysis was by reverse phase LC-MS/MS, using a Hewlett Packard 1100 LC equipped with a Phenomenex Luna C18 (length, 5 cm; internal diameter, 2 mm; particle size, 3 µm; pore size, 100 Å) column, coupled to an API3000 triple quadrupole mass spectrometer (Applied Biosystems, Foster City, CA) with a turbo ionspray source. The mass spectrometer was operated in positive ion mode, with acquisition by multiple reaction monitoring (MRM). Peak areas were determined using Analyst 1.4.2 (build 1236) software (Applied Biosystems).

Stable Isotope Labeled Synthetic Peptides

Synthetic peptide standards (8-12 mer), each containing one amino acid heavy labeled with ^{13}C [98 %] and ^{15}N [95 %], were purchased from Thermo Electron (Thermo Scientific, Waltham, MA). Two of the peptides were uniquely representative of human UGT1A1 and three were uniquely representative of human UGT1A6. The peptides were selected according to manufacturer recommendations and previously published guidelines [Beynon et al. 2005, Gerber et al. 2003]. The amino acid sequences (for UGT1A1 and UGT1A6) were obtained using the Universal Protein Resource Knowledge Base (UniProtKB)(funded mainly by the National Institutes of Health). Peptide uniqueness of tryptic fragments was verified by NCBI Blast (National Center for Biotechnology Information Basic Local Alignment Search Tool). Amino acid analysis was conducted on each peptide to determine exact amount present. The analysis involved acid hydrolysis, derivatization with phenylisothiocyanate and

separation of the phenylthiocarbamyl-amino acid derivatives by reverse phase HPLC. The analysis was conducted at the Center for Structural Biology, Wake Forest University School of Medicine, Winston-Salem, NC, USA. Some amino acids were excluded from the analysis because of known acid hydrolysis effects (e.g. bonds between isoleucine and valine [peptide 3] are not easily broken) and the possible cyclization and isomerization of aspartic acid adjacent to glycine or isoleucine (peptides 2 and 3) [Vinther et al. 1996, Fledelius et al. 1997]. The peptides purchased are listed in Table **1.** Selection criteria included peptides which were not too hydrophilic or hydrophobic, did not contain reactive amino acids (e.g. M, C), and did not contain chemically unstable sequences (e.g. N-terminal Q, N-terminal N).

Known variable Single Nucleotide Polymorphisms (SNPs) were also considered during selection (see discussion). It was intended to obtain two peptides for each UGT isoform, but a third was obtained for UGT1A6 because initial investigations suggested that there may be difficulties with peptide 3. This proved not to be the case. One peptide, initially selected for UGT1A6 (peptide 5, Table **1**) was ignored for most of the investigations when a large co-eluting peak was consistently observed for one of its two MRMs. All five peptide sequences were found to lack the predicted posttranslational modifications using the software indicated in parentheses: N-linked glycosylation (NetNGlyc), O-linked glycosylation (NetOGlyc), sulfation (Sulfinator), methylation (MeMO), acetylation (NetAcet), palmitoylation (NBA-Palm), myristoylation (NMT), and sumoylation (SUMOsp). Results of analysis for predicted phosphorylation sites lacked

agreement and depend on the software used (Kinase Phos or NetPhos). No sites were identified in the two UGT1A1 peptides. Kinase Phos identified tyrosine-77 in peptide 5 as a potential site, whereas NetPhos suggested that serine-50 in peptide 3, threonine-110 in peptide 4, and tyrosine-112 in peptide 4 are likely phosphorylation sites. These predictions do not take into account the endoplasmic reticulum localization of the UGTs where they likely have restricted access to most cellular kinases. Stock solutions of each peptide were prepared in 50 % acetonitrile/50 % acetic acid 1.6 % and stored, in 300 and 400 µL aliquots, at -20 ºC in polypropylene vials.

Sample Preparation and digestion

Calibrators, containing 1.5, 3, 6, 12 and 25 µg of commercially available recombinant UGTs 1A1 and 1A6, with protein normalized to 200 µg by the addition of RLMs, a blank containing 50 µg of UGT control supersomes, with protein normalized in the same way, and HLM samples (pooled and individual donor samples) containing 200 µg of protein, were prepared. Samples were denatured and reduced by heating at 95 ºC for 11 min in 5 mM dithiothreitol (sample volume 90 µL; buffer 50 mM ammonium bicarbonate). This was followed by alkylation with iodoacetamide (10 µL of 100 mM solution added) for 20 min in the dark. Heavy labeled peptides were then added as internal standards (10 µL of solution containing 10 pmol of peptides 1, 3, 4, 5 and 20 pmol of peptide 2) and the residual acetonitrile (< 5 µL) was removed by evaporation under nitrogen for ~5 min. Samples were then digested with trypsin in 50 mM ammonium

bicarbonate; enzyme/protein ratio = 1:50; for 4 h at 37 ºC, which was found to provide maximal response to peptides monitored from recombinant UGTs. The reaction was then quenched by addition of three volumes of acetonitrile. Following centrifuging at 800 x *g* for 10 min the organic content was removed by evaporation under nitrogen for ~10 min. Ammonium bicarbonate (50 mM, 0.9 mL) was then added in preparation for solid phase extraction. SPE cartridges were conditioned with 1 mL methanol and 1 mL distilled water. Samples were then added and the cartridges were washed with 1 mL 50 mM ammonium bicarbonate. Cartridges were eluted with 1 mL acetonitrile/25 mM formic acid (40:60). The eluate was evaporated to dryness under nitrogen at 42 ºC in a water bath and samples were reconstituted with 100 µL acetonitrile/25 mM formic acid at pH 3 (pH was adjusted to 3 by drop wise addition of ammonium hydroxide). Samples were stored at -20 ºC until analyzed by LC-MS/MS.

LC conditions

Mobile phase was acetonitrile (solvent B) and 25 mM formic acid with pH adjusted to 3 (solvent A) by addition of ammonium hydroxide. Injection volume was 50 µL (50 % of sample), and flow rate was 0.4 mL/min. Gradient; 10 % solvent B to 100 % at 4 min, to 10 % at 5 min, held at 10 % for equilibration until 10 min. Sample was split before introduction into the turbo ionspray source of the mass spectrometer (half of effluent was allowed into the source).

MS/MS conditions

All heavy labeled peptides were found to be doubly charged when infused into the mass spectrometer in ~2 μM concentrations in mobile phase (50:50). Two MRM transitions, with product ion for each > 500 Da (and precursor ion as doubly charged ion), were chosen for each heavy labeled peptide following optimization. Using these, two further MRM transitions were elucidated for the corresponding unlabeled peptides from digested recombinant enzyme and microsomal samples. Thus there were four MRM transitions monitored per peptide, giving a total of 20 MRMs which were acquired. As the peptides eluted within a narrow time frame the MRMs were not grouped and were therefore all acquired within each cycle. Following optimization, dwell time was set at 60 ms, with a pause time of 5 ms. Cycle time was therefore 1.3 s. MRM product ions were named according to peptide fragmentation nomenclature [Roepstorff and Fohlman 1984] (Table **2**).

Calibration Curves

The concentration of enzyme in recombinant material (pmol/mg recombinant protein) was calculated, following preparation and analysis of five replicate calibrant sets (total 25 samples; a calibrant set consisted of five samples, each a different concentration within the calibration range), from the known amount of heavy labeled peptide added to each sample as internal standard. The amount of heavy labeled peptide added was designed to fall within the (unweighted) linear range, and equality of response between labeled and unlabeled peptide was

assumed. Complete trypsin digestion was also assumed as increasing time of digestion did not improve responses. The same batches of recombinant UGTs 1A1 and 1A6 were used throughout the study. Calibration curves were constructed by plotting recombinant enzyme concentration against the peak area of each MRM representing unlabeled (recombinant) tryptic peptide relative to the peak area of each corresponding MRM representing labeled synthetic peptide internal standard, using a weighted ($1/x^2$) linear regression fit. The calibration and assignment of enzyme concentration was based upon the known amount of labeled synthetic peptide internal standard added to each sample, and assuming equality of response, as commonly done for isotope dilution methods. Thus for each peptide there were two calibration curves, and for each enzyme there were at least four calibration curves, from which the optimal peptides and MRM transitions could be determined.

Validation

Solid phase extraction efficiency

Solid phase extraction efficiency was determined for the labeled internal standard peptides in calibrant samples which were put through the entire sample preparation procedure. Two concentrations of calibrant were used. For each concentration the labeled standards were added to three samples just before solid phase extraction, and to three further samples just after solid phase extraction.

Sample preparation – denaturation and trypsinization

The use of heating (95 ºC for 11 min), in our method, to denature the protein samples was compared with use of an organic co-solvent, TFE [Roepstorff and Fohlman 1984], to denature. For the co-solvent method TFE (35 µL of the final 90 µL volume) was added at the very beginning, and samples were incubated with shaking at 37 ºC for 2 h. Two samples from the HLM library were analyzed in triplicate by each method and average concentrations calculated. To examine use of a lower temperature to denature, two samples of a high concentration within the calibration range were denatured at 60 ºC for 30 min and compared to five replicate calibrant samples of the same concentration denatured at 95 ºC for 11 min.

Intra- and inter-day assay variability

For intra-day variability, five replicate calibration curves were prepared on the same day, and analyzed. Peak area ratios were examined as a measure of variability. This was repeated with a further five replicate calibrant sets, without adding rat liver microsomes to normalize protein content, to examine for matrix effects. For inter-day variability two batches of pooled human liver microsome samples, from different sources, were analyzed with each calibrant set.

Human liver microsome (HLM) library

To test the application of the developed method, samples from a library of ten individual HLM donors were analyzed in triplicate, with a calibrant set and pooled HLM inter-day control samples.

Human intestinal microsomes (HIMs)

Samples from one batch of HIMs were analyzed in triplicate, with a calibrant set and pooled HLM inter-day control samples.

Western blot analysis of HLM library and digested and non-digested samples

As demonstration of the reliability of the developed LC-MS/MS method, the HLM library was analyzed for UGTs 1A1 and 1A6 by (relative quantification) Western blot. Correlations between the results for each method were evaluated. Two immunoblots were prepared, one for UGT1A1 and one for UGT1A6. The primary antibodies, one for each isoform, were both developed in the Ritter lab [Chen et al. 2005, Ritter et al. 1999]. For each blot a 7.5 % polyacrylamide resolving gel and a 4 % polyacrylamide stacking gel were poured and 25 µg of protein loaded for each HLM sample. Samples were electrophoresed at 150 V through the stacking gel and 175 V through the resolving gel. After transfer of the proteins to a nitrocellulose membrane, the blots were probed for expression of the relevant UGT isoform, at a 1:1000 dilution of the primary antibody, by incubation for an hour at room temperature. The blots were then probed for the

secondary antibody (sheep anti-mouse HRP linked) which was added at a dilution of 1:15,000, also for an hour at room temperature. Amersham ECL products were used to detect and visualize expression of peptides. Also analyzed with each immunoblot were four samples (each of highest calibrant concentration) which had been put through the initial stages of the LC-MS/MS sample preparation procedure, but taken no further than the digestion step. Two of the samples were digested (procedure stopped following 4 h digestion step at 37 ºC) and two were not digested (procedure stopped following addition of internal standard). All four samples were evaporated to dryness under nitrogen and reconstituted in 10 µL 50 mM ammonium bicarbonate for analysis by Western blot.

C. RESULTS

Selection of MRMs

For MRM transitions the product ions of highest intensity, > 500 Da, obtained from infusion of the heavy labeled peptides were chosen (Fig. (**1)**). If any MRMs were subsequently shown to give unsatisfactory calibration curves, as in the case of peptide 5, the product ion of next highest intensity was also examined. In the case of peptide 5 this was also unsatisfactory, due to a co-eluting peak. Product ions in all cases were y ions (Table **2**). All product ions chosen for the heavy labeled synthetic standards, except that for the lower mass product ion of peptide 2, contained the heavy label. All MRM transitions used in the analyses are shown in Table **2** (the MRM2 shown for peptide number 5 was the last MRM tested for that peptide).

Chromatography

Following application of the sample preparation procedure MRM chromatograms were obtained for calibrant samples, blank samples and pooled and individual donor human liver microsome samples. Representative chromatograms are shown in Fig. (**2)**. All peaks, except those of MRM2 for unlabeled enzyme derived peptides 4 and 5, were free of co-eluting peaks. For peptide 4 MRM2 the interfering peak, only seen in the blank control, was sufficiently small for the blank peak area ratio to be subtracted for each calibrant, for all calibrant sets prepared. The interfering peak was shown to originate from the rat liver microsomes used to normalize total protein amount in calibrants and blanks, thus it was not observed in human liver microsome samples. For enzyme derived peptide 5 MRM2 (747.5/1217.8) a large co-eluting peak was seen in calibrant, blank control and HLM samples such that peak areas could not be accurately determined. Data for this MRM and peptide was therefore not subsequently studied as two other peptides could be reliably employed for the UGT1A6 quantification.

Calibration Curves and Extraction Efficiency

The concentrations (pmol/mg protein) of each enzyme isoform in recombinant material, used to construct calibration curves, and calculated as described in the Methods section, are shown in Table **3**. Representative curves, which were linear and reproducible, are shown in Fig. (**3)**. The lowest concentrations shown in Table **3** represent limits of quantification (~5 pmol/mg protein for UGT1A1, and ~2 pmol/mg protein for UGT1A6). Limits of detection were approximately one third of these values. Correlation (r) values for calibration curves were generally > 0.98. Solid phase extraction efficiencies of synthetic heavy labeled peptide internal standards were found to be > 87 % for peptides 1, 3 and 4, and > 73 % for peptide 2.

Sample preparation – denaturation and trypsinization

Concentrations determined by co-solvent denaturation were slightly higher than those obtained by heating (95 ºC for 11 min) in HLM samples analyzed. For example, for HLM 216 the average UGT1A1 concentration increased from 25.3 to 27.5 pmol/mg protein. The average UGT1A6 concentration increased from 4.0 to 6.0 pmol/mg protein. When a lower temperature was used to denature samples, peak area ratios (PARs) were less reproducible.

Intra- and Inter-day Assay Variation

Intra-day variation, represented by the range of %C.V.s (n=5) of peak area ratios over the standard curves for each MRM, varied depending on the peptide

and MRM. Peptide 1 and peptide 4 MRMs gave the best reproducibility for UGT1A1 and UGT1A6, respectively. Intra-day C.V.s were below 20 % for peptide 1 and below 25 % for peptide 4. Human liver microsome matrix was found to be “cleaner” than rat liver microsome matrix (which was used to normalize for total protein in calibrant samples) and hence lower concentration variability was observed for this matrix (Table **5**; n=3). Inter-day assay variation data is shown in Table **4**. Peptides 1 and 4 were again superior with respect to %C.V.s, and the choice of MRM influenced reproducibility.

Human Liver Microsome Library (LC-MS/MS and Western Blot Analysis)

Absolute quantification results from LC-MS/MS analysis of the human liver microsome library of ten individual donors are shown in Table **5**. Using peptides 1 and 4, representing UGTs 1A1 and 1A6 respectively, and mean values of the two MRMs, there was a seven fold difference between the highest and lowest UGT1A1 concentration (HLM 222, 52 pmol/mg protein; HLM 228, 7.8 pmol/mg protein) and a 3.1 fold difference between the corresponding UGT1A6 concentrations (HLM 233, 7.9 pmol/mg protein; HLM 218, 2.6 pmol/mg protein). Ratios of UGT1A1 to UGT1A6 for each sample ranged from 1.6 for HLM 228 to 9.3 for HLM 225. There was no correlation between UGT1A1 and UGT1A6 concentrations within individuals ($r = 0.335$, using peptides 1 and 4). Results of Western blot analysis of the HLM library are shown in Fig. (**4**). Correlations (r)

between the absolute concentrations obtained by LC-MS/MS and the relative values obtained by Western blot (normalized to 100 % for the lowest density) for each MRM of peptides 1 and 4, are shown in Fig. (**5**).

Human Intestinal Microsomes

The UGT1A1 concentration determined in one batch of pooled human intestinal microsomes, analyzed in triplicate, was on average (n=3), peptide 1, MRM1, 5.8 pmol/mg protein, MRM2, 7.4 pmol/mg protein. These data were in good agreement for the MRMs monitored. Peptide 2 concentrations (data not shown) were in a similar range, but showed higher variability. UGT1A6 concentrations in intestinal microsomes were below the limit of quantification.

D. DISCUSSION

This study demonstrates the use of stable isotope labeled synthetic peptides for the absolute quantification of endogenous enzyme proteins by tandem mass spectrometry operated in the MRM mode. The approach is applied here to Phase II metabolic enzymes for the first time. Specifically it is applied to UGT1A1 and UGT1A6, two enzymes with specific antibodies, to enable a comparison and evaluation of the new approach.

Selection of stable isotope labeled synthetic peptide is clearly an important step, both for enzyme identification purposes (the peptide must be unique to the enzyme being quantified) and for analytical reasons (the peptide needs to have good chromatographic properties, ionize well, and give sensitive and selective

MRM signals). Each of the nine functional known UGTs in the 1A subfamily of enzymes is comprised of approximately 530 amino acids (Uniprot). There is sequence identity at the C terminus region, which is encoded for each isoform by the common exons 2 to 5 of the UGT1A gene. Therefore, the N terminus region, which is less homologous, and encoded for by a unique exon 1 for each isoform was the site for unique peptides. We found, when searching for suitable peptides for labeling, that there were no apparent unique sequences beyond approximate amino acid number 210. For the isoforms quantified here, UGTs 1A1 and 1A6, there were few tryptic peptides that fit the criteria for use in the method. For UGT1A1 the enzyme sequence D_{70}GAF(^{13}C5,^{15}N)YTLK$_{77}$ was selected as the second peptide (peptide 2) because it was the only remaining peptide of sufficient length (< 16 amino acids), even though it was known that the DG linkage could possibly undergo cyclization or isomerization [Vinther et al. 1996, Fledelius et al. 1997], particularly at neutral or basic pH. This peptide could also be affected by a reported G71R polymorphism (UGT1A1*6) that is more common in Asians and found to produce Gilbert Syndrome [Akaba et al. 1998, Maruo et al. 2005]. For UGT1A6 one other peptide could possibly have been used. This was S_{185}PDPVSYIPR$_{194}$. It was not chosen because of a reported R184S polymorphism [Basu et al. 2005], which if present would alter the length of the tryptic peptide. Some additional SNPs for UGT1A1 have been reported for the peptides employed, though these were relatively rare with allele frequencies that are very low. Certainly, one must consider nonsynonymous SNPs when interpreting quantitative proteomic data, but it may also be possible to use this

method to measure expression of the variant isoforms in subjects that are heterozygous. The other concern with the method is that it does not consider possible posttranslational modifications. The peptides selected here (Table **1**) did not include asparagine (N), a possible site for glycosylation, but were replete with serine (S) and tyrosine (Y), which are possible sites for phosphorylation. To date there is limited information on phosphorylation of UGTs [Basu et al. 2004, Ciotti et al. 1997]. Alternative methods based on antibody detection may also, in any case, be affected by phosphorylation.

The use of dithiothreitol and iodoacetamide for reduction and alkylation of protein samples is well established. The use of heating to denature is less common. Our method was validated by showing little difference between heating at 95 ºC and using TFE to denature samples. A lower temperature produced peak area ratios that were less reproducible. The use of detergents sodium dodecyl sulfate and CHAPS [3-((3-cholamidopropyl)dimethylammonio)-1-propane-sulfonic acid] to denature the proteins was also examined. However, these were found to produce interfering peaks by full scan mass spectrometry, thereby possibly affecting ionization and mass spectrometry performance. Detergents could also possibly affect chromatography performance. Our sample work up, using SPE, was simple and provided samples that easily interfaced with LC-MS/MS. A point worth noting is that trypsinization is assumed to be 100%. Other than optimizing the conditions for trypsinization, for example with respect to time and trypsin concentration, as was done in our method development, it is difficult to examine the efficiency of the reaction. It is also assumed that there are

no protein losses during denaturation and reduction. Labeled peptides are added prior to digestion and SPE to compensate for possible peptide losses during these steps. Loss of peptide would mean under calculation of UGT concentration.

For initial method development a 15 cm column was tested due to the complexity of the digested peptides. Peak shape was not optimal with a longer column, therefore the 5 cm column was evaluated and found to provide adequate chromatography with much shorter run times and higher sensitivity. Product ions of > 500 Da were chosen for MRMs because of increased selectivity at higher mass values (Fig. (**1**)) [Anderson and Hunter 2006]. The peak intensities between MRMs were in good agreement for each peptide (MRM1/MRM2 ratio range for peptides 1 to 4 was ≥ 0.45 ≤ 1.51). The dwell time (60 ms) was chosen as a compromise between sensitivity needed and cycle time. The cycle time (1.3 s) was sufficient for approximately 15 data points per peak, most peaks being approximately 20 s wide. Peak intensities for peptide 2 MRMs were lower than for the other peptides, possibly a consequence of the potential DG cyclization and isomerization described earlier [Chen et al. 2005, Ritter et al. 1999]. The peak intensity of MRM2 in particular was low. This was interesting because the product ion of this MRM was the only product ion of all MRMs selected that did not contain the synthetic peptide label (Table **2**).

Calculated concentrations of enzyme in recombinant material were consistent between MRMs and between peptides for each UGT isoform. However, reproducibility and the sensitivity are improved if optimization for the best peptide

and MRM is performed. Intra- and inter-day assay variation results indicated that peptides 1 and 4 were the best peptides to use for the UGTs 1A1 and 1A6 quantification respectively. Peptides 2 and 3 could be used as support verification. Intra-day variation would have been expected to be less than inter-day variation, but examination of the data suggested that this was not so. This could possibly be explained by the use of rat liver microsomes in calibrants (intra-day samples) to normalize total protein content. The rat liver microsomal matrix appeared to be more complex, with greater background interference than the human liver microsomal matrix. Analysis of the human liver microsome library provided a form of intra-day measure (samples were prepared and analyzed in triplicate) free from rat liver microsomal matrix, with %C.V.s being better than those obtained when rat liver microsomal matrix was present (Table **5**). Results again showed that peptides 1 and 4 were best because of the lower %C.V.s obtained for those peptides.

Concentrations of UGT1A1 were greater than UGT1A6 in all 10 HLM library samples when measured by LC-MS/MS (Table **5**). Comparisons of concentrations are not possible with Western blots since different antibodies would be employed for distinct enzymes. For UGT1A enzymes, because they share a common C-terminus via exon sharing, one could use the 1A common antibody to estimate relative concentrations between isoforms assuming the response is similar. However, the LC-MS/MS method employed here is generally applicable to diverse proteins and provides greater precision than is commonly obtained with Western blot combined with densitometry. There was no

correlation between the concentrations of the two isoforms (r = 0.335, for peptides 1 and 4). High correlations were observed between the absolute concentrations of UGT1A1 determined by LC-MS/MS and the relative concentrations determined by Western blot (Fig. (**5**)). The dynamic range for LC-MS/MS was greater and was thus more discriminatory (Fig. (**5**)), while Western blot is easily saturated, and thus provides a possible explanation for the UGT1A1 correlation lines of Fig. **5** not crossing the y-axis at the origin. The corresponding correlations (Western blot v. LC-MS/MS) for UGT1A6 were not as high. Reasons for this may have included that the UGT1A6 concentrations occurred at the lower end of the LC-MS/MS calibration curve (the dynamic range of the UGT1A6 concentrations was also lower than that of the UGT1A1 concentrations). Also, we believe that the specificity of the UGT1A1 antibody is greater than that for UGT1A6 since there appear to be two bands in the UGT1A6 Western blot (Fig. (**4**)). The correlations, and improvements in dynamic range observed when using LC-MS/MS (Fig. (**5**)), demonstrated nonetheless the applicability of the LC-MS/MS method for the absolute quantification of the UGTs in human liver microsomes.

Application of the LC-MS/MS method to HIMs was also successful, with concentrations of UGT1A1 being approximately 30 % those of HLMs. This is in broad agreement with the findings of Wen et al. [Wen et al. 2007] who, using etoposide as a UGT1A1 probe substrate *in vitro*, showed the $V_{(max)}$ of HIMs to be approximately half that of the $V_{(max)}$ of HLMs. UGT1A6 concentrations were also

lower than in HLMs but could not be measured as they were below the limit of quantification using the method and equipment employed here.

A method for the absolute quantification of the human UGT isoforms 1A1 and 1A6, using heavy labeled peptide standards, by tandem LC-MS, has been developed. The method assumes 100% digestion with trypsin, and no protein losses during denaturation and reduction. It can be employed in a variety of matrices, in this case HLMs, HIMs, RLMs and supersomes. As mentioned in the introduction, these methods evolved from previous efforts in proteomic analysis using LC-MS, often employed for relative quantification, and are being extended to provide absolute quantification with accurate and precise quantification through the use of heavy labeled peptides. Targeted absolute quantification to study Phase I enzymes [Wang et al. 2006] and transporters [Kamiie et al. 2008] are being reported, thus the methods may become common procedures in drug metabolism and drug development studies. Results indicate that the method is robust and reproducible and can be employed over a wide dynamic range, sample-dependent matrix effects notwithstanding. The sensitivity of LC-MS/MS is in the fmole - amole range on-column, which translates to low pmole/mg detection as presented here, and should improve to sub pmole/mg protein with the use of capillary LC and newer equipment than the API-3000 employed. This sensitivity is competitive with other methods such as DIGE [Friedman 2007, Tonge et al. 2001] for protein analysis, and LC-MS/MS with stable isotope standards benefits from improved reproducibility and the ability for absolute quantification rather than relative quantification in most other methods.

Pre-selection of peptide is important, for example to minimize polymorphic effects on concentrations determined, and time and attention needs to be given to the validation of each peptide. Use of multiple peptides per protein supports the validity of results obtained, and provides verification of results that may be confounded by known or unknown nonsynonymous SNPs. It is important for the use of this method to carefully consider protein variants. However, the method also has the potential benefit of being able to measure relative levels of expression of such variants, if known, and if present in a peptide amenable to the method.

We found that peptide 1, representative of UGT1A1, and peptide 4, representative of UGT1A6, gave greater reproducibility than the corresponding isoform representative peptides 2 and 3, though peptides 2 and 3 (UGT1A1, 1A6, respectively) gave similar average concentrations of proteins. HLMs contain more UGT1A1 (~0.140 % w/w; ~23.4 pmol/mg protein; peptide 1: Table **5**) than UGT1A6 (~0.029 % w/w; ~4.8 pmol/mg protein; peptide 4: Table **5**). Human intestinal microsomes contain less of each enzyme (UGT1A1 concentrations were approximately 30 % those of HLMs, and UGT1A6 concentrations were below the limit of quantification). Concentrations obtained by LC-MS/MS were found to correlate with relative values obtained by Western blot analysis. Excellent correlations seen for UGT1A1 were better than for UGT1A6, possibly due to UGT1A6 concentrations being at the lower end of the calibration curve and/or possibly due to greater specificity of the UGT1A1 antibody. The method can potentially be applied to the entire UGT family of proteins and other

endogenous proteins and enzymes. Targeted quantitative proteomics using heavy labeled peptides allows absolute rather than relative quantification and should revolutionize the measurement of specific proteins in complex biological matrices. Application of these methods will enhance the study of drug metabolism, and hence drug discovery and development, by providing accurate and precise measurement of specific proteins, including many not previously amenable to measurement due to the lack of specific antibodies. Moreover, this LC-MS approach for protein quantification will be easily translated from species to species via the wealth of genomic data available today.

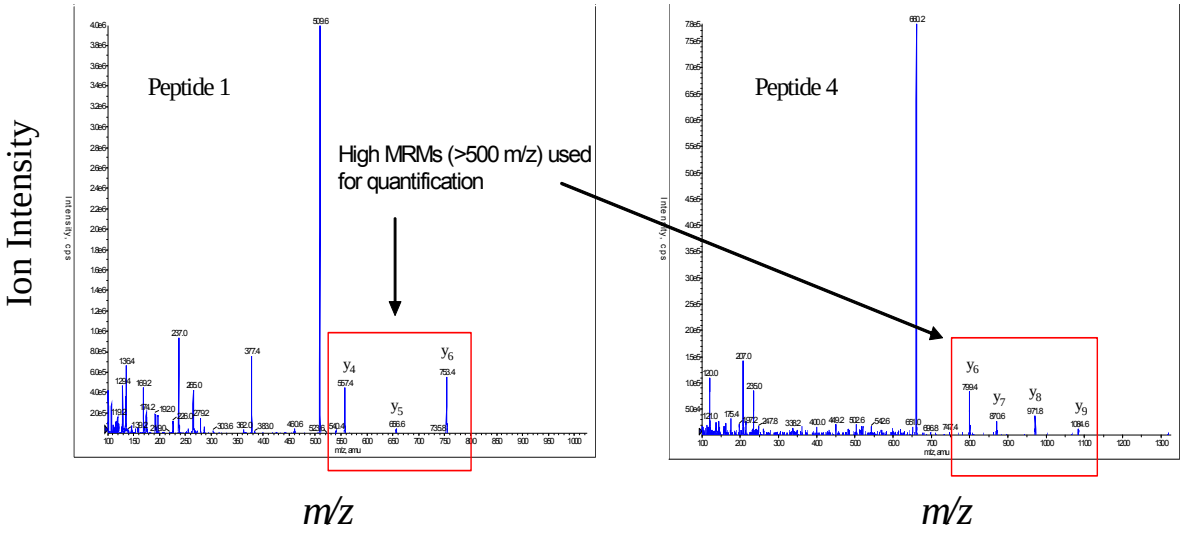

Figure 6.1. MRM optimization scans for peptides 1 and 4, highlighting prominent product ions of mass > 500 Da. Two MRMs, using the two product ions of highest intensity, were chosen for each peptide. The ions y4 and y6 for peptide 1, and y6 for peptide 4, are more intense due to the 'proline effect' whereby formation of y-ions by amide bond cleavage N-terminal to proline is preferred.

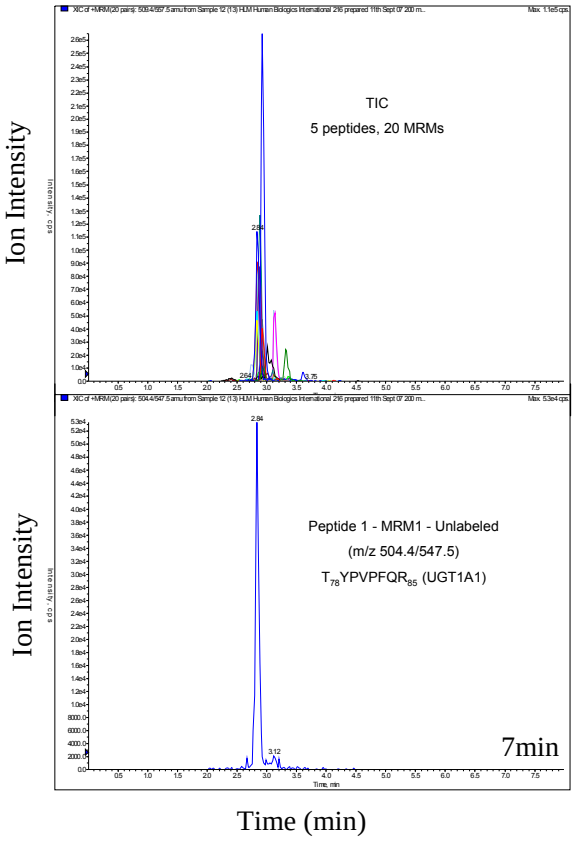

Figure 6.2. MRM chromatograms following isolation of tryptic peptides from a human liver microsomal donor sample, showing total ion chromatogram (5 peptides, 20 MRMs)(top), and extracted chromatogram of enzyme derived MRM1 peptide 1 (T78YPVPFQR85, UGT1A1 representative). The sample was prepared from 200 µg of microsomal protein.

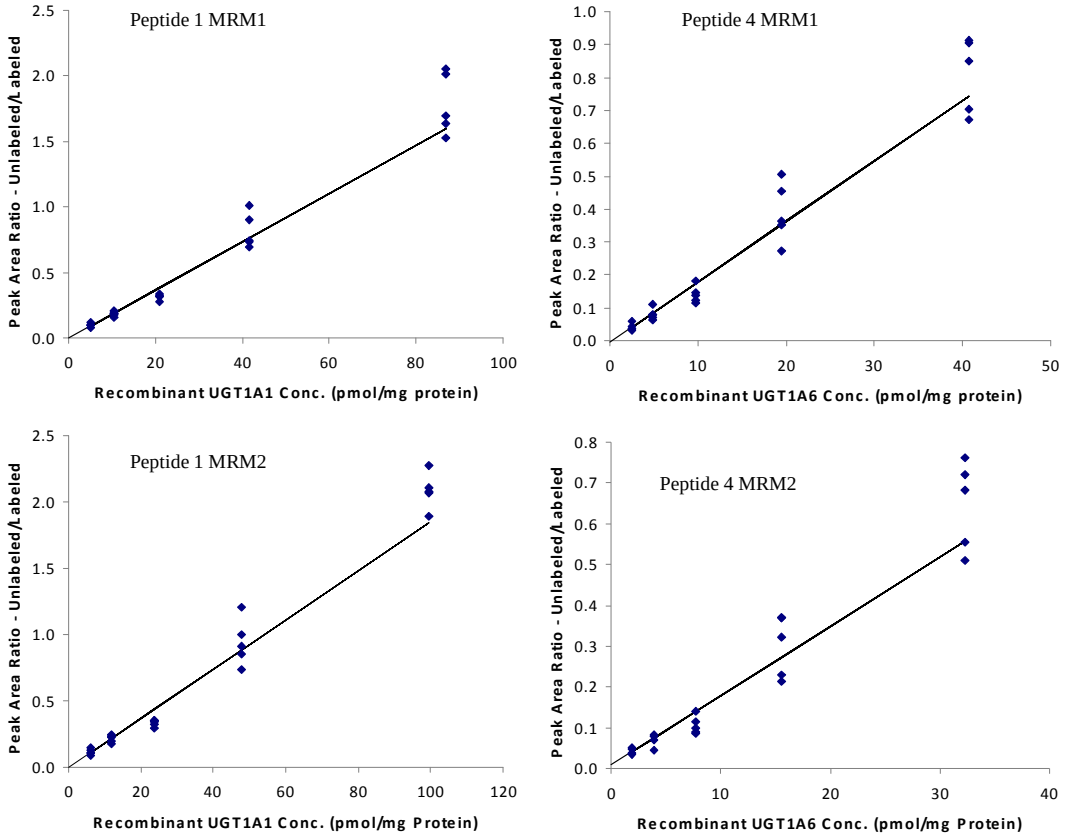

Figure 6.3. Representative calibration curves (n = 5 replicate samples for each concentration), constructed using a weighted (1/x2) linear regression fit, for MRMs 1 and 2 of peptides 1 and 4. Peptide 1 is uniquely representative of human UGT1A1. Peptide 4 is uniquely representative of human UGT1A6. Concentration of enzyme in recombinant material was calculated for each MRM of each peptide from the known amount of heavy labeled peptide added as internal standard. The amount added was designed to fall within the (unweighted) linear range. Equality of response between labeled and unlabeled peptide MRMs was assumed.

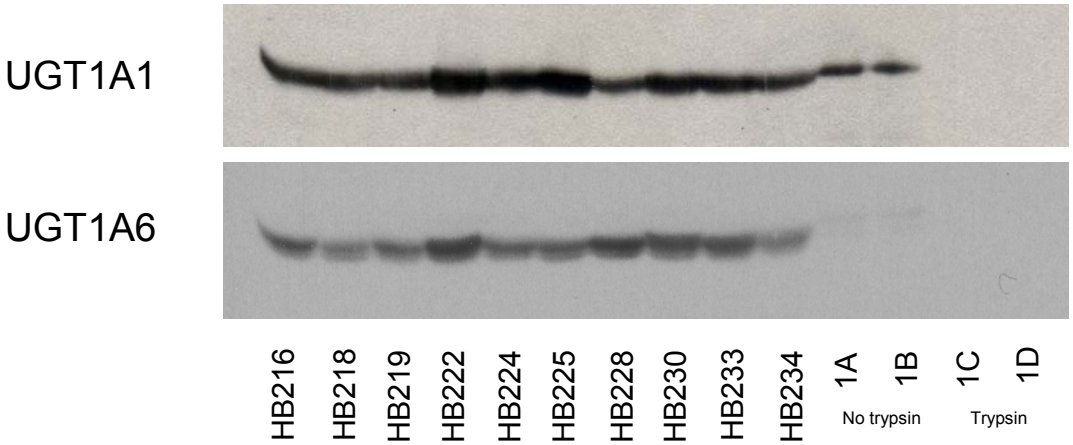

Figure 6.4. Western immunoblot analysis of human liver microsome library of ten individual donors. Also shown are images of four highest concentration calibrant samples, two of which had not been digested by trypsin and two of which had been digested.

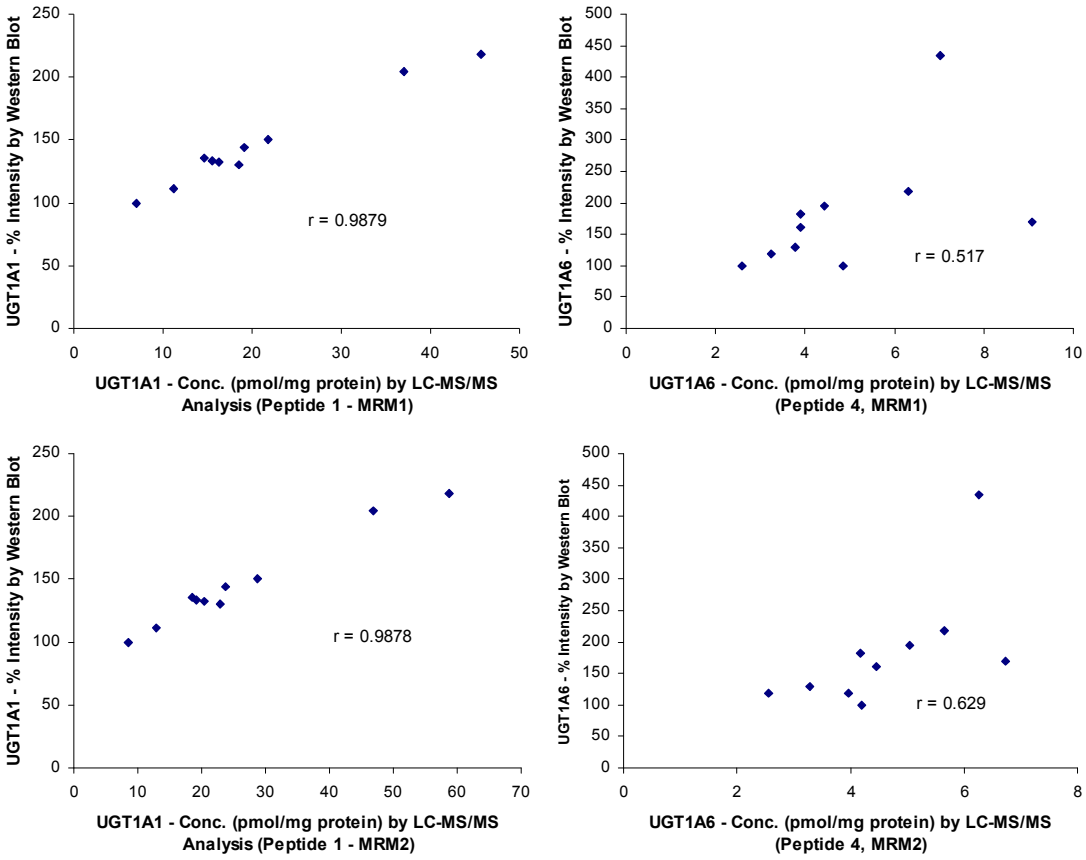

Figure 6.5. Human liver microsome library analysis of ten individual donors; correlation of absolute quantification values obtained by LC-MS/MS with relative quantification values obtained by Western immunoblot, for both MRMs of peptides 1 (UGT1A1 representative) and 4 (UGT1A6 representative). The Western blot with the lowest densitometry reading was assigned a value of 100%, with others relative to this.

Table 6.1. Unique human UGTs 1A1 and 1A6 representative heavy labeled peptides selected for use as internal standards for absolute quantification.

Peptide Number	UGT Isoform	Amino Acid Sequence
Peptide 1	UGT1A1	T78YPVPF(13C9,15N)QR85
Peptide 2	UGT1A1	D70GAF(13C9,15N)YTLK77
Peptide 3	UGT1A6	D44IVEV(13C5,15N)LSDR52
Peptide 4	UGT1A6	S103FLTAP(13C5,15N)QTEYR113
Peptide 5	UGT1A6	I77YPVP(13C5,15N)YDQEELK88

Table 6.2 MRM Transitions for UGT stable isotope standards

	Peptide 1		Peptide 2		Peptide 3		Peptide 4		Peptide 5	
	MRM1	MRM2	MRM1	MRM2	MRM1	MRM2	MRM1	MRM2	MRM1	MRM2
Product Ion	y4	y6	y4	y5	y6	y7	y6	y8	y8	y10
Labeled (internal standards)										
MRM	509.4/557.5	509.4/753.7	462.8/524.4	462.8/681.5	526.5/724.6	526.5/823.6	660.1/799.6	660.1/971.6	750.5/1027.5	750.5/1223.8
Label a	Yes	Yes	No	Yes	Yes	Yes	Yes	Yes	Yes	Yes
Unlabeled (calibrants)										
MRM	504.4/547.5	504.4/743.7	457.8/524.4	457.8/671.5	523.5/718.6	523.5/817.6	657.1/793.6	657.1/965.6	747.5/1021.5	747.5/1217.8

a: Retention of heavy isotope label in product ion.

Table 6.2. Chosen MRM transitions (transitions of highest sensitivity product ions) for synthetic heavy labeled and recombinant enzyme derived tryptic peptides showing product ion position in peptide, and whether product ions for the internal standards contain the labeled amino acid. Peptides 1 and 2 are uniquely representative of human UGT1A1, and peptides 3, 4 and 5 are uniquely representative of human UGT1A6.

Table 6.3 Recombinant enzyme amount unit conversions to pmol/mg protein

Recombinant microsome	UGT1A1 (pmol/mg protein)				UGT1A6 (pmol/mg protein)			
	Peptide 1		Peptide 2		Peptide 3		Peptide 4	
(µg)	MRM1	MRM2	MRM1	MRM2	MRM1	MRM2	MRM1	MRM2
1.5	5.2	6.0	7.9	7.6	2.5	3.1	2.4	1.9
3	10.4	11.9	15.7	15.2	4.9	6.2	4.9	3.9
6	20.8	23.9	31.4	30.4	9.8	12.5	9.8	7.8
12	41.6	47.7	62.9	60.8	19.7	24.9	19.5	15.5
25	86.7	99.5	131	127	40.9	51.9	40.7	32.3

Table 6.3. Calculation of enzyme amounts (pmol/mg protein) in recombinant UGT microsomes. Amounts were calculated following preparation and analysis of five replicate calibrant sets (total 25 samples) from the known amount of heavy labeled peptide added to each sample as internal standard. The amount added was designed to fall within the (unweighted) linear range. Equality of response between labeled and unlabeled peptide MRMs was assumed. The lowest values shown were limits of quantification when added to RLM to provide 200 □g total protein per sample.

Table 6.4 Interday precision data for UGT isoforms 1A1 and 1A6

	UGT1A1 (pmol/mg protein)				UGT1A6 (pmol/mg protein)			
	Peptide 1		Peptide 2		Peptide 3		Peptide 4	
HLM	MRM1	MRM2 MRM2	MRM1		MRM1	MRM2 MRM2	MRM1	
Batch 1	18.4	21.1	26.2	29.6	3.3	2.8	3.6	3.0
Average	7.9	11	18	13	17	15	18	28
(% C.V.)								
Batch 2	21.4	24.0	35.5	32.4	3.7	3.2	4.6	3.9
Average	6.7	10	24	17	43	37	19	28
(% C.V.)								

Table 6.4. Inter-day precision data for absolute quantification of the human UGT enzyme isoforms 1A1 and 1A6. Two batches of pooled human liver microsome samples (200 µg), obtained from different sources, were used in the determinations (n=5).

Table 6.5. Absolute quantification of UGTs 1A1 and 1A6 in human liver microsome library of ten individual donors by LC-MS/MS.

		UGT1A1 (pmol/mg protein)a				UGT1A6 (pmol/mg protein)a			
		Peptide 1		Peptide 2		Peptide 3		Peptide 4	
Sample		MRM1		MRM1		MRM1		MRM1	
		MRM2		MRM2		MRM2		MRM2	
HLM 216		21.8	28.8	37.1	27.5	5.4	2.4	3.9	4.2
Average		13	5.4	14	6.1	6.4	81	15	10
	%								
C.V.									
HLM 21	Average	14.7	18.5	19.8	25.4	2.8	1.8	2.6	2.6
	%	6.1	7.0	28	12	14	51	12	4.7
C.V.									
HLM 219		16.2	20.4	27.4	23.7	5.3	1.9	3.9	4.5
Average		7.6	6.0	13	6.1	14	58	11	21
	%								
C.V.									
HLM 222		45.7	58.9	91.5	68.2	6.3	3.9	7.0	6.3
Average		9.7	2.6	20	8.5	13	23	2.0	5.8
	%								
C.V.									
HLM 224		19.1	23.7	27.8	29.1	4.0	1.5	3.8	3.3
Average		5.0	8.4	37	4.9	9.2	55	7.8	5.0
	%								
C.V.									
HLM 225		37.0	46.9	60.9	48.4	5.8	3.3	4.8	4.2
Average		1.4	14	9.5	6.5	19	25	7.0	10
	%								
C.V.									
HLM 228		7.0	8.5	13.6	11.0	3.4	2.0	4.4	5.0
Average		16	5.4	16	7.9	38	84	12	6.5

% C.V.								
HLM 230	15.6	19.1	25.7	22.2	4.6	3.5	6.3	5.7
Average	3.8	13	26	1.6	9.6	59	8.3	9.4
% C.V.								
HLM 233	18.5	22.9	27.6	26.6	11.2	9.4	9.1	6.7
Average	12	5.3	17	10	12	27	7.3	4.7
% C.V.								
HLM 234	11.2	12.9	20.6	20.0	4.3	3.1	3.2	4.0
Average	18	17	26	15	15	42	4.9	6.3
% C.V.								
Average (MRM)	20.7	26.1	35.2	30.2	5.3	3.3	4.9	4.6
(all ten HLM) % C.V.	57	59	67	54	44	70	41	28

a n=3 for all individual microsome data

Table 6.5. Microsomes (200 µg) from each donor were analyzed in triplicate and concentrations were extrapolated from calibration curves constructed from the analysis of calibrant samples containing recombinant UGTs 1A1 and 1A6. Calibrant samples also contained rat liver microsomes to normalize total protein content to 200 µg.

E. References

Akaba K, Kimura T, Sasaki A, Tanabe S, Ikegami T, Hashimoto M, Umeda H, Yoshida H, Umetsu K, Chiba H, Yuasa I, Hayasaka K. Neonatal hyperbilirubinemia and mutation of the bilirubin uridine diphosphate-glucuronosyltransferase gene: a common missense mutation among Japanese, Koreans and Chinese. *Biochem. Mol. Biol. Int.,* **1998,** *46*(1), 21-6.

Anderson L, Hunter CL. Quantitative Mass Spectrometric Multiple Reaction Monitoring Assays for Major Plasma Proteins. *Mol. Cell Proteomics,* **2006**, *5*(4), 573-88.

Barnidge DR, Goodmanson MK, Klee GG, Muddiman DC. Absolute quantification of the model biomarker prostate-specific antigen in serum by LC-Ms/MS using protein cleavage and isotope dilution mass spectrometry. *J. Proteome Res.*, **2004**, *3*(3), 644-52.

Barr JR, Maggio VL, Patterson DG. Jr, Cooper GR, Henderson LO, Turner WE, Smith SJ, Hannon WH, Needham LL, Sampson EJ. Isotope dilution--mass spectrometric quantification of specific proteins: model application with apolipoprotein A-I. *Clin. Chem.,* **1996**, *42*(10), 1676-82.

Basu NK, Kovarova M, Garza A, Kubota S, Saha T, Mitra PS, Banerjee R, Rivera J, Owens IS. *Proc. Nat. Acad. Sci.,* **2005**, *102*(18), 6285-90.

Basu NK, Kubota S, Meselhy MR, Ciotti M, Chowdhury B, Hartori M, Owens IS. *J. Biol. Chem.,* **2004**, *279*(27), 28320-29.

Beynon RJ, Doherty MK, Pratt JM, Gaskell SJ. Multiplexed absolute quantification in proteomics using artificial QCAT proteins of concatenated signature peptides. *Nat. Methods,* **2005**, *2*(8), 587-9.

Chen S, Beaton D, Nguyen N, Senekeo-Effenberger K, Brace-Sinnokrak E, Argikar U, Remmel RP, Trottier J, Barbier O, Ritter JK, Tukey RH. Tissue-specific, inducible, and hormonal control of the human UDP-glucuronosyltransferase-1 (*UGT1*) locus. *J. Biol. Chem.,* **2005**, *280*(45), 37547–557.

Ciotti M, Marrone A, Potter C, Owens IS. Genetic polymorphism in the human UGT1A6 (planar phenol) UDP-glucuronosyltransferase: pharmacological implications. *Pharmacogenetics,* **1997**, *7*(6), 485-95.

Evans WE, Relling MV. Pharmacogenomics: translating functional genomics into rational therapeutics. *Science,* **1999**, *286*(5439), 487-91.

Fledelius C, Johnsen AH, Cloos PA, Bonde M, Qvist P. Characterization of urinary degradation products derived from type I collagen. Identification of a beta-isomerized Asp-Gly sequence within the C-terminal telopeptide (alpha1) region. *J. Biol. Chem.,* **1997***, 272*(15), 9755-63.

Friedman DB. Quantitative proteomics for two-dimensional gels using difference gel electrophoresis. *Methods Mol. Biol.,* **2007**, *367*, 219-39.

Gerber SA, Rush J, Stemman O, Kirschner MW, Gygi SP. Absolute quantification of proteins and phosphoproteins from cell lysates by tandem MS. *Proc. Natl. Acad. Sci. U S A,* **2003**, *100*(12), 6940–45.

Guillemette C. Pharmacogenomics of human UDP-glucuronosyltransferase enzymes. *Pharmacogenomics J.,* **2003**, *3*(3), 136-58.

Gygi SP, Rist B, Gerber SA, Turecek F, Gelb MH, Aebersold R. Quantitative analysis of complex protein mixtures using isotope-coded affinity tags. *Nat. Biotechnol.,* **1999**, *17*(10), 994-9.

Jenkins RE, Kitteringham NR, Hunter CL, Webb S, Hunt TJ, Elsby R, Watson RB, Williams D, Pennington SR, Park BK. Relative and absolute quantitative expression profiling of cytochromes P450 using isotope-coded affinity tags. *Proteomics,* **2006**, *6*(6), 1934-47.

Kamiie J, Ohtsuki S, Iwase R, Ohmine K, Katsukura Y, Yanai K, Sekine Y, Uchida Y, Ito S, Terasaki T**.** Quantitative atlas of membrane transporter proteins: development and application of a highly sensitive simultaneous LC/MS/MS method combined with novel in-silico peptide selection criteria. **2008** *Pharm. Res.,* Jan 25 [Epub ahead of print].

Kirsch S, Widart J, Louette J, Focant JF, De Pauw E. Development of an absolute quantification method targeting growth hormone biomarkers using liquid chromatography coupled to isotope dilution mass spectrometry. *J. Chromatogr. A*, **2007**, *1153*(1-2), 300-6.

Kuhn E, Wu J, Karl J, Liao H, Zolg W, Guild B. Quantification of C-reactive protein in the serum of patients with rheumatoid arthritis using multiple reaction monitoring mass spectrometry and ^{13}C-labeled peptide standards. *Proteomics,* **2004**, *4*(4), 1175-86.

Lin S, Shaler TA, Becker CH. Quantification of intermediate-abundance proteins in serum by multiple reaction monitoring mass spectrometry in a single-quadrupole ion trap. *Anal. Chem.,* **2006**, *78*(16), 5762-7.

Maruo Y, Iwai M, Mori A, Sato H, Takeuchi Y. Polymorphism of UDP-glucuronosyltransferase and drug metabolism. *Curr. Drug Metab.,* **2005**, *6*(2), 91-9.

Meech R and Mackenzie PI. Structure and function of uridine diphosphate glucuronosyltransferases. *Clin. Exp. Pharmacol. Physiol.,* **1997**, *24*(12), 907-15.

Ong SE, Blagoev B, Kratchmarova I, Kristensen DB, Steen H, Pandey A, Mann M. Stable isotope labeling by amino acids in cell culture, SILAC, as a simple and accurate approach to expression proteomics. *Mol. Cell Proteomics,* **2002**, *1*(5), 376–86.

Ritter JK, Kessler FK, Thompson MT, Grove AD, Auyeung DJ, Fisher RA. Expression and inducibility of the human bilirubin UDP-glucuronosyltransferase UGT1A1 in liver and cultured primary hepatocytes: evidence for both genetic and environmental influences. *Hepatology,* **1999**, *30*(2), 476–84.

Roepstorff P and Fohlman J. Proposal for a common nomenclature for sequence ions in mass spectra of peptides. *Biomed. Mass Spectrom.*, **1984**, *11*(11), 601.

Ross P.L.; Huang Y.N.; Marchese J.N.; Williamson B.; Parker K.; Hattan S.; Khainovski N, Pillai S, Dey S, Daniels S, Purkayastha S, Juhasz P, Martin S, Bartlet-Jones M, He F, Jacobson A, Pappin DJ. Multiplexed protein quantitation in Saccharomyces cerevisiae using amine-reactive isobaric tagging reagents. *Mol. Cell Proteomics,* **2004***, 3*(12), 1154-69.

Skalnikova H, Rehulka P, Chmelik J, Martinkova J, Zilvarova M, Gadher SJ, Kovarova H. Relative quantitation of proteins fractionated by the ProteomeLabtrade mark PF 2D system using isobaric tags for relative and absolute quantitation (iTRAQ). *Anal. Bioanal. Chem.,* **2007**, *389*(5), 1639-45.

Smolka MB, Zhou H, Purkayastha S, Aebersold R. Optimization of the isotope-coded affinity tag-labeling procedure for quantitative proteome analysis. *Anal. Biochem.,* **2001**, *297*(1), 25-31.

Tonge R, Shaw J, Middleton B, Rowlinson R, Rayner S, Young J, Pognan F, Hawkins E, Currie I, Davison M. Validation and development of fluorescence two-dimensional differential gel electrophoresis proteomics technology. *Proteomics,* **2001**, *1*(3), 377-96.

Tukey RH and Strassburg CP. Human UDP-glucuronosyltransferases: metabolism, expression, and disease. *Annu. Rev. Pharmacol. Toxicol.,* **2000**, *40*, 581-616.

Turecek F. Mass spectrometry in coupling with affinity capture-release and isotope-coded affinity tags for quantitative protein analysis. *J. Mass Spectrom.,* **2002***, 37*(1), 1-14.

Vinther A, Holm A, Hoeg-Jensen T, Jespersen A.M, Klausen NK, Christensen T, Sorensen HH. Synthesis of stereoisomers and isoforms of a tryptic heptapeptide fragment of human growth hormone and analysis by reverse-phase HPLC and capillary electrophoresis. *Eur. J. Biochem.,* **1996**, *235*(1-2), 304-9.

Wang H, Qian WJ, Mottaz HM, Clauss TR, Anderson DJ, Moore RJ, Camp DG, Khan AH, Sforza DM, Pallavicini M, Smith DJ, Smith RD. Development and evaluation of a micro- and nanoscale proteomic sample preparation method.*J. Proteome Res.,* **2005**, *4*(6), 2397-403.

Wang MZ, Wu Q, Bridges AS, Smith PC, Kornbluth S, Tidwell RR, Paine MF, Hall JE. A gel-free MS-based quantitative proteomic approach accurately measures cytochrome P450 protein concentrations in human liver microsomes. *ISSX 14th National Meeting*, San Juan, Puerto Rico, October 22-26, **2006**.

Wellmann A, Wollscheid V, Lu H, Ma ZL, Albers P, Schutze K, Rohde V, Behrens P, Dreschers S, Ko Y, Wernert N. Analysis of microdissected prostate tissue with ProteinChip(R) arrays - a way to new insights into carcinogenesis and to diagnostic tools. *Int. J. Mol. Med.,* **2002**, *9*(4), 341-7.

Wells PG, Mackenzie PI, Chowdhury JR, Guillemette C, Gregory PA, Ishii Y, Hansen AJ, Kessler FK, Kim PM, Chowdhury NR, Ritter JK. Glucuronidation and the UDP-glucuronosyltransferases in health and disease. *Drug Metab. Dispos.,* **2004**, *32*(3), 281-90.

Wen Z, Tallman MN, Ali SY, Smith PC. UDP-glucuronosyltransferase 1A1 is the principal enzyme responsible for etoposide glucuronidation in human liver and intestinal microsomes: structural characterization of phenolic and alcoholic glucuronides of etoposide and estimation of enzyme kinetics. *Drug Metab. Dispos.,* **2007***, 35*(3), 371-80.